FIELD SOLUTION AND ELECTRICAL CHARACTERISTICS OF SLOTTED CIRCULAR WAVEGUIDES AND COAXIAL LINES

by

ESSAM EL-DIN M. HASSAN

A Thesis

Submitted to the Faculty of Graduate Studies

The University of Manitoba

In Partial Fulfillment of the Requirements for the Degree

of

DOCTOR OF PHILOSOPHY

IN ELECTRICAL ENGINEERING

Department of Electrical Engineering

Winnipeg, Manitoba

Canada

1977

FIELD SOLUTION AND ELECTRICAL CHARACTERISTICS OF SLOTTED CIRCULAR WAVEGUIDES AND COAXIAL LINES

BY

ESSAM EL-DIN M. HASSAN

A dissertation submitted to the Faculty of Graduate Studies of the University of Manitoba in partial fulfillment of the requirements of the degree of

DOCTOR OF PHILOSOPHY

'Praise be to Allah, the Lord of the Universe'

The "Quran"
1.1

Dedicated to

My Parents, my Friends and my Teachers.

In recognition of the great gifts I am indebted to them.

Abstract

The tangential field on the surface of a narrow axial slot on the wall of a hollow waveguide or a coaxial line due to an incident TE_{11} excitation is obtained. The slot length is initially assumed to be semi-infinite in length, but the results are then extended to a finite slot by including the reflected field at the slot far end. The propagating modes in the slotted guide are obtained by using the transverse resonance method. A modal expansion of the fields with unknown coefficients in both slotted and complete sections of the guide are assumed, and the continuity of the field components at the plane separating the two sections is utilized to obtain two matrix equations for the unknown coefficients. These equations are solved to determine the required coefficients. It is shown that these coefficients together with the slot static field can be used to obtain a closed-form solution for the slot tangential field. The solution satisfies the edge conditions and is valid only for narrow slots. An examination of the results shows that the slot field is localized, which allows the extention of the solution to successive slotted sections. Using this approach a solution for the field of periodic leaky wave structures is presented.

ACKNOWLEDGEMENT

The author of this work wishes to acknowledge the relentless effort and continuous help and support of Dr. L. Shafai of the Electrical Engineering Department, University of Manitoba, throughout all phases of this work. An effort, without which, this work would not have come to its present form.

The author also expresses his gratitude and appreciation to all who helped him in different phases of this work. In particular, Dr. W. M. Boerner, Prof. E. Bridges and Dr. O. Aboul-Atta for their valuable assistance and advice.

Thanks and sincere appreciation are also due to all friends and colleagues of this Department, especially to my friends Mr. B. Azarbar, Mr. A. Shoamanesh and Mr. N. Youssef for long hours of discussion and help.

The skillful typing and sincere efforts by a group of friends, particularly Ms. J. Moroz Bade, are greatly appreciated.

The auther also wishes to acknowledge the help offered him by the University of Manitoba Computer Center,and the valuable financial support forwarded to him by the National Research Council of Canada (NRC) in the form of a scholarship and by the University of Manitoba in the form of a University fellowship.

TABLE OF CONTENTS

		Page
Abstract		i
Acknowledgement		ii
Table of Contents		iii
List of Figures		vi
List of Tables		x
List of Symbols		xiii
CHAPTER 1.	INTRODUCTION	1
CHAPTER 2.	LITERATURE SURVEY	5
2.1	Introduction	5
2.2	Variational technique	7
2.3	Transverse resonance method	10
2.3.1	Radial transmission line modes	11
2.3.2	Transverse resonance applied to slotted cylindrical waveguide	12
2.3.3	Perturbation solution for the wave number	13
2.3.4	Aperture admittance	15
2.4	Computer method of determining the propagation constant of slotted waveguides	17
2.5	Integral equation for the field of circumferential aperture	20
CHAPTER 3	FIELD SOLUTION ON THE APERTURE OF A HOLLOW SLOTTED WAVEGUIDE	23
3.1	Introduction	23
3.2	Propagation constant for axially slotted hollow waveguide 'arbitrary slot location'	24
3.2.1	Numerical results for the propagation constant . .	28
3.3	Two identical and symmetrically located slots . .	32
3.3.1	Propagation constant for two identical slots symmetrically located with respect to the origin .	32
3.3.2	Numerical results for the propagation constant of a double slotted waveguide section	36

Page

3.4	Formulation of the scattering problem	40
3.4.1	Field representation interior to the waveguide . .	41
3.4.2	Mode orthogonality	45
3.4.3	Mode matching	49
3.4.4	Solution of the unknown coefficients	52
3.5	Electric field on the slot	51
3.6	Numerical results for the slot fields	54
CHAPTER 4.	FIELD SOLUTION ON THE APERTURE OF AN AXIALLY SLOTTED COAXIAL WAVEGUIDE	74
4.1	Introduction	74
4.2	Propagating TE modes in axially slotted coaxial waveguide	75
4.2.1	Slot impedance	76
4.2.2	Perturbation solution for the coaxial guide wave number	78
4.2.3	Numerical examples of the coaxial wave number . .	80
4.3	Two identically symmetrically located slot	83
4.3.1	Propagation constant in a coaxial line with identical, diagonally symmetric axial slots	84
4.3.2	Numerical results for the propagation constant of a double slotted coaxial guide	87
4.4	Formulation of the scattering problem	90
4.4.1	Field representation inside the coaxial waveguide (TE modes)	91
4.4.2	Mode orthogonality	95
4.4.3	Mode matching	98
4.4.4	Solution of the unknown coefficients	101
4.5	Electric field on the slot surface	114
4.6	Numerical results for the slot field	114
CHAPTER 5.	RADIATION CHARACTERISTICS OF SINGLE AND CASCADED SLOTTED SECTIONS	124
5.1	Field on a finite slot	126
5.1.1	Formulation and field solution	127
5.1.2	Numerical results of the finite slot fields . . .	132

Page

5.2	Radiation characteristics of axial slots	144
5.2.1	Radiation pattern of a single or double axial slots	144
5.2.2	Numerical examples of the radiation pattern of one slotted waveguide section	144
5.3	Cascaded radiating slotted sections	159
5.3.1	Analysis of the radiation pattern of cascaded slotted sections	160
5.3.2	The radiation pattern of cascaded slotted sections	165
CHAPTER 6	CONCLUSION AND DISCUSSION	170
	Suggestions for future investigations	174
Appendix A	. . . . .	177
Appendix B	. . . . .	178
Appendix C	. . . . .	180
Appendix D	. . . . .	182
Appendix E	. . . . .	189
Appendix F	. . . . .	192
Appendix G	. . . . .	195
Appendix H	. . . . .	197
Appendix I	. . . . .	201
Bibliography		203

LIST OF FIGURES

Figure		Page
2.1	Slotted rectangular waveguide	7
2.2	Slotted cylindrical waveguide	7
2.3	Direction of viewing the impendance in the Slotted cylindrical hollow waveguide	10
2.4	Transmission line representation of the slotted cylindrical hollow waveguide.	12
2.5	Thick slotted cylindrical waveguide	17
2.6	Circumferential slotted coaxial waveguide	20
3.1	Axially slotted waveguide with arbitrary slot location.	24
3.2	TE_{11} field distribution in axially slotted waveguide	31
3.3	Symmetrically double slotted waveguide	33
3.4	Transmission line representation of the symmetrically double slotted waveguide	33
3.5	Axially slotted waveguide with arbitrary slot location.	41
3.6	Reflection coefficient versus the ratio a/λ_0 of different slot widths. Single slotted waveguide	56
3.7	Reflection coefficient versus the ratio a/λ_0 of different slot widths. Symmetrically slotted hollow waveguide	58
3.8	The slot tangential field E_0 versus the distance z along the slot for single slotted hollow waveguide. Different slot parameters.	66
3.9	The slot tangential field E_0 versus the distance z along the slot for single slotted hollow waveguide. Different operating frequency.	67
3.10	The slot tangential field E_0 versus the distance z along the slot for single slotted hollow waveguide. Different operating frequency.	68
3.11	The slot tangential field E_0 versus the distance z along the slot for double slotted hollow waveguide. Different slot parameters.	69
3.12	The slot tangential field E_0 versus the distance z along the slot for double slotted hollow waveguide. Different operating wavelength.	70

Figure		Page
3.13	The slot field for both single and double slotted hollow waveguides	71
3.14	The slot field for both single and double slotted hollow waveguides	72
4.1	Axially slotted coaxial waveguide	76
4.2	Symmetrically double slotted coaxial guide	84
4.3	Transmission line representation of the symmetrically double slotted coaxial guide	85
4.4	Axially slotted coaxial waveguide.	91
4.5	Reflection coefficient versus the ratio a/λ_0 for different slot widths. Single slotted coaxial guide.	107
4.6	Reflection coefficient versus the ratio a/λ_0 for different slot widths. Symmetrically double slotted coaxial guide .	110
4.7	Slot tangential field E_0 versus the distance z along the slot. Single slotted coaxial guide with different slot parameters.	116
4.8	Slot tangential field E_0 versus the distance z along the slot. Single slotted coaxial guide with different operating wavelength.	117
4.9	Slot tangential field E_0 versus the distance z along the slot. Single slotted coaxial guide with different operating frequency.	118
4.10	Slot tangential field E_0 versus the distance z along the slot. Symmetrically double slotted coaxial guide with different parameters.	119
4.11	Slot tangential field E_0 versus the distance z along the slot. Symmetrically double slotted coaxial guide with different operating wavelength.	120
4.12	The slot field for both single and double slotted coaxial guide.	121
4.13	The slot field for both single and double slotted coaxial guide	122
5.1	Finite axially slotted waveguide	127
5.2	Tangential field E_0 on a finite slot of length $3\lambda_0$, $\phi_0 = 2^o$. Single slotted waveguide	133
5.3	Tangential field E_0 on a finite slot of length λ_0 , $\phi_0 = 2^o$. Single slotted waveguide	134

Figure		Page
5.4	Tangential field E_0 on a finite slot of length $0.5\lambda_0, \phi_0 = 2^o$. Single slotted waveguide	135
5.5	Tangential field E_0 on a finite slot of length $3\lambda_0$, $\phi_0 = 5^o$. Single slotted waveguide	136
5.6	Tangential field E_0 on a finite slot of length $3\lambda_0$, $\phi_0 = 5^o$. Symmetrically double slotted waveguide.	137
5.7	Tangential field E_0 on a finite slot of length $3\lambda_0$, $\phi_0 = 5^o$. Single slotted coaxial line.	138
5.8	Tangential field E_0 on a finite slot of length λ_0 , $\phi_0 = 5^o$. Single slotted coaxial line.	139
5.9	Tangential field E_0 on a finite slot by length $0.5\lambda_0$, $\phi_0 = 5^o$. Single slotted coaxial line.	140
5.10	Tangential field E_0 on a finite slot of length $3\lambda_0$, $\phi_0 = 2^o$. Single slotted coaxial line.	141
5.11	Tangential field E_0 on a finite slot of length $3\lambda_0$, $\phi_0 = 2^o$. Double symmetrically slotted coaxial guide.	142
5.12	Radiation pattern of a finite slot in the ϕ-direction. Single slotted waveguide $a/\lambda_0 = 0.4$ $\lambda_0 = 5^o$ $\alpha = 0.0$	150
5.13	Radiation pattern of a finite slot in the ϕ-direction. Double symmetrical slots $a/\lambda_0 = 0.4$ $\phi_0 = 5^o$ $\alpha = 0.0, 180^o$ $c = 1.5$	151
5.14	Radiation pattern of a finite slot in the ϕ-direction. Double slotted waveguide. $a/\lambda_0 = 0.5$ $\phi_0 = 5^o$ $\alpha = 0.0^o, 180^o$ $c = 1.5$	152
5.15	Radiation pattern of a finite slot in the θ-direction. Single slotted waveguide. $L = 0.5\lambda_0$	153
5.16	Radiation pattern of a finite slot in the θ-direction. Single slotted waveguide. $L = \lambda_0$	154
5.17	Radiation pattern of a finite slot in the θ-direction. Single slotted waveguide. $L = 3\lambda_0$	155
5.18	Radiation pattern of a finite slot in the θ-direction. Single slotted waveguide. $L = 10\lambda_0$ $a/\lambda_0 = 0.4$	156
5.19	Radiation pattern of a finite slot in the θ-direction. Single slotted waveguide. $L = 10\lambda_0$ $a/\lambda_0 = 0.35$	157

Figure		Page
5.20	Successive slotted waveguide sections.	100
5.21	Radiation pattern in the Θ direction of four and eight successive double slotted sections. $\alpha = 0.0, 180^{o}$. $L = 0.5\lambda_0$ $L' = 0.77\lambda_0, \phi_0 = 5^{o}$	166
5.22	Radiation pattern in the Θ-direction of 10 successive double slotted sections. $\alpha = 0.0, 180^{o}$ $L = 0.5\lambda_0$ $L' = 0.77\lambda_0$, $\phi_0 = 5^{o}$	167
5.23	Radiation pattern in the Θ-direction of 10 successive double slotted sections. $\alpha = 0.0, 180^{o}$. $L = .3\lambda_0$ $L' = 0.956\lambda_0, \phi_0 = 5^{0}$	168
A-1	Transverse resonance circuit.	177
D.1	Symmetrically double slotted waveguide.	182
D.2	Transmission line representation of the double slotted waveguide	182

LIST OF TABLES

Table		PAGE
3.1	Values of δ and γ for different slot locations. $\phi_0 = 5^o$. Hollow waveguide.	28
3.2	Values of δ and γ for different slot locations. $\phi_0 = 3^o$. Hollow waveguide.	29
3.3	Values of δ and γ for different slot locations. $\phi_0 = 2^o$. Hollow waveguide.	29
3.4	Values of δ and γ for different hollow waveguide mode	30
3.5	Values of δ and γ for double slotted hollow waveguide. $\phi_0 = 2^o$, $a/\lambda_0 = 0.5$	37
3.6	Values of δ and γ for double slotted waveguide. $\phi_0 = 5^o$, $a/\lambda_0 = 0.5$	37
3.7	Comparison between single and double slotted waveguide $\phi_0 = 4^o$	38
3.8	Comparison between single and double slotted waveguide. Different slot widths.	39
3.9	Transmission and reflection coefficients for incident TE_{11} waveguide mode. $\phi_0 = 2^o$, $\alpha = 0.0^o$	54
3.10	Transmission and reflection coefficients for incident TE_{11} waveguide mode. $\phi_0 = 2^o$, $\alpha = 45^o$	54
3.11	Transmission and reflection coefficients for incident TE_{11} waveguide mode. $\phi_0 = 5^o$, $\alpha = 0.0^o$ and M = 8.	55
3.12	Transmission and reflection coefficients for incident TE_{11} waveguide mode. $\phi_0 = 5^o$, $\alpha = 0.0^o$ and M = 6	55
3.13	Transmission and reflection coefficients for incident TE_{11} waveguide mode. Double slotted guide with $\phi_0 = 2^o$ and $\alpha = 0.0^o$	57
3.14	Transmission and reflection coefficients for incident TE_{11} waveguide mode. Double slotted guide with $\phi_0 = 2^o$ and $\alpha = 45^o$	57

LIST OF TABLES

Table		Page
3.15	Transmission and reflection coefficients for incident TE_{11} waveguide mode. Double slotted guide with $\phi_0 = 5^o, \alpha = 0.0^o$	59
4.1	Values of δ and γ for different slot locations. $\phi_0 = 5^o$. Coaxial line	81
4.2	Values of δ and γ for different slot locations. $\phi_0 = 3^o$. Coaxial line	82
4.3	Values of δ and γ for different slot locations. $\phi_0 = 2^o$. Coaxial line	82
4.4	Values of δ and γ for different coaxial waveguide modes	83
4.5	Values of δ and γ for double slotted coaxial line. $\phi_0 = 2^o$, $a/\lambda_0 = .35$	88
4.6	Values of δ and γ for double slotted coaxial line $\phi_0 = 5^o$, $a/\lambda_0 = 0.35$	88
4.7	Comparison between single and double slotted coaxial guide. $\phi_0 = 4^o$	87
4.8	Comparison between single and double slotted coaxial guide. Different slot widths.	90
4.9	Transmission and reflection coefficients for incident TE_{11} coaxial mode. $\phi_0 = 2^o, \alpha = 0.0^o$	103
4.10	Transmission and reflection coefficients for incident TE_{11} coaxial mode. $\phi_0 = 2^o, \alpha = 45^o$	104
4.11	Transmission and reflection coefficients for incident TE_{11} coaxial mode. $\phi_0 = 5^o, \alpha = 0.0^o$. $M = 5$	105
4.12	Transmission and reflection coefficients for incident TE_{11} coaxial mode $\phi_0 = 5^o, \alpha = 0.0^o$. $M = 4$	106
4.13	Transmission and reflection coefficients for incident TE_{11} coaxial mode. Double slotted guide with $\phi_0 = 2^o, \alpha = 0.0$	108

LIST OF TABLES

Table		Page
4.14	Transmission and reflection coefficients for incident TE_{011} coaxial mode. Double slotted guide with $\phi_0 = 2^o, \alpha = 45^o$	108
4.15	Transmission and reflection coefficients for incident TE_{011} coaxial mode. Double slotted guide with $\phi_0 = 5^o, \alpha = 0.0^o$	109

LIST OF PRINCIPAL SYMBOLS

I. Latin Symbols

a	Hollow waveguide radius or inner radius of the coaxial guide.
b	Outer radius of the coaxial -uide.
c	Ratio b/a
d	Stands for either a or b according to the equation.
dB	Decibels.
E ±nn	$10^{\pm nn}$
e_{nm}	Electric field mode function.
h_{nm}	Magnetic field mode function.
$H_n^{(1)}(K_\rho)$	Hankel function of the first kind of argument K_ρ and order n.
$J_n(K_\rho)$	Bessel function of argument K_ρ and order n
j	$\sqrt{-1}$
K_ρ	Propagation constant of the slotted guide section in the ρ-direction.
L.H.S.	Left hand side.
R.H.S.	Right hand side.
P_r	Power reflection coefficient.
L	Slot length.
L'	Separation distance between any two cascaded slots.
X_{nm}	M^{th} root of $J_n'(X_{nm}) = 0.0$
z_{nm}	M^{th} root of equation (4.20).

$F(cz_{1m})$	Is defined by equation (4.12).
$C_n(z_{nm}\rho/a)$, $C_n'(z_{nm}\rho/a)$, $D_n(K_{\rho_{nm}}\rho)$, $D_n'(K_{\rho_{nm}}\rho)$	Are given by equation (4.17).
$G_n(cz_{nm})$	Is given by equation (4.32).
B_s	Slot susceptance of the slotted waveguide.
G_s	Slot conductance of the slotted waveguide.
B_s^c	Slot susceptance of the slotted coaxial waveguide.
G_s^c	Slot conductance of the slotted coaxial waveguide.
E_s	Surface field on a finite slot.
E_0	Surface field on a semi-infinite slot.

II. Greek Symbols

α	Slot location with respect to $\phi = 0.$ axis.
α_z, α_ρ	Attenuation constants in the z and ρ-directions, respectively.
β_z, β_ρ	Phase shift constants in the z and ρ-directions, respectively.
ω	Angular frequency.
γ	Propagation constant in the slotted waveguide section in the axial direction.

δ	Value of the small perturbation of the transverse wave-number of the slotted guide around its value of the complete waveguide.
θ_{nm}	Propagation constant in the axial direction of the complete waveguide.
ϕ_0	Slot half angular width.
λ_0	Free space wavelength.
λ_s	Slot field wavelength.
ϵ_n	Neumann number, equals 1 for n= 0, and 2 for n $\neq$ 0.
Π_z^e & Π_z^m	Electric and magnetic vector potentials, respectively.

CHAPTER I

INTRODUCTION

The ever increasing progress of the communication technology is continuously demanding more sophisticated and precise devices to achieve efficient convoyance of information. Antennas, the matching devices between the systems transmitting or receiving signal and the free space, have always been the subject of extensive research work. Among the most widely used antenna structures in microwave communication are the slotted waveguides and the slotted coaxial lines. These two structures have found numerous applications in both microwave systems and antennas. As antennas they are used in multiple feed systems for cylindrical, spherical and conical reflectors [1-6], or as a broadband balun transformer for matching the balanced antenna impedance to the unbalanced coaxial feed [7].

The axially slotted waveguide is a structure capable of supporting leaky waves along its aperture. As the wave travels down the structure, energy leaks in a prescribed direction through the aperture. Extensive analyses of the leaky wave nature have been made in the past decade. These waves were first pointed out by Marcuvitz [8] in 1956. The treatment of guided waves along open structures was further established by Tamir and Oliner [9]. The influence of the guided leaky waves on the radiation pattern was treated by Collin [10], Hessel [11], and Tamir and Oliner [12]. It is shown by several authors [13-15] that these waves are characterized by a complex propagation constant $K_z = \beta_z + j\alpha_z$ (with time variation exp $(-j\omega t)$) along the structure. This shows a continuous leakage of energy as the waves

travel along the z direction. The wave is a fast wave with a phase velocity faster than that of light (i.e. $\beta_z < K_0$). A direct result of this condition is that the wavenumber in the transverse direction ρ takes the form $K_\rho = \beta_\rho - i\alpha_\rho$, which shows an improper wave travelling in the ρ-direction with ever increasing amplitude. It should be emphasized, however, that the radiation from the leaky wave antenna is essentially confined to certain regions and that the solution is restricted within this region[13]-[14]. The leaky wave radiation is normally in the forward direction [14]. However, in non- conventional structures such as waveguides with dielectric rod or guides employing plasma or ferrite structures, radiation could be achieved in the backward region. This is demonstrated in the work of Clarricoats et al[16]-[17],Trivelpiece et al[18]-[19]and Tamir and Oliner [20].

The particular leaky wave problem of the axially slotted or coaxial line waveguide has received limited investigations in the past. Collin [21] has calculated the characteristic impedance of a slotted coaxial line. This was subsequently used by Duncan in designing a broad-band balun[7]. Quite recently the characteristic impedance of the partially filled slotted hollow and coaxial guides have been numerically calculated by Hatsuda [22]. The possible leaky modes supported by the slotted structure was first investigated by Rumsey [23] who obtained a variational expression for the complex propagation constant of the field interior to the rectangular slotted waveguide. Harrington,using a similar variational expression,solved the problem in the cylindrical waveguide case [24]. Later in 1960, Goldstone and Oliner [25] employed the transverse resonance method based on the knowledge of the slot impedance. Their work agreed well with the work

of Harrington [24] for narrow slots, but showed discrepancy at wide slot case due to the approximation involved in their expression. Recently, Clarricoats and Slinn [26] solved the same problem numerically by matching the field expanations in three regions (assuming a finite thickness for the waveguide). The condition that the determinant of the system vanishes,allows the determination of the wave number. However, in all these cases the slot field was usually assumed to have a certain suitable form and was never calculated. It is the main objective of this thesis to obtain this slot field and investigate its behavior for various slot and waveguide parameters. Initially the slot is assumed to be semi-infinite in length and be excited by a TE_{11} incident mode.

As mentioned previously the problem of determining the slot field has not been attempted before. The form of this field and the parameters influencing its intensity, distribution and the radiated power may be important to many microwave, antenna and communication engineers. Assuming TE_{11} excitation, an exact integral equation formulation of the slot field could be obtained similar to the work of Chang and Wu [46], and Wu [47] for the circumferential slot in coaxial guides. The solution of this integral equation, however, may be difficult to generate. Therefore, one may look for other suitable techniques to tackle the problem. The solution presented in this thesis is a quasi analytical solution, where the problem is solved by a combination of analytical and numerical techniques. In Chapter 2 the different modes supported by the structure are obtained using the technique of Goldstone and Oliner [25]. This technique is later modified to allow the solution for any single and double symmetrical slots with arbitrary slot

locations. In Chapter 3 the fields in both the slotted and the complete sections of the hollow waveguide are expanded in their respective modes with two sets of unknown coefficients. Matching these fields on the plane separating the two waveguide sections converts the continuity condition into two sets of infinite equations. These two sets of equations are cast in a matrix form and are solved together to yield the required unknown coefficients. When these coefficients are obtained, it is shown that for a narrow slot the coefficients of the TE_{1m} modes in the slotted section are sufficient to determine the slot field. Using this particular set of coefficients one can arrive at a closed form solution for the tangential component of the field on a narrow slot. In Chapter 4 the same technique is applied to axially slotted coaxial waveguides, and the slot field is obtained in a manner much similar to the method used in Chapter 3. The solution for a finite slot is presented in Chapter 5 by considering the reflection at the slot far end. When this field is obtained, one can study the radiation characteristics of a finite slotted waveguide section . This is carried out in the second part of Chapter 5 and is extended to successive slotted waveguide sections. It is shown that the results obtained compare well with the limited data available in the literature on slotted waveguides [14], [33], [35].

The work is concluded in Chapter 6 by a general discussion of the results and possible extensions of the work to other related problems.

CHAPTER II

LITERATURE SURVEY

2.1. Introduction

The problem of slots on the surface of a waveguide is as old as the waveguide itself. It was first utilized for two major objectives; to provide means of entry into the waveguide to study the internal field, such that the presence of the slot does not influence the original field configuration to any great degree [36] and to study the radiation due to the tangential field on the surface of the slot. This field, however, in most earlier work was assumed to be known [33]-[35].

Quite recently, with the increasing interest in communication technology, the problem of coupling between internal and external fields of a waveguide or coaxial cable through holes or slots has received a rather thorough investigation[37-41]. As mentioned before most of the work dealt with either small holes on the outer surface for which a perturbation approach was employed [41] or a circumferential slot on the outer sheath for which an integral equation was developed for the tangential slot field [37-40].

The axially slotted waveguide, a structure which is capable of supporting leaky waves along its surface[13-15]has drawn some attention recently because of its possible use as an efficient feed source for conducting reflectors [1-6]. Most of the work done in this area, however, dealt with the possible propagating modes inside the structure [23-27] or along the surface of the finite slot [42-43].

Since the knowledge of the propagation constant inside the slotted waveguide enables one to gain considerable knowledge about the leaky wave

field, determination of this constant is thus essential for any further analysis of the field either inside or outside the slotted waveguide. Rumsey [23] in 1953 has established a variational expression for the propagation constant γ which has been used by Harrington [24] for both TE and TM cases. Goldstone and Oliner [25] employed the transverse resonance technique with an equivalent susceptance for the slot to obtain an explicit expression for γ. Their method was quite accurate for narrow slots, but showed discrepancies from the measured results and from that of Harrington's for wide slots. Finally Clarricoats and Slinn solved the problem numerically by matching the fields on both sides of the slot [26]. The result of their work is reported to be in good agreement with the experimental results of Goldstone and Oliner [25]. The scattering parameter technique has also been used by Chen [27], which yields an expression identical to Harrington's variational expression.

In order to gain a better understanding of the problem, the first part of this Chapter deals, in some detail, with the work of Harrington as well as with that of Goldstone and Oliner, and Clarricoats and Slinn. In the second part the integral equation approach for the tangential field on a narrow circumferential slot is presented. It is shown that the static solution as obtained by Hurd [37] and Chang [38] is a fairly acceptable solution for the electric field as long as the slot is quite narrow, a result which shall be used in later chapters to arrive at a closed form formula for the axial slot field. The integral equation formulation is exact. However, the solution presented is limited to narrow slots. For wide slots the solution may not be valid since the basic assumptions are violated. In addition, mode coupling is highly probable, in which case the formulation of the problem itself may no

longer be accurate.

With these limitations in mind, we now proceed to present the different analytical solutions for the propagation constant of an axially slotted waveguide as discussed by Harrington [24], Goldstone and Oliner [25], and Clarricoats and Slinn [26]

2.2. Variational Technique

Consider a rectangular waveguide with an infinitely long axial slot of width w cut on one of its sides as shown in Fig. 2.1 . Rumsey has shown that a stationary expression for the propagation constant γ is given by [23]

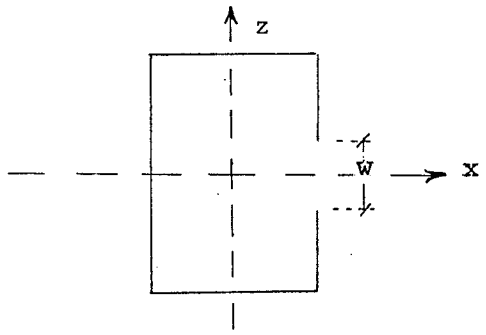

Fig. 2.1 Slotted rectangular waveguide

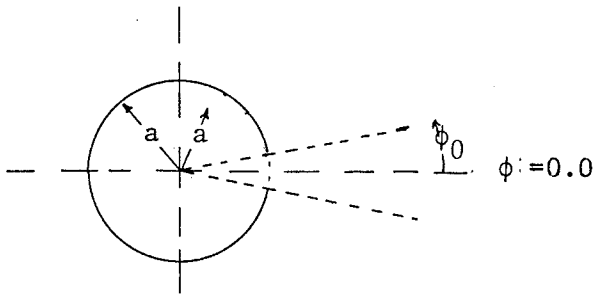

Fig. 2.2 Slotted cylindrical waveguide

$$\int_{-w/2}^{w/2} \{E_y(H_z^i - H_z^e) + E_z(H_y^i - H_y^e)\}dz = 0 \qquad (2.1)$$

where the superscript e and i refer to the external and internal fields respectively. For the cylindrical cross-section of Fig. 2.2 the expression could be shown to be [28]

$$\int_{-\phi_0}^{\phi_0} \{E_\phi(H_z^i - H_z^e) + E_z(H_\phi^i - H_\phi^e)\}d\phi = 0 \qquad (2.2)$$

Assuming an expression for the field in the outside region to be in the form

$$H_z^e(\rho,\phi) = \sum_{n=0}^{\infty} b_n H_n^{(1)}(K_\rho \rho) \cos n\phi \qquad (2.3)$$

where

$H_z^e(\rho,\phi)$ is the external z component of the magnetic field,

$H_n^{(1)}(K,\rho)$ is the Hankel function of the first kind of order n,

b_n is the Fourier coefficient,

K_ρ is the complex propagation constant in ρ direction given by

$$K_\rho^2 + \gamma^2 = K_0^2 \qquad (2.4)$$

The coordinates ρ, ϕ and ϕ_0 are as shown in Fig. 2.2 . The internal magnetic field $H_z^i(\rho,\phi)$ can similarly be assumed as

$$H_z^i(\rho,\phi) = \sum_{n=0}^{\infty} a_n J_n(K_\rho \rho) \cos n\phi \qquad (2.5)$$

with J_n and a_n being the cylindrical Bessel function and the Fourier coefficient respectively.

Using Maxwell's equations and assuming constant electric field on the slot in the azimuthal direction, Harrington has obtained the coefficients a_n and b_n. By substituting the results in equation (2.2), he has arrived at an expression which, for the TE modes, is given by

$$\sum_{n=0}^{\infty} \varepsilon_n \left[\frac{J_n(K_\rho a)}{J_n'(K_\rho a)} - \frac{H_n^{(1)}(K_\rho a)}{H_n^{(1)\prime}(K_\rho a)}\right] \left(\frac{2 \sin n\phi_0}{n}\right)^2 = 0 \qquad (2.6)$$

where ε_n is the Neumann number. This equation gives K_ρ as a function of the waveguide radius a, and the slot half-angle ϕ_0. It has an infinite number of solutions each corresponding to a waveguide mode

similar to those of a closed circular waveguide. Thus assuming that $K_\rho a$ is nearly equal to a closed waveguide mode constant $K_{nm}a$, one can set

$$K_\rho a = K_{nm}a + \delta \tag{2.7}$$

where δ is a small complex number. Thus expanding the Bessel and the Hankel functions around $K_{nm}a$ and retaining only terms up to the second order in δ, one can arrive at an equation of the form

$$a_2\delta^2 + a_1\delta + a_0 = 0 \tag{2.8}$$

where a_0, a_1 and a_2 are constants which depend on J_n and H_n in a manner determined by the form of the excitation [24] and [28]. Once δ is known, γ can be found using the relation

$$\gamma = -\frac{1}{\lambda_0}\sqrt{[(K_\rho a)/(a/\lambda_0)]^2 - (2\pi)^2} \tag{2.9}$$

with λ_0 being the operating wavelength.

This technique adopted by Harrington is quite general and has several advantages over the technique used by Goldstone and Oliner[25]. It retains terms of the order δ^2 which makes it valid for both narrow and wide slots. The stationary characteristic of (2.6) in relation to the type of the assumed tangential slot field also adds to its advantages. The expression, however, has a major disadvantage. For small slot half angle ϕ_0, it is insensitive to the variation of the slot location α. Regardless of the change in the integration interval, one obtains a solution which is always the same as the solution for the case $\alpha = 0°$ (or $\alpha = 180°$). This particular problem is discussed later in Section (3.2.1).

Because of this drawback, it becomes necessary to resort to another technique, which may be less accurate but more adaptable for arbitrary slot location. This technique is the transverse resonance method used by Goldstone and Oliner[25]. Because of frequent use of this technique in the early stages of this thesis, a comprehensive review of their work is given in the next Section.

2.3. Transverse Resonance Method

In this method the cross section of the structure is represented by a transmission line network. The resonance of this network yields values of K_ρ and hence γ for the travelling wave structure. Quantitatively the resonance of a network occurs when the impedance looking in one direction is equal and opposite in sign to the impedance looking in the opposite direction as discussed in Appendix [A]. Thus if a network representation of a structure is set in ρ direction, then according to [15] :

$$\overleftarrow{Z} + \overrightarrow{Z} = 0$$

or equivalently (2.10)

$$\overleftarrow{Y} + \overrightarrow{Y} = 0$$

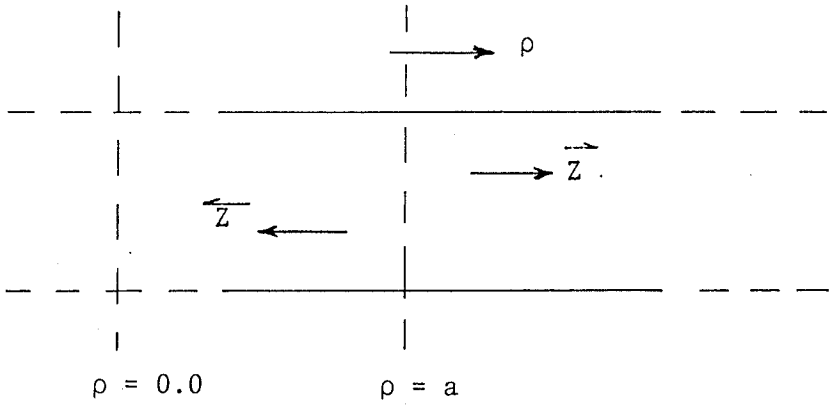

Fig. 2.3 Direction of viewing the impedance

where Z and Y represent the impedance and the admittance respectively. The arrows to the left mean the quantity Z or Y is viewed in the direction of decreasing ρ and an arrow to the right means viewing them in the direction of increasing ρ, as shown in Fig. 2.3 .

2.3.1. Radial Transmission Line Modes

In general the field inside a waveguide can be expressed as a product of two functions. The first is a function of only the coordinates along which the transmission line representation is effected. It is called the modal amplitude. The other function, which is called the mode function, is usually independent of the modal amplitude coordinates [29].

In the treatment of the present problem, Goldstone and Oliner [25] modified the mode function to permit it to be a function of ρ which is taken to be the direction along which the network representation of the slotted waveguide is set.

The transverse (to ρ) field can be represented by [29]

$$E_t(\rho,\phi) = \sum_n V_n^e(\rho)\, e_n^e(\rho,\phi) + V_n^h(\rho)\, e_n^h(\rho,\phi)$$
$$H_t(\rho,\phi) = \sum_n I_n^e(\rho)\, h_n^e(\rho,\phi) + I_n^h(\rho)\, h_n^h(\rho,\phi) \qquad (2.11)$$

where the z dependence $\exp(-\gamma z)$ has been dropped. In this equation $e(\rho,\phi)$ and $h(\rho,\phi)$ are the mode functions and the superscripts e and h refer to TM and TE modes respectively. $V(\rho)$ and $I(\rho)$ are the modal amplitudes such that $I_n^h(\rho)$ and $V_n^e(\rho)$ satisfy Bessel's differential equation

$$\left[\frac{1}{\rho}\frac{\partial}{\partial\rho}\left(\rho\frac{\partial}{\partial\rho}\right) + \left(K_\rho^2 - \frac{n^2}{\rho^2}\right)\right] \begin{Bmatrix} I_n^h \\ V_n^e \end{Bmatrix} = 0 \qquad (2.12)$$

Furthermore

$$\frac{dV_n}{d\rho} = -j(K_\rho^2 - \frac{n^2}{\rho^2})\ Z_{0n}\ I_n$$

$$\frac{dI_n}{d\rho} = -j(K_\rho^2 - \frac{n^2}{\rho^2})\ Y_{0n}\ V_n \qquad (2.13)$$

$$Y_{0n}^e = 1/Z_{0n}^e = \frac{\omega\varepsilon\rho}{K_\rho^2}\ (K_\rho^2 - \frac{n^2}{\rho^2})^{\frac{1}{2}},\ Y_{0n}^h = \frac{1}{Z_{0n}^h} = \frac{K_\rho^2}{\omega\mu\rho} \cdot \frac{1}{(K_\rho^2 - \frac{n^2}{\rho^2})^{\frac{1}{2}}} \qquad (2.14)$$

The mode functions and their orthogonality relations are given elsewhere [25].

2.3.2. Transverse Resonance Applied to Slotted Cylindrical Waveguide

The slotted guide shown in Fig. 2.2 could be represented by a radial transmission line of length a terminated by an admittance Y_s which is due to the presence of the slot (see Fig. 2.4).

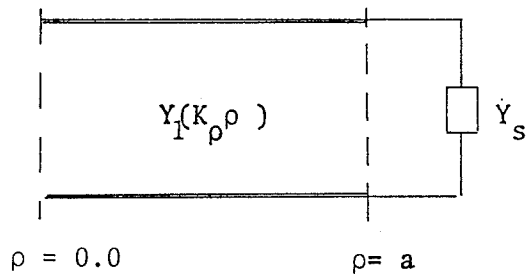

Fig. 2.4 Transmission line representation of the slotted waveguide

If $Y_1(K_\rho\rho)$ is the admittance of the radial transmission line, the transverse resonance equation may be written as

$$\overleftarrow{Y}_1(K_\rho a) + \overrightarrow{Y}_s = 0 \qquad (2.15)$$

where arrows on admittances indicate the direction of observation of each admittance. Consider the TE_{11} case, $\overleftarrow{Y}_1(K_\rho a)$ is given by [29]

$$\overleftarrow{Y}_1(K_\rho a) = - I_1^h / V_1^h$$

Using equations (2.11) - (2.14) or referring to references [25], [28], $\overleftarrow{Y}_1(K_\rho a)$ is given by

$$\overleftarrow{Y}_1(K_\rho a) = \frac{K_\rho}{j\omega\mu a} \frac{J_1(K_\rho a)}{J_1'(K_\rho a)} \tag{2.16}$$

Substituting back in (2.15) and with the knowledge of the slot admittance Y_s, one may solve for K_ρ using a suitable perturbation technique, which will be given next for future reference.

2.3.3. Perturbation Solution for the Wave Number

As has been discussed in Section (2.2), the wave number in ρ-direction $K_\rho a$ can be set equal to a corresponding waveguide mode number plus a small complex number as given by equation (2.7), which is rewritten here for convenience as

$$K_\rho a = K_{mn} a + \delta \tag{2.7}$$

The transverse resonance condition of equation (2.10) can be written as

$$\overleftrightarrow{Z}(K_\rho a) = 0 \tag{2.17}$$

where

$$\overleftrightarrow{Z}(K_\rho a) = \overleftarrow{Z}_1(K_\rho a) + R_s - jX_s \tag{2.18}$$

and from equation (2.16)

$$\overleftarrow{Z}_1(K_\rho a) = - \frac{\omega\mu a}{jK_\rho} \frac{J_1'(K_\rho a)}{J_1(K_\rho a)}$$

the functions R_s and X_s are given by

$$R_s = \frac{G_s}{G_s^2 + B_s^2} \qquad X_s = \frac{B_s}{G_s^2 + B_s^2}$$

where G_s and B_s are the slot conductance and susceptance respectively.

Expanding (2.7) about $K_{11}a$, i.e., X_{11}, it gives

$$\overleftrightarrow{Z}(K_\rho a) \simeq \overleftrightarrow{Z}(K_{11}a) + \delta\, \overleftrightarrow{Z}'(K_{11}a) = 0$$

where the prime denotes differentiation with respect to $K_\rho a$. It is simple to show that

$$\overleftrightarrow{Z}'(K_{11}a) \simeq \frac{1 - (K_{11}a)^2}{j(K_{11}a)^2} \; \frac{-\omega\mu a}{K_\rho}$$

where the derivatives of R_s and X_s are neglected [25]. Thus for the TE_{11} mode δ reduces to

$$\delta = \frac{(K_{11}a)^2}{(K_{11}a)^2 - 1} \; \{X_s' + j\, R_s'\} \tag{2.19}$$

where

$$X_s' = -X_s/(\omega\mu a/K_\rho) \quad \text{and} \quad R_s' = -R_s/(\omega\mu a/K_\rho)$$

The complex perturbation δ cannot be fully known before the slot admittance Y_s is calculated. This problem is quite involved. One may employ such methods as the integral equation method, the equivalent static method or the transformation method. A comprehensive account of these methods can be found in the work of Schwinger[31], Marcuvitz[29], and others. In the following Section a brief account of the integral equation method is presented. The details may be found in references [25],[28],[29] and[31]

2.3.4. Aperture Admittance

Referring to Fig. 2.2 an expression for the slot conductance G_s of the TE_{11} mode can be written as [25], [28] and Appendix [D]

$$G_s = \frac{\int_{-\phi_0}^{\phi_0} d\phi \int_{-\phi_0}^{\phi_0} d\phi' \; E_\phi(a,\phi)\; G''(a;\phi,\phi')\; E_\phi(a,\phi')}{\left| \int_{-\phi}^{\phi} h''_{zn}\; E_\phi(a,\phi)\, d\phi \right|^2} \tag{2.20}$$

where $E_\phi(a,\phi)$ is the electric field on the slot and

$$h''_{zn} = \sqrt{\frac{\varepsilon_n}{2\pi}} \cos n\phi \tag{2.21}$$

$$G''(a,\phi,\phi') = \mathrm{Re} \left\{ \sum_{n=0}^{\infty} \vec{Y}''_n(a)\; h''_{zn}(\phi)\; h''_{zn}(\phi') \right\}$$

with

$$\vec{Y}''_n(a) = \frac{K_\rho}{j\omega\mu a} \frac{H_n^{(1)}(K_\rho a)}{H_n^{(1)'}(K_\rho a)} \tag{2.22}$$

The expression for the conductance can be shown to be stationary with respect to the variation of the aperture field about its correct value [25]. Using the static slot electric field [37-38]

$$E_\phi = 1/\sqrt{1 - (\phi/\phi_0)^2} \tag{2.23}$$

which is derived from the integral equation solution given in Appendix [B], one finds

$$G_s = \frac{1}{\pi\omega\mu a^2} \sum_{n=0}^{\infty} \frac{\varepsilon_n}{\left|H_n^{(1)}(K_\rho a)\right|^2} \left| \frac{J_0(n\phi_0)}{J_0(\phi_0)} \right|^2 \tag{2.24}$$

The susceptance portion of the equivalent circuit can be calculated from the following equation [25] and Appendix [D]

$$V_1'' = \frac{-M_z}{j\omega\varepsilon} I_1'' h_1''(a,0)\, h_1''^{*}(a,0) \tag{2.25}$$

where

V'' is the modal voltage of the $n = 1$ mode at the slot

I_1'' is the discontinuity in the modal current of the n = 1 mode

M_z is the magnetic polarizability of the slot given by [25]:

$$M_z = \frac{\pi}{2} \frac{K_0^2}{K_\rho^2} \cdot \frac{1}{\ln(2/\phi_0)} \tag{2.26}$$

A brief account of the derivation of equation (2.25) is given in Appendix [B]. Now, using (2.25) and (2.26), the slot susceptance is readily obtained as

$$\frac{I_1''}{V_1''} = jB_s = -j\omega\varepsilon\left(\frac{K_\rho}{K_0}\right)^2 2\ln(2/\phi_0) \tag{2.27}$$

A straightforward substitution of (2.24) and (2.27) in equation (2.19) determines δ, which together with (2.7) and (2.9) fully determines both K_ρ and γ. Further details and numerical results are given in reference [25].

This method has several advantages. The slot impedances of many structures have been thoroughly studied and are either available in the literature or easily derived using known techniques, which makes the method applicable to variety of structures. Also, when the perturbation technique is applied, a relatively simple and explicit expression for δ is obtained which saves a substantial computational time compared to Harrington's method. Furthermore, the expression can be modified as will be shown later allowing a solution for different slot locations to be derived. The technique, however, has its disadvantages. For the

case of wide slots, the results may not be accurate enough because of the perturbation procedure used and due to the lumped susceptance analysis performed in the small aperture limit. This particular drawback, however, has no effect on the work of this thesis. In all the analysis to follow, it is assumed that the slot is quite narrow, and thus the work of Goldstone and Oliner may be utilized. In defining the term narrow, the criterion adapted by Silver[35] is used.This states that the slot is narrow if $2 \log_{10} \frac{\text{length}}{\text{width}} >> 1$. This definition will be used throughout this work.

The numerical solution of the problem is presented next. The procedure is simple and straightforward, but the computational task is tremendous and has its disadvantages as will be discussed later.

2.4. Computer Method of Determining the Propagation Constant of Slotted Waveguides

In this method a field expansion in three regions is assumed. The configuration of the slotted guide and the three regions are shown in Fig. 2.5 .

The electric and magnetic fields in the aperture plane of the discontinuity are expanded in terms of normal modes appropriate for the region. Applying orthogonality relations at the surface of the discontinuity converts the discontinuity equations into two sets of infinite

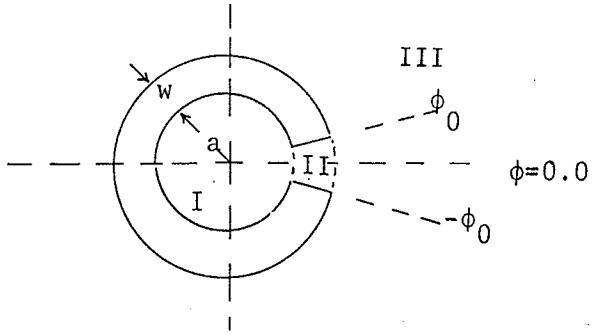

Fig. 2.5 Thick slotted cylindrical waveguide

equations. They are truncated after a suitable number of terms and the resulting finite sets may be solved together for the propagation constant.

In this analysis Clarricoats and Slinn [26] adopted the modal representation introduced by Goldstone and Oliner [25] described in the preceeding section. The modal functions for the TE modes assume the following expressions

i) Region I

$$V_n^h(\rho) = A_n^{(1)} \frac{j\omega\mu_0}{K_\rho^2} K_\rho \rho \; J_n'(K_\rho\rho)$$

$$I_n^h(\rho) = A_n^{(1)} J_n(K_\rho\rho)$$

ii) Region II

$$V_n^h(\rho) = A_n^{(2)} \frac{j\omega\mu_0}{K_\rho^2} K_\rho\rho[J_p'(K_\rho\rho) + \frac{B_n^{(2)}}{A_n^{(2)}} Y_p'(K_\rho\rho)]$$

$$I_n^h(\rho) = A_n^{(2)} [J_p(K_\rho\rho) + \frac{B_n^{(2)}}{A_n^{(2)}} Y_p(K_\rho\rho)]$$

with

$$p = n\pi/\phi_0$$

iii) Region III

$$V_n^h(\rho) = A_n^{(3)} \frac{j\omega\mu_0}{K_\rho^2} K_\rho\rho \; H_n^{(1)'}(K_\rho\rho)$$

$$I_N^h(\rho) = A_n^{(3)} H_n^{(1)}(K_\rho\rho)$$

where notations are the same as those of the previous Section, and A_n and B_n are unknown coefficients. Applying the condition of continuity of H_t at both $\rho = a$ and $\rho = a + w$ within the domain $-\phi_0 < \phi < \phi_0$ will yield a set of four homogeneous equations in the four unknowns $A_n^{(1)}$, $A_n^{(2)}$, $B_n^{(2)}$ and $A_n^{(3)}$. The condition that the determinant of the

system should vanish permits the evaluation of the propagation constant K_ρ. Clarricoats et al [26] using this approach has solved for the TE_{11} case [26] and has obtained results which are in good agreement with the reported experimental results of Goldstone and Oliner [25].

Further details on the numerical procedure as well as numerical results are given in reference [26]. The method, however, suffers from several drawbacks. The numerical procedure is quite tedious and time consuming. Moreover, for narrow slots only the first term $n = 0$ of the field expansion in region II can practically be assumed since for higher orders the order of the Bessel and the Neumunn functions becomes very high In this case the ϕ variation of the field in region II becomes numerically insignificant,which makes the overall expansion insensitive to the variation of the slot location. More serious is the parameter w, which is the width of the window in Fig. 2.5 . The final expression apparently depends on w which makes the evaluation of the propagation constant γ a function of an uncontrolled parameter. Thus by using different values of w one obtains different values for δ. Even though this may seem logical, an application of this method reverals that as w approaches zero its solution for δ does not yield the expected solution obtained by the Harrington or the Goldstone and Oliner methods.

For the above reasons, together with the discussion of Sections (2.2) and (2.3), the technique adopted by Goldstone et al [25] proves most suitable for the work of this thesis and is used later for the analysis of both the hollow and the coaxial slotted waveguides.

The remaining task of this Chapter is to present the integral equation technique used in solving a closely related problem. The problem

in question is to obtain the field on the surface of a circumferential slot cut in the outer sheath of a coaxial waveguide. Several authors have attempted this problem using different techniques [37 - 40],[44] and [45]. These techniques are not, however, related to the problem of this thesis, therefore only the formulation of the integral equation for the aperture field is presented. More specific details on the techniques used and on the numerical results are given in references [37 - 40], [44] and [45]

2.5. Integral Equation for the Field of Circumferential Apertures

Consider a coaxial cylinder of infinite extent with inner and outer radii a and b respectively and a circumferential slot of width 2d on the outer sheath as shown in Fig. 2.6 .

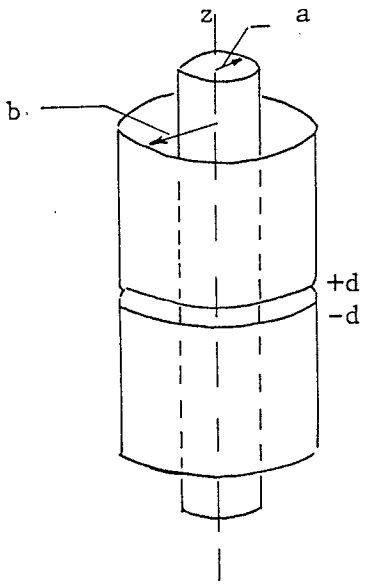

Fig. 2.6 Circumferential slotted coaxial waveguide

Let the relative permittivity of the inner region be ε, and assume that the exterior region to be free space. An incident TEM current mode of unit amplitude is assumed in the form $\frac{1}{\rho} e^{-j(\omega t - K_z a)}$, where K_z is the wavenumber in the dielectric in the z-direction.

In the coaxial region, the ϕ component of the magnetic field can be expressed in terms of the tangential electric field at the aperture according to [46] - [47] as

$$H_\phi(\rho,z) = \frac{1}{2\pi\rho} e^{jK_z z} + \frac{iK_z b}{\eta} \int_{-d}^{d} E_z(b, z') G_c(\rho;z,z') \, dz' \qquad (2.28)$$

where

$$G_c(\rho;z,z') = \frac{i}{2} \sum_{m=0}^{\infty} (\gamma_m A_m)^{-1} \phi_m(\rho) \phi_m(b) e^{i\gamma_m |z-z'|}$$

$$\phi_m(\rho) = J_1(\beta_m \rho) H_0^{(1)}(\beta_m a) - J_0(\beta_m a) H_1^{(1)}(\beta_m \rho)$$

$$A_m = 2(\pi\beta_m)^{-2} [(1 - J_0^2(\beta_m b))/J_0^2(\beta_m a)]$$

and

$$\gamma_m = (K_z^2 - \beta_m^2)^{\frac{1}{2}}$$

with β_m being the cut-off wavenumber of a TM_{0m} mode and $\eta = 120\pi/\sqrt{\varepsilon}\ \Omega$ is the intrinsic wave impedance of the interior region.

In the exterior region $\rho > b$, one has

$$H_\phi(\rho,z) = \frac{-iK_0 b}{\eta_0} \int_{-d}^{d} E_z(b, z') \, G_0(\rho; z, z') \, dz' \qquad (2.29)$$

where

$$G_0(\rho;z,z') = -(\pi b)^{-1} \int_0^{\infty} \frac{H_1^{(1)}(u\rho)}{u H_0^{(1)}(u\rho)} \cos[\alpha(z - z')] d\alpha$$

and

$$u = (K_0^2 - \alpha^2)^{\frac{1}{2}} = i(\alpha^2 - K_0^2)^{\frac{1}{2}}$$

$$\eta_0 = 120\pi\ \Omega$$

An exact integral equation for the aperture field can be obtained from (2.28) and (2.29) and the boundary conditions at the aperture $|z| \leq d$ and $\rho = b$ as

$$\int_{-d}^{d} E_z(b,z')\,[G_c(b;z,z') + \varepsilon^{-1}\, G_0(b;z,z')]\,dz' = \frac{i\eta}{2\pi\, K_z b^2}\exp(iK_z z) \tag{2.30}$$

The solution for this equation may not be simple, and it depends usually on the approximations involved. For the axially slotted waveguide, it is possible to formulate a similar integral equation. However, because of the different limitations and dimensions, the solution may not be easily feasible as in the case of the circumferential slot.

In the next Chapter a totally different approach for solving the problem of hollow and axially slotted waveguides is attempted. Based on the knowledge of the different propagating modes in the slotted waveguide as presented in Sec. (2.3) in conjunction with a scattering technique, a closed-form formula for the field on the aperture is obtained.

It is shown that the technique could be extended to multi-slot loadings as well as to other structures of interest such as the coaxial waveguide. A comprehensive analysis of this problem will be presented in a later Chapter.

CHAPTER III

FIELD SOLUTION ON THE APERTURE OF A HOLLOW SLOTTED WAVEGUIDE

3.1. Introduction

The ultimate aim of any antenna structure is to radiate (receive) the electromagnetic power in a prescribed manner from certain directions in space . To this end the distribution of the field on the surface of the antenna is of prime importance since the knowledge of this field gives the external field everywhere in the space (the uniqueness theorem).

Thus in order to investigate the form of the radiation from a slotted waveguide, the electric field on the slot has to be known. This electric field will vary according to several factors such as the type of excitation, the slot width and orientation, and the dimension of the waveguide.

In this Chapter an attempt is made to solve for the tangential electric field on a narrow axial slot on the surface of a hollow waveguide, due to an incident dominant TE_{11} mode. For simplicity the slot is assumed to be long compared to the wavelength; such that no coupling between modes (TE and TM) may occur.

Extending the technique presented in Section (2.3) to cover any azimuthal slot location one may solve for different modes supported by the structure. Based on these modes a scattering problem is then formulated at the interface between the solid and the slotted sections of the waveguide. With the enforcement of the boundary conditions on the metallic walls of the structure a closed-form formula for the tangential electric field on the aperture is obtained. The solution is then extended to waveguide sections with a set of two identical slots,symmetric with

respect to the origin (i.e. 180° apart), but arbitrarily located on the guide surface. It is of interest to note that because of the highly localized nature of the field of each slot, as evident from the results of this thesis (Sec. 3.6 and Sec. 4.6) and also reported in reference [38], the result may also be extended to several successive slotted sections. This allows a solution of problems such as the periodically slotted leaky wave structures, or the penetration of an external field into an interrupted shielded cable.

3.2. Propagation Constant for Axially Slotted Hollow Waveguide 'Arbitrary Slot Location'

Consider an axially slotted waveguide as shown in Fig. 3.1 with the slot location shifted an angle α from the reference angle $\phi = 0$, the slot angle being $2\phi_0$ and semi-infinite in length.

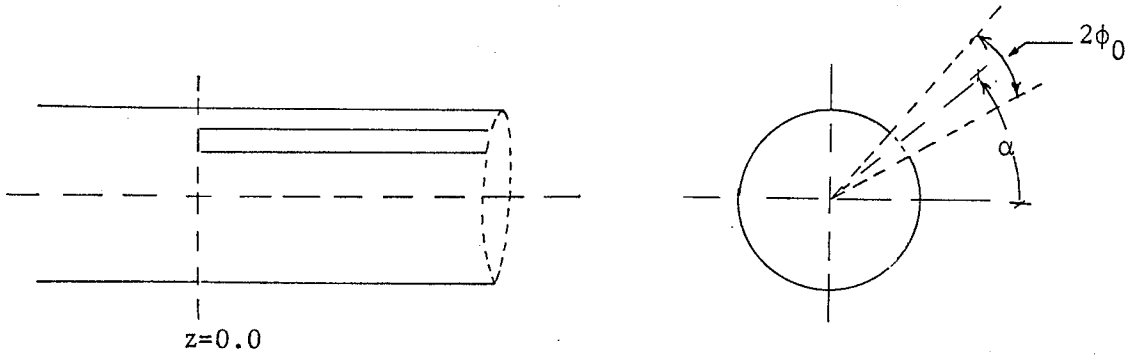

Fig. 3.1 Axially slotted waveguide with arbitrary slot location

Application of equation (2.20) for the TE_{11} case in the slotted region for the slot conductance G_s yields

$$G_s = \frac{\int_{\alpha-\phi_0}^{\alpha+\phi_0} d\phi \int_{\alpha-\phi_0}^{\alpha+\phi_0} d\phi' \quad E_\phi(a,\phi) \quad G''(a;\phi,\phi') \quad E_\phi(a,\phi')}{\left| \int_{\alpha-\phi_0}^{\alpha+\phi_0} h''_{z1} \, E_\phi \, (a,\phi) d\phi \right|^2} \tag{3.1}$$

with

$$G''(a;\phi,\phi') = \mathrm{Re}\ \{ \sum_{n=0}^{\infty} \vec{Y}_n''(a)\ \ h_{zn}''(\phi')\ \ h_{zn}''(\phi)\}$$

$$h_{zn}''(\phi) = \sqrt{\frac{\varepsilon_n}{2\pi}}\ \cos n\phi$$

and

$$\vec{Y}_n''(a) = \frac{K_\rho}{j\omega\mu a}\ \frac{H_n^{(1)}(K_\rho a)}{H_n^{(1)\prime}(K_\rho a)}$$

Since $h_{zn}''(\phi)$ is real, then

$$G''(a;\phi,\phi') = h_{zn}''(\phi)\ h_{zn}''(\phi')\ \cdot\ \mathrm{Re}\ \{\vec{Y}_n''(a)\}$$

But

$$\mathrm{Re}\ \{\vec{Y}_n''(a)\} = \frac{1}{2}[\vec{Y}_n''(a) + \vec{Y}_n''^{*}(a)] = \frac{2}{\pi\omega\mu a^2}\ \frac{1}{|H_n^{(1)\prime}(K_\rho a)|^2}$$

Therefore

$$G''(a;\phi,\phi') = \sum_{n=0}^{\infty} \frac{2}{\pi\omega\mu a^2}\ \frac{1}{|H_n^{(1)\prime}(K_\rho a)|^2}\ \frac{\varepsilon_n}{2\pi}\ \cos n\phi\ \ \cos n\phi' \qquad (3.2)$$

It is now recalled that the expression (3.1) is stationary with respect to the variation of the aperture field about its true value (Sec. 2.3.4).

Thus instead of the exact aperture field, one may use the static aperture field, modified by a factor $\cos\alpha$ (to take into account the reduced field intensity as one moves away from the location of the maximum field). Accordingly E_ϕ is given by [37] and [38] :

$$E_\phi(\phi) = \frac{\cos\alpha}{\sqrt{1 - \left(\frac{\phi-\alpha}{\phi_0}\right)^2}} \tag{3.3}$$

Using (3.2) and (3.3) in equation (3.1) one finds

$$G_s = \frac{1}{\pi\omega\mu a^2} \sum_{n=0}^{\infty} \frac{\varepsilon_n}{|H_n^{(1)'}(k_\rho a)|^2} \frac{\int_{\alpha-\phi_0}^{\alpha+\phi_0} \frac{\cos n\phi\, d\phi}{\sqrt{1-[(\phi-\alpha)/\phi_0]^2}} \int_{\alpha-\phi_0}^{\alpha+\phi_0} \frac{\cos n\phi\, d\phi}{\sqrt{1-[(\phi''-\alpha)/\phi_0}}}{\left| \int_{\alpha-\phi_0}^{\alpha+\phi_0} \frac{\cos\phi}{\sqrt{1-[(\phi-\alpha)/\phi_0]^2}} d\phi \right|^2} \tag{3.4}$$

Now, consider the integral

$$I(n) = \int_{\alpha-\phi_0}^{\alpha+\phi_0} \frac{\cos n\phi\, d\phi}{\sqrt{1-[(\phi-\alpha)/\phi_0]^2}} \tag{3.5}$$

Introducing the change of variables $u = \phi - \alpha$, $I(n)$ becomes

$$I(n) = \int_{-\phi_0}^{\phi_0} \frac{\cos n(u+\alpha)}{\sqrt{1-(u/\phi_0)^2}} du$$

$$= \cos n\alpha \int_{-\phi_0}^{\phi_0} \frac{\cos nu}{\sqrt{1-(u/\phi_0)^2}} du - \sin n\alpha \int_{-\phi_0}^{\phi_0} \frac{\sin nu}{\sqrt{1-(u/\phi_0)^2}} du$$

let $\chi = u/\phi_0$, thus

$$I(n) = \cos(n\alpha)\cdot\phi_0 \int_{-1}^{1} \frac{\cos(\chi \quad n\phi_0)}{\sqrt{1-\chi^2}} d\chi - \sin(n\alpha)\cdot\phi_0 \int_{-1}^{1} \frac{\sin(\chi \quad n\phi_0)}{\sqrt{1-\chi^2}} d\chi \tag{3.6}$$

In the Appendix [C] it is shown that the second term of the right side vanishes, while the first term yields

$$I(n) = \cos n\alpha \quad \phi_0 \quad \pi J_0(n\phi_0) \tag{3.7}$$

Accordingly, (3.4) becomes

$$G_s = \frac{1}{\pi\omega\mu a^2} \sum_{n=0}^{\infty} \frac{\varepsilon_n}{|H_n^{(1)'}(K_\rho a)|^2} \cdot \left(\frac{\cos n\alpha}{\cos\alpha} \frac{J_0(n\phi_0)}{J_0(\phi_0)}\right)^2 \qquad (3.8)$$

This gives the value of the conductance for an axial slot shifted by an angle α from the reference location $\phi = o$. It is worth noticing that as α approaches 90° the value of the conductance approaches infinity. It is shown in the following analysis that the slot susceptance also approaches infinity as α approaches 90°. This means that the slot is, in effect, a short circuit, i.e. is not seen by the wave. Accordingly it has no effect on the internal field. This is in agreement with the experimental results [36] and with physical reasonings since the azimuthal surface current at this location is identically zero, and hence is never interrupted by the presence of the slot. Another way of looking at this result is to consider the power radiated through the slot given by $V_1^2 G_s$. Although G approaches infinity, the slot voltage V_1 approaches zero and in the limit the power radiated is zero as is evident from equation (D-12) together with (D-14) of Appendix [D]. This again is consistent with the previous argument and with the results of this thesis where it is shown in Tables (3-1) - (3-3) that the value of δ approaches zero as α approaches 90°. This indicates that the system has minimal disturbance as the slot location α approaches 90°.

Now, having investigated the slot conductance, we proceed to evaluate the slot susceptance. Application of equation (D-20) of Appendix [D] for the case of a single slot yields

$$j B_s = -j\omega\varepsilon \left(\frac{K_\rho}{K_0}\right)^2 \quad 2\ln(2/\phi_0)/\cos^2\alpha \qquad (3.9)$$

Introducing the values of the conductance and susceptance obtained in this section into equation (2.19) one may obtain values of δ_m (as defined by equation (2.7)) for any TE_{1m} mode as

$$\delta_m = \frac{(X_{1m})^2}{(X_{1m})^2 - 1} \{X_s' + jR_s'\} \qquad (3.10)$$

where X_{1m} are the roots of $J_1'(z) = 0$ and

$$X_s' = \frac{-X_s}{(\omega\mu a/K_\rho)} \quad , \quad R_s' = \frac{-R_s}{(\omega\mu a/K_\rho)}$$

with

$$X_s = \frac{B_s}{G_s^2 + B_s^2} \quad , \quad R_s = \frac{G_s}{G_s^2 + B_s^2}$$

Using (2.7) and (2.9) the propagation constant in both z and ρ direction is completely determined. Tables 3.1, 3.2, 3.3 and 3.4 give some computed values of both δ and γ, which are discussed in the following Section.

3.2.1. Numerical Results for the Propagation Constant

Equation (3.10) is solved for several slot locations and different slot widths. Some of the results are shown in Tables 3.1 - 3.4 below

TABLE 3.1. Computer values of δ and γ for different slot locations α. First mode ($X_{11}' = 1.841$)$\cdot \phi_0 = 5°$, $a/\lambda_0 = 0.5$

Location α	δ Real	δ Imag.	$\gamma\lambda_0$ Real	$\gamma\lambda_0$ Imag.
0°	0.1174 E 0	- 0.2558 E-1	0.4080 E-1	-0.4913 E 1
20°	0.1057 E 0	- 0.1740 E-1	0.2747 E-1	-0.4931 E 1
30°	0.9085 E-1	- 0.1121 E-1	0.1749 E-1	-0.4954 E 1
45°	0.6100 E-1	- 0.5470 E-2	0.8323 E-2	-0.5000 E 1
60°	0.3047 E-1	- 0.2878 E-2	0.4271 E-2	-0.5045 E 1
75°	0.8137 E-2	- 0.9090 E-3	0.1323 E-2	-0.5079 E 1

TABLE 3.2. Value for δ and γ for different slot locations α. First mode $(X'_{11} = 1.841)$ $\phi_0 = 3°$. $a/\lambda_0 = 0.5$

Location α	δ		$\gamma\lambda_0$	
	Real	Imag.	Real	Imag.
0°	0.1021 E 0.0	-0.1920 E-1	0.3024 E-1	-0.4937 E1
20°	0.9153 E-1	-0.1297 E-1	0.2025 E-1	-0.4953 E1
30°	0.7842 E-1	-0.8324 E-2	0.1285 E-1	-0.4973 E1
45°	0.5255 E-1	-0.4054 E-2	0.7126 E-2	-0.5013 E1
60°	0.2626 E-1	-0.2140 E-2	0.3164 E-2	-0.5052 E1
75°	0.7018 E-2	-0.6769 E-3	0.9850 E-3	-0.5080 E1

TABLE 3.3. Values for δ and γ for different slot locations α. First mode $(X'_{11} = 1.8412)$, $\phi_0 = 2°$ $a/\lambda_0 = 0.5$

Location α	δ		$\gamma\lambda_0$	
	Real	Imag.	Real	Imag.
0°	0.9249 E-1	-0.1567 E-1	0.2447 E-1	-0.4952 E1
20°	0.8267 E-1	-0.1055 E-1	0.1634 E-1	-0.4967 E1
30°	0.7071 E-1	-0.6756 E-2	0.1036 E-1	-0.4985 E1
45°	0.4734 E-1	-0.3287 E-2	0.4946 E-2	-0.5021 E1
60°	0.2305 E-1	-0.1736 E-2	0.2562 E-2	-0.5056 E1
75°	0.6326 E-2	-0.5498 E-3	0.7996 E-3	-0.5081 E1

TABLE 3.4. Values for δ and γ for different modes $\alpha = 0.0$ $\phi_0 = 5°$ $a/\lambda_0 = 0.5$

X_{1m}	δ		$\gamma\lambda_0$	
	Real	Imag.	Real	Imag.
1.8412	0.1174 E0	-0.2559 E-1	0.4080 E-1	-0.4913 E1
5.3314	0.2953 E-1	-0.6665 E-2	0.8687 E 1	-0.1645 E-1
8.5363	0.1815 E-1	-0.3824 E-2	0.1591 E2	-0.8223 E-2
11.706	0.1326 E-1	-0.2495 E-2	0.2258 E2	-0.5180 E-2
14.863	0.1051 E-1	-0.1706 E-2	0.2907 E2	-0.3490 E-2

It is apparent from these tables that, for any fixed slot location, the attenuation constant increases with the slot width. As an example for a waveguide of $a/\lambda_0 = 0.5$ and a fixed slot location, the attenuation constant increased from $0.0244\,Np/\lambda_0$ to $0.0408\,Np/\lambda_0$ as the slot width increases from 4° to 10°. This simply indicated a higher loss of energy due to the radiation through the wider slot. It is also clear from these tables that as the slot location moves from a maximum tangential field of $\phi = 0.0°$, the attenuation constant decreases. Again considering the waveguide dimension $a/\lambda_0 = 0.5$, the attenuation constant for a slot width of 6° decreases from $0.0302\,Np/\lambda_0$ to $0.00316\,Np/\lambda_0$ as the slot moves from its initial location at $\alpha = 0°$ to $\alpha = 60°$. That is, the attenuation constant decreases by a factor of 10 within a 60° change in the slot location. Both results are physically expected ones. Since, due to the nature of the field configuration for the TE_{11} mode in the waveguide, the slot field decays as one moves away from the $\phi = 0.0°$ location. Thus, the radiated field decreases with increasing slot location. Harrington's

technique , although appearing quite general, does not yield accurate results except for slot locations $\alpha = 0^{o}$ or 180^{o}. This is possibly because the field expansion of both internal and external fields in the radial direction as assumed by Harrington is incomplete. These assumed fields,as given by equs. (2.3) and (2.5), should be extended to cover all possible ρ-variations. this means one must introduce an extra infinite summation over the roots of Bessel and Hankel functions. When the slot is at $\alpha = 0^{o}$ or 180^{o} its disturbance to the ρ-component of the field is,however,minimal (see Fig. 3.2). In this case a single summation over the azimuthal variations as given by (2.3) and (2.5) is sufficient for accurate results. This argument is further pursued to test cases where the presence of the slot has little effect on the radial field component. When α is close to 90^{o},good results were obtained using Harrington's technique that compares favourably with the results obtained by the extended Goldstone and Oliner's technique. This is in agreement with the present discussion,since at such locations the slot has very little effect on the field inside the waveguide. For this reason Goldstone et al technique, as extended in

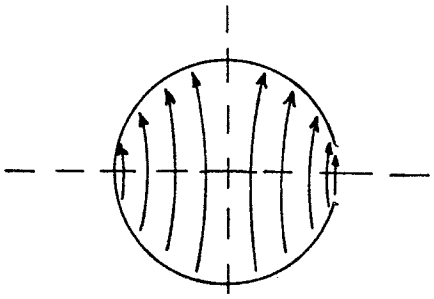

Fig. 3.2 TE_{11} field inside axially slotted waveguide.

this Section to cover any arbitrary slot location along the guide surface, seems to be superior to Harrington's method. The technique,however, has its shortcomings. It is valid only for narrow slots, and may not be easily modified for considering the interaction among several slots distributed azimuthally on the waveguide surface. This is due to the fact that the

analysis of the combined susceptance becomes extremely difficult. In the next Section this particular difficulty, however, is overcome for the special case of two symmetrically located slots. The problem in this case becomes easier due to the symmetry of the surface azimuthal current at the discontinuities as shown in Appendix [D].

3.3. Two Identical and Symmetrically Located Slots

In the previous Section, the propagation constant of propagating modes supported by a waveguide section with an arbitrarily located single slot has been solved in order to determine the surface field distribution and hence the radiation pattern in free space. It may be advantageous, however, to utilize more than one slot per section of the waveguide since this provides a wider range of flexibility and control over the radiation pattern. The problem is quite involved since the interaction between various slots has to be considered. In this Section an attempt is made to obtain the propagation constant of a waveguide section with two identical slots symmetrically located with respect to the origin. The analysis takes into consideration the possible interaction between the slots and yields results that compare favourably with that of the single available result for double slots using Harrington's technique (at $\alpha = 0.0^{\circ}$ and 180°).

3.3.1. Propagation Constant for Two Identical Slots Symmetrically Located With Respect to the Origin

The work of Section (3.2) for the propagation constant of a slotted waveguide (one axial slot) can be readily extended to cover the case of a waveguide with two identical narrow axial slots separated by 180° as shown in Fig. 3.3 .

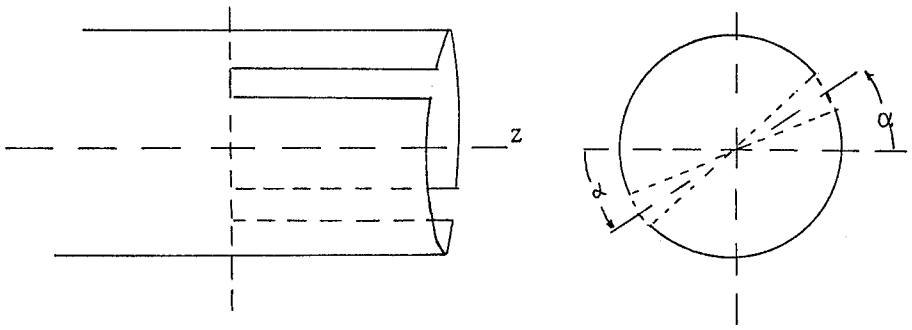

Fig. 3.3
Double slotted waveguide

As before, to determine the propagation constant of the structure, one has to calculate the impedance or the admittance of two slots combined together so that they represent the terminating load when effecting the transmission line representation of the slotted waveguide as seen in Fig. 3.4 .

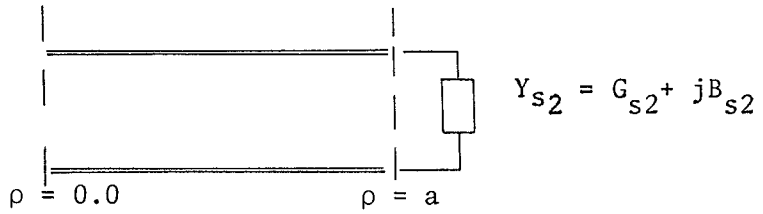

Fig. 3.4 Transmission line representation of the symmetrically double slotted waveguide.

Referring to Appendix [D], the conductance G_{s2} of two slots located as shown in Fig. (3.2) is given by equation (D-13) as

$$G_{s2} = P/\left| \int_{\alpha-\phi_0}^{\alpha+\phi_0} h_{z1}(a,\phi)E_{\phi}(a,\phi)ad\phi + \int_{\pi+\alpha-\phi_0}^{\pi+\alpha+\phi_0} h_{z1}(a,\phi)E_{\phi}(a,\phi)ad\phi \right|^2 \tag{3.11}$$

with

$$P = \mathrm{Re}\left\{ \sum_{n=0}^{\infty} \vec{Y}_n \left(\int_{\alpha-\phi_0}^{\alpha+\phi_0} E_\phi(a,\phi) h_{zn}(a,\phi)\, a\,d\phi + \int_{\pi+\alpha-\phi_0}^{\pi+\alpha+\phi_0} E_\phi(a,\phi) h_{zn}(a,\phi)\, a\,d\phi \right)^2 \right\}$$

(3.12)

$$h_{zn}(a,\phi) = \sqrt{\frac{\varepsilon_n}{\pi}} \cos n\phi$$

and

$$\mathrm{Re}\{\vec{Y}_n\} = \frac{2}{\pi\omega\mu a^2} \frac{1}{\left|H_n^{(1)'}(K_\rho a)\right|^2}$$ as established in Sec. (3.2.)

Assuming the slot field to vary as [App. D].

$$E_\phi(a,\phi) = E_0 \cos\alpha / \sqrt{1 - \left(\frac{\phi-\alpha}{\phi_0}\right)^2} \qquad (3.13)$$

Substituting (3.13) in (3.12) one finds

$$P = \frac{1}{\pi\omega\mu a^2} \sum_{n=0} \frac{E_0^2}{\left|H_n^{(1)'}(K_\rho a)\right|^2} \frac{\varepsilon_n}{\pi} \left\{ \cos\alpha \int_{\alpha-\phi_0}^{\alpha+\phi_0} \frac{\cos n\phi\, a\,d\phi}{\sqrt{1 - \left(\frac{\phi-\alpha}{\phi_0}\right)^2}} + \right.$$

$$\left. + \cos(\pi + \alpha) \int_{\pi+\alpha-\phi_0}^{\pi+\alpha+\phi_0} \frac{\cos n\phi\, a\,d\phi}{\sqrt{1 - \left[\frac{\phi - (\pi+\alpha)}{\phi_0}\right]^2}} \right\} \qquad (3.14)$$

The integration in (3.14) is identical to I(n) of eq. (3.5) whose result is given by (3.7). Accordingly P could be written as

$$P = \frac{1}{\pi\omega\mu a} \sum_{n=0}^{\infty} \frac{E_0^2}{\left|H_n^{(1)'}(K_\rho a)\right|^2} \frac{\varepsilon_n}{\pi} (\phi_0 \pi \cos\alpha)^2 \left[(\cos n\alpha - \cos n(\pi+\alpha)) \right.$$

$$\left. J_0(n\phi_0) \right]^2$$

$$= \frac{4}{\pi\omega\mu a} \frac{E_0^2}{\pi} (\phi_0 \pi \cos\alpha)^2 \sum_{n=1,3,5} \frac{2}{\left|H_n^{(1)'}(K_\rho a)\right|^2} \left[\cos n\alpha\, J_0(n\phi_0)\right]^2$$

(3.15)

The denominator of eq. (3.11) may be written as

$$\left|\int_{\alpha-\phi_0}^{\alpha+\phi_0} \frac{1}{\sqrt{\pi}} \cos\phi \frac{\cos\alpha\, E_0}{\sqrt{1-(\frac{\phi-\alpha}{\phi_0})^2}}\, ad\phi + \int_{\pi+\alpha-\phi_0}^{\pi+\alpha+\phi_0} \frac{1}{\sqrt{\pi}} \cos\phi \cdot \frac{\cos(\pi+\alpha)\, ad\phi}{\sqrt{1-(\frac{\phi-(\pi+\alpha)}{\phi_0})^2}}\right|^2$$

$$= \frac{a}{\pi} \quad 4(\pi\ \phi_0\ \cos\alpha)^2\ F_0 \cdot \cos^2\alpha\ J_0^2(\phi_0) \qquad (3.16)$$

where the integration is carried out similar to (3.14). Combining (3.15) and (3.16) yields the slot conductance for two slots as

$$G_{s2} = \frac{1}{\pi\omega\mu a^2} \sum_{n=1,3,5} \frac{2}{|H_n^{(1)'}(K_\rho a)|^2} \left(\frac{\cos n\alpha}{\cos\alpha} \cdot \frac{J_0(n\phi_0)}{J_0(\phi_0)}\right)^2 \qquad (3.17)$$

This gives the value of the combined conductance of two slots with the interaction between them taken into consideration. For the susceptance, one may employ equation (D-20) of Appendix [D] where the value of B_{s2} is given by

$$B_{s2} = -\frac{\omega\ \varepsilon\ \pi}{M_z \cdot 2\cos^2\alpha}$$

$$= -\omega\varepsilon\left(\frac{K_\rho}{K_0}\right)^2 \ln\ (2/\phi_0)/\cos^2\alpha \qquad (3.18)$$

Now, the value of δ_m as defined by equation (2.7) is readily obtained by application of eq. (3.10). Thus

$$\delta_m = \frac{X_{1m}^2}{X_{1m}^2 - 1}\,(X_{s2}' + jR_{s2}') \qquad (3.19)$$

where

X_{1m} is the root of $J_1'(Z) = 0$

$$X'_{s_2} = \frac{X_{s2}}{-\omega\mu a/K_\rho} \quad , \qquad R'_{s_2} = \frac{R_{s2}}{-\omega\mu a/K_\rho} \tag{3.20}$$

with

$$X_{s2} = \frac{G_{s_2}}{B^2_{s_2} + G^2_{s2}} \quad , \qquad R_{S2} = \frac{G_{s2}}{R^2_{s2} + B^2_{s2}}$$

Using (2.7) and (2.9), the propagation constant in the slotted section of the waveguide is completely determined. Tables 3.5 and 3.6 below give computed values for δ and γ for different slot locations and slot widths. In the next Section these results are presented and are discussed.

3.3.2. Numerical Results for the Propagation Constant of a Double Slotted Waveguide Section

The value of δ is evaluated using equation (3.19) for several locations of the two-slot set and for different slot widths. Some of these results are given in Tables 3.5 - 3.6 . The results shown in these tables follow the general trend noticed before in Sec. (3.2.1). The attenuation constant drops considerably as the slot location moves far from the location $\phi = 0$. Considering for instance the case of $\phi_0 = 2°$ and $a/\lambda_0 = 0.5$ (Table 3.5), the attenuation constant drops from 0.0480 Np/λ_0 to 0.00387 Np/λ_0 within $60°$. This is about an 8% reduction of the attenuation constant. It is also apparent that as the slot width increases, the attenuation constant increases indicating a higher power radiation into the free space. It may also be of interest to investigate the relation between the results of a single and of double slots. One such case is the case of a single slot located at an angle α and a two-slot-set one at $\phi = \alpha$ and the other at $\phi = 180° + \alpha$. The related

information is tabulated in Table 3.7 for the slot width of 4^{o} .

TABLE 3.5. Computed values of δ and γ for arbitrary located two slot set 180° apart. TE_{11} mode. $\phi_0 = 2^{o}$, $a/\lambda_0 = 0.5$

Location α	δ		$\gamma\lambda_0$	
	Real	Imag.	Real	Imag.
0.0	0.18595 E 0	-0.2842 E-1	0.48012 E-1	-0.48006 E1
30	0.14135 E 0	-0.1393 E-1	0.2266 E-1	-0.4874 E1
45	0.9459 E-1	-0.7230 E-2	0.1131 E-1	-0.4948 E1
60	0.4743 E-1	-0.2576 E-2	0.3876 E-2	-0.5021 E1
75	0.1274 E-1	-0.2492 E-3	0.3644 E-3	-0.5072 E1

TABLE 3.6. Computed values of δ and γ for arbitrary located two-slot set 180° apart. TE_{11} mode, $\phi_0 = 5°$, $a/\lambda_0 = 0.5$

Location α	δ		$\gamma\lambda_0$	
	Real	Imag.	Real	Imag.
0.0	0.23679 E 0	-0.4662 E-1	0.8220 E-1	-0.47139 E1
30	0.18153 E 0	-0.2312 E-1	0.3891 E-1	-0.48079 E1
45	0.1218 E 0	-0.1199 E-1	0.1919 E-1	-0.4905 E1
60	0.61197 E-1	-0.4252 E-2	0.6472 E-2	-0.5000 E1
75	0.1646 E-1	-0.4105 E-3	0.6020 E-3	-0.5067 E1

TABLE 3.7. Comparison between the results of a single and double slot set $\phi_0 = 4°$

α	a/λ_0	Case	Attenuation constant α_z Np/λ_0	Ratio $(\alpha_{z_2}/\alpha_{z_1})$
0.0°	0.5	single slot	0.0244	1.967
		double slot	0.0480	
	0.35	single slot	0.0826	2.32
		double slot	0.192	
60°	0.5	single slot	0.00256	1.51
		double slot	0.00387	
	0.5	single slot	0.00794	1.55
		double slot	0.01233	

It is evident that two identical slots, symmetrically located, do not radiate twice as much power as a single slot located at the same location. The ratio of the radiated power for a two-slot-set is dependent on several factors, such as the frequency of operation and the slot location. In addition, Table 3.8 shows that the radiation power also depends on the slot width.

TABLE 3.8. Comparison between single and double slots $a/\lambda_0=0.5$ $\alpha = 0.0$

Slot width	case	Attenuation constant α_z Np/λ_0	Ratio $(\alpha_{z_2}/\alpha_{z_1})$
4°	single slot	0.0244	1.967
	double slot	0.0480	
10°	single slot	0.0408	2.014
	double slot	0.0822	

One, however, can see certain trends in the available results. The interaction between the slots enhances the radiation when the slots are located around $\alpha = 0$, or when a/λ_0 approaches its cut-off value, for wider slots, the interaction causes a higher radiation power than for that of narrow slots, and a single slot of width $2\phi_0$ radiates less power than two slots each of width ϕ_0. For example, referring to Table 3.8 , two slots of width 4° give an attenuation constant of .048 Np/λ_0, while a single slot of width 10° yields 0.0408Np/λ_0. That is two slots would disturb the system more than one slot even if its width is more than their combined widths. These are general trends, which could be used initially for design purposes. However, every single case should be investigated individually. In a later Section the field variation on the slot surface due to their mutual interaction will be studied, where other features will be investigated.

Now, having studied the propagation constant of a single as well as of double symmetrical slots, one may carry on to the next Section

where a modal expansion of the field with unknown coefficients on both sections of the waveguide is assumed. When these coefficients are determined, one may solve for the field on the slot surface(s).

3.4. Formulation of the Scattering Problem

In Sections (3.2) and (3.3) the wavenumbers of the different propagating modes supported by the slotted structure has been obtained. Using these wavenumbers, the field in the slotted section of the waveguide can be expanded into summation of infinite modes with an unknown sets of coefficients in a way similar to the modes in the normal closed waveguide. However, these modes differ from the familiar closed waveguide modes in that they are not completely orthogonal to each other in the sense defined in reference [52]. They are, however, orthogonal in the azimuthal direction. The field in each section of the waveguide is expanded in its respective modes, each with a set of unknown coefficients. When the field components are matched on the plane separating the closed and the slotted waveguide, one may get two infinite sets of equations for two infinite sets of unknown coefficients. Further, each one of these equations contains infinite summations on both sides. Employing the orthogonality relations among the modes, one may considerably reduce their complexity. It is shown that the problem is reduced to two infinite independent matrix equations in two sets of unknown coefficients. When these equations are truncated after an appropriate number of terms, the unknown coefficients on both sides of the waveguide may be obtained. In a later Section these coefficients will be used to completely determine the slot field.

3.4.1. Field Representation Interior to the Waveguide

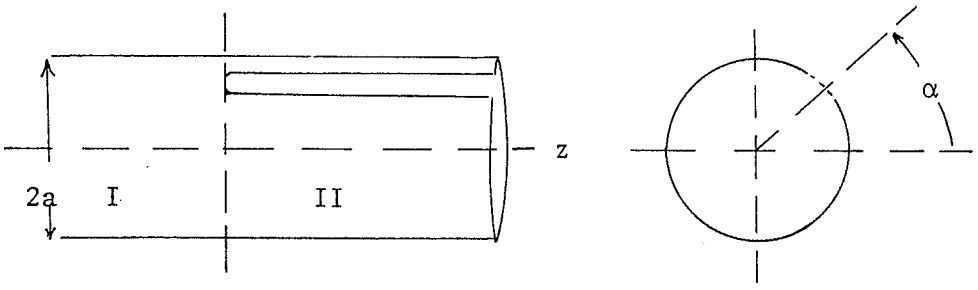

Fig. 3.5 Axially slotted waveguide with arbitrary slot location

Let the incident field in region I of Fig. 3.5 be the dominant TE_{11} mode with a wave function in the form

$$\psi^i = T \quad J_1\left(\frac{X_{11}}{a}\rho\right) \cos\phi \exp(j\theta_{11}z) \tag{3.21}$$

where T is the intensity of the incident field, a is the waveguide radius and a time variation $e^{-j\omega t}$ is assumed. Let the wave function of the reflected field in the same region (region I) be represented by

$$\psi^r = T \sum_{p=0}^{\infty} \sum_{q=1}^{\infty} B_{pq} J_\rho(X_{pq}\rho/a) \cos p\phi \exp(-j\theta_{pq}z) \tag{3.22}$$

where p and q are integers and

B_{pq} S are unknown constants to be determined

X_{pq} is the qth root of $J_p'(Z) = 0$.

and

$$\theta_{pq}^2 + (X_{pq}/a)^2 = K_0^2 \tag{3.23}$$

Let the transmitted field in region II be represented by the wave function

$$\phi = T \sum_{r=0}^{\infty} \sum_{s=0}^{\infty} A_{rs} J_r(K_{\rho_{rs}}\rho) \cos r\phi \exp(-\gamma_{rs}z) \tag{3.24}$$

where r and s are integers and

$$\gamma_{rs} = \alpha_z - j\beta_z = -\sqrt{K_{\rho_{rs}}^2 - K_0^2} = -j\sqrt{(\frac{2\pi}{\lambda_0})^2 - K_\rho^2} \tag{3.25}$$

A_{rs}'s are constants to be determined

$K_{\rho_{rs}}$'s are known for each mode and for each slot location according to the analysis of Sections (3.2) or (3.3).

The field components on both regions can be derived from the relation [30]

$$E_\rho = -\frac{1}{\rho}\frac{\partial F}{\partial \phi} \qquad H_\rho = \frac{-1}{j\omega\mu}\frac{\partial^2 F}{\partial \rho \partial z}$$

$$E_\phi = \frac{\partial F}{\partial \rho} \qquad H_\phi = \frac{-1}{j\omega\mu}\frac{1}{\rho}\frac{\partial^2 F}{\partial \phi \partial z} \tag{3.26}$$

$$E_z = 0 \qquad H_z = \frac{-1}{j\omega\mu}(\frac{\partial^2}{\partial z^2} + K_0^2)F$$

where F stands for any of the TE wave functions of eqns. (3.21), (3.22) and (3.24).

It is convenient to introduce the mode functions, e^I_{nm} and h^I_{nm} for region I, and e^{II}_{nm} and h^{II}_{nm} for region II, defined for region I as:

$$e^I_{nm} = e^I_{\phi_{nm}} \vec{a}_\phi + e^I_{\rho_{nm}} \vec{a}_\rho \tag{3.27}$$

$$h^I_{nm} = h^I_{\phi_{nm}} \vec{a}_\phi + h^I_{\rho_{nm}} \vec{a}_\rho$$

where $\vec{a}_\phi$ and $\vec{a}_\rho$ are unit vectors in ϕ and ρ directions respectively and

$$e^{I}_{\phi_{nm}} = \frac{X_{nm}}{a} J_n'(X_{nm}\,\rho/a)\cos n\phi$$

$$e^{I}_{\rho_{nm}} = \frac{n}{\rho} J_n(X_{nm}\,\rho/a) \quad \sin n\phi$$

$$h^{I\mp}_{\phi_{nm}} = \mp \frac{j\theta_{nm}}{j\omega\mu} e^{I}_{\rho_{nm}} \tag{3.28}$$

$$h^{I\mp}_{\rho_{nm}} = \pm \frac{j\theta_{nm}}{j\omega\mu} e^{I}_{\phi_{nm}}$$

where the upper and lower signs hold for $e^{-j\theta_{nm}z}$ and $e^{+j\theta_{nm}z}$ respectively.

In region II

$$e^{II}_{nm} = e^{II}_{\phi_{nm}} \vec{a}_\phi + e^{II}_{\rho_{nm}} \vec{a}_\rho$$

$$h^{II}_{nm} = h^{II}_{\phi_{nm}} \vec{a}_\phi + h^{II}_{\rho_{nm}} \vec{a}_\rho \tag{3.29}$$

with

$$e^{II}_{\phi_{nm}} = K_{\rho_{nm}} J_n'(K_{\rho_{nm}}\,\rho) \quad \cos n\phi$$

$$e^{II}_{\rho_{nm}} = \frac{n}{\rho} J_n(K_{\rho_{nm}}\,\rho) \sin n\phi$$

$$h^{II}_{\phi_{nm}} = -\frac{\gamma_{nm}}{j\omega\mu} e^{II}_{\rho_{nm}} \tag{3.30}$$

$$h^{II}_{\rho_{nm}} = \frac{\gamma_{nm}}{j\omega\mu} e^{II}_{\phi_{nm}}$$

With these mode representations and with the aid of (3.21), (3.22), (3.24) and (3.26), the field components in regions I and II can be written as

Region I

$$E_{\phi}^{I} = T \quad e_{\phi_{11}}^{I} \exp(j\theta_{11}z) + T \sum_{p=0} \sum_{q=1} B_{pq} \, e_{\phi_{pq}}^{I} (-j\theta_{pq}z)$$

$$E_{\rho}^{I} = T \quad e_{\rho_{11}}^{I} \exp(j\theta_{11}z) + T \sum_{p=0} \sum_{q=1} B_{pq} \, e_{\rho_{pq}}^{I} \exp(-j\theta_{pq}z)$$

$$H_{\phi}^{I} = T \quad h_{\phi_{11}}^{I+} \exp(j\theta_{11}z) + T \sum_{p=0} \sum_{q=1} B_{pq} \, h_{\phi_{pq}}^{I-} \exp(-j\theta_{pq}z)$$

$$H_{\rho}^{I} = T \quad h_{\rho_{11}}^{I+} \exp(j\theta_{11}z) + T \sum_{p=0} \sum_{q=1} B_{pq} \, h_{\rho_{pq}}^{I-} \exp(-j\theta_{pq}z) \qquad (3.31)$$

Region II

$$E_{\phi}^{II} = T \sum_{r=0} \sum_{s=1} A_{rs} \, e_{\phi_{rs}}^{II} \exp(-\gamma_{rs}z)$$

$$E_{\rho}^{II} = T \sum_{r=0} \sum_{s=1} A_{rs} \, e_{\rho_{rs}}^{II} \exp(-\gamma_{rs}z)$$

$$H_{\phi}^{II} = T \sum_{r=0} \sum_{s=1} A_{rs} \, h_{\phi_{rs}}^{II} \exp(-\gamma_{rs}z) \qquad (3.32)$$

$$H_{\rho}^{II} = T \sum_{r=0} \sum_{s=1} A_{rs} \, h_{\rho_{rs}}^{II} \exp(-\gamma_{rs}z)$$

These equations give the field everywhere in regions I and II in terms of the modes e_{nm} and h_{nm}. Certain mathematical relations among these modes hold. These relations will be needed later to reduce the complexity of the analysis in order to set the unknown coefficients in a form that can be numerically solved. The next Section is devoted to the task of developing these relations.

3.4.2. Mode Orthogonality

In this subsection, some of the basic mathematical relationships among the modes given by (3.28) and (3.30) will be established. These relationships will constitute the main frame of the scattering formulations to be followed in the next Section. Consider the integral relation

$$M^{\mp}_{\substack{nm\\pq}} = \int_S (e^I_{nm} \times h^{I\mp}_{pq}) \cdot \vec{a}_z \, ds \tag{3.33}$$

where S is the cross sectional area of the waveguide, $\vec{a}_z$ is a unit vector in the z-direction. Substituting (3.27) in (3.33) gives

$$M^{\mp}_{\substack{nm\\pq}} = \int_s (e^I_{\phi_{nm}} \vec{a}_\phi + e^I_{\rho_{nm}} \vec{a}_\rho) \times (h^{I\mp}_{\phi_{pq}} \vec{a}_\phi + h^{I\mp}_{\phi_{pq}}) \cdot \vec{a}_z \, ds$$

$$= \int_{\rho=0}^{a} \int_{\phi=0}^{2\pi} (e^I_{\rho_{nm}} h^I_{\phi_{pq}} - e^I_{\phi_{nm}} h^I_{\rho q}) \rho \, d\rho d\phi$$

which upon substitution of the mode functions (3.28) gives

$$M^{\mp}_{\substack{nm\\pq}} = \int_{\rho=0}^{a} \int_{\phi=0}^{2\pi} \left(-\frac{X_{nm}}{a} J_n'(X_{nm}\rho/a) \cos n\phi \mp \frac{j\theta_{pq}}{j\omega\mu} \frac{X_{pq}}{a} J_p'(X_{pq}\rho/a) \cos p\phi \right.$$

$$\left. + \frac{n}{\rho} J_n(X_{nm}\rho/a) \sin n\phi \mp \frac{j\theta_{pq}}{j\omega\mu} \frac{p}{\rho} J_p(X_{pq}\rho/a) \sin p\phi \right) \rho \, d\rho d\phi$$

where again the upper and the lower signs hold for $e^{-j\theta_{nm}z}$ and $e^{j\theta_{nm}z}$ respectively. Now using the orthogonality relationship

$$\int_0^{2\pi} \cos n\phi \cos p\phi \, d\phi = \int_0^{2\pi} \sin n\phi \sin p\phi d\phi = 0 \quad n \neq p$$

$$= \pi \quad n = p \neq 0$$

$$= 2\pi \quad n = p = 0$$

(3.34)

$$M^{\mp}_{\substack{nm \\ pq}} = M^{\mp}_{\substack{nm \\ q}} = \mp \frac{2\pi}{\varepsilon_n} \frac{j\theta_{nq}}{j\omega\mu} \int_{\rho=0}^{2\pi} \left(\frac{n^2}{\rho} J_n(X_{nm}\rho/a)\ J_n(X_{nq}\rho/a)\right.$$

$$\left. + \frac{X_{nm}}{a} \frac{X_{nq}}{a} J_n'(X_{nm}'\rho/a)\ J_n'(X_{nq}'\rho/a)\right) \rho d\rho$$

which by change of variable $y = \rho/a$ becomes

$$M^{\mp}_{\substack{nm \\ q}} = \mp \frac{2\pi}{\varepsilon_n} \frac{j\theta_{nq}}{j\omega\mu} \left\{\int_0^1 \frac{n^2}{y} J_n(X_{nm}y)\ J_n(X_{nm}y)\ dy\right.$$

$$\left. + X_{nm} X_{nq} \int_0^1 J_n'(X_{nm}y)\ J_n'(X_{nq}y)\ y\ dy\right. \qquad (3.35)$$

It is shown in Appendix[E]that the integral in (3.35) exists only for $m = q$ and is equal to [Eq. (C-9)].

$$\frac{X_{nm}^2}{2}\left(1 - \frac{1}{X_{nm}^2}\right) J_n^2(X_{nm})$$

Accordingly

$$M^{\mp}_{nm} = \int_S (e^I_{nm} \times h^{I\mp}_{pq}) \cdot \vec{a}_z\ ds$$

$$= \mp \frac{2\pi}{\varepsilon_n} \frac{j\theta_{nm}}{j\omega\mu} \frac{X_{nm}^2}{2}\left(1 - \frac{1}{X_{nm}^2}\right) J_n^2(X_{nm}) \qquad (3.36)$$

which establishes the orthogonality relation between the modes e^I and h^I.

Another relation which should prove important in later analyses is the integral:

$$N_{\substack{nm \\ pq}} = \int_S (e^I_{nm} \times h^{II}_{pq}) \cdot \vec{a}_z\ ds \qquad (3.37)$$

Following similar steps as before and using the mode functions

(3.30) and (3.28), one obtains

$$N_{\substack{nm\\pq}} = \int_{\rho=0}^{a}\int_{\phi=0}^{2\pi} \left(-\frac{X_{nm}}{a} J_n'(X_{nm}\rho/a)\cos n\phi \quad \frac{\gamma_{pq}}{j\omega\mu} \quad K_{\rho_{pq}} J_\rho(K_{\rho_{pq}}\rho)\cos p\phi \right.$$

$$\left. + \frac{n}{\rho} J_n(X_{nm}\rho/a) \quad \sin n\phi \quad \left(-\frac{\gamma_{pq}}{j\omega\mu}\right) \frac{p}{\rho} J_\rho(K_{\rho_{pq}}\rho) \cdot \sin p\phi\right)\rho d\rho d\phi$$

let again $y = \rho/a$ and using the orthogonality relation of the trigonometric functions (3.34), an equation similar to (3.35) can be obtained as

$$N_{\substack{nm\\pq}} = N_{nmq} = -\frac{2\pi}{\varepsilon_n} \quad \frac{\gamma_{nq}}{j\omega\mu} \quad \left\{\int_0^1 n^2 \quad \frac{J_n(X_{nm}y) \quad J_n(K_{\rho_{nq}} a\, y)}{y} dy \right.$$

$$\left. + X_{nm} \quad (K_{\rho_{nq}} a) \int_0^1 y\, J_n'(X_{nm}y)\, J_n'(K_{\rho_{nq}} a) dy\right\} \qquad (3.38)$$

It is shown in Appendix [E] that the integral in (3.38) exists and is equal to (eq. E-6)

$$X_{nm}^2 (K_{\rho_{nq}} a) \frac{J_n(X_{nm})\, J_n'(K_{\rho_{nq}} a)}{X_{nm}^2 - (K_{\rho_{nq}} a)^2}$$

Accordingly

$$N_{nmq} = \int_s (e_{nm}^{I} \times h_{pq}^{II}) \cdot \vec{a}_z \, ds$$

$$= -\frac{2\pi}{\varepsilon_n} \quad \frac{\gamma_{nq}}{j\omega\mu} \quad X_{nm}^2 (K_{\rho_{nq}} a) \quad \frac{J_n(X_{nm})\, J_n'(K_{\rho_{nq}} a)}{X_{nm}^2 - (K_{\rho_{nq}} a)^2} \qquad (3.39)$$

which establishes the second important relation of this Section. Finally, consider the integral:

$$Q_{\substack{nm\\pq}}^{\mp} = \int_s (h_{nm}^{I\mp} \times e_{pq}^{II}) \cdot \vec{a}_z \, ds \qquad (3.40)$$

From (3.28) we have

$$h^{I\mp}_{nm} = \mp \frac{j\theta_{nm}}{j\omega\mu} (e^{I}_{\rho_{nm}} \vec{a}_{\phi} - e^{I}_{\phi_{nm}} \vec{a}_{\rho}) \tag{3.41}$$

and from (3.30)

$$e^{II}_{pq} = \frac{j\omega\mu}{\gamma_{pq}} (h^{II}_{\rho_{pq}} \vec{a}_{\phi} - h^{II}_{\phi_{pq}} \vec{a}_{\rho}) \tag{3.42}$$

Using (3.42) and (3.41) in (3.40) one obtains

$$\begin{aligned} Q^{\mp}_{\substack{nm \\ pq}} &= \mp \frac{j\theta_{nm}}{j\omega\mu} \frac{j\omega\mu}{\gamma_{pq}} \int_s (e^{I}_{\rho} \vec{a}_{\phi} - e^{I}_{\phi} \vec{a}_{\rho}) \times (h^{II}_{\rho} \vec{a}_{\phi} - h^{II}_{\phi} \vec{a}_{\rho}) \cdot \vec{a}_z \, ds \\ &= \mp \frac{j\theta_{nm}}{\gamma_{pq}} \int_s (e^{I}_{\rho_{nm}} h^{II}_{\phi_{pq}} - e^{I}_{\phi_{nm}} h^{II}_{\rho_{pq}}) \vec{a}_z \cdot \vec{a}_z \, ds \\ &= \mp \frac{j\theta_{nm}}{\gamma_{pq}} \int_s (e^{I}_{nm} + h^{II}_{pq}) \cdot \vec{a}_z \, ds \end{aligned} \tag{3.43}$$

But by virtue of (3.37), the integral

$$\int_s (e^{I}_{nm} \times h^{II}_{pq}) \cdot \vec{a}_z \, ds = N_{nmq}$$

Substituting back in (3.43) one finds

$$\begin{aligned} Q^{\mp}_{\substack{nm \\ pq}} = Q^{\mp}_{nmq} &= \int (h^{I\mp}_{nm} \times e^{II}_{pq}) \cdot \vec{a}_z \, ds \\ &= \mp \frac{j\theta_{nm}}{\gamma_{nq}} N_{nmq} \\ &= \mp \frac{2\pi}{\varepsilon_n} \frac{j\theta_{nm}}{j\omega\mu} X^2_{nm} (K_{\rho_{nq}} a) \frac{J_n(X_{nm}) J'_n(K_{\rho_{nq}} a)}{X^2_{nm} - (K_{\rho_{nq}} a)^2} \end{aligned} \tag{3.44}$$

Relations (3.36), (3.39) and (3.44) are the basic formulas which will be used for the formulation of the scattering problem as discussed in the

following Section.

3.4.3. Mode Matching

With the aid of the field representation in the slotted waveguide of Fig. 3.2 and the orthogonal relations among the mode functions, the field components on both sides can be determined by matching its tangential components at the interface between the slotted and the solid sections of the waveguide (i.e. at the plane $z = 0$). The technique used here is similar to that used in reference [49], and is based on the integral relation [52].

$$\int (e_m \times h_n) \cdot \vec{a}_z \, ds = \delta_{mn}$$

which is valid for any two non-degenerate modes in a waveguide of uniform cross-section provided that e_m and h_n are normalized. This relation has been established before for the TE_{11} mode in Sec. (3.4.2).

Consider the two identities:

$$\int_s (E^I \times h^I_{nm})\Big|_{z=0} \cdot \vec{a}_z \, ds = \int_s (E^{II} \times h^I_{nm})\Big|_{z=0} \cdot \vec{a}_z \, ds \qquad (3.45)$$

and

$$\int_s (H^I \times e^I_{nm})\Big|_{z=0} \cdot \vec{a}_z \, ds = \int_s (H^{II} \times e^I_{nm})\Big|_{z=0} \cdot \vec{a}_z \, ds \qquad (3.46)$$

which are based on the fact that at the plane $z = 0$, the tangential electric field E_t and the tangential magnetic field H_t are continuous, i.e.

$$E^I_t = E^{II}_t$$

and

$$H_t^I = H_t^{II}$$

Consider first equation (3.45), the L.H.S. could be written as:

$$\int_s E^I \times h_{mn}^{I\mp}\Big|_{z=0} \cdot \vec{a}_z \, ds = T \int_s (e_{11}^I \times h_{nm}^{I\mp} + \sum_{p=0} \sum_{q=1} B_{pq} e_{pq}^I \times h_{nm}^{I\mp}) \cdot \vec{a}_z ds$$

But from (3.36) we have

$$\int_s e_{11}^I \times h_{nm}^{I\mp}\Big|_{z=0} \cdot \vec{a}_z \, ds = \mp \pi \frac{j\theta_{11}}{j\omega\mu} \frac{X_{11}^2}{2} \left(1 - \frac{1}{X_{11}^2}\right) J_1^2(X_{11})$$

$$= M_{11}^{\mp}$$

and

$$\int_s e_{pq}^I \times h_{nm}^{I\mp}\Big|_{z=0} \cdot \vec{a}_z \, ds = \mp \pi \frac{j\theta_{nm}}{j\omega\mu} \frac{X_{nm}^2}{2} \left(1 - \frac{1}{X_{nm}^2}\right) J_n^2(X_{nm})$$

$$= M_{nm}^{\mp}$$

Thus

$$\int_s (E^I \times h_{nm}^{I\mp})\Big|_{z=0} \cdot \vec{a}_z \, ds = T M_{11}^{\mp} + T B_{nm} M_{nm}^{\mp} \qquad (3.47)$$

Similarly the R.H.S. of equation (3.45) gives:

$$\int_s (E^{II} \times h_{nm}^{I\mp})\Big|_{z=0} \cdot \vec{a}_z \, ds = T \sum_{r=0} \sum_{s=1} A_{rs} \int e_{rs}^{II} \times h_{nm}^{I\mp}\Big|_{z=0} \cdot \vec{a}_z \, ds$$

$$= -T \sum_{s=1} A_{ns} Q_{nsm}^{\mp} \qquad (3.48)$$

where in the last formula, use has been made of equation (3.44). Combining (3.47) and (3.48), equation (3.45) could finally be written as:

$$M_{11}^{\mp} + B_{nm} M_{nm}^{\mp} = - \sum_{s=1}^{\infty} A_{ns} Q_{nsm}^{\mp} \qquad (3.49)$$

where $Q^{\mp}_{nsm}$ and $M^{\mp}_{mn}$ are given by (3.44) and (3.36) respectively.

In a similar way an expansion of the L.H.S. of equation (3.46) gives

$$\int_s (H^I \times e^I_{nm})\Big|_{z=0} \cdot \vec{a}_z \, ds = \int_s (T\, h^{I+}_{11} + T \sum_{p=0} \sum_{q=1} B_{pq} h^{I-}_{pq}) \times e^I_{nm} \cdot \vec{a}_z \, ds$$

Again using (3.36) gives

$$\int_s (H^I \times e^I_{nm})\Big|_{z=0} \cdot \vec{a}_z \, ds = - T M^+_{11} - T B_{nm} M^-_{nm}$$

$$= T M^-_{11} - T B_{nm} M^-_{nm}$$

where $-M^+_{11}$ is replaced by M^-_{11}

The R.H.S. of equation (3.46) gives

$$\int_s H^{II} \times e^I_{nm}\Big|_{z=0} \cdot \vec{a}_z \, ds = T \sum_{r=0} \sum_{s=1} A_{rs} \int_s h^{II}_{rs} \times e^I_{nm}\Big|_{z=0} \cdot \vec{a}_z \, ds$$

which by virtue of (3.39) yields

$$= -T \sum_s A_{ns} N_{nms}$$

Therefore, collecting terms and substituting back in (3.46) gives

$$-M^-_{11} + B_{nm} M^-_{nm} = \sum_s A_{ns} N_{nms} \qquad (3.50)$$

where again M_{nm} is given by (3.36) and N_{nms} is given by (3.39).

Equations (3.49) and (3.50) are solved together for the unknowns B_{nm}'s and A_{ns}'s. It is to be understood that allowing both n, m and s to take discrete values 1, 2, 3,... up to infinity, an infinite number of matrix equations is generated. Each matrix containing an infinite number of terms. However, it is shown in the following Section

that to determine the tangential electric field on the slot, it is sufficient to consider only the case $n = 1$ together with a few terms in each matrix. For the $n \neq 1$ cases the excitation terms are zero, but the respective coefficients are not required for the slot field due to the orthogonality enforced on the slot field. Although it is not our interest to find the field inside the waveguide, it could, however, be determined once the slot field is known using the reciprocity theorem in a procedure similar to that used by Silver[35].

3.4.4. Solution of the Unknown Coefficients

Consider the case $n = 1$ of equation (3.49) and (3.50). It is more instructive to write them in a matrix form as:

$$\begin{bmatrix} 1 \\ 0 \\ \vdots \\ 0 \end{bmatrix} + \begin{bmatrix} B_{11} \\ B_{12} \\ \\ B_{1K} \end{bmatrix} = - \begin{bmatrix} \bar{Q}_{111}/\bar{M}_{11} & \bar{Q}_{121}/\bar{M}_{11} & \cdots & \bar{Q}_{1K1}/\bar{M}_{11} \\ \bar{Q}_{112}/\bar{M}_{12} & \bar{Q}_{122}/\bar{M}_{12} & \cdots & \bar{Q}_{1K2}/\bar{M}_{12} \\ \vdots & \vdots & & \vdots \\ \bar{Q}_{11K}/\bar{M}_{1K} & \bar{Q}_{12K}/\bar{M}_{1K} & \cdots & \bar{Q}_{1KK}/\bar{M}_{1K} \end{bmatrix} \begin{bmatrix} A_{11} \\ A_{12} \\ \vdots \\ A_{1K} \end{bmatrix} \tag{3.51}$$

In a similar way equation (3.50) may be written as

$$-\begin{bmatrix} 1 \\ 0 \\ \vdots \\ 0 \end{bmatrix} + \begin{bmatrix} B_{11} \\ B_{12} \\ \vdots \\ B_{1K} \end{bmatrix} = \begin{bmatrix} \bar{N}_{111}/\bar{M}_{11} & \bar{N}_{112}/\bar{M}_{11} & \cdots & \bar{N}_{11K}/\bar{M}_{11} \\ \bar{N}_{121}/\bar{M}_{12} & \bar{N}_{122}/\bar{M}_{12} & \cdots & \bar{N}_{12K}/\bar{M}_{12} \\ \vdots & \vdots & & \vdots \\ \bar{N}_{1K1}/\bar{M}_{1K} & \bar{N}_{1K2}/\bar{M}_{1K} & \cdots & \bar{N}_{1KK}/\bar{M}_{1K} \end{bmatrix} \begin{bmatrix} A_{11} \\ A_{12} \\ \vdots \\ A_{1K} \end{bmatrix} \tag{3.52}$$

These matrix equations (3.51) and (3.52) are obtained by truncating equations (3.49) and (3.50) after an appropriate number of terms K. Subtracting (3.52) from (3.51) cancels the unknown coefficients B_{1n} (n = 1,2,K) and gives

$$\begin{bmatrix} 2 \\ 0 \\ \vdots \\ 0 \end{bmatrix} = - \begin{bmatrix} \frac{Q^-_{111} + N_{111}}{M^-_{11}} & \frac{Q^-_{121} + N_{112}}{M^-_{11}} & \cdots & \frac{Q^-_{1K1} + N_{11K}}{M^-_{11}} \\ \frac{Q^-_{112} + N_{121}}{M^-_{12}} & \frac{Q^-_{122} + N_{122}}{M^-_{12}} & \cdots & \frac{Q^-_{1K2} + N_{12K}}{M^-_{12}} \\ \vdots & \vdots & \vdots & \\ \frac{Q^-_{11K} + N_{1K1}}{M^-_{1K}} & \frac{Q^-_{12K} + N_{1K2}}{M^-_{1K}} & \cdots & \frac{Q^-_{1KK} + N_{1KK}}{M^-_{1K}} \end{bmatrix} \begin{bmatrix} A_{11} \\ A_{12} \\ \vdots \\ A_{1K} \end{bmatrix} \tag{3.53}$$

The solution of this equation gives the unknown transmission coefficients (A_{11}, A_{12}, .. A_{1K}) in the slotted sections of the waveguide. Substituting them back in (3.52) or (3.51) the scattering coefficients B_{11}, B_{12} ... B_{1K} in the solid section can readily be obtained. Here, one may stress the fact that physically B_{11} actually represents the reflection coefficient of the electric field at the interface between the slotted and the solid section, while A_{11} represents the transmission coefficient at this plane.

A computer program is prepared to calculate both the coefficients A_{1n} and B_{1n} as given by (3.53) and either of (3.51) or (3.52). Tables 3.9 - 3.12 give some of the computed results for a single slot while Tables 3.13 - 3.15 give corresponding values for double symmetrically located slots.

TABLE 3.9. The Transmission and Reflection Coefficients for TE_{11} Mode

$\phi_0 = 2^o$ $\alpha = 0.0^o$ K* = 8 $a/\lambda_0 = 0.5$

Scattering Coeff. in Region II Real	Imag.	Reflect. Coeff. in Region I Real	Imag.	n
0.9944 E 0.0	-0.3637 E-03	0.1378 E-01	0.2574 E-02	1
-0.7875 E-02	-0.6589 E-02	0.9705 E-02	-0.3452 E-02	2
0.3705 E-02	0.1938 E-02	-0.4116 E-02	0.5086 E-03	3
-0.2278 E-02	-0.9547 E-03	0.2448 E-02	-0.8993 E-04	4
0.1604 E-02	0.5819 E-03	-0.1675 E-02	-0.1778 E-04	5
-0.1293 E-02	-0.4084 E-03	-0.1241 E-02	0.5063 E-04	6
0.9443 E-03	0.2895 E-03	0.9676 E-03	-0.5981 E-04	7
-0.7637 E-03	-0.2220 E-03	0.7820 E-03	0.6047 E-04	8

* K is the number of terms in the summation (3.49) or (3.50) before truncating

TABLE 3.10. Transmission and Reflection Coefficients for TE_{11} Mode

$\phi_0 = 2^o$ $\alpha = 45^o$ K = 8 $a/\lambda_0 = 0.5$

Scattering Coefficients in Region II Real	Imag.	Reflect. Coeff. in Region I Real	Imag.	n
0.9962 E 0.0	-0.1440 E-03	0.6902 E-02	0.5198 E-03	1
-0.4211 E-02	-0.2872 E-02	0.4582 E-02	-0.2240 E-02	2
0.1918 E-02	0.7642 E-03	-0.2000 E-02	0.4755 E-03	3
-0.1184 E-02	-0.3541 E-03	0.1201 E-02	-0.1767 E-03	4
-0.1098 E-03	-0.3971 E-04	-0.8263 E-03	0.8137 E-04	5
0.2181 E-05	0.6619 E-06	0.6140 E-03	-0.4158 E-04	6
-0.4418 E-06	-0.1150 E-06	-0.4790 E-03	0.2226 E-04	7
-0.3048 E-06	-0.7096 E-07	0.3882 E-03	-0.1195 E-04	8

TABLE 3.11. Transmission and Reflection Coefficients for TE_{11} Mode

$\phi_0 = 5^o$ $\alpha = 0.0^o$ K = 8 a/λ_0=0.5

Scattering Coefficient in Region II	Reflection Coefficient in Region I	n
0.9938 E 0.0 -0.2308 E-03	0.1769 E-01 0.4317 E-02	1
-0.9782 E-02 -0.9018 E-02	0.1280 E-01 -0.3755 E-02	2
0.4676 E-02 0.2758 E-02	-0.5360 E-02 0.3648 E-03	3
-0.2893 E-02 -0.1392 E-02	0.3173 E-02 0.5574 E-04	4
0.2038 E-02 -0.8632 E-03	-0.2166 E-02 -0.1400 E-03	5
-0.1617 E-02 -0.6152 E-03	0.1602 E-02 0.1518 E-03	6
0.1203 E-02 0.4397 E-03	-0.1247 E-02 -0.1445 E-03	7
-0.9758 E-03 -0.3401 E-03	0.1007 E-02 0.1324 E-03	8

TABLE 3.12. Transmission and Reflection Coefficients for TE_{11} Mode

$\phi_0 = 5^o$ $\alpha = 0.0^o$ K = 6 a/λ_0=0.5

Scattering Coefficient in Region II	Reflection Coefficients in Region I	n
0.9938 E 0.0 -0.2330 E-03	0.1769 E-01 0.4314 E-02	1
-0.9784 E-02 -0.9019 E-02	0.1280 E-01 -0.3755 E-02	2
0.4678 E-02 0.2759 E-02	-0.5354 E-02 0.3652 E-03	3
-0.2895 E-02 -0.1393 E-02	0.3172 E-02 0.5544 E-04	4
0.0240 E-02 0.8644 E-03	-0.2166 E-02 -0.1398 E-03	5
-0.1621 E-02 -0.6173 E-03	0.1602 E-02 0.1516 E-03	6

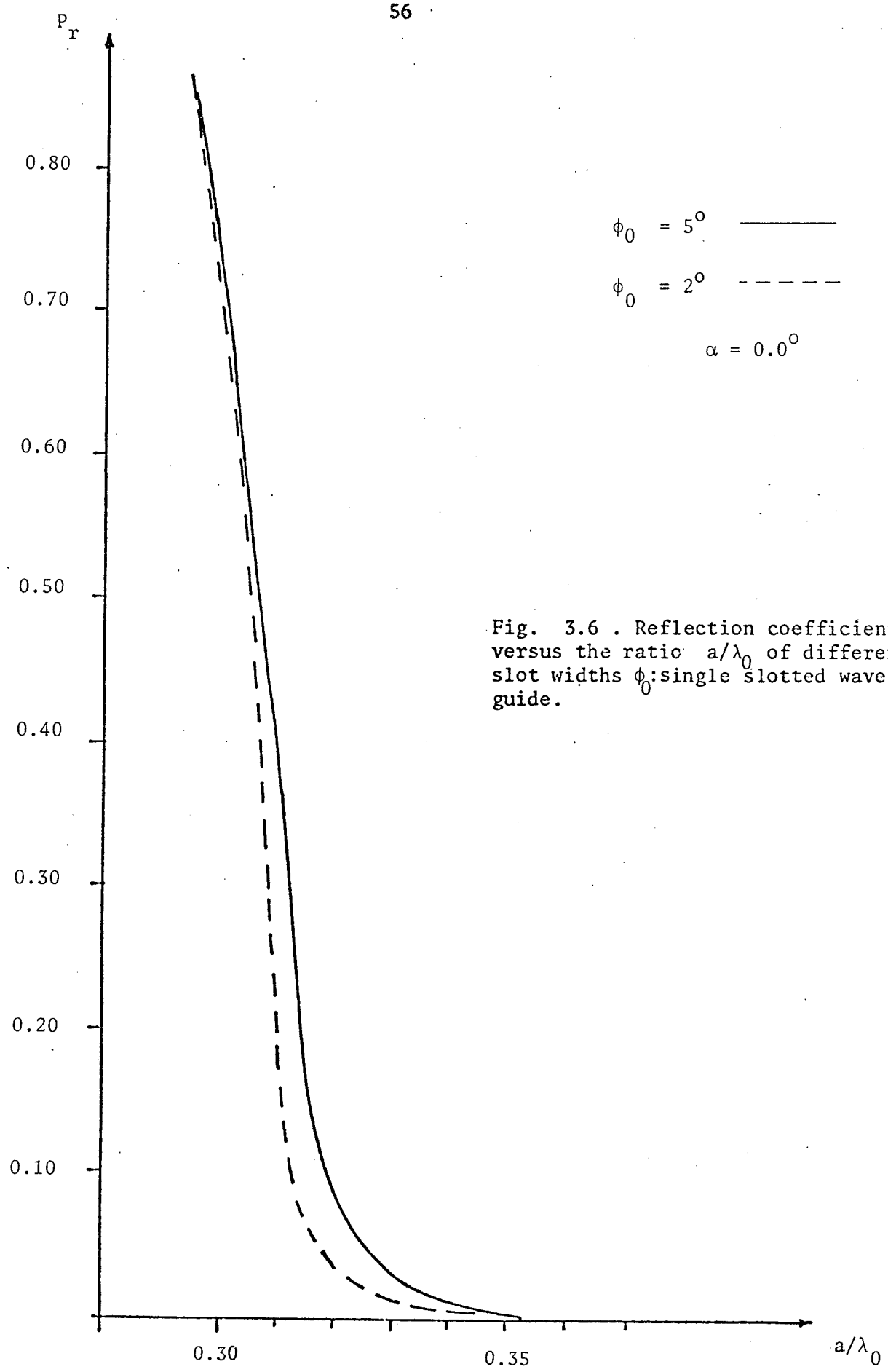

Fig. 3.6 . Reflection coefficient versus the ratio a/λ_0 of different slot widths ϕ_0:single slotted waveguide.

TABLE 3.13. Transmission and Reflection Coefficients:Two Slots 180°

Apart $\phi_0 = 2^o$ $\alpha = 0.0^o$ K = 6 $a/\lambda_0 = 0.5$

n	Transmission Coefficient Real		Image.		Reflect. Coefficient Real		Image.	
1	0.0042	E 0	-0.2028	E-2	0.2916	E-1	-0.5432	E-2
2	-0.1676	E-1	0.1339	E-1	0.2045	E-1	0.7086	E-2
3	0.7873	E-2	-0.3979	E-2	-0.8633	E-2	-0.1038	E-2
4	-0.4841	E-2	0.1966	E-2	0.5132	E-2	0.1843	E-3
5	0.3388	E-2	-0.1196	E-2	-0.3513	E-2	0.3558	E-4
6	-0.2631	E-2	0.8270	E-3	0.2603	E-2	-0.1027	E-3

TABLE 3.14. Transmission and Reflection Coefficients:Two Slots 180°

Apart $\phi_0 = 2^o$ $\alpha = 45^o$ K = 6 $a/\lambda_0 = 0.5$

n	Transmission Cofficient Real		Imag.		Reflection Coefficient Real		Imag.	
1	0.9944	E 0	0.1229	E-3	0.1415	E-1	-0.1254	E-2
2	-0.8561	E-2	0.5875	E-2	0.9461	E-2	0.4423	E-2
3	0.3920	E-2	-0.1592	E-2	-0.4104	E-2	-0.9105	E-3
4	-0.2389	E-2	0.7401	E-3	0.2461	E-2	0.3271	E-3
5	0.1673	E-2	-0.4315	E-3	-0.1691	E-2	-0.1438	E-3
6	-0.1342	E-2	0.2947	E-3	0.1256	E-2	0.6880	E-4

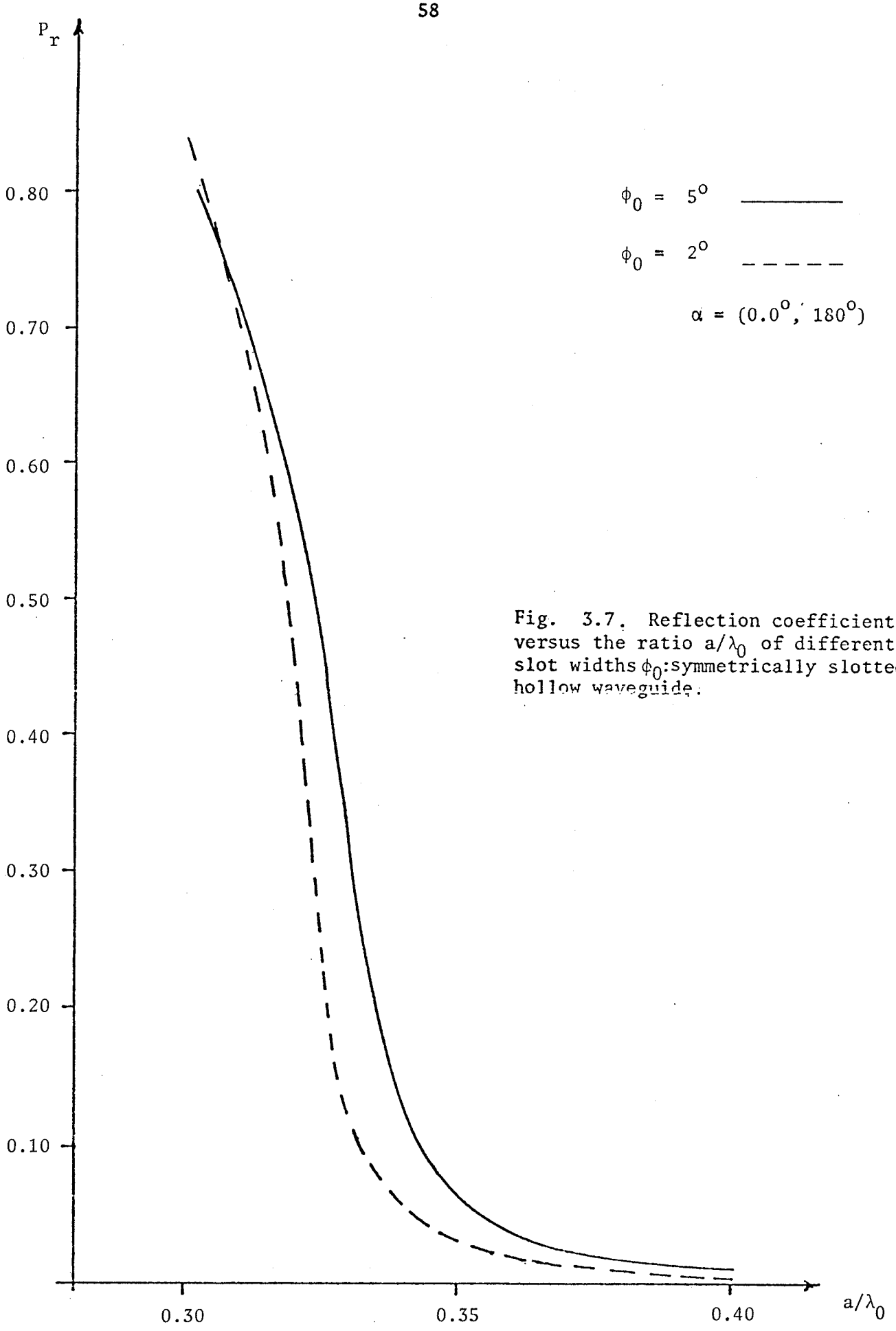

Fig. 3.7. Reflection coefficient versus the ratio a/λ_0 of different slot widths ϕ_0: symmetrically slotted hollow waveguide.

TABLE 3.15 Transmission and Reflection Coefficients: Two Slots 180° Apart

$\phi_{i0} = 5^{o}$ $\alpha = 0.0^{o}$ $K = 6$ $a/\lambda_0 = 0.5$

n	Transmission Coefficient Real		Transmission Coefficient Imag.		Reflection Coefficient Real		Reflection Coefficient Imag.	
1	0.9958	E 0	-0.3107	E-2	0.3804	E-1	-0.9417	E-2
2	-0.2124	E-1	0.1856	E-1	0.2740	E-1	0.7609	E-2
3	0.1012	E-1	-0.5771	E-2	-0.1139	E-1	-0.6910	E-3
4	-0.6254	E-2	0.2922	E-2	0.6742	E-2	-0.1471	E-3
5	-0.5415	E-2	0.6313	E-2	-0.4605	E-2	0.3092	E-3
6	0.5934	E-4	-0.3257	E-4	0.3407	E-2	-0.3276	E-3

It is of interest to point out the fact that basically the first few terms in each group (A_{1n} and B_{1n}) are sufficient to determine the field, and that the rest of the coefficients are increasingly negligible as seen from Tables 3.9 - 3.15 . This result is physically clear since higher modes are actually non-propagating and have little effect on the field.

It is also apparent from Tables 3.9 and 3.10 for the single slot or Tables 3.13 and 3.14 for double slot that the reflection coefficient decreases as the slot moves away from the position of maximum surface current. This confirms the fact that the slot effect on the internal field decreases as it moves towards smaller surface current regions[36].This has its important application in microwave measurements since it allows probe penetration into the waveguide interior with a least perturbation of the field configuration [36]. The reflection coefficient is also a function of the operating frequency as is evident from Fig. 3.6 and

3.7 . It increases rapidly as one approaches the cut-off frequency, and decays smoothly to a very small value for higher frequencies. It is also instructive to note that the presence of two slots would disturb the system (especially near the cut-off frequency) far more than what one slot would do, even if the width of the single slot is equal to the widths of the two slots combined together. Referring to Fig. 3.6 for one slot together with Fig. 3.7 for two slots, one can see that the power reflection coefficient, P_r, (which is the magnitude squared of the field reflection coefficient) due to double slots, each of width 4° (Fig. 3.7), is always higher than the corresponding power reflection coefficient of a single slot of width 10° (Fig. 3.6). For example at $a/\lambda_0=0.34$ the first curve shows a P_r of about 0.055, while the second curve shows a value of 0.014. This is about 4 times greater. It is seen, however, that at an $a/\lambda_0=0.4$ or more, which is generally the practical case, the reflection coefficient in both single and double slot cases becomes negligibly small. This seems to be the best operating frequency. However, as noticed before in Table 3.7 , the radiated power (as indicated by the value of the attenuation constant) drops sharply as the ratio a/λ_0 increases. This suggests an optimum operating point in order to achieve an acceptable P_r with reasonable power radiation in free space.

The accuracy of the numerical procedure seems acceptable. Tables 3.11 and 3.12 give results for the same slot case ($\phi_0 = 5°$ and $\alpha = 0.0$) with different numbers of terms considered before truncating equation (3.53). It is clear from these tables that the result is very stable and almost independent of the number of terms considered. The relative error (absolute error divided by the value of the coefficient)

of balancing each individual equation of the set(3.43)was calculated (not shown in the tables) and was found to vary between 10^{-5} and 10^{-6} in a single precision calculation. Different cases were examined to check the accuracy of the procedure, and the results in all cases were satisfactory and within the limit of 10^{-5} or less. This allows one to carry on to the next step to evaluate the slot field as will be discussed in the following Section.

3.5. Electric Field on the Slot

As it has been discussed earlier, the fundamental objective of this Chapter is to evaluate the electric field on the surface of the slot due to an incident TE_{11} dominant mode. Based on the scattering coefficients determined in the previous Section and with the assumption of a narrow slot, it is possible to work out a closed form formula for the tangential field on the slot. The analysis is quite general and applied to both single and double slotted waveguide sections.

For a narrow and long slot, the only tangential field that may exist on the slot is the ϕ polarized field E_ϕ [24]. From equation (3.32) and using (3.30) the electric field in the azimuthal direction of the slotted region is given by

$$E_\phi(\rho,\phi,z) = T \sum_{n=0}^{\infty} \sum_{m=1}^{\infty} A_{nm} K_{\rho_{nm}} J_n'(K_{\rho_{nm}}\rho) \cos n\phi \exp(-\gamma_{nm} z) \tag{3.54}$$

This expression is valid for both single and double slotted sections as long as the appropriate coefficients A_{nm} and $K_{\rho_{nm}}$ are used.

It has been shown by several authors [25], [37], [38], [50], however, that a reasonable representation for the ϕ variation of the

field on a narrow slot may be assumed in the form

$$E_\phi(a,\phi) = \frac{E_0}{\sqrt{1 - (\phi/\phi_0)^2}} \qquad -\phi_0 \leq \phi \leq \phi_0 \tag{3.55}$$

When the z variation and the slot location α are incorporated into (3.55), the slot field may be assumed as

$$E_\phi(a,\phi,z) = \frac{E_0(a,z)\ \cos\alpha}{\sqrt{1 - (\frac{\phi - \alpha}{\phi_0})^2}} \qquad \alpha - \phi_0 < \phi < \alpha + \phi_0 \tag{3.56}$$

where the factor $\cos\alpha$ is introduced here merely to adjust for the appropriate direction of the field as the slot location α varies between $0.0°$ and $360°$. Combining (3.54) and (3.56) gives

$$\frac{E_0(a,z)\ \cos\alpha}{\sqrt{1 - (\frac{\phi - \alpha}{\phi_0})^2}} = T \sum_{n=0}^{\infty} \sum_{m=1}^{\infty} A_{nm} K_{\rho_{nm}} J_n'(K_{\rho_{nm}} a) \cos n\phi \exp(-\gamma_{nm} z) \tag{3.57}$$

where

$$\alpha - \phi_0 < \phi < \alpha + \phi_0 \qquad \text{for single slot}$$

and

$$\left.\begin{aligned} &\alpha - \phi_0 < \phi < \alpha + \phi_0 \\ &\pi + \alpha - \phi_0 < \phi < \pi + \alpha + \phi_0 \quad \text{with } \alpha + \pi \text{ replacing } \alpha \\ &\qquad\qquad \text{in the expression (3.57)} \end{aligned}\right\} \text{for double symmetric slots}$$

Multiplying both sides by $\cos\phi$ and integrating over the slot (slots) gives

$$E_0(a,z)\ f(\alpha,\phi_0) = T \sum_{n=0}^{\infty} \sum_{m=1}^{\infty} A_{nm} K_{\rho_{nm}} J_n'(K_{\rho_{nm}} a) \exp(-\gamma_{nm} z) \int_0^{2\pi} \cos n\phi \cos\phi\, d\phi \tag{3.58}$$

Where the integration of the R.H.S. is extended over the whole waveguide wall since E_ϕ is zero at the metallic walls, and

$$f(\alpha,\phi_0) = \cos\alpha \int_{\alpha-\phi_0}^{\alpha+\phi_0} \frac{\cos\phi}{\sqrt{1 - (\frac{\phi - \alpha}{\phi_0})^2}} d\phi \qquad \text{for single slot}$$

$$= \cos\alpha \left\{\int_{\alpha-\phi_0}^{\alpha+\phi_0} \frac{\cos\phi}{\sqrt{1 - (\frac{\phi-\alpha}{\phi_0})^2}} d\phi - \int_{\pi+\alpha-\phi_0}^{\pi+\alpha+\phi_0} \frac{\cos\phi\, d\phi}{\sqrt{1 - [\frac{\phi-(\pi+\alpha)}{\phi_0}]^2}}\right\}$$

for two symmetric slots

(3.59)

The integration of the function $f(\alpha,\phi_0)$ has been dealt with before in Sec. (3.2) and was shown to be equal to (equation (3.5) and (3.7)):

$$\int_{\alpha-\phi_0}^{\alpha+\phi_0} \frac{\cos\phi}{\sqrt{1 - (\frac{\phi-\alpha}{\phi_0})^2}} = \cos\alpha \quad \phi_0 \, \pi \, J_0(\phi_0) \tag{3.60}$$

Therefore $f(\alpha,\phi_0)$ is equal to

$$f(\alpha,\phi_0) = \cos^2\alpha \quad \phi_0 \, \pi \, J_0(\phi_0) \quad \text{for single slot}$$

$$= 2 \quad \cos^2\alpha \, \phi_0 \, \pi \, J_0(\phi_0) \quad \text{for two symmetric slots} \tag{3.61}$$

The R.H.S. of equation (3.58) is equal to zero except for $n = 1$, since

$$\int_0^{2\pi} \cos n\phi \cos\phi \, d\phi = \pi \qquad n = 1$$

$$= 0 \qquad n \neq 1 \tag{3.62}$$

Using (3.61) and (3.62), equation (3.58) takes the form

$$N \quad \cos\alpha \, \phi_0 \quad J_0(\phi_0) \quad E_0(a,z) \quad \cos\alpha$$

$$= T \sum_{m=1}^{\infty} A_{nm} \, K_{\rho_{nm}} \, J_1'(K_{\rho_{1m}} a) \exp(-\gamma_{1m} z) \tag{3.63}$$

where $N = 1$ for single slot

$= 2$ for double slot

Using the value of $E_0(a,z)$ as given by (3.63) in equation (3.56), a closed form formula for the slot field is finally obtained as

$$E_\phi(a,\phi,z) = \frac{T}{\phi_0 \; J_0(\phi_0) \; N \cos\alpha} \cdot \frac{\sum_{m=1} A_{1m} K_{\rho_{1m}} J_1'(K_{\rho_{1m}} a) \exp(-\gamma_{1m} z)}{\sqrt{1 - (\frac{\phi - \alpha}{\phi_0})^2}} \tag{3.64}$$

The coefficients $A_{11}, A_{12}, \ldots A_{1K}$ are known according to the discussion of Sec. (3.4). The values of $K_{\rho_{1m}}$ and γ_{1m} are also known [Sec. (3.2) and (3.3)]. Thus equation (3.64) completely determines the slot field for either single or double symmetrically located slots.

In the following Section equation (3.64) is utilized to study the slot field. For different slot parameters some results are presented, examined and discussed.

3.6. Numerical Results for the Slot Fields

In this Section some numerical results of the slot field as a function of the distance along the guide as well as slot parameters, such as the slot width $2\phi_0$ and location α, are presented. The values of the slot field E_0 presented in this Section are such that the coefficient T of the incident wave function (3.21) equals unity. The results cover both the single and the double slot cases in accordance with equation (3.64).

The main features of the field such as the decay of its magnitude along the z direction and the reduction in its intensity as the slot location α moves from the position of maximum azimuthal surface current

(ϕ = 0.0) are clear from Fig. 3.8 and Fig. 3.11 for the single and double slots, respectively. The results also show that for any two slots of different widths, keeping other parameters equal, the field intensity on the narrower one is higher in value than the corresponding wider slot, Fig. 3.8 and Fig. 3.11 . However, it is shown later in Chapter 5 that the integration of the field on the slot surface area $\int_{slot} E_{\phi}\, ds$ is higher for the wider slot, indicating higher power radiation. This is in agreement with the results for the attenuation constant obtained previously for different slot widths as presented in Sec. 3.2 for a single slot, and in Sec. 3.3 for double slots. Thus, one may control the radiated power in different sections of space by choosing adequate combinations of slot number , length , size and location . This will be discussed in more details in Chapter 5. It is also interesting to note that the field intensity on the slot increases as we approach the cut-off frequency as is evident from Figs. 3.9 , 3.10 and 3.12 . This result, again, is in agreement with the discussion of Sec. (3.4.4) and with the results of Table 3.7 Sec. (3.3.2). It shows that as a/λ_0 decreases, the attenuation constant increases indicating higher power radiation in the space.

Figs. 3.13 and 3.14 compare the fields of a two-slot set, located at $\phi - \alpha$ and $\phi = \pi + \alpha$, with that of a single slot located at $\phi = \alpha$. This is equivalent to studying the change of the field of one slot when another slot is introduced on the waveguide surface diagonally across from the first one. The analysis reveals the important and interesting result that the slot field is more or less localized especially, as shown in (3.14), where the ratio a/λ_0 is larger (i.e. at higher frequencies). For example at $a/\lambda_0 = 0.5$ and $\alpha = 60°$, the field changes

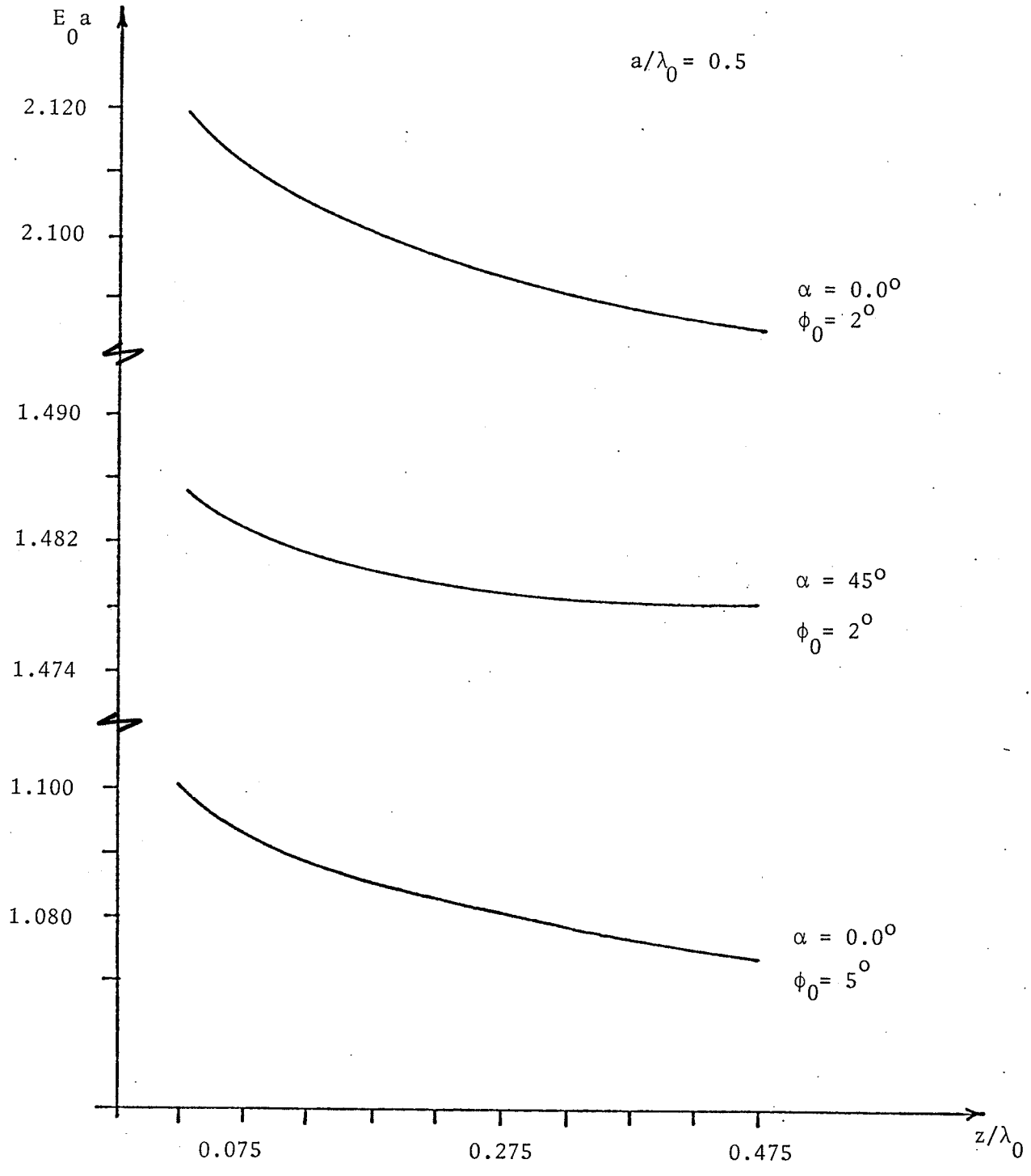

Fig. 3.8 . The slot tangential field E_0 versus the distance z along the slot for single slotted hollow waveguide. Different slot parameters.

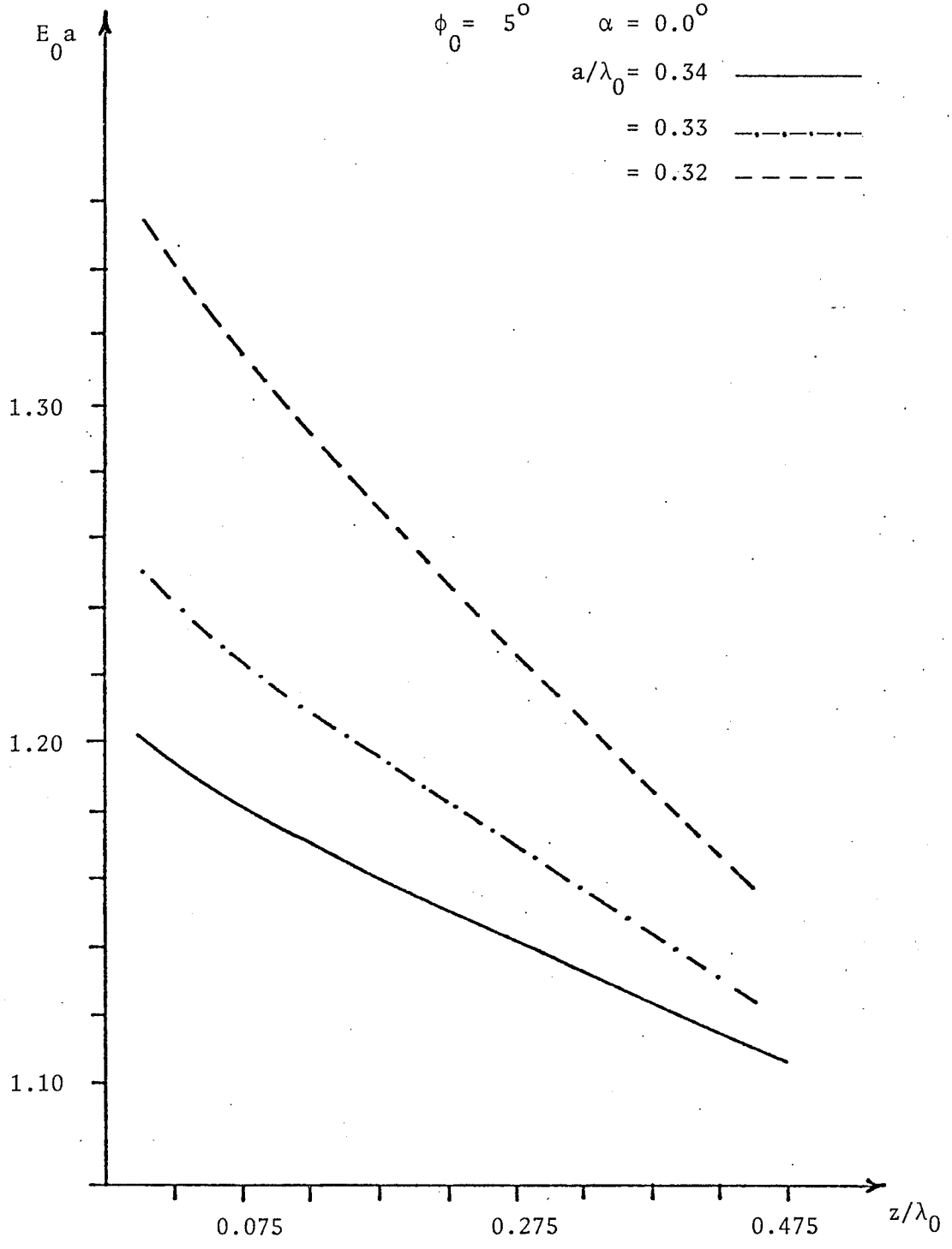

Fig. 3.9 . The slot tangential field E_0 versus the distance z along the slot for single slotted hollow waveguide. Different operating frequency.

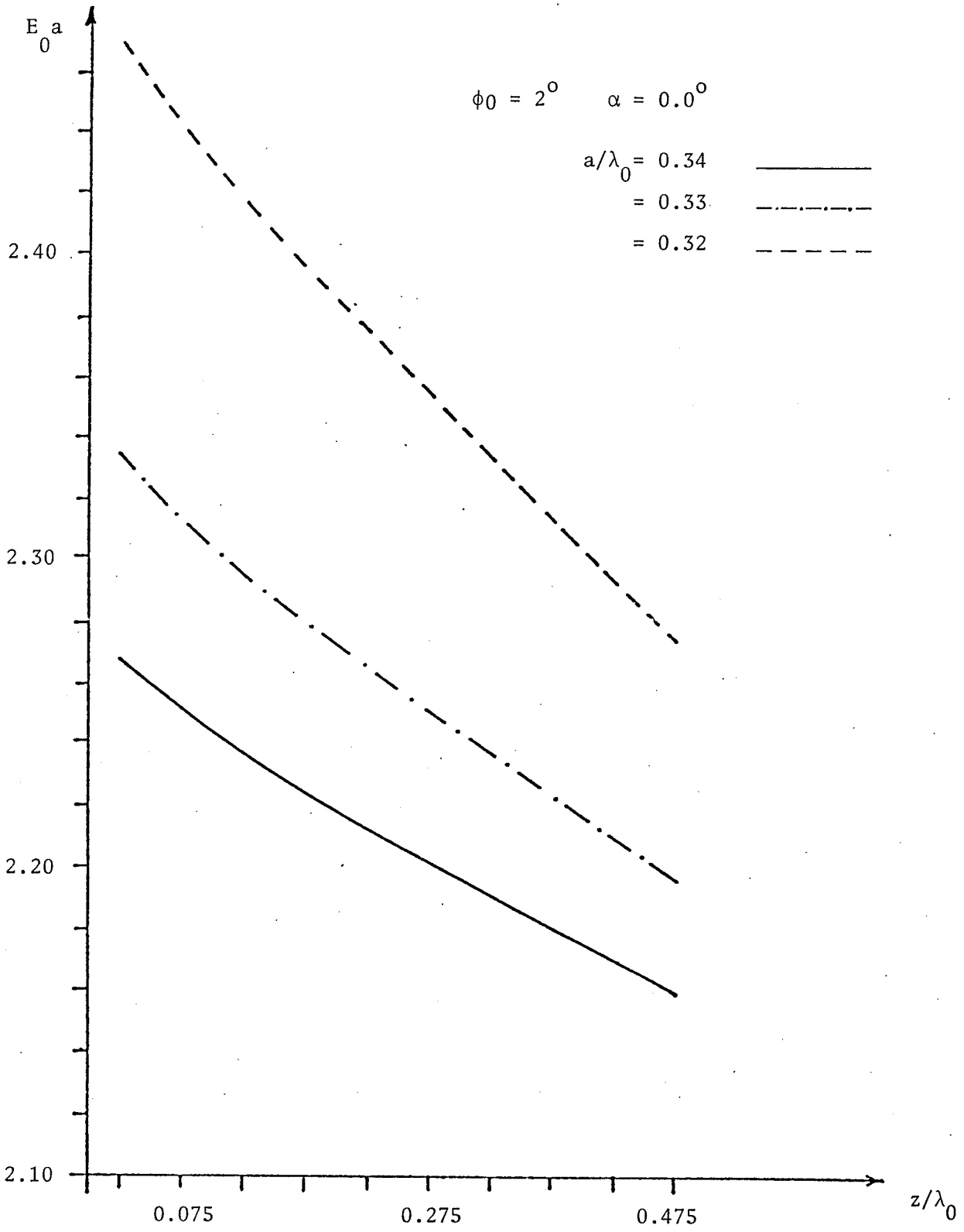

Fig. 3.10 . The slot tangential field E_0 versus the distance z along the slot for single slotted hollow waveguide. Different operating frequency.

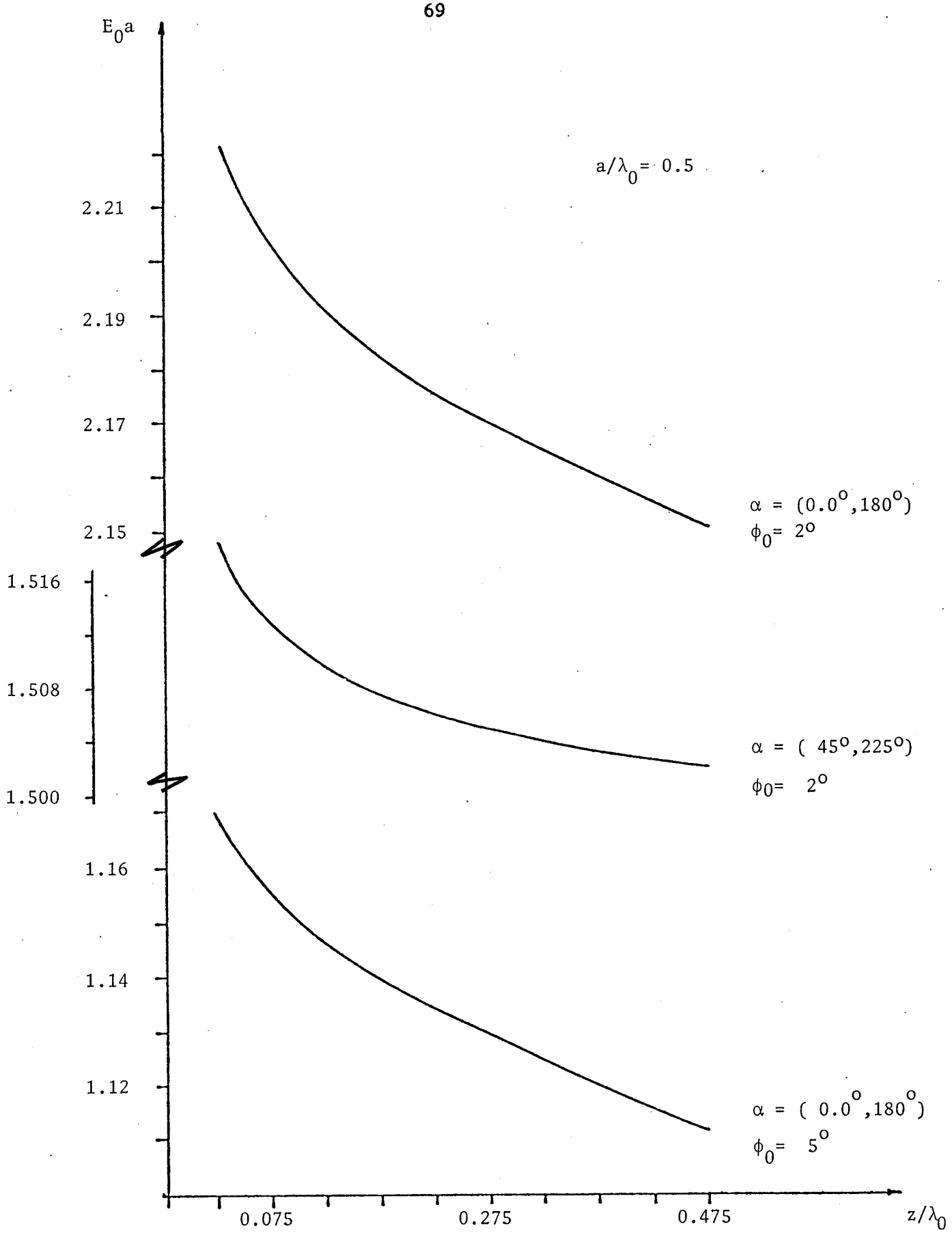

Fig. 3.11 . The slot tangential field E_0 versus the distance z along the slot for double slotted hollow waveguide. Different slot parameters.

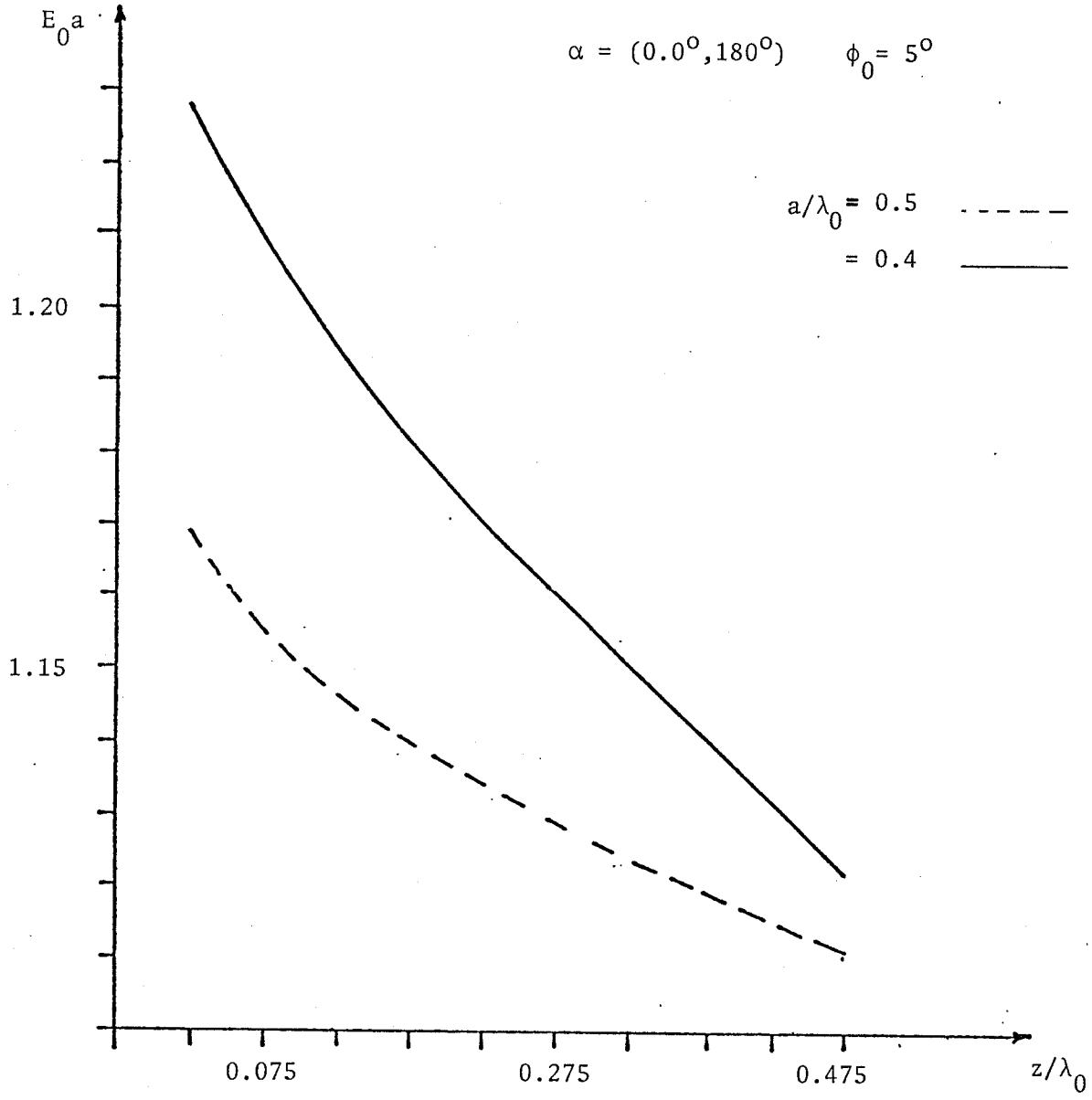

Fig. 3.12 . The slot tangential field E_0 versus the distance z along the slot for double slotted hollow waveguide. Different operating wavelength.

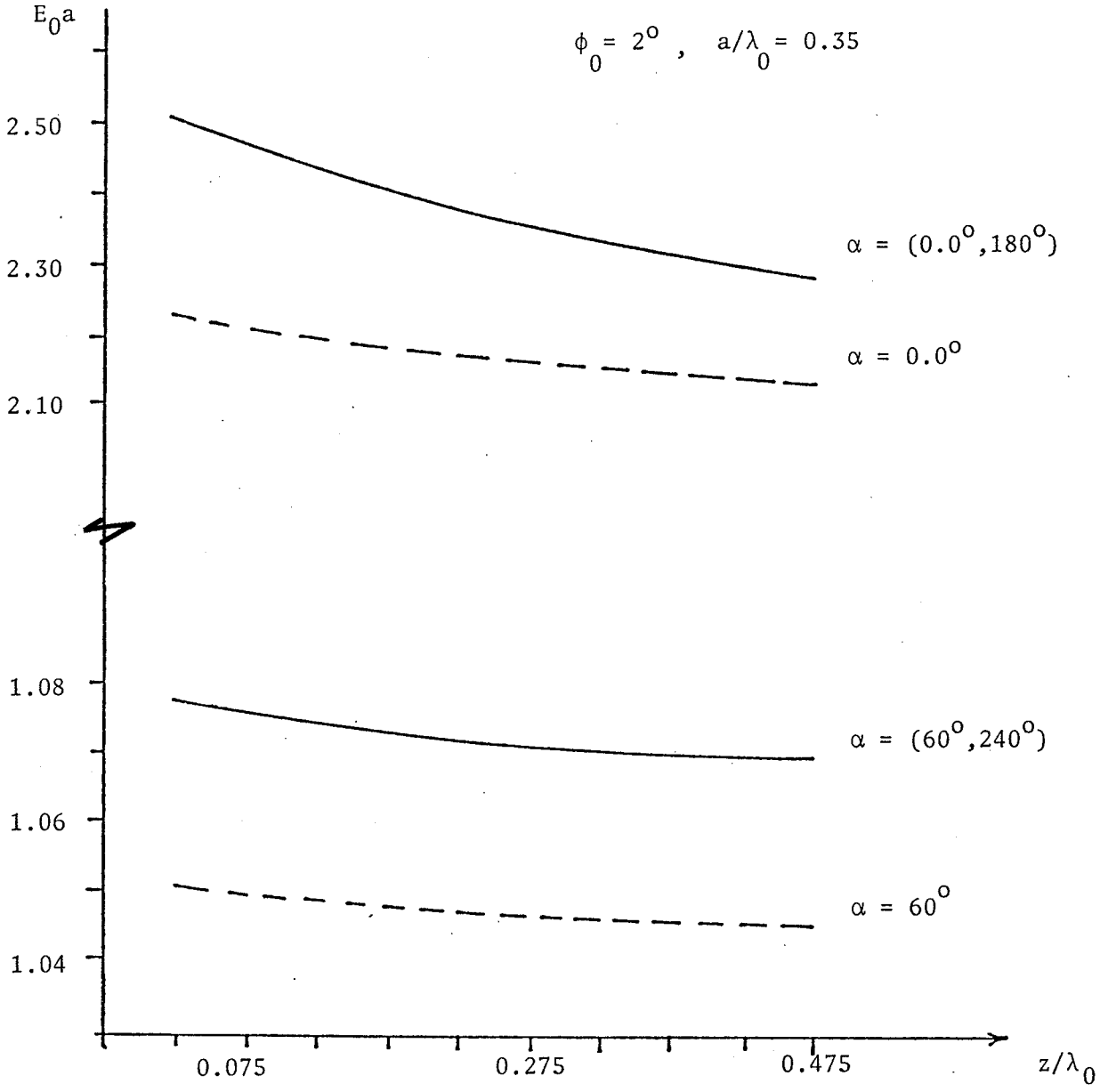

Fig. 3.13 . The slot field for both single and double slotted hollow waveguide.

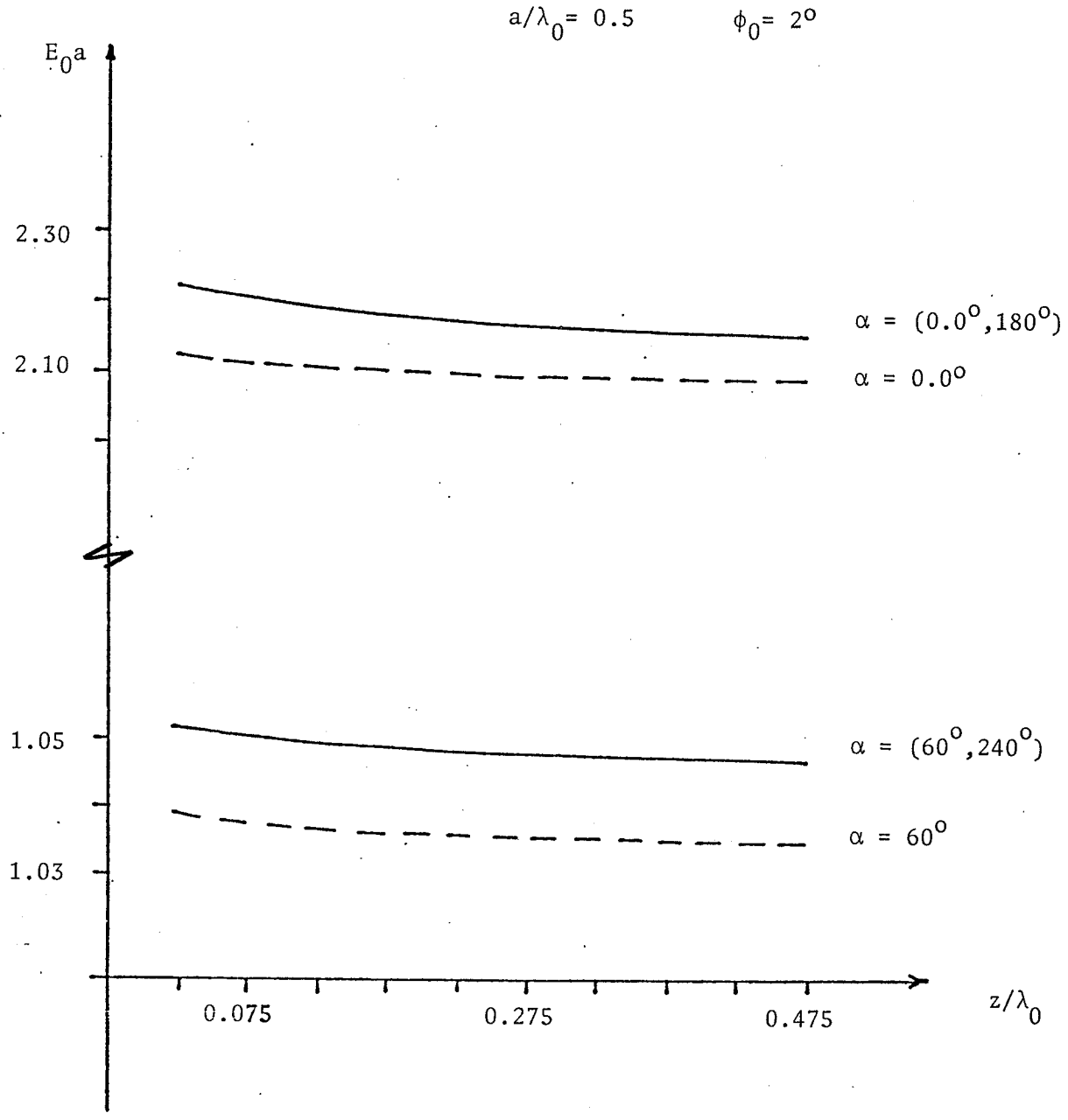

Fig. 3.14 . The slot field for both single and double slotted hollow waveguide.

by about 1% of its value when another slot is introduced. The same range of change is also noticed for $\alpha = 0°$. The change increases as a/λ_0 decreases but remains comparatively small. At $a/\lambda_0 = .35$, it is about 3%. This observation has been reported before by Chang in his treatment of a circumferential slot in a radiating cylinder [38]. The result is important in that it allows extension of this work to multi-slotted sections or to periodic structures where the solution of the field on one section may be extended to other similar adjacent structures. This will have its application later in Chapter 5.

In conclusion, this Chapter has studied and presented the nature of the field on the slot surface of both single and doubly slotted waveguides. This may prove important for several technical problems such as the possible coupling between adjacent waveguides, or using the structure as a periodic feed line, etc. A more interesting and possibly more practical problem is the slotted coaxial line with its varied applications in microwave communications. In the next Chapter an attempt is made to investigate this problem. The mathematical treatment may be more lengthy and tedious, yet it follows precisely the same major lines as those of the present Chapter.

CHAPTER IV

FIELD SOLUTION ON THE APERTURE OF AN AXIALLY SLOTTED COAXIAL WAVEGUIDE

4.1. Introduction

Slotted coaxial waveguides, apart from the academic interest, have rather important applications in modern communication. Interests in slotted coaxial lines stem from their wide application in microwave systems such as antenna feeds [35],[21],[22], wide band balun transformers [7] or feeds for multiply-fed long cylindrical antenna [38]. Recently, interest in problems such as sleeve antennas, coupling between external and internal fields through a cracked shield of a coaxial cable, prompted several authors to study the field distribution on a circumferential slot cut in the outer sheath of a coaxial line as presented in Chapter 2. Yet not much has been done to study the field distribution on the surface of slots of different shapes and orientation.

In this Chapter, the problem of a narrow, infinitely long axial slot cut in the outer surface of a coaxial line, excited by an incident TE_{11} mode is investigated. This problem reveals along with the circumferential case, that in all applications varying the shape and location of the slot greatly modifies the radiation pattern of the structure. The treatment here follows the same lines as the work of Chapter 3 for the case of the hollow waveguide. First, the solution of the possible modes supported by the structure is obtained. A modal expansions of the field with unknown coefficients in both the closed and the slotted sections of the coaxial guide are assumed. The field is then matched along the interface between two sections where the unknown

coefficients are determined. Finally, enforcing the boundary conditions on the outer wall of the coaxial line leads to a closed-form formula for the tangential electric field on the slot much similar to the formula obtained previously for the slotted hollow waveguide. The work is extended to cover coaxial line sections with a set of two identical slots diagonally symmetrical and arbitrarly located around the waveguide surface. The coupling between slots is still small, but is shown to be higher than the corresponding case of the hollow waveguide.

Now, in view of the analysis of the previous Chapter, and in order to investigate the present problem, one first has to determine the slot admittance (impedance) as a necessary step to evaluate the propagating modes of the structure. This is the subject of the following Section.

4.2 Propagating TE Modes in Axially Slotted Coaxial Waveguide

In this Section different propagating TE modes in the slotted part of the coaxial line are investigated. The problem is solved using the transverse resonance technique given previously in Sec. (2.3).

Harrington's technique could not be used here for the same reasons discussed before in Sec. (2.2) and (3.2.1). They are, generally, the difficulties encountered when the method is applied to study different slot locations. Moreover, in this particular problem of a coaxial line, the resulting expression for δ proves to be rather cumbersome and the solution may be difficult to generate. The analysis, therefore, is limited to narrow slots and is valid for any slot location in the same way as that of the hollow waveguide discussed in Sec. (3.2).

4.2.1. Slot Impedance

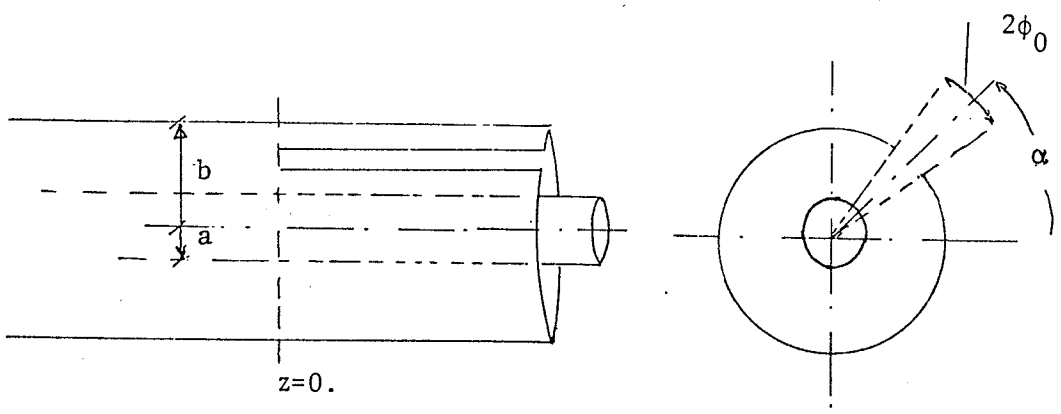

Fig. 4.1 Axially slotted coaxial waveguide

Consider the axially slotted coaxial waveguide shown in Fig. 4.1. Application of equation (2.20) for the hollow waveguide conductance is possible here, since the same radial transmission line mode representation is applicable to both structures. Accordingly, the slot conductance G_s^c for the TE_{11} incident mode is given by [28] and Appendix [D]

$$G_s^c = \frac{\int_{\alpha-\phi_0}^{\alpha+\phi_0} d\phi' \int_{\alpha-\phi_0}^{\alpha+\phi_0} d\phi \; E_\phi(b,\phi)\, G''(b;\phi,\phi')\, E_\phi(b,\phi')}{\left| \int_{\alpha-\phi_0}^{\alpha+\phi_0} h_{z1}'' \; E_\phi(b,\phi)\, d\phi \right|^2} \qquad (4.1)$$

where $$G''(b;\phi,\phi') = \mathrm{Re}\left\{ \sum_{n=0}^{\infty} \vec{Y}''(b)\, h_{zn}''(\phi)\, h_{zn}''(\phi') \right\}$$

$$h_{zn}''(\phi) = \sqrt{\frac{\varepsilon_n}{2\pi}} \cos n\phi$$

and $\vec{Y}''(b)$ is the impedance of a radial waveguide at $\rho = b$ looking

toward the outside region. It has the same form as in the case of the hollow waveguide, and is given by

$$Y''(b) = \frac{K_\rho}{j\omega\mu b} \frac{H^{(1)}(K_\rho b)}{H^{(1)'}(K\rho b)} \qquad (2.22)$$

Thus, one can see that all parameters involved in determining the slot conductance of the coaxial line are exactly similar to these of the hollow waveguide. Therefore, the slot conductance in the present case is similar to that of equation (3.8) for the hollow waveguide and assumes the form

$$G_s^c = \frac{1}{\pi\omega\mu b^2} \sum_{n=0}^{\infty} \frac{n}{|H_n^{(1)'}(K_\rho b)|^2} \left(\frac{\cos n\alpha}{\cos\alpha} \frac{J_0(n\phi_0)}{J_0(\phi_0)}\right)^2 \qquad (4.2)$$

where the waveguide radius a in eqn.(3.8) is replaced in (4.2) by the outer coaxial line radius b since G_s here is evaluated at $\rho = b$.

Similarly, using the same argument, the susceptance of the slot B_s^c is given by equation (2.25) as

$$B_s^c = -\frac{j\omega\varepsilon}{M_z} \frac{1}{\cos^2\alpha} \qquad (4.3)$$

where M_z is the magnetic polarizability of the slot. The analysis leading to the determination of M_z involves the radial transmission line susceptance at $\rho = b$ looking in the direction of decreasing ρ (see Appendix B). For the coaxial line, this susceptance differs from its counterpart of the hollow waveguide due to the presence of the metal surface at $\rho = a$. However, it is shown in Appendix[F]that,in spite of this fact, the final expression for M_z remains unchanged. It is, therefore given by

$$M_z = \frac{\pi}{2} \left(\frac{K_0}{K\rho}\right)^2 / \ln(2/\phi_0) \qquad (2.26)$$

which upon substitution in (4.3) immediately yields

$$B_s^c = -\omega\varepsilon \left(\frac{K_\rho}{K_0}\right)^2 2 \ln (2/\phi_0) / \cos^2\alpha \qquad (4.4)$$

This gives an expression for the slot susceptance, which is the same as that of the hollow waveguide. The expressions for B_s^c and G_s^c represent a short circuit condition as the slot location α approaches 90°. This indicates that the slot at this location is not seen by the wave, and accordingly has no effect on the field inside the coaxial line. This point has been discussed previously in Sec. (3.2).

The determination of the propagation constant using a perturbation technique follows the same line as given in Section (2.3.3), but because of different modal amplitudes in the present case, the resulting equation differs from that of (2.19) as shown in the following Section.

4.2.2. Perturbation Solution for the Coaxial Guide Wave Number

The transverse resonance condition as discussed in Section (2.3.3) is given by

$$\overleftrightarrow{Z}(K_\rho b) = 0 \qquad (4.5)$$

where

$$\overleftrightarrow{Z}(K_\rho b) = \overleftarrow{Z}_1(K_\rho b) + R_s^c - jX_s^c \qquad (4.6)$$

and $\overrightarrow{Z}_1(K_\rho b)$ is given by [29],[54].

$$\overleftarrow{Z}_1(K_\rho b) = -\frac{j\omega\mu b}{K_\rho}\left[\frac{J_1'(K_\rho b)\, Y_1'(K_\rho a) - J_1'(K_\rho a)\, Y_1'(K_\rho b)}{J_1(K_\rho b)\, Y_1'(K_\rho a) - J_1'(K_\rho a)\, Y_1(K_\rho b)}\right. \qquad (4.7)$$

In the coaxial waveguide, the mode constants z_{1m} of the TE_{1m} excitation are solutions of the equation [29]

$$J_1'(cz_{1m})\, Y_1'(z_{1m}) - J_1'(z_{1m})\, Y_1'(cz_{1m}) = 0 \qquad (4.8)$$

where $c = b/a$. Now, assuming that the mode constants of the slotted sections $K_\rho a$ are very close to the corresponding mode constants of the closed sections, one may set

$$K_\rho a = z_{1m} + \delta_{1m} a \tag{4.9}$$

where δ_{1m} is a small complex number. Substituting (4.9) into (4.5) and expanding the resulting expression in Taylor's series around z_{1m} and retaining only the first term, gives

$$\delta_{1m} = -\overleftrightarrow{Z}_1(cz_{1m}) \; / \; \overleftrightarrow{Z}_1'(c\, z_{1m}) \tag{4.10}$$

where the prime indicates differentiation with respect to K_ρ.
It is shown in Appendix G that

$$\overleftrightarrow{Z}_1'(cz_{1m}) = - ja \frac{\omega\mu b}{K_\rho} \quad F(c\, z_{1m}) \tag{4.11}$$

where $F(Cz_{1m})$ is given by

$$F(cz_{1m}) = (1 - \frac{1}{z_{1m}^2}) \left[\frac{Y_1'(cz_{1m})J_1(z_{1m}) + J_1'(cz_{1m})Y_1(z_{1m})}{Y_1'(z_{1m})J_1(cz_{1m}) - J_1'(z_{1m})Y_1(cz_{1m})}\right] - c(1 - \frac{1}{c^2 z_{1m}^2}) \tag{4.12}$$

Substituting (4.11) and (4.6) into (4.10) and with the aid of (4.8), (4.2) and (4.4), an expression for δ_{1m} is obtained as

$$\delta_{1m} a = (X_s'(z_{1m}) + jR_s'(z_{1m}))/F(cz_{1m}) \tag{4.13}$$

where

$$X_s'(z_{1m}) = \frac{B_s'(z_{1m})}{G_s^{2'}(z_{1m}) + B_s'^2(z_{1m})}$$

and

$$R_s'(z_{1m}) = \frac{G_s'(z_{1m})}{G_s^{2'}(z_{1m}) + B_s^{2'}(z_{1m})}$$

$$G_s'(z_{1m}) = \frac{G_s^c}{Y_0}$$

$$B_s'(z_{1m}) = \frac{B_s^c}{Y_0}$$

with

$$Y_0 = -K_\rho/\omega\mu b$$

Equation (4.13) has been used to determine the different propagation modes in the slotted coax. line as presented in the following Section.

4.2.3. Numerical Examples of the Coaxial Wavenumber

Solution for the waveguide modes for different slot locations and widths are considered for the case $c = 1.5$, such that, mainly the TE_{11} mode is allowed to propagate in the solid region [29],[54]. Some of the results are given in Tables 4.1 - 4.4 similar to Tables 3.1 - 3.4, given previously in Section (3.2.1) for the hollow waveguide.

The general features of the results and their variation with the slot parameters are in complete agreement with the physical expectations and are similar to those discussed in Sec. (3.2.1). Consider for example the effect of slot locations α on the results. For a coaxial waveguide dimension $a/\lambda_0 = 0.35$, $c = 1.5$ and slot width $10°$ Table 4.1 shows that the attenuation constant varies from $0.0429\ Np/\lambda_0$ at $\alpha = 0.0$ to 0.00438 at $\alpha = 60°$. This is about a 90% drop in the power radiated within a change of location of $60°$. This shows that the radiation power drops appreciably as the slot location moves away from the location of the maximum azimuthal surface current. The slot width has also a notable effect on the radiation power. As an example, comparing Tables 4.1 and 4.3 reveals that though the wider slot radiates higher power than the narrower one, yet doubling the slot surface area would not double

the radiation power. The tables show that for slot widths 10° and 4°, the power ratio is always around 1.7 regardless of the slot location. In fact, it has been shown before in Chapter 3 Sec. (3.3.2) and it is confirmed here in Sec. (4.3.2), that to enhance the power radiation one should use a greater number of narrow slots per section rather than use few wider slots.

The higher order modes are next investigated. Table 4.4 gives some values of δ_{1m} for m = 2,3....,etc. It is clear from the table that these modes are non-propagating and they vanish within a small fraction of a wavelength.

location α	δ Real	Imag.	$\gamma\lambda_0$ Real	Imag.
0°	0.1538 E 0	-0.3103 E-1	0.4296 E-1	-0.5655 E 1
20°	0.1372 E 0	-0.2393 E-1	0.3243 E-1	-0.5677 E 1
30°	0.1175 E 0	-0.1744 E-1	0.2303 E-1	-0.5703 E 1
45°	0.7905 E-1	-0.8921 E-2	0.1119 E-1	-0.5752 E 1
60°	0.3968 E-1	-0.3692 E-2	0.4389 E-2	-0.5800 E 1
75°	0.1064 E-1	-0.9314 E-3	0.1063 E-2	-05.834 E 1

TABLE 4.1 Values of δ and γ for different slot location α for the first mode(z_{11}= 0.8052).

$a/\lambda_0 = 0.35$ $\phi_0 = 5°$

TABLE 4.2 Values of δ and γ for different slot location α and for the first mode (z_{11} = 0.8052). a/λ_0=0.35 ϕ_0 = 3°

location α	δ Real	δ Imag.	$\gamma\lambda_0$ Real	$\gamma\lambda_0$ Imag.
0°	0.1336 E 0	-0.2319 E-1	0.3127 E-1	-0.5682 E 1
20°	0.1189 E 0	-0.1783 E-1	0.2359 E-1	-0.5701 E 1
30°	0.1016 E 0	-0.1296 E-1	0.1675 E-1	-0.5724 E 1
45°	0.6819 E-1	-0.6609 E-2	0.8172 E-2	-0.5766 E 1
60°	0.3420 E-1	-0.2733 E-2	0.3225 E-2	-0.5807 E 1
75°	0.9170 E-2	-0.6902 E-3	0.7862 E-3	-0.5836 E 1

TABLE 4.3 Values of δ and γ for different slot locations α and for the first mode (z_{11} = 0.8052). a/λ_0=0.35 ϕ_0 = 2°

location α	δ Real	δ Imag.	$\gamma\lambda_0$ Real	$\gamma\lambda_0$ Imag.
0°	0.1209 E 0	-0.1888 E-1	0.2505 E-1	-0.5699 E 1
20°	0.1074 E 0	-0.1450 E-1	0.1889 E-1	-0.5716 E 1
30°	0.9170 E-1	-0.1052 E-1	0.1343 E-1	-0.5736 E 1
45°	0.6147 E-1	-0.5359 E-2	0.6566 E-2	-0.5774 E 1
60°	0.3081 E-1	-0.2215 E-2	0.2601 E-2	-0.5811 E 1
75°	0.8260 E-2	-0.5596 E-3	0.6366 E-3	-0.5837 E 1

TABLE 4.4 Values of δ and γ for different modes
$\alpha = 0$ $\phi_0 = 5°$ $a/\lambda_0 = 0.35$

z_{1m}	δ_{1m} Real	Imag.	$\gamma_{1m}\lambda_0$ Real	Imag.
0.8052	0.1538 E 0	-0.3103 E-1	0.4296 E-1	-0.5655 E 1
6.376	0.2433 E-1	-0.4962 E-2	0.1717 E 2	-0.1509 E-1
12.612	0.6322 E-2	-0.8010 E-3	0.3550 E 2	-0.2324 E-2
18.88	0.1762 E-1	-0.8372 E-3	0.5362 E 2	-0.2408 E-2
25.156	0.7188 E-4	-0.1139 E-5	0.7159 E 2	-0.3268 E-5

The technique used in this Section to determine δ is similar to the technique used by Goldstone and Oliner [25], which has been employed in Chapter 3 . As discussed in Sec. (2.3.4), this technique is valid only for narrow slots and the accuracy of the results presented here should be considered within this limit. Moreover, in solving for multi-slotted waveguide sections one should also consider the interaction among the slots, which usually adds to the complexity of the problem. It is shown in the following Section that the problem lends itself easily to a solution for the special case of two identical, diagonally symmetrical slots similar to the solution presented in Sec. (3.3).

4.3. Two Identical Symmetrically Located Slots

In Section (4.2) the propagation constants of different modes supported by a coaxial line with a single axial slot along its surface has been investigated. The knowledge of these propagation constants would enable one to proceed to solve for the slot field distribution and to study the factors that may influence it. It is clear, however, that adding extra slots on the guide surface provides a more flexible parameter

for controlling the radiation of the structure. The problem as discussed in Chapter 3 may not be quite as simple since the interaction among these slots has to be appropriately considered. In this Section the problem of two identical and diagonally symmetric slots on the surface of a coaxial guide is investigated. The analysis to follow is similar to the work of Sec. (3.3.1), and therefore, will be given briefly.

4.3.1 Propagation Constants In A Coaxial Line With Two Identical Diagonally Symmetric Axial Slots

In Sec. (4.2.1) the impedance (admittance) of a single axial slot in an arbitrary location α on the surface of a coaxial guide has been determined. This work can be extended to the present case of two identical slots, $180°$ apart, as shown in Fig. 4.2.

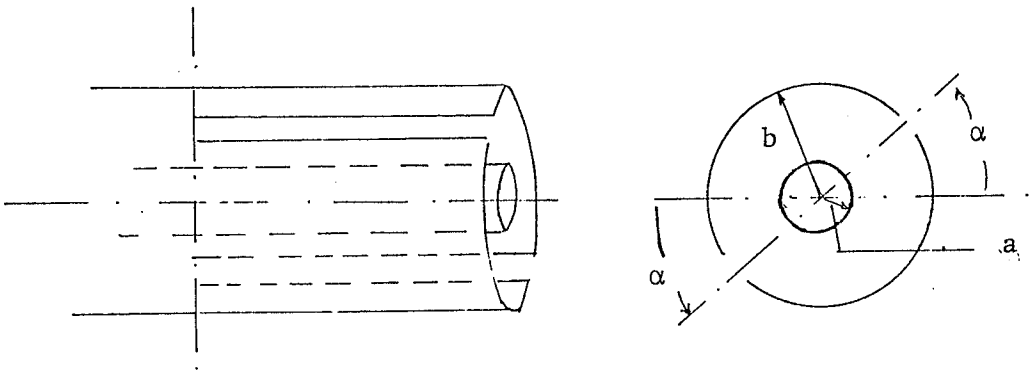

Fig. 4.2 Symmetrically double slotted coaxial guide

As discussed before in Sec. (2.3), the structure could be represented by a transmission line in ρ direction terminated at $\rho = b$ by the effective impedance (admittance) of two slots combined together,

Fig. 4.3

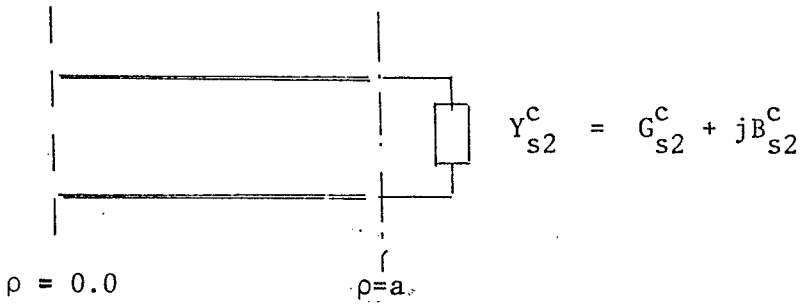

Fig. 4.3 Transmission line representation of the symmetrically double slotted coaxial guide

The radial transmission line mode representation is exactly the same for both the hollow and the coaxial waveguide [29]. Therefore, the equations for both the conductance and the susceptance of hollow waveguides developed in Appendix [D] could as well be used for the present case of the coaxial line. Accordingly, the effective slot conductance of the double-slotted coaxial line of Fig. 4.2 is given by equation (D.3) as

$$G^c_{s2} = P \Big/ \left| \int_{\alpha-\phi_0}^{\alpha+\phi_0} h''_{z1}(a,\phi)\ E_\phi(a,\phi)\ ad\phi + \int_{\pi+\alpha-\phi_0}^{\pi+\alpha+\phi_0} h''_{z1}(a,\phi)\ E_\phi(a,\phi)\ ad\phi \right|^2$$

$$P = \mathrm{Re}\left\{ \vec{Y}_n(K_\rho b) \left(\int_{\alpha-\phi_0}^{\alpha+\phi_0} h''_{zn}(a,\phi)\ E_\phi(a,\phi) + \int_{\pi+\alpha-\phi_0}^{\pi+\alpha+\phi_0} h''_{zn}(a,\phi)\ E_\phi(a,\phi) ad\phi \right)^2 \right\}$$

It has been shown in Sec. (4.2.1) that $\vec{Y}_n(K\rho b)$ in the coaxial waveguide takes the same form as the hollow waveguide case. We also recall that the mode functions $h''_{zn}(a,\phi)$ are similar for both cases. Therefore, the combined conductance G^c_{s2} of two slots takes a form identical to the effective conductance G_{s2} of the double slotted hollow waveguide

presented in Sec. (3.3.1) by eqn. (3.17), that is

$$G^c_{s2} = \frac{1}{\pi\omega\mu b^2} \sum_{n=1,3,5}^{\infty} \frac{2}{|H_n^{(1)'}(K_\rho b)|^2} \left(\frac{\cos n\alpha}{\cos\alpha} \frac{J_0(n\phi_0)}{J_0(\phi_0)}\right)^2 \tag{4.14}$$

Similarly, the effective susceptance of two slots is given by equation (D-20) as

$$B^c_{s2} = -\frac{\omega\varepsilon\pi}{2 M_z \cos^2\alpha}$$

where M_z, according to Appendix [F] together with the discussion of Section (4.2.1), takes again the same form for both coaxial and hollow waveguides. It is, therefore, given by eqn. (2.26) as

$$M_z = \frac{\pi}{2} \left(\frac{K_0}{K_\rho}\right)^2 / \ln(2/\phi_0)$$

Therefore, B^c_{s2} takes the form

$$B^c_{s2} = -\omega\varepsilon \left(\frac{K_\rho}{K_0}\right)^2 \ln(2/\phi_0) / \cos^2\alpha \tag{4.15}$$

Now, the value of δ_{1m} defined by equation (4.9) is obtained by direct substitution of (4.14) and (4.15) in eqn. (4.13) as

$$\delta_{1m} = [X'_s(z_{1m}) + j R'_s(z_{1m})] / F(cz_{1m}) \tag{4.16}$$

where $F(cz_{1m})$ is given by (4.12) and

$$X'_s(z_{1m}) = \frac{B'_s}{B'^2_s + G'^2_s} \quad , \quad R'_s(z_{1m}) = \frac{G'_s}{B'^2_s + G'^2_s}$$

with

$$B'_s = \frac{B^c_{s2}}{-\omega\mu b/K} \qquad G'_s = \frac{G^c_{s2}}{-\omega\mu b/K}$$

Equation (4.16) together with (4.9) determine the different propagating modes in the slotted structure. The propagation constant is readily obtained using equation (2.9). In the following Section some of the results obtained using these equations are presented and compared with the case of a single slot of Sec. (4.2.2).

4.3.2. Numerical Results for the Propagation Constant of a Double Slotted Coaxial Waveguide

The value δ as given by (4.16) is evaluated for several parameters such as the operating wavelength, the slot location and the slot width. Some of the results are presented in Tables 4.5 and 4.6 . Upon studying these results, one would notice the same trend as one noticed in Sections (3.3.2). The radiated power decreases with the decrease of the slot width or with the slot approaching locations where the surface current is very small. However, the variation in this case is noticed to be sharper, when compared to the corresponding double slotted waveguide of Sec. (3.3). Consider for example the results given by Table 4.5 . As α varies from $0.0°$ to $60°$ the attenuation constant drops from 0.656 Np/λ_0 to 0.00345 Np/λ_0. This is a drop of about 95% compared to 92% in the hollow waveguide case presented in Sec. (3.3.2). It may also be interesting to compare cases of single and double slots that may be geometrically related. Table 4.7 compares the results of a double slot set located at $\phi = \alpha$ and $\phi = \pi + \alpha$, with those of a single slot located at $\phi = \alpha$. The slots are assumed identical and have a $4°$ width.

TABLE 4.5 Computed values of δ and γ for arbitrary located two-slot set, 180° apart. First mode excitation

$\phi_0 = 2$ $a/\lambda_0 = 0.35$ $c = 1.5$

location α	δ Real	δ Imag.	$\gamma\lambda_0$ Real	$\gamma\lambda_0$ Imag.
0.0	0.2402 E 0	-0.4255 E-1	0.6567 E-1	-0.5529 E 1
30	0.1826 E 0	-0.2400 E-1	-0.3448 E-1	-0.5614 E 1
45	0.1229 E 0	-0.1088 E-1	0.1448 E-1	-0.5696 E 1
60	0.6181 E-1	-0.2825 E-2	0.3463 E-2	-0.5774 E 1
75	0.1660 E-1	-0.2105 E-3	0.2423 E-3	-0.5827 E 1

TABLE 4.6 $\phi_0 = 5°$ $a/\lambda_0 = 0.35$ $c = 1.5$

location α	δ Real	δ Imag.	$\gamma\lambda_0$ Real	$\gamma\lambda_0$ Imag.
0.0	0.3043 E 0	-0.6965 E-1	0.11619 E 0	-0.5429 E 1
30	0.2334 E 0	-0.3966 E-1	0.6070 E 0	-0.5539 E 1
45	0.1580 E 0	-0.1804 E-1	0.2518 E-1	-0.5648 E 1
60	0.7978 E-1	-0.4709 E-2	0.5914 E-2	-0.5752 E 1
75	0.2144 E-1	-0.3511 E-3	0.4069 E-3	-0.5822 E 1

TABLE 4.7 Comparison between results of single and double slotted coaxial guide

$\phi_0 = 4°$

α	a/λ	case	Atten. Const. α_z	Ratio $(\alpha_{z_2})/(\alpha_{z_1})$
0.0°	0.3	Single slot	0.0355	2.66
		Double slot	0.0944	
	0.2	Single slot	0.1029	3.10
		Double slot	0.3171	
60°	0.3	Single slot	0.00365	1.33
		Double slot	0.00487	
	0.2	Single slot	0.00987	1.36
		Double slot	0.01346	

Here again, it is clear that two identical slots symmetrically located do not radiate twice as much as a single set at the same location. The ratio of the radiated power varies with the slot location, the wavelength and the slot width as is evident from the following table.

TABLE 4.8 Comparison between results of a single and double slotted coaxial guides.

$a/\lambda_0 = 0.35$ $\alpha = 0.0^o$

Slot Width	Case	Attenu. Const. α_z	Ratio $(\alpha_{z_2})/(\alpha_{z_1})$
4°	Single Slot	0.0250	2.62
	Double Slot	0.0656	
10°	Single Slot	0.0429	2.70
	Double Slot	0.1161	

It is also worth mentioning that as before the field disturbance due to a wide angle slot is less than two narrow ones. It is evident from Table 4.8 that two slots of width 4° would have an attenuation constant of 0.0656 Np/λ_0 while one slot of width 20° has an attenuation of only 0.0429 Np/λ_0. However, one may notice that, the variation in this case, is sharper than the corresponding case of the hollow waveguide of Section (3.3.2).

The effect of the interaction between the fields of two slots will be studied further in a later Section when the slot field is obtained. To this end, and with the knowledge of the eigen-values of the slotted section, it is possible now to proceed to the next Section. There, the unknown coefficients of the modal expansion of the field on both sides of the slotted coaxial line with TE_{11} excitation are obtained. This step allows the determination of the field solution on the slot surface as will be discussed in Section (4.4).

4.4 Formulation of the Scattering Problem

The analysis of the previous Section helps determining the propagating TE modes supported by the slotted structure. In this Section

these modes are used to form a modal expansion of the field in both closed and slotted sections of the coaxial line each with a set of unknown coefficients. These coefficients are then obtained in a way similar to that followed in Sec. (3.3), where the field components are matched at the plane separating the two waveguide sections. In a later Section these coefficients will be used to completely determine the slot field.

4.4.1. Field Representation Inside the Coaxial Waveguide (TE modes)

The field inside a coaxial guide is usually given by a combination of both the Bessel functions and the Neumann functions. It may be convenient before introducing the mathematical form of this field to define a set of functions that will be used extensively in the analysis of this Chapter. Define the functions $C_n(z_{nm}\rho/a)$ and $D_n(K_{\rho_{nm}}\rho)$ and their derivatives as

$$
\begin{aligned}
C_n(z_{nm}\rho/a) &= Y_n'(z_{nm})\, J_n(z_{nm}\rho/a) - J_n'(z_{nm})\, Y_n(z_{nm}\rho/a) \\
C_n'(z_{nm}\rho/a) &= \frac{z_{nm}}{a}\left[Y_n'(z_{nm})\, J_n'(z_{nm}\rho/a) - J_n'(z_{nm})\, Y_n'(z_{nm}\rho/a)\right] \\
D_n(K_{\rho_{nm}}\rho) &= Y_n'(K_{\rho_{nm}}a)\, J_n(K_{\rho_{nm}}\rho) - J_n'(K_{\rho_{nm}}a)\, Y_n(K_{\rho_{nm}}\rho) \\
D_n'(K_{\rho_{nm}}\rho) &= K_{\rho_{nm}}\left[Y_n'(K_{\rho_{nm}}a)\, J_n'(K_{\rho_{nm}}\rho) - J_n'(K_{\rho_{nm}}a)\, Y_n'(K_{\rho_{nm}}\rho)\right]
\end{aligned}
\tag{4.17}
$$

Now, let an incident field in region I of Fig. 4.4 be

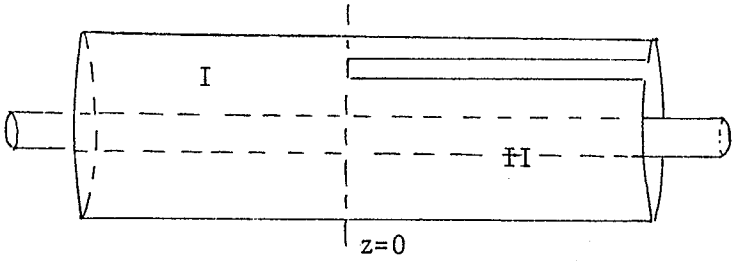

Fig. 4.4 Axially slotted coaxial guide

TE_{11} with a wave function in the form [29]

$$\psi^i = T[C_1(z_{11}\rho/a)]\cos\phi \exp(j\theta_{11}z) \tag{4.18}$$

where T is the intensity of the incident field, a is the inner radius of the coaxial waveguide, θ_{11} is the propagation constant of the TE_{11} mode, and $e^{-j\omega t}$ time variation is assumed. Let the wave function of the scattered field in the same region (region I) be represented by

$$\psi^s = T \sum_{p=0} \sum_{q=1} B_{pq} [C_p(z_{pq}\rho/a)] \cos p\phi \exp(-j\theta_{pq}z) \tag{4.19}$$

where p and q are integers and

B_{pq}'s are unknown constants to be determined

z_{pq} is the q^{th} root of the equation

$$Y'_p(z_{pq})\, J'_p(cz_{pq}) - J'_p(z_{pq})\, Y'_p(cz_{pq}) = 0 \tag{4.20}$$

with $c = b/a$ and b is the outer radius of the waveguide and

$$\theta^2_{pq} + (z_{pq}/a)^2 = K_0^2$$

The scattered field in region II can be represented by the wave-function

$$\phi = T \sum_{r=0} \sum_{s=1} A_{rs} [D_n(K_{\rho_{rs}}\rho)] \cos r\phi \cdot \exp(-\gamma_{rs}z) \tag{4.21}$$

where r and s are integers and

$$\gamma_{rs} = \alpha_z - j\beta_z = \sqrt{K^2_{\rho_{rs}} - K_0^2} \tag{4.22}$$

$K_{\rho_{rs}}$'s are known for each mode and each slot location according to Sec. 4.2.

A_{rs}'s are constants to be determined.

For convenience, the letter K will be used, in what follows, in place of $K_{\rho_{rs}}$ except in certain special cases to avoid confusion.

The field components in both regions can be derived from the relations (3.26) stated in Sec. (3.4). As in Chapter 3 , it is convenient to introduce the mode functions e_{nm} and h_{nm} in both region I and II;defined as:

Region I:

$$\begin{aligned} \overset{I}{e}_{nm} &= \overset{I}{e}_{\phi_{nm}} \vec{a}_\phi + \overset{I}{e}_{\rho_{nm}} \vec{a}_\rho \\ \overset{I}{h}_{nm} &= \overset{I}{h}_{\phi_{nm}} \vec{a}_\phi + \overset{I}{h}_{\rho_{nm}} \vec{a}_\rho \end{aligned} \tag{4.23}$$

where

$$\begin{aligned} \overset{I}{e}_{\phi_{nm}} &= C_n'(z_{nm}\rho/a) \cos n\,\phi \\ \overset{I}{e}_{\rho_{nm}} &= \frac{n}{\rho} C_n(z_{nm}\rho/a) \sin n\,\phi \\ \overset{I}{h}^{\pm}_{\phi_{nm}} &= \pm \frac{j\theta_{nm}}{j\omega\mu} \overset{I}{e}_{\rho_{nm}} \\ \overset{I}{h}^{\pm}_{\rho_{nm}} &= \mp \frac{j\theta_{nm}}{j\omega\mu} \overset{I}{e}_{\phi_{nm}} \end{aligned} \tag{4.24}$$

and the lower and upper signs hold for $\exp(-j\theta_{nm} z)$ and $\exp(j\theta_{nm} z)$ variations,respectively.

Region II:

$$\begin{aligned} \overset{II}{e}_{nm} &= \overset{II}{e}_{\phi_{nm}} \vec{a}_\phi + \overset{II}{e}_{\rho_{nm}} \vec{a}_\rho \\ \overset{II}{h}_{nm} &= \overset{II}{h}_{\phi_{nm}} \vec{a}_\phi + \overset{II}{h}_{\rho_{nm}} \vec{a}_\rho \end{aligned} \tag{4.25}$$

where

$$
\begin{aligned}
{}^{II}e_{\phi_{nm}} &= D_n'(K_{\rho_{nm}}\rho)\cos n\phi \\
{}^{II}e_{\rho_{nm}} &= \frac{n}{\rho} D_n(K_{\rho_{nm}}\rho)\sin n\phi \\
{}^{II}h_{\phi_{nm}} &= -\frac{\gamma_{nm}}{j\omega\mu} {}^{II}e_{\rho_{nm}} \\
{}^{II}h_{\rho_{nm}} &= \frac{\gamma_{nm}}{j\omega\mu} {}^{II}e_{\phi_{nm}}
\end{aligned}
\tag{4.26}
$$

These mode represenations with the aid of (4.18), (4.19), (4.21) and (3.26) give the field components in both regions I and II, which takes the form

Region I:

$$
\begin{aligned}
{}^{I}E_{\phi} &= T\,{}^{I}e_{\phi_{11}} \exp(j\theta_{11}z) + T \sum_{p=q} \sum_{q=1} B_{pq}\,{}^{I}e_{\phi_{pq}} \exp(-j\theta_{pq}z) \\
{}^{I}E_{\rho} &= T\,{}^{I}e_{\phi_{11}} \exp(j\theta_{11}z) + T \sum_{p=q} \sum_{q=1} B_{pq}\,{}^{I}e_{\rho_{pq}} \exp(-j\theta_{pq}z) \\
{}^{I}H_{\phi} &= T\,{}^{I}h^{+}_{\phi_{11}} \exp(j\theta_{11}z) + T \sum_{p=0} \sum_{q=1} B_{pq}\,{}^{I}h^{-}_{\phi_{pq}} \exp(-j\theta_{pq}z) \\
{}^{I}H_{\rho} &= T\,{}^{I}h^{+}_{\rho_{11}} \exp(j\theta_{11}z) + T \sum_{p=0} \sum_{q=1} B_{pq}\,{}^{I}h^{-}_{\rho_{pq}} \exp(-j\theta_{pq}z)
\end{aligned}
\tag{4.27}
$$

Region II:

$$
\begin{aligned}
{}^{II}E_{\phi} &= T \sum_{r=0} \sum_{s=1} A_{rs}\,{}^{II}e_{\phi_{rs}} \exp(-\gamma_{rs}z) \\
{}^{II}E_{\rho} &= T \sum_{r=0} \sum_{s=1} A_{rs}\,{}^{II}e_{\rho_{rs}} \exp(-\gamma_{rs}z) \\
{}^{II}H_{\phi} &= T \sum_{r=0} \sum_{s=1} A_{rs}\,{}^{II}h_{\phi_{rs}} \exp(-\gamma_{rs}z)
\end{aligned}
\tag{4.28}
$$

$$H_{\rho}^{II} = T \sum_{r=0} \sum_{s=1} A_{rs} h_{\rho_{rs}}^{II} \exp(-\gamma_{rs} z)$$

These equations give the field everywhere in regions I and II in terms of the e_{nm} and h_{nm} modes.

Certain relations between these modes exist.. These relations will help in reducing the resulting equations of the unknown sets A and B to a simple form that can be numerically solved. The next Section deals exclusively with these relations.

4.4.2. Mode Orthogonality

In this Section mathematical relations among the modes given by (4.24) and (4.26) will be introduced. These relations are similar to those discussed before in Sec. (2.4.2) and will be used extensively in the formulation of the scattering problem to follow in a later Section.

Consider the integral relation

$$M_{\substack{nm \\ pq}}^{\pm} = \int_S (e_{nm}^{I} \times h_{pq}^{I\pm}) \cdot \vec{a}_z \, ds \qquad (4.29)$$

where S is the cross-sectional area of the waveguide. Substituting (4.23) in (4.29) gives

$$M_{\substack{nm \\ pq}}^{\pm} = \int_s (e_{\phi_{nm}}^{I} \vec{a}_{\phi} + e_{\rho_{nm}}^{I} \vec{a}_{\rho}) \times (h_{\phi_{pq}}^{I\pm} \vec{a}_{\phi} + h_{\rho_{pq}}^{I\pm} \vec{a}_{\rho}) \cdot \vec{a}_z \, ds$$

$$= \int_{\rho=a}^{b} \int_{\phi=0}^{2\pi} (e_{\rho_{nm}}^{I} h_{\phi_{pq}}^{I\pm} - e_{\phi_{nm}}^{I} h_{\rho_{pq}}^{I\pm}) \, \rho d\rho \, d\phi$$

which upon substituting the mode values given by(4.24) gives

$$M_{\substack{nm \\ pq}}^{\pm} = \int_{\rho=a}^{b} \int_{0}^{2\pi} (\frac{n}{\rho} C_n(z_{nm}\rho/a) \, C_p(z_{pq}\rho/a) \pm \frac{j\theta_{pq}}{j\omega\mu} \frac{p}{\rho} \sin n\phi \sin p\phi$$

+

$$\pm C'_n(z_{nm}\rho/a)\, C'_p(z_{pq}\rho/a)\cos n\phi \cos p\phi)\, \theta_{pq}/\ \omega\mu\ \ \rho d\rho d\phi$$

Using the orthogonality of the trigonometric functions as presented by (3.34), this equation becomes

$$M^{\pm}_{\substack{nm \\ pq}} = M^{\pm}_{\substack{nm \\ q}} = \pm \frac{2\pi}{\varepsilon_n} \frac{j\theta_{nq}}{j\omega\mu} \int_{y=1}^{c} \left(\frac{n^2}{y} C_n(z_{nm}y)\, C_n(z_{nq}y) + C'_n(z_{nm}y)\, C'_n(z_{nq}y)\, y\right)dy \tag{4.30}$$

where $y = \rho/a$.

This integration is evaluated in Appendix[H], and is shown to exist only for $z_{nm} = z_{nq}$ and is equal to zero otherwise. Using the result (H - 8) of appendix H, equation (4.30) may be written as

$$M^{\pm}_{\substack{nm \\ q}} = M^{\pm}_{nm} = \int_s (e^I_{nm} \times h^{I_{\pm}}_{pq}) \cdot \vec{a}_z\, ds$$

$$= \pm \frac{2\pi}{\varepsilon_n} \frac{j\theta_{nm}}{j\omega\mu} \frac{z^2_{nm}}{2} \left\{c^2\left(1 - \frac{1}{c^2 z^2_{nm}}\right) C^2_n(cz_{nm}) - c\left(1 - \frac{1}{z^2_{nm}}\right) C_n(z_{nm})\, G_n(cz_{nm})\right\} \tag{4.31}$$

where

$$C_n(cz_{nm}) = J_n(cz_{nm})\, Y'_n(z_{nm}) - Y_n(cz_{nm})\, J'_n(z_{nm})$$

$$G_n(cz_{nm}) = J_n(z_{nm})\, Y'_n(cz_{nm}) - Y_n(z_{nm})\, J'_n(cz_{nm}) \tag{4.32}$$

Equation (4.31) establishes the orthogonality relation between the modes e^I and h^I for the coaxial line.

Another integral which is of importance in later analyses is the integral relation

$$N_{\substack{nm \\ pq}} = \int_s (e^{I}_{nm} \times h^{II}_{pq}) \cdot \vec{a}_z \, ds \tag{4.33}$$

Substituting the mode values given by (4.24) and (4.26) into (4.33) and evaluating the trigonometric orthogonality relations, (3.34) gives

$$N_{\substack{nm \\ pq}} = N_{nmq} = -\frac{2\pi}{\varepsilon_n} \frac{\gamma_{nq}}{j\omega\mu} \left\{ \frac{n^2}{y} \int_{y=1}^{c} C_n(z_{nm}y) \cdot D_n(K_{\rho_{nm}} ay)dy + a^2 \int_{y=1}^{c} C'_n(z_{nm}y) \right.$$

$$\left. D'_n(K_{\rho_{nm}} ay) \; y dy \right.$$

where $y = \rho/a$

The result of this integration is given by (H-6) of Appendix[H]. Accordingly, one finds

$$N_{nmq} = \int_s (e^{I}_{nm} \times h^{I}_{pq}) \cdot \vec{a}_z \, ds = \frac{-2\pi}{\varepsilon_n} \frac{\gamma_{nq}}{j\omega\mu} \frac{z^2_{nm} \, (K\rho_{nm}a)}{z^2_{nm} - (K\rho_{nm}a)^2}$$

$$\{ c \; C_n(cz_{nm}) \; D'_n \; (c \, K_{\rho_{nm}} a) - C_n(z_{nm}) \; D'_n(K\rho_{nm}a) \}$$

(4.34)

Where $C_n(cz_{nm})$ is given by (4.32) and

$$C'_n(cz) = J'_n(cz) \; Y'_n(z) - Y'_n(cz) \; J'_n(z) \tag{4.35}$$

This establishes the second integral relation to be encountered later in the formulation of the scattering problem.

The third important relationship to be considered is

$$Q^{\pm}_{\substack{nm \\ pq}} = \int_S (h^{I_{\pm}}_{nm} \times e^{II}_{pq}) \cdot \vec{a}_z \, ds \tag{4.36}$$

where S is the same as that in (4.29).

Using (4.24) and (4.26) and following the same steps as in Sec. (3.4.2) in the derivation of (3.43), one can easily show that (4.36) may be written as

$$Q^{\pm}_{\substack{nm \\ pq}} = \pm \frac{j\theta_{nm}}{\gamma_{pq}} \int_s (e^{I}_{nm} \times h^{\pm II}_{pq}) \cdot \vec{a}_z \, ds \tag{4.37}$$

which upon using (4.34) gives

$$Q^{\pm}_{\substack{nm \\ pq}} = Q^{\pm}_{nmq} = \int (h^{I}_{nm} \times e^{\pm II}_{pq}) \cdot \vec{a}_z \, ds = \pm \frac{j\theta_{nm}}{\gamma_{nq}} N_{nmq} = \pm \frac{2\pi}{\varepsilon_n} \frac{j\theta_{nm}}{j\omega\mu}$$

$$\frac{z^2_{nm} (K_{nq}a)}{z^2_{nm} - (K_{nq}a)^2} \{c \, C_n(cz_{nm}) \, C'_n(cK_{nq}a) - C_n(z_{nm}) \, C'_n(K_{nq}a)\} \tag{4.38}$$

This concludes the derivation of the three basic integral relations needed for the formulation of the scattering problem as will be discussed in the next Section.

4.4.3. Mode Matching

The next step in this analysis is to match the tangential components of the field on both sections of the coaxial line (at the plane $z = 0$). To this end, the technique presented in Sec. (3.4.3) is applied here, employing the different relationships obtained previously in (4.31), (4.34) and (4.38).

Consider the two identities

$$\int_s (E^{I}_t \times h^{\pm I}_{nm}) \Big|_{z=0} \cdot \vec{a}_z \, ds = \int_s (E^{II}_t \times h^{\pm I}_{nm}) \Big|_{z=0} \cdot \vec{a}_z \, ds \tag{4.39}$$

and

$$\int_s (\overset{I}{H_t} \times \overset{I}{e_{nm}}) \Big|_{z=0} \cdot \vec{a}_z \, ds = \int_s (\overset{II}{H_t} \times \overset{I}{e_{nm}}) \Big|_{z=0} \cdot \vec{a}_z \, ds \qquad (4.40)$$

which are based on the fact that the tangential electric field E_t and magnetic field H_t are continuous at the plane separating the two waveguide sections. Analytically this means

$$\overset{I}{E_t} = \overset{II}{E_t}$$

and

$$\overset{I}{H_t} = \overset{II}{H_t}$$

Consider first equation (4.39). The R.H.S., using (4.27), could be written as:

$$\int_s \overset{I}{E_t} \times \overset{I}{h^{\pm}_{nm}} \Big|_{z=0} \cdot \vec{a}_z \, ds = (T \int_s \overset{I}{e_{11}} \times \overset{I}{h^{\pm}_{nm}} + T \sum_{p=0} \sum_{q=1} B_{pq} \int_s \overset{I}{e_{pq}} \times \overset{I}{h^{\pm}_{nm}}) \cdot \vec{a}_z \, ds$$

But from (4.31)

$$\int_s \overset{I}{e_{nm}} \times \overset{I}{h^{\pm}_{pq}} \cdot \vec{a}_z \, ds = -M^{\pm}_{nm}$$

Therefore

$$\int_s \overset{I}{E} \times \overset{I}{h^{\pm}_{nm}} \Big|_{z=0} \cdot \vec{a}_z \, ds = T \, M^{\pm}_{11} + T \, B_{nm} \, M^{\pm}_{nm} \qquad (4.41)$$

Similarly, using (4.28), the R.H.S. of (4.40) gives

$$\int_s \overset{II}{E_t} \times \overset{I}{h^{\pm}_{nm}} \Big|_{z=0} \cdot \vec{a}_z \, ds = T \sum_{r=0} \sum_{s=1} A_{rs} \int \overset{II}{e_{rs}} \times \overset{I}{h^{\pm}_{nm}} \Big|_{z=0} \cdot \vec{a}_z \, ds$$

which upon using (4.36) becomes

$$\int_s \overset{II}{E_t} \times \overset{I}{h^{\pm}_{nm}} \Big|_{z=0} \cdot \vec{a}_z \, ds = -T \sum_{s=1} A_{ns} \, Q^{\pm}_{nsm} \qquad (4.42)$$

Combining (4.41) and (4.42), equation (4.39) could finally be written as

$$M_{11}^{\pm} + B_{nm} M_{nm}^{\pm} = - \sum_{s=1} A_{ns} Q_{nsm}^{\pm} \tag{4.43}$$

Equation (4.43) is similar, in form, to equation (3.49) of Chapter 3 for the hollow waveguide. However, the values of $M_{nm}^{\pm}$ and $Q_{nsm}^{\pm}$ given here by equations (4.31) and (4.38) are fundamentally different from their counterpart of Chapter 3.

Now, consider equation (4.40), in a similar way the L.H.S. using (4.27) becomes

$$\int_s \overset{I}{H_t} \times \overset{I}{e_{nm}} \Big|_{z=0} \cdot \vec{a}_z \, ds = \int_s (T \overset{I}{h_{11}^{+}} + T \sum_{p=0} \sum_{q=1} B_{pq} \overset{I}{h_{pq}^{-}}) \times \overset{I}{e_{nm}} \cdot \vec{a}_z \, ds$$

$$= - TM_{11}^{+} - T B_{nm} M_{nm}^{-}$$

$$= T M_{11}^{-} - T B_{nm} M_{nm}^{-}$$

where the result of (4.31) was employed, and $-M_{11}^{+}$ is replaced by M_{11}^{-}. The R.H.S. of (4.40), using equation (4.28), gives

$$\int (\overset{II}{H_t} \times \overset{I}{e_{nm}}) \Big|_{z=0} \cdot \vec{a}_z \, ds = T \sum_{r=0} \sum_{s=1} A_{rs} \int_s \overset{II}{h_{rs}} \times \overset{I}{e_{nm}} \cdot \vec{a}_z \, ds$$

which when using (4.34) becomes

$$\int H_t \times e_{nm} \Big|_{z=0} \cdot \vec{a}_z \, ds = - T \sum_{s} A_{ns} N_{nms}$$

Thus, equation (4.40) becomes

$$- M_{11}^{-} + B_{nm} M_{nm}^{-} = \sum_{s=1} A_{ns} N_{nms} \tag{4.44}$$

The unknown A's and B's could be determined by solving (4.43) and (4.44) in a manner similar to that of Section (3.4.3). Allowing n, m and s to take discrete values 1, 2, 3, ... these two equations form a set of infinite simultaneous equations.

However, as in the case of the hollow waveguide, it is shown that the n=1 mode and a few terms in each series are sufficient to determine the slot field. For the $n \neq 1$ modes, the excitation is zero. By enforcing the orthogonality relationship on the slot field, it is shown that these modes are not required to determine the slot tangential field.

4.4.4. Solution of the Unknown Coefficients

The solution of (4.43) and (4.44) follows exactly the same lines as that of Sec. (3.4.4). Therefore, it will be briefly mentioned here. Consider the case of n=1, equation (4.43) and (4.44) becomes

$$M_{11}^{-} + B_{1m} M_{1m}^{-} = - \sum_{s=1} A_{1s} Q_{1sm}^{-} \tag{4.45}$$

$$-M_{11}^{-} + B_{1m} M_{1m}^{-} = \sum_{s=1} A_{1s} N_{1ms} \tag{4.46}$$

Subtracting (4.46) from (4.45), and truncating after an appropriate number of terms L , gives a matrix equation similar to (3.53) which is of the form

$$\begin{bmatrix} 2 \\ 0 \\ \vdots \\ 0 \end{bmatrix} = - \begin{bmatrix} \dfrac{Q_{111}^{-} + N_{111}}{M_{11}^{-}} & \cdots & \dfrac{Q_{1L1}^{-} + N_{11L}}{M_{11}^{-}} \\ \vdots & & \vdots \\ \dfrac{Q_{11L}^{-} + N_{1L1}}{M_{1L}^{-}} & & \dfrac{Q_{1LL}^{-} + N_{1LL}}{M_{1L}^{-}} \end{bmatrix} \begin{bmatrix} A_{11} \\ \vdots \\ A_{1L} \end{bmatrix} \tag{4.47}$$

The coefficients A_{11}, A_{12} ... A_{1L} are easily obtained from equation (4.72) by a simple matrix inversion. Substituting the results back in either (4.45) or (4.46), the coefficients B_{11}, B_{12} ... B_{1L} can readily be obtained. Again, one should point out that B_{11} and A_{11} represent the reflection and the transmission coefficients, respectively.

A computer program is established to calculate these coefficients using (4.47) and either (4.45) or (4.46). Tables 4.9 - 4.12 give some of the computed results for a single slot, while Tables 4.13 - 4.15 give corresponding values for the double slotted case. It is apparent that the first few terms are enough to determine the field, and that the rest of the coefficients are increasingly negligible as seen from above tables. This result is physically feasible since, as in the case of the hollow waveguide, higher modes are non-propagating and they vanish within very short distance.

Most of the observations noticed before in Sec. (3.4.4) are encountered here again. The reflection coefficients for any mode decay as the slot moves far from the position of maximum azimuthal field as is shown in Tables 4.9-4.10 for the single slot and in 4.13 - 4.14 for the double slot. This, again, has its important application in microwave measurements. It allows a probe entry to the waveguide in places where the slot has minimum effect on the field. Thus one may conduct experimental investigation with the least disturbance to the interior field. The reflection coefficient is also shown to be a function of the wavelength. Figs. 4.5 and 4.6 for single and double slots, respectively, shows that the value of the power reflection coefficient rises fast near the cut-off frequency, and decays smoothly as the frequency increases. It is clear also from these curves that the presence of two slots will cause higher

TABLE 4.9 The Transmission and reflection coefficients for TE_{11} coaxial line mode.

$\phi_0 = 2°$ $\alpha = 0.0$ $a/\lambda_0 = 0.36$ $L = 5$

M	Transmission Coefficients (TE_{1m}) in Region II		Reflection Coefficients (TE_{11}) in Region I	
	Real	Imag.	Real	Imag.
1	0.1174 E 1	0.2837 E-1	0.1278 E-1	0.2226 E-2
2	-0.4127 E-1	-0.2176 E-1	0.3187 E-1	-0.4877 E-2
3	-0.5188 E-4	-0.2738 E-4	0.3187 E-2	0.3309 E-4
4	-0.1538 E-4	-0.5268 E-5	0.3115 E-2	0.1987 E-3
5	0.2720 E-7	0.7787 E-8	0.2227 E-4	0.2016 E-5

TABLE 4.10 The scattering and reflection coefficients for TE_{11} coaxial line mode.

$\phi_0 = 2°$ $\alpha = 45°$ $a/\lambda_0 = 0.35$ $L = 5$

M	Transmission Coefficients (TE_{1m}) in Region II		Reflection Coefficients (TE_{1m}) in Region I	
	Real	Imag.	Real	Imag.
1	0.1085 E 1	0.7917 E-2	0.6207 E-2	0.5759 E-3
2	-0.2121 E-1	-0.9264 E-2	0.1515 E-1	-0.3615 E-2
3	-0.1351 E-4	-0.4599 E-5	0.1532 E-2	-0.1072 E-3
4	-0.3823 E-5	-0.8739 E-6	0.1508 E-2	-0.2399 E-4
5	0.4011 E-8	0.7195 E-9	0.1080 E-4	0.1187 E-6

TABLE 4.11 Transmission and Reflection Coefficients for TE_{11} coaxial line mode.

$\phi_0 = 5^o$ $\alpha = 0.0^o$ $a/\lambda_0 = 0.35$ $L = 5$

M	Transmission Coefficients in Region II (TE_{1m})		Reflection Coefficients in Region I (TE_{1m})	
	Real	Imag.	Real	Imag.
1	0.1223 E 1	0.4739 E-1	0.1664 E-1	0.3845 E-2
2	-0.5237 E-1	-0.3113 E-1	0.4211 E-1	-0.4073 E-2
3	-0.8750 E-4	-0.4867 E-4	0.4163 E-2	0.2690 E-3
4	-0.2574 E-4	-0.1016 E-4	0.4069 E-2	0.4800 E-3
5	0.4590 E-7	0.1522 E-7	0.2905 E-4	0.4206 E-5

TABLE 4.12 Transmission and Reflection Coefficients for TE_{11} coaxial line mode.

$\phi_0 = 5^o$ $\alpha = 0.0^o$ $a/\lambda_0 = .35$ $L = 4$

M	Transmission Coefficients in Region II (TE_{1m})		Reflection Coefficients in Region I (TE_{11})	
	Real	Imag.	Real	Imag.
1	0.1223 E 1	0.4739 E-1	0.1664 E-1	0.3845 E-2
2	-0.5237 E-1	-0.3113 E-1	0.4211 E-1	-0.4073 E-2
3	-0.8750 E-4	-0.4867 E-4	0.4163 E-2	0.2690 E-3
4	-0.2574 E-4	-0.1016 E-4	0.4069 E-2	0.4800 E-3

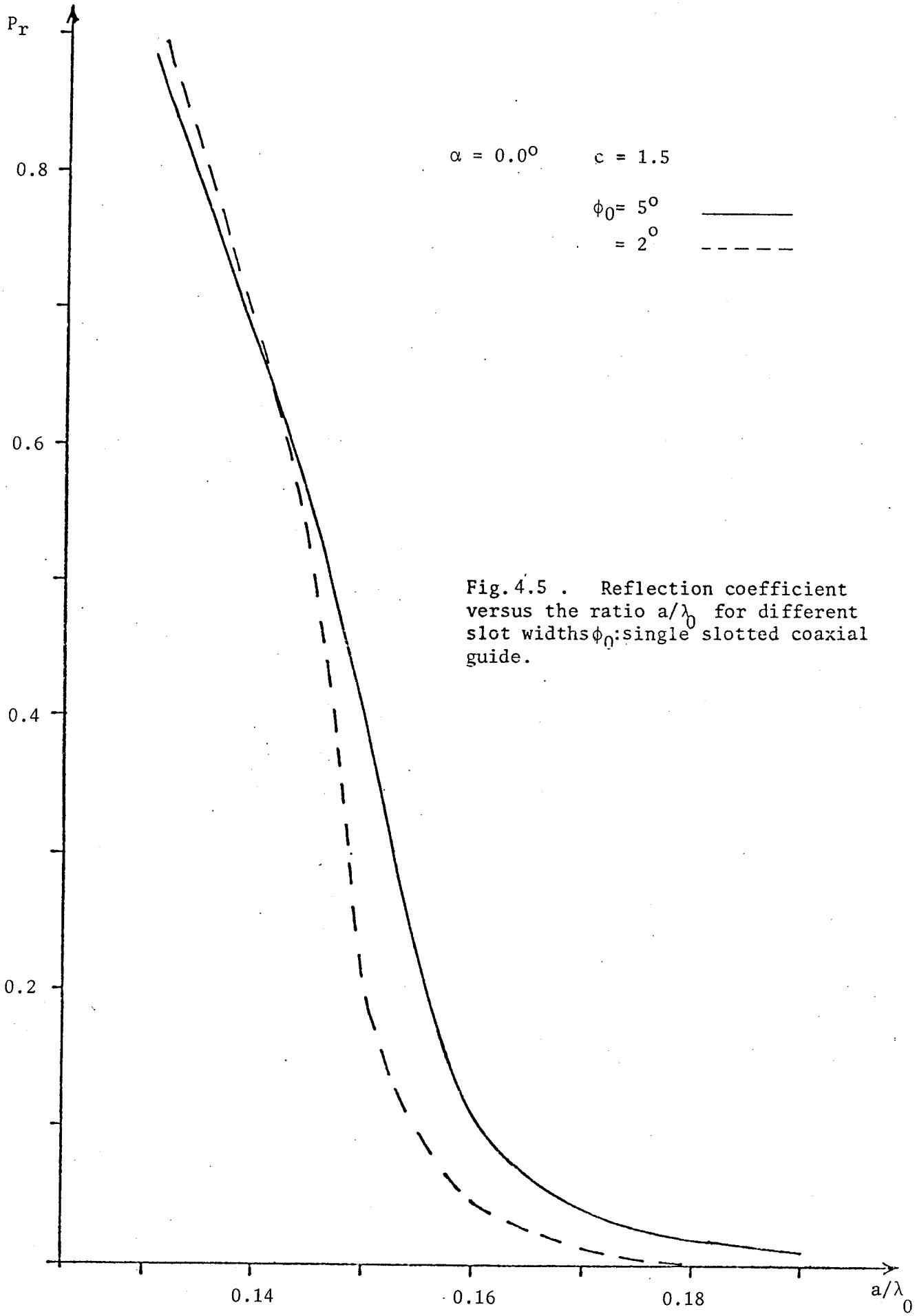

Fig. 4.5 . Reflection coefficient versus the ratio a/λ_0 for different slot widths ϕ_0: single slotted coaxial guide.

TABLE 4.13 Transmission and Reflection Coefficients

c = 1.5 Two slots, 180° apart, $\phi_0 = 2^\circ$ $\alpha = 0.0^\circ$

L = 5 $a/\lambda_0 = 0.35$

n	Transmission Coefficient		Reflection Coefficient	
	Real	Imag.	Real	Imag.
1	0.1357 E 1	0.6837 E-1	0.2780 E-1	0.6059 E-2
2	-0.8697 E-1	-0.4930 E-1	0.6950 E-1	-0.7302 E-2
3	-0.2209 E-3	-0.1281 E-3	0.6877 E-2	0.3641 E-3
4	-0.6654 E-4	-0.2501 E-4	0.6729 E-2	0.7066 E-3
5	0.1284 E-6	0.4412 E-7	0.4807 E-4	0.6305 E-5

TABLE 4.14 Transmission and Reflection Coefficients

c = 1.5 Two slots, 180° apart, $\phi_0 = 2^\circ$ $\alpha = 45^\circ$

L = 5 $a/\lambda_0 = 0.35$

n	Transmission Coefficient		Reflection Coefficient	
	Real	Imag.	Real	Imag.
1	0.1177 E 1	0.1638 E-1	0.1303 E-1	0.1302 E-2
2	-0.4308 E-1	-0.1900 E-1	0.3176 E-1	-0.7239 E-2
3	-0.5637 E-4	-0.1984 E-4	0.3204 E-2	-0.1984 E-3
4	-0.1603 E-4	-0.3709 E-5	0.3152 E-2	-0.2706 E-4
5	0.2798 E-7	0.5728 E-8	0.2258 E-4	0.4055 E-6

TABLE 4.15 Transmission and Reflection Coefficients

c = 1.5 Two slots, 180^{o} apart, $\phi_0 = 5^{o}$ $\alpha = 0.0^{o}$

L = 5 $a/\lambda_0 = 0.35$

n	Transmission Coefficient		Reflection Coefficient	
	Real	Imag.	Real	Imag.
1	0.1461 E 1	0.1166 E 0.0	0.3676 E-1	0.1089 E-1
2	-0.1118 E 0	-0.7319 E-1	0.9331 E-1	-0.2807 E-2
3	-0.3778 E-3	-0.2355 E-3	0.9133 E-2	0.1142 E-2
4	-0.1131 E-3	-0.4985 E-4	0.8908 E-2	0.1576 E-2
5	0.2154 E-6	0.8620 E-7	0.6355 E-4	0.1291 E-4

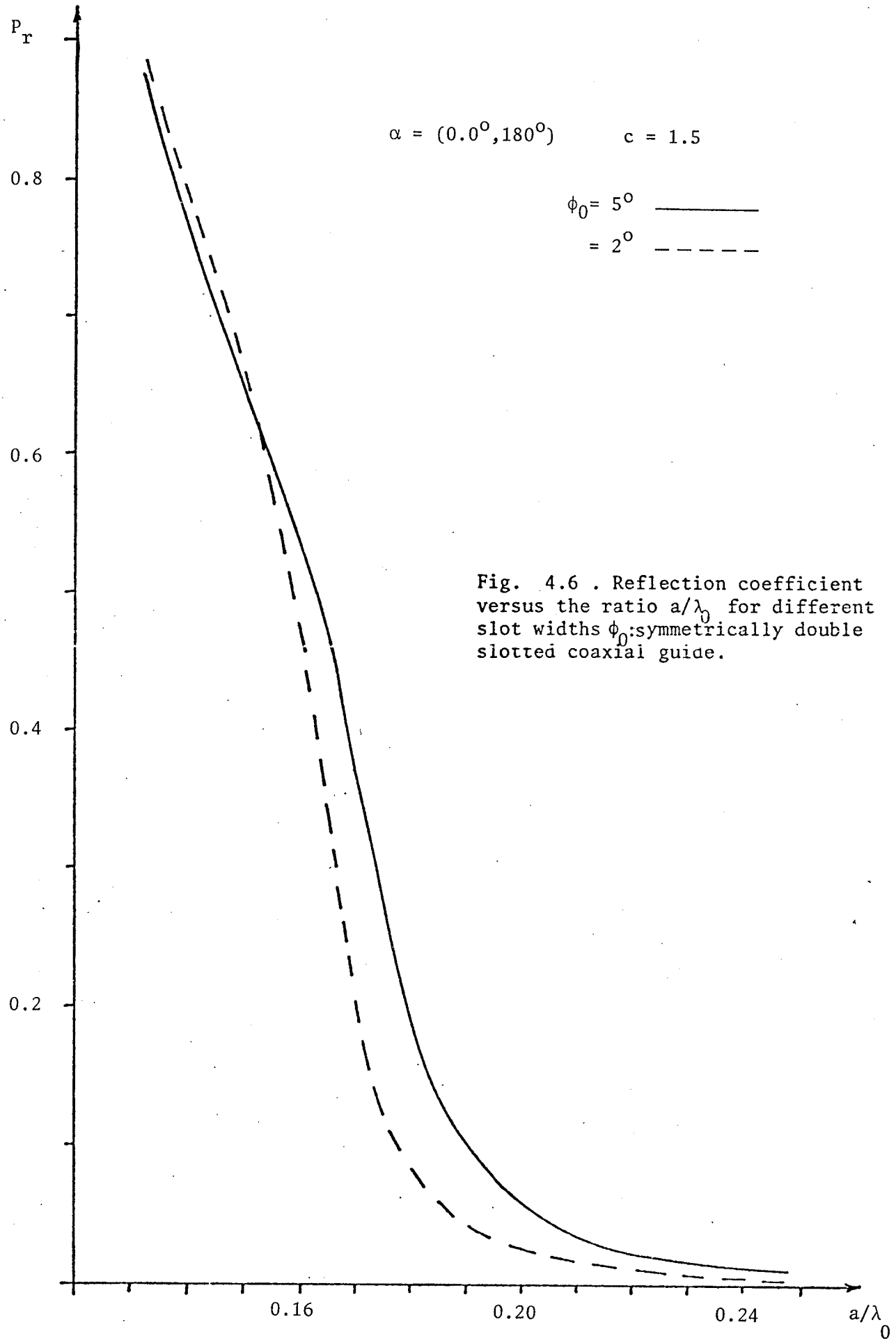

Fig. 4.6 . Reflection coefficient versus the ratio a/λ_0 for different slot widths ϕ_0:symmetrically double slotted coaxial guide.

power reflection coefficient than one single slot, even if the surface area of the single slot is equivalent to the surface area of both slots together for $a/\lambda_0=0.17$. Figs. 4.5 and 4.6 show that the P_r for a single slot of width $20°$ is about .04, while the corresponding value for two slots, each of width $4°$, is about 0.2. The change here is noticed to be sharper than the corresponding case of the hollow waveguide of Sec. (3,4.4). One may also point out that while the power reflection coefficient decreases as a/λ_0 increases, it was shown in Section (4.3.2) that the radiated power in this case decreases. This suggests an optimum operating frequency to compromise between the required radiation power in the space and the minimum P_r in the waveguide, depending on the practical needs.

Finally, the stability and accuracy of the numerical procedure again seems quite acceptable. Tables 4.11 and 4.12 give the values of the coefficients A and B with two different number of terms considered. It is obvious from these tables that the results are very stable, and good to the fifth significant figure. The accuracy of the results is tested by substituting the values of the coefficients back into each equation and calculating the error. This error was always in the range of 10^{-6} or less in a single precision calculation. Different cases were tested to check the accuracy, and the results in all cases were within the above limit.

This concludes the analysis of this Section, allowing one to carry on to the next step to evaluate the field on the surface of the slot(s).

4.5. Electric Field on the Slot Surface

The final stage of this Chapter is to evaluate the tangential electric field on the slot surface due to the incident TE_{11} coaxial

line mode. To this end, the scattering coefficients obtained in Sec. (4.3) together with the assumption of a long narrow slot are employed to arrive at a closed-form formula for this field. The approach is similar to that of Sec. (3.5) for the hollow waveguide case, and applies for both single and double slotted coaxial guide sections.

It is shown by Harrington that for a long narrow slot the field remains essentially either TE or TM depending upon the excitation [24] This suggests that there is only a tangential component of the field on the slot surface and in this case it is the ϕ-polarized E_ϕ. Accordingly, by virtue of equations (4.26) and (4.28), the slot field could be written explicitly as:

$$E_\phi(b,\phi,z) = T \sum_{r=0} \sum_{s=1} A_{rs} D'_r(K_{\rho_{rs}} b) \cos r\phi \exp(-\gamma_{rs} z) \qquad (4.48)$$

where $D'_r(K_{\rho_{rs}} b)$ is given by (4.17).
This expression is valid for both single and double slotted sections as long as the appropriate coefficients A_{rs} and $K_{\rho_{rs}}$ are used. Further, the field on a narrow slot could be shown to take the form [25], [37-38], [45] and [50].

$$E_\phi(b,\phi) = \frac{E_0}{\sqrt{1-(\phi/\phi_0)^2}} \qquad -\phi_0 < \phi < \phi_0 \qquad (4.49)$$

which, when introducing the slot location α and the z variation, may take the form

$$E_\phi(b,\phi,z) = \frac{E_0(b,z)\cos\alpha}{\sqrt{1-\left(\frac{\phi-\alpha}{\phi_0}\right)^2}} \qquad \alpha - \phi_0 < \phi < \alpha + \phi_0 \qquad (4.50)$$

where the factor $\cos\alpha$ is introduced here merely to adjust for the appropriate direction of the field as the slot location α varies between $0.0°$ and $360°$ around the guide surface. Combining (4.48) and (4.50) gives

$$\frac{E_0(b,\phi)\cos\alpha}{\sqrt{1-\left(\frac{\phi-\alpha}{\phi_0}\right)^2}} = T \sum_{r=0}^{\infty} \sum_{s=1}^{\infty} A_{rs} D_r'(K_{\rho_{rs}} b) \cos r\phi \exp(-\gamma_{rs} z) \qquad (4.51)$$

with $\alpha - \phi_0 < \phi < \alpha + \phi_0$ for a single slot

and

$\alpha - \phi_0 < \phi < + \phi_0$

$\pi + \alpha - \phi_0 < \phi < \pi + \alpha + \phi_0$ for double slots

with $\pi + \alpha$ replaces α in (4.51)

Multiplying both sides by $\cos\phi$ and integrating over the slot (slots) gives

$$E_0(b,z)\, f(\alpha,\phi_0) = T \sum_{r=0} \sum_{s=1} A_{rs} D_r'(K_{\rho_{rs}} b) \exp(-\gamma_{rs} z) \int_0^c \cos r\phi \cos\phi \, d\phi \qquad (4.52)$$

where the integration on the R.H.S. is extended over the whole waveguide since the field is zero on the metal wall, and $f(\alpha,\phi_0)$ is given by

$$f(\alpha,\phi_0) = \cos\alpha \int_{\alpha-\phi_0}^{\alpha+\phi_0} \frac{\cos\phi}{\sqrt{1-\left(\frac{\phi-\alpha}{\phi_0}\right)^2}} \, d\phi \qquad \text{single slot}$$

$$= \cos\alpha \left\{ \int_{\alpha-\phi_0}^{\alpha+\phi_0} \frac{\cos\phi \, d\phi}{\sqrt{1-\left(\frac{\phi-\alpha}{\phi_0}\right)^2}} - \int_{\pi+\alpha-\phi_0}^{\pi+\alpha+\phi_0} \frac{\cos\phi \, d\phi}{\sqrt{1-\left[\frac{\phi-(\pi+\alpha)}{\phi_0}\right]^2}} \right.$$

double slot

(4.53)

The integration of (4.53) is given by (3.61) as

$$f(\alpha,\phi_0) = \cos^2\alpha \;\; \phi_0 \;\; \pi \, J_0(\phi_0) \qquad \text{single slot} \tag{4.54}$$

$$= 2\cos^2\alpha \;\; \phi_0 \;\; \pi \;\; J_0(\phi_0) \qquad \text{double slots}$$

Also, since

$$\int_0^{2\pi} \cos r\phi \cos\phi \, d\phi = \pi \quad r = 1 \tag{4.55}$$

$$= 0 \quad r \neq 1$$

therefore, the integration to the R.H.S. of eqn. (4.52) is equal to zero except for $r = 1$.

Combining (4.52), (4.54) and (4.55) one can show that

$$E_0(b,z)\cos\alpha = \frac{T}{\phi_0 J_0(\phi_0)\, N\cos\alpha} \sum_{s=1}^{\infty} A_{1s} D_1'(K\rho_{1s} b)\exp(-\gamma_{1s} z) \tag{4.56}$$

where $N = 1$ for single slot

$= 2$ for double slot

Substituting from (4.56) into (4.50), a closed form formula for the slot field is finally obtained so that

$$E_\phi(b,\phi,z) = \frac{T}{\phi_0 J_0(\phi_0)\, N\cos\alpha} \sum_{s=1}^{\infty} A_{1s} \; D_1'(K\rho_{1s} b) \; \frac{\exp(-\gamma_{1s} z)}{\sqrt{1 - \left(\frac{\phi - \alpha}{\phi_0}\right)}} \tag{4.57}$$

The coefficients A_{1s} are known through the analysis of Sections (4.3) and (4.4) and the values of $K_{\rho_{1s}}$ and γ_{1s} are all known according to Sections(4.2.2) and (4.3.1). Thus equation (4.57) completely determines the slot field. Some numerical examples for different parameters are presented in the next Section.

4.6. Numerical Results for the Slot Field

With the aid of equation (4.51) the field on the slot(s) surface for both the single and double slotted coaxial lines are evaluated for several

slot parameters. These are presented in Figs. 4.7 - 4.13 . In all these figures the value of the slot field E_0 is such that the constant T of the incident wave function (4.18) equals unity.

The field preserves the same general features as noticed in Sec. (3.6). The intensity decays as the slot location moves from the position of maximum azimuthal field as is apparent from Figs. 4.7 and 4.10 for single and double slots, respectively. It is also shown that for two slots of different width with all other parameters kept equal, one finds the field on the narrower slot higher than that on the wider one. However, the field integration $\int_S ds$ on the slot surface is higher for the wider slot indicating higher power radiation into space. This is in agreement with the previous results of Sections (4.2.3) and (4.3.2) for both the single and the double slotted Sections, respectively.

The operating frequency has a strong influence on the slot field. It is shown in Figs. 4.8 and 4.9 for the single slot, and in Fig.4.11 for the double slotted section, that as the ratio a/λ_0 decreases the slot field increases, indicating higher power radiation. This is again in complete agreement with the results of Sections (4.2.3) and (4.3.2), which shows a higher attenuation constant in the slotted section (i.e. higher power radiation) as the ratio a/λ_0 decreases.

Finally, it may be instructive to compare the field of the two-slot set located at $\phi = \alpha$ and $\phi = \alpha + \pi$ with that of a single slot located at $\phi = \alpha$. This is equivalent to studying the field on one slot when another slot is introduced diagonally across from the first one. Figs. 4.12 and 4.13 shows that there exists a moderate degree of interaction between slot fields and that this interaction increases with the field

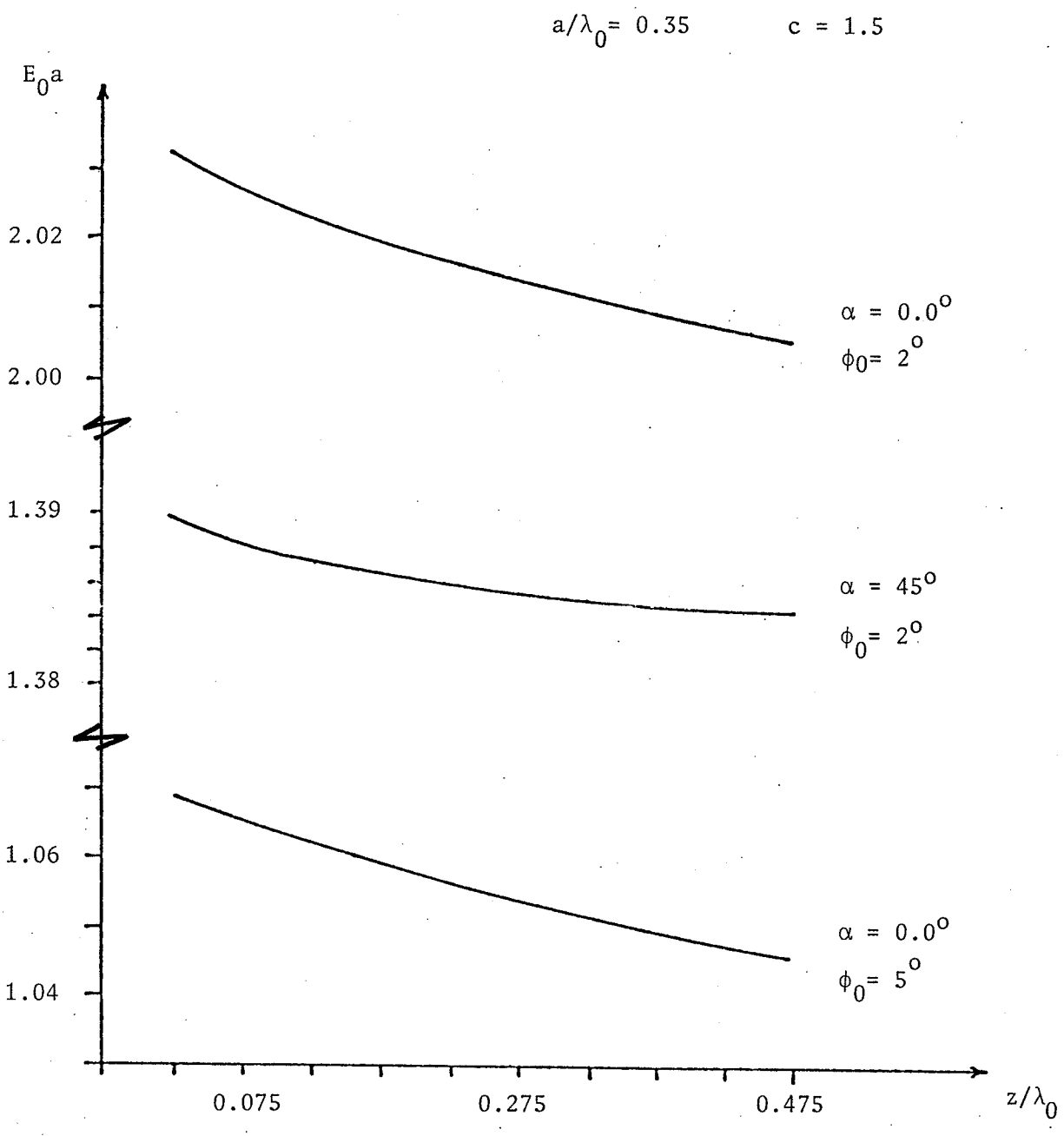

Fig. 4.7 . Slot tangential field E_0 versus the distance z along the slot. Single slotted coaxial guide with different slot parameters.

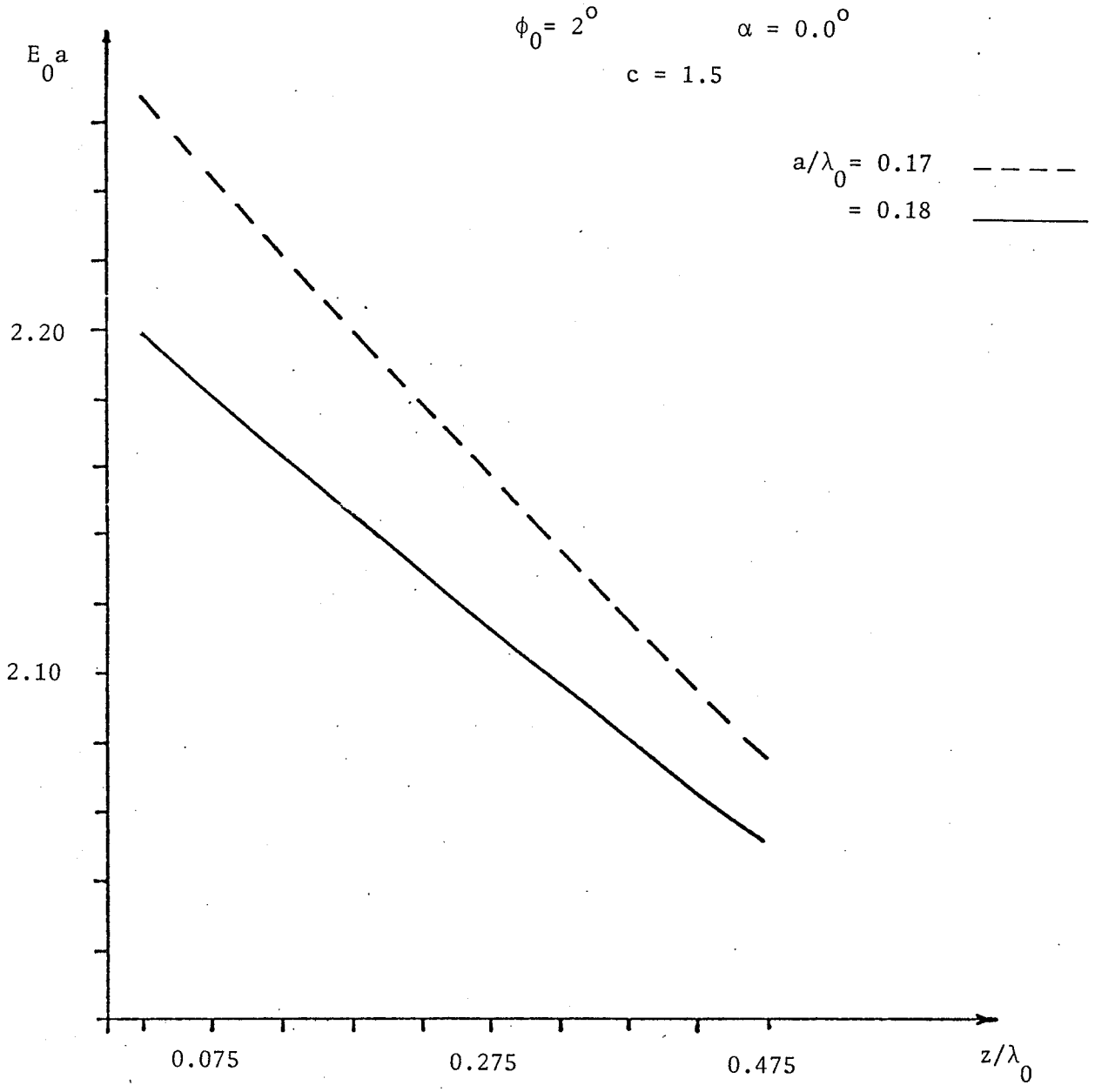

Fig. 4.8 . Slot tangential field E_0 versus the distance z along the slot. Single slotted coaxial guide with different operating wavelength.

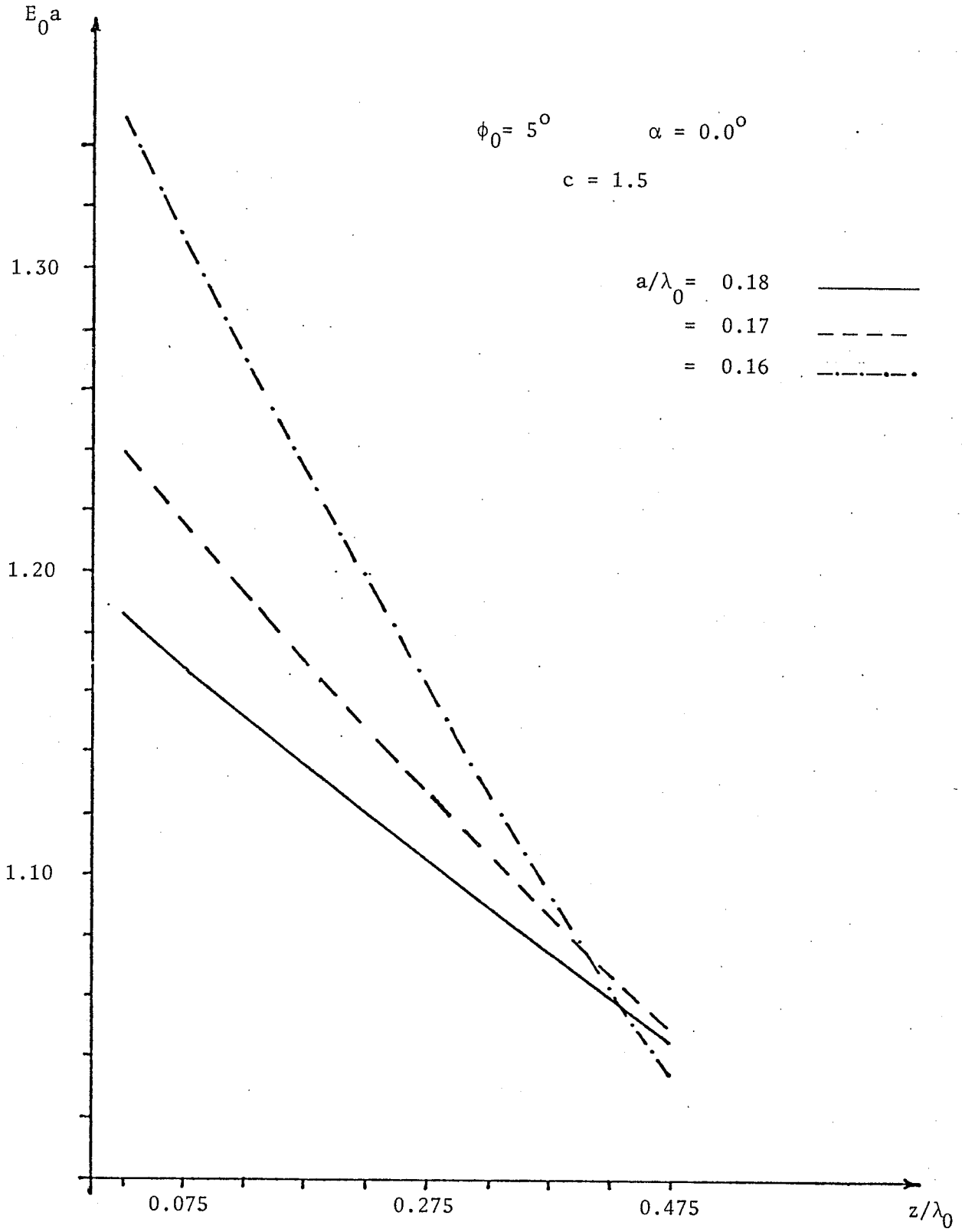

Fig. 4.9 . Slot tangential field E_0 versus the distance z along the slot. Single slotted coaxial guide with different operating frequency.

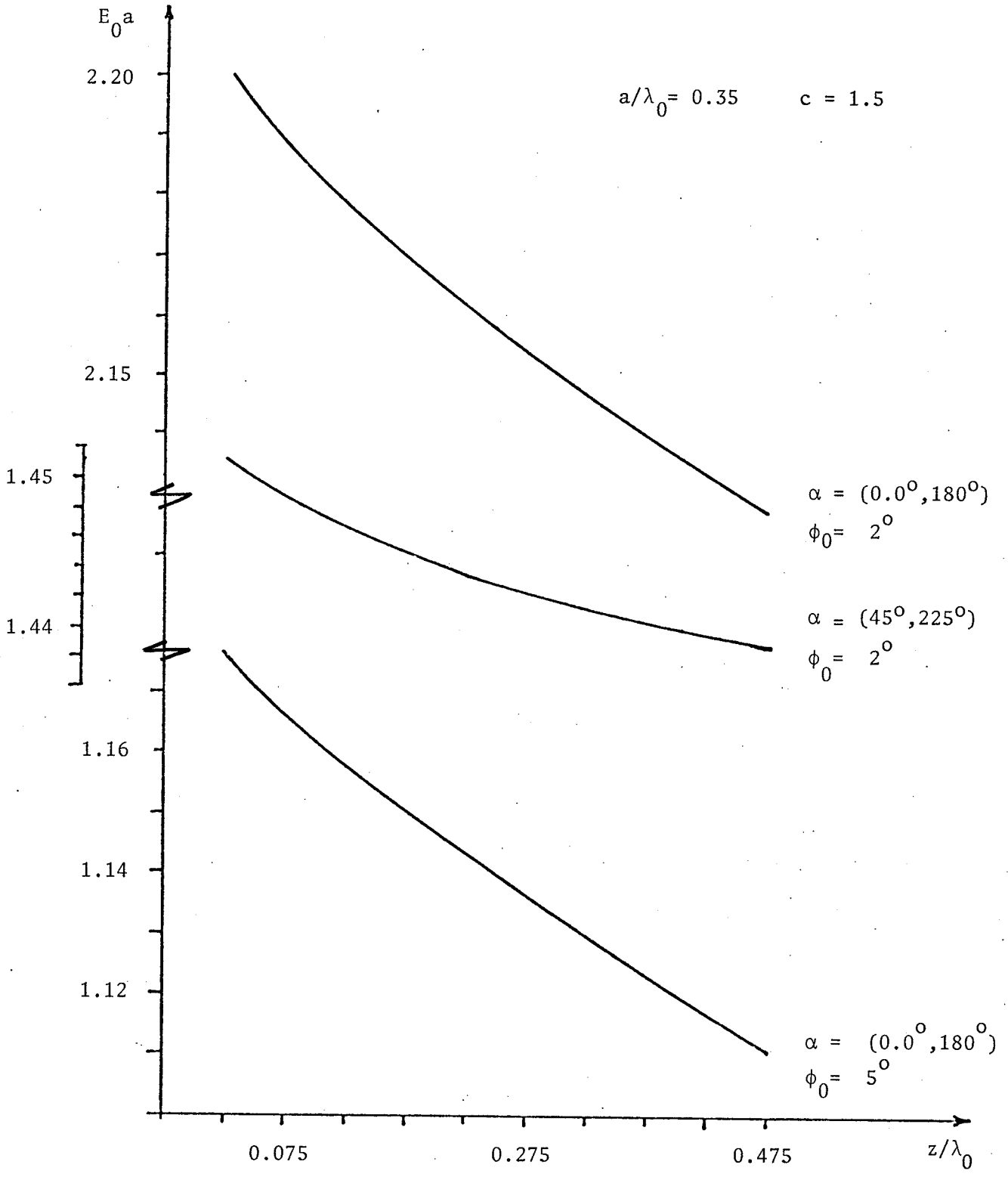

Fig. 4.10 . Slot tangential field E_0 versus the distance z along the slot. Symmetrically double slotted coaxial guide with different parameters.

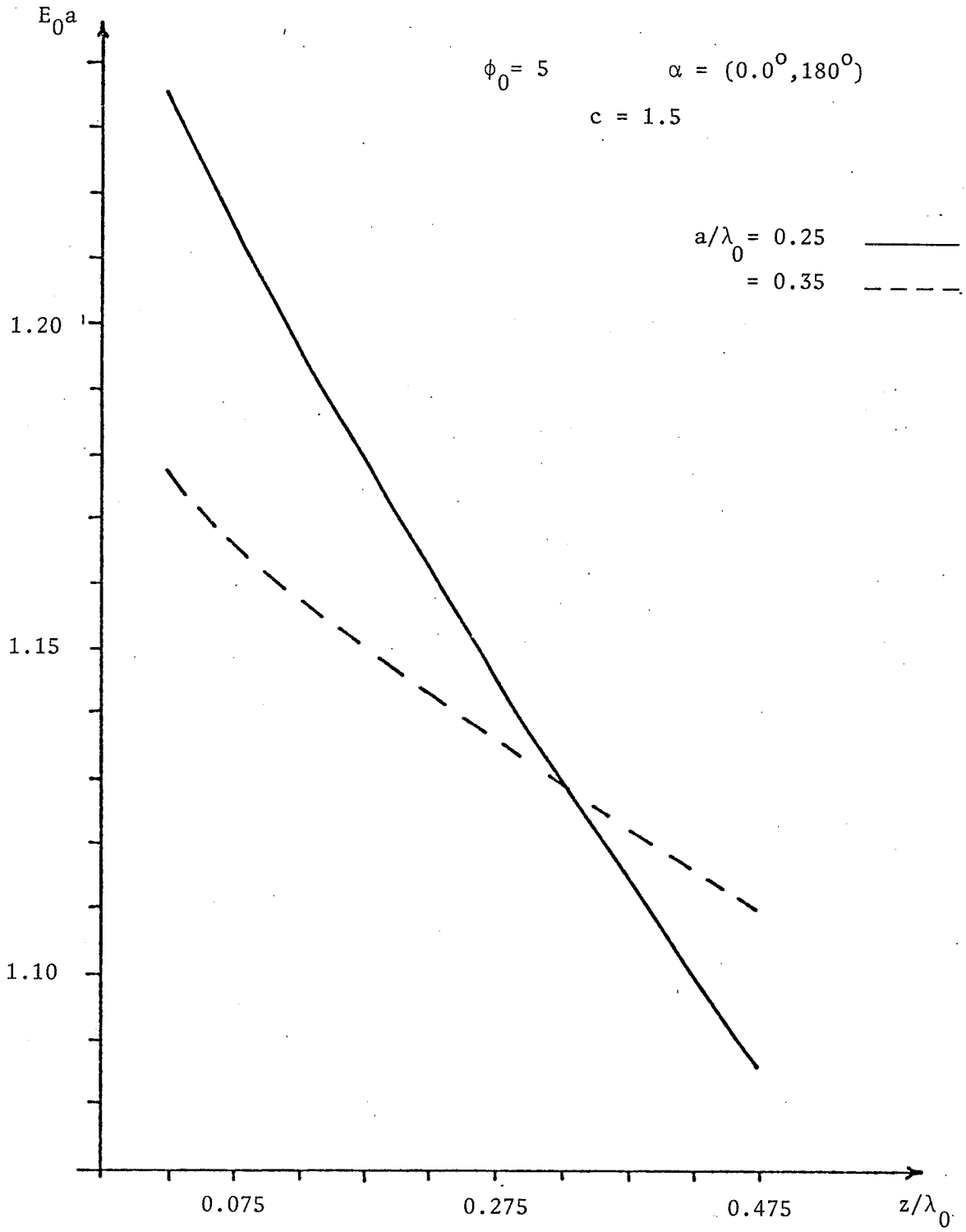

Fig. 4.11 . Slot tangential field E_0 versus the distance z along the slot. Symmetrically double slotted coaxial guide with different operating wavelength.

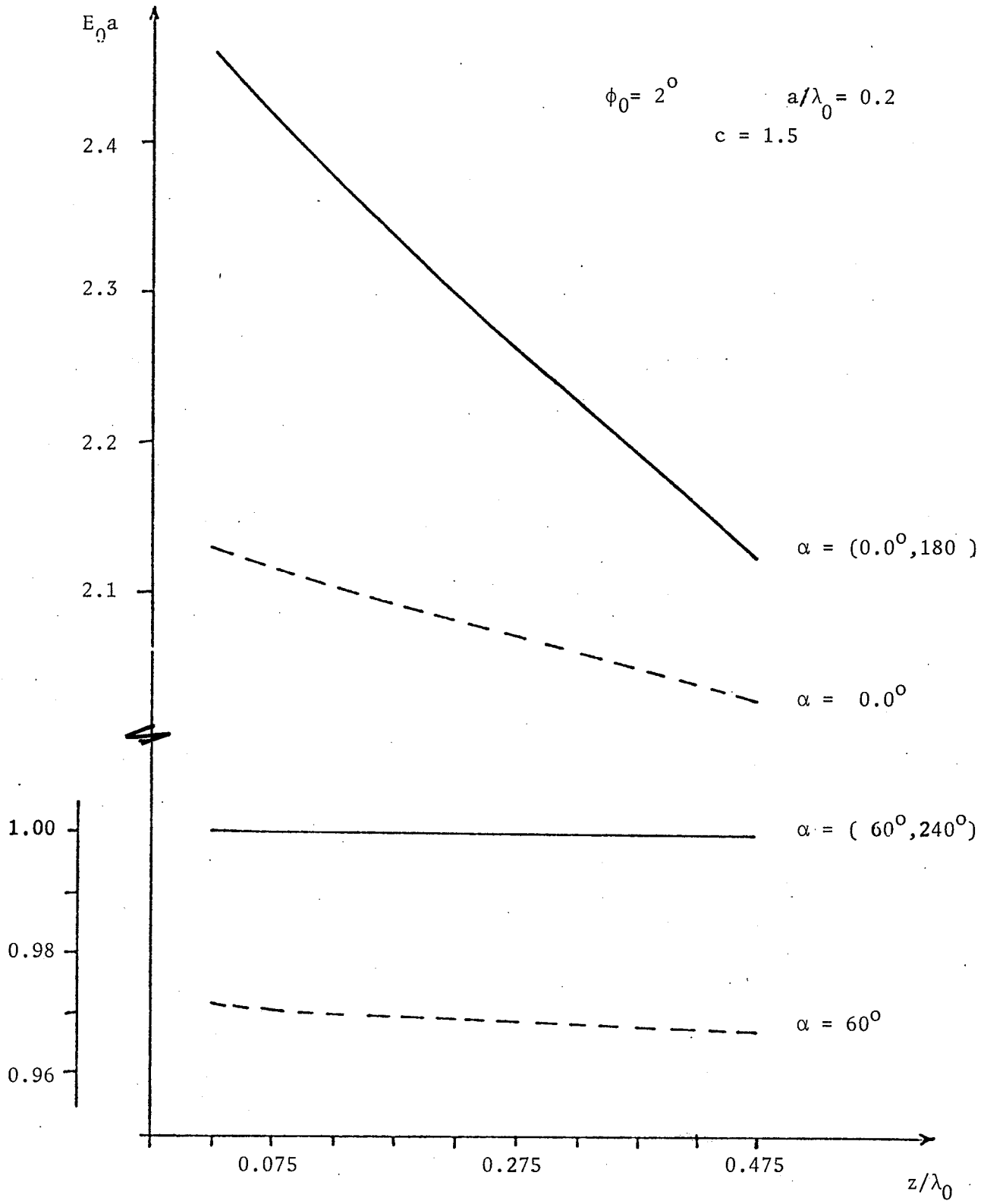

Fig. 4.12. The slot field for both single and double slotted coaxial guide.

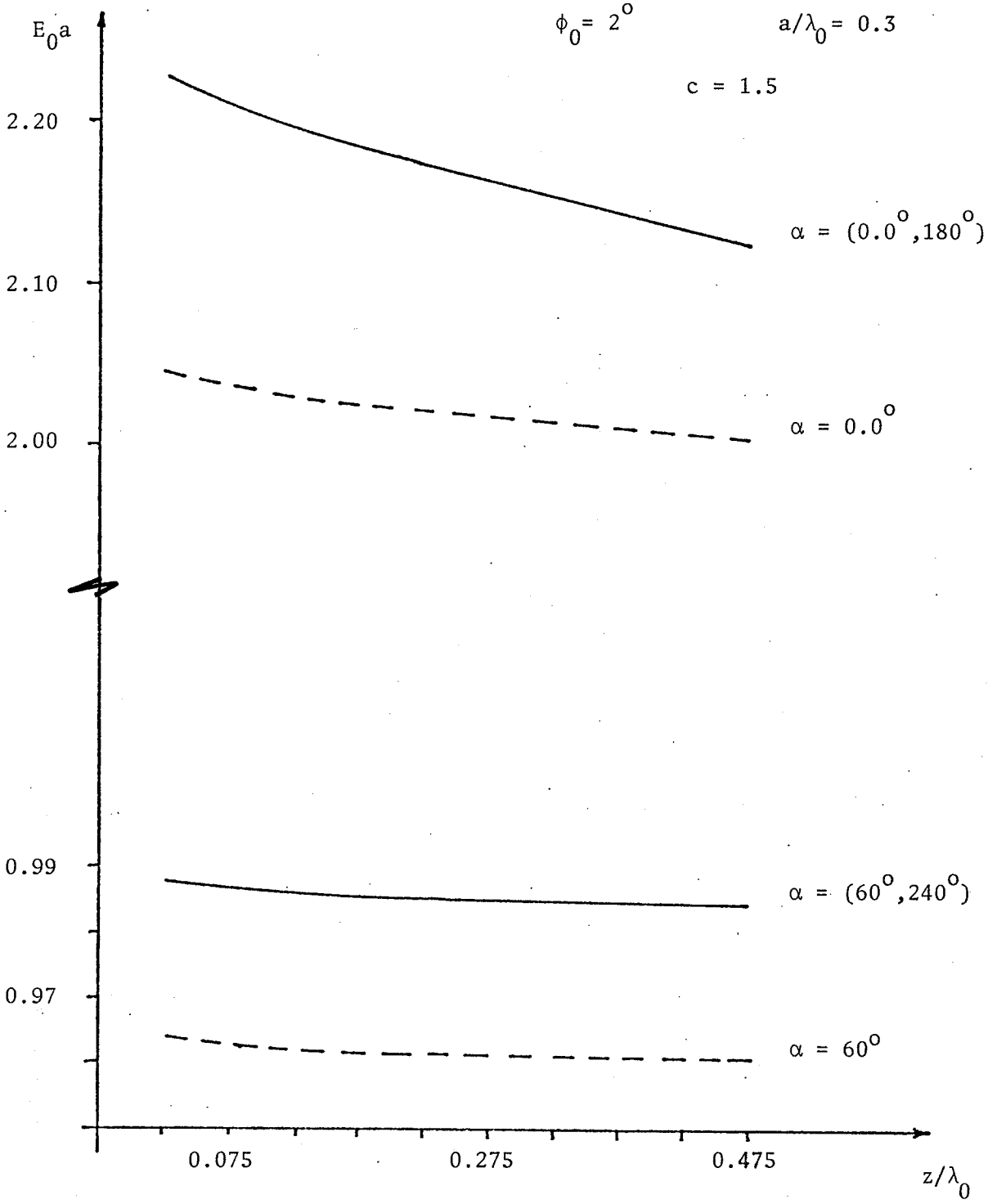

Fig. 4.13 . The slot field for both single and double slotted coaxial guide.

intensity. Referring to Fig. (4.12) we notice that when another slot is introduced at $a/\lambda_0=0.2$ and $\alpha = 0.0$, the field changes by an average of about 8%. This change reduces to about 3% for $\alpha = 60°$. The change also decreases slightly as a/λ_0 increases (i.e. as the slot field decreases). These results show that the interaction between slots in coaxial lines is sometimes appreciable and should not be neglected.

In conclusion, the work of this Chapter covers the determination of the possible propagating modes and the slot field of a single or doubly slotted coaxial line for a TE_{11} coaxial mode excitation. The coaxial waveguide is an important element in microwave communications, and the results of this Chapter may prove to be useful in analyzing leaky wave antennas supported by periodically spaced slots, or coaxial slotted lines as multiple feeds for reflectors.

Now that the field on the slot(s) for both hollow and coaxial waveguides has been determined, one may proceed to study the radiation due to these slots. This analysis as well as the possible utilization of the results are the main study objectives of the following Chapter.

CHAPTER V

RADIATION CHARACTERISTICS OF SINGLE AND CASCADED SLOTTED SECTIONS

The main objective of this Chapter is to investigate the radiation characteristics of the axially slotted waveguide structure from the slot tangential field as generated by an incident waveguide mode. There are many published works which deal with solving this type of external boundary value or radiation problem [33], [35]. However, the slot field is always assumed to be known. This assumption may not be accurate in cases which attempt to utilize the slotted waveguide or coaxial line as a feed system for reflectors or radiating elements, since the true pattern is still unkown. In Chapters 3 and 4 , the field on the surface of a narrow semi-infinite slot on a hollow or coaxial waveguide was obtained. Practically, any slot on the waveguide surface has a finite length. The field on the surface of a finite slot may be different from the semi-infinite case studied in the previous Chapters. Therefore, for a more accurate radiation characteristic, the modified field due to the slot finiteness has to be investigated first. Once this field is obtained, the radiation characteristics can be determined easily through the well known techniques [33], [35] , [53].

In this Chapter, the field on the finite slots is investigated for both the hollow and the coaxial waveguide. The problem is solved approximately by including the reflections at the slot ends and retaining only the first order reflection at the far end of the slot. This

approximation is a reasonable one as long as the slot length is sufficiently long. The reflections contribute to the slot field according to the magnitude and phase of the reflected waves. The analysis follows the same steps of Chapters 3 and 4 where different wave functions with unknown coefficients are assumed on both the slotted and the closed sections of the waveguide. These coefficients are later obtained by matching the tangential field components at planes separating the two waveguide sections. The slot field is then obtained by using the method of Sec.(3.5)and Sec.(4.5). Once the analysis of the finite slot field is completed, the radiation characteristics of a single or doubly slotted waveguide section can be obtained by using well known relationships. The remaining part of this Chapter is devoted to this analysis and for investigating the effect of different slot and waveguide parameters on this radiation pattern. The technique adopted here follows closely that of Tyras [53] for the treatment of an aperture on an infinite circular cylinder. Since, in the radiation problem, the boundary conditions for both the coaxial line and the waveguide are identical, the treatment of the problem, as presented here, covers both cases.

The objective of this Chapter could be divided into two different, but inseparable problems. These are the determination of the finite slot field and investigation of the radiation patterns of that field. The following Section is devoted completely to the study and discussion of the field on a finite slot. The analysis of the other problem, i.e of the radiation characteristics, will follow in a later Section.

5.1 Field on a Finite Slot

In the treatment of the axially slotted guide in both Chapters 3 and 4 , the slot is assumed to be narrow and infinitely long. From a practical point of view, any slot always has a finite length. This fact introduces additional complexity to the problem. At each end of the slot the wave is partially reflected back, which modifies the slot field according to the phase and magnitude of the reflected field. Moreover, if the slot is too short TM_{nm} modes may be generated, in addition to the existing TE_{nm} modes. The problem is greatly simplified, however, if the slot is long and narrow. In this case, the mode coupling is unlikely to be appreciable and the field remains essentially TE in accordance with the excitation [24]. The reflections at each end of the slot however, remain and regardless of the slot dimension may not be neglected. This is especially true near the cut-off frequency, where the reflection coefficient has an appreciable value, as shown in Sec. (3.4.4) and Sec. (4.4.4). It will be assumed, however, that the slot length is large enough so that only the first order reflection at the far end need be considered. That is, all other reflections can be neglected without significantly affecting the slot field.

In this Section, the finite slot field for both hollow and coaxial guide is studied assuming that the slot is long enough to suppress mode coupling. The reflection coefficients at the far end of the slot are calculated by matching the field in the slotted and closed waveguide sections in a manner similar to the analysis of Chapters 3 and 4. The reflected field is added to the previously calculated field

in the slotted section to give the total slot field. In a later Section the resulting standing wave pattern of the field is presented and is analyzed.

5.1.1 Formulation and Field Solution

Let a dominant TE_{11} mode be incident from region I toward region II in the slotted circular waveguide shown in Fig. 5.1 . Let the

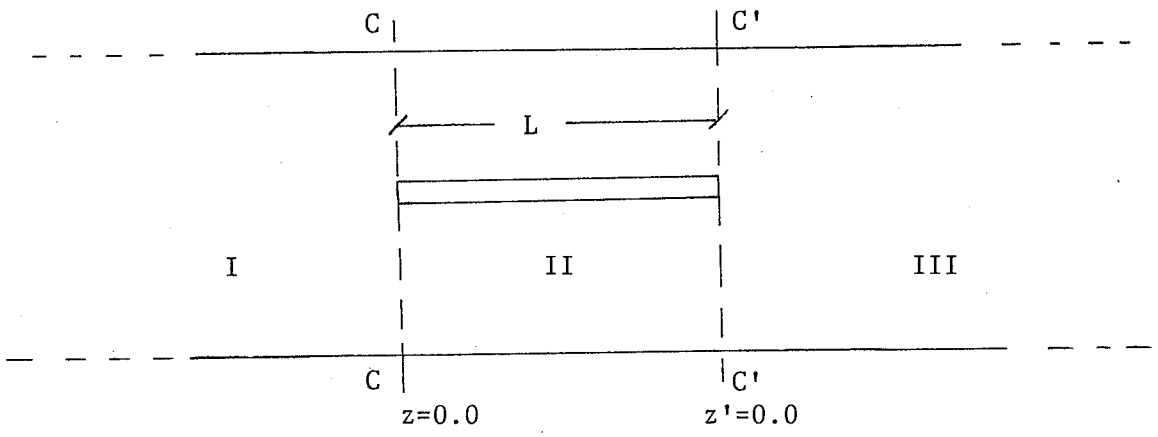

Fig. 5.1 Finite axially slotted waveguide

mode function of the incident field be given by eqn. (3.21), which takes the form

$$\phi^i = T.J_1(x_{11}\rho/a)\cos\phi \exp(j\theta_{11}z) \qquad (5.1)$$

where T is the amplitude of the incident wave function, x_{11} is the first root of $J_1'(z) = 0$ and

$$\theta_{11}^2 = K_0^2 - (x_{11}/a)^2$$

Let the reflected mode function ϕ^r (in region I) and the transmitted mode functions ψ^t (in region II) be given, respectively, by

$$\phi^r = T \cdot \sum_{n=0}^{\infty} \sum_{m=1}^{\infty} B_{nm} J_n(x_{nm}\rho/a) \cos n\phi \exp(-j\theta_{nm} z) \tag{5.2}$$

$$\psi^t = T \cdot \sum_{n=0}^{\infty} \sum_{m=1}^{\infty} A_{nm} J_n(K_\rho \rho) \cos n\phi \exp(-\gamma_{nm} z) \tag{5.3}$$

where B_{nm} and A_{nm} are constants.

From these wavefunctions, the field components in region I and II are obtained using eqn. (3.26). In the analysis of Chapter 3, the coefficients B_{nm} and A_{nm} were obtained, and the slot field was shown to be

$$E_\phi(a,\phi,z) = \frac{1}{\phi_0 J_0(\phi_0) N \cos\alpha} \cdot \frac{\sum_{m=1}^{\infty} A_{1m} K_{\rho_{1m}} J_1'(K_{\rho_{1m}} a) \exp(-\gamma_{1m} z)}{\sqrt{1 - \left(\frac{\phi - \alpha}{\phi_0}\right)^2}} \tag{5.4}$$

The field in region II will continue to propagate as a summation of different modes, each with a different attenuation constant as given by eqn. (5.3). If the slot length is not too short, all but the first mode will vanish as the wave approaches the plane C' - C' (see Fig. 5.1). Introducing the coordinate transformation

$$z = z' + L$$

where L is the slot length. This transfers the origin from the plane C - C to the plane C' - C'. In this case one may write an expression

for the first mode in region II as

$$\phi'^{i} = T'J_1(K_{\rho 11}a)\cos\phi\, e^{-\gamma_{11}z'} \tag{5.5}$$

where $T' = T \cdot A_{11}\exp(-\gamma_{11}sL)$. This first mode could now be considered as an incident mode from region II toward region III. Let the reflected wave function ϕ'^{r} in region II and the transmitted wave function ψ'^{t} in region III be given, respectively, by

$$\phi'^{r} = T' \cdot \sum_{n=0} \sum_{m=1} A'_{nm} J_n(K_\rho \rho)\cos n\phi \exp(\gamma_{mn}z') \tag{5.6}$$

$$\psi'^{t} = T' \cdot \sum_{n=0} \sum_{m=1} B'_{nm} J_n(x_{nm}\rho/a)\cos n\phi \exp(j\theta_{nm}z') \tag{5.7}$$

where A'_{nm} and B'_{nm} are constants to be determined. Now, using eqn. (3.26) the field components in both regions II and III can be obtained. The tangential components of these fields are matched at $z=0$. Employing the proper orthogonalities among the mode functions, and following the same steps as those of Chapter 3, one may arrive at the following two equations:

$$-B'_{nm} M^{\pm}_{nm} = \sum_{s=1}^{\infty} A'_{ns} Q^{\pm}_{nsm} + Q^{\pm}_{11m} \tag{5.8}$$

and

$$B'_{nm} M^{-}_{nm} = \sum_{s=1}^{\infty} A'_{ns} N_{nms} - N_{1m1} \tag{5.9}$$

where $M^{\pm}_{nm}$, $Q^{\pm}_{nsm}$ and N_{nms} are given by eqns. (3.36), (3.44) and (3.39), respectively. In order to obtain the slot field, one need only consider

the case $n = 1$ of both (5.8) and (5.9). For the modes $n \neq 1$ the excitation is zero and, as shown previously, the respective coefficients are not needed to solve for the slot field. Solving equations (5.8) and (5.9) for the $n = 1$ case by eliminating the coefficients B'_{1m} and truncating the infinite series after an appropriate number of terms L gives

$$\begin{bmatrix} (Q^-_{111} + N_{111}) & \cdots & (Q^-_{1L1} + N_{11L}) \\ \vdots & & \vdots \\ (Q^-_{11L} + N_{1L1}) & \cdots & (Q^-_{1LL} + N_{1LL}) \end{bmatrix} \begin{bmatrix} A'_{11} \\ A'_{12} \\ \vdots \\ A'_{1L} \end{bmatrix} = \begin{bmatrix} (N_{111} - Q^-_{111}) \\ (N_{121} - Q^-_{112}) \\ \vdots \\ (N_{1L1} - Q^-_{11L}) \end{bmatrix} \tag{5.10}$$

Upon solving eqn. (5.10) by simple matrix inversion, the coefficients $A'_{11}, A'_{12}, \ldots A'_{1L}$ of the reflected field in region II are obtained. Substituting these coefficients in either (5.8) or (5.9) for the $n = 1$ case, the transmission coefficients in region III, i.e. B'_{11}, B'_{12} . . . can also be obtained. Having determined the coefficients A'_{1m}, one can easily find the slot field by following the same steps as those of Section (3.4.4). It is simple to show that this field takes a form similar to eq. (3.26) and is given by

$$E^r_\phi(a,\phi,z) = \frac{T'}{\phi_0 J_0(\phi_0) N \cos\alpha} \frac{\sum_{m=1}^{\infty} A'_{1n} K'_{\rho_{1m}} J'_1(K_{\rho_{1m}} a) \exp(\gamma_{1m} z')}{\sqrt{1 - \left(\frac{\phi - \alpha}{\phi_0}\right)^2}} \tag{5.11}$$

where $z' = z - L$ and $T' = T.A_{11}\exp(-\gamma_{11} L)$.

The total slot field $E_s(a,\phi,z)$ is obtained by adding (5.4)and(5.11) and is given by

$$E_s(a,\phi,z) = \frac{T}{\phi_0 J_0(\phi_0) N \cos\alpha} \frac{1}{\sqrt{1 - (\frac{\phi - \alpha}{\phi_0})^2}} \{ \sum_{m=1} A_{1m} K_{\rho_{1m}} J_1'(K_{\rho_{1m}} a) \cdot$$

$$\exp(-\gamma_{1m} z) + A_{11} \exp(-\gamma_{11} L) \sum_{m=1}^{\infty} A_{1m}' K_{\rho_{1m}} J_1'(K_{\rho_{1m}} a) \cdot$$

$$\exp(-\gamma_{1m}(L - z))\} \qquad (5.12)$$

where $N = 1$ for a single slot

$N = 2$ for two diagonally symmetrical slots.

The analysis for the coaxial guide is similar to the above method and uses the results of Chapter 4. Carrying out this analysis, one easily arrives at two equations similar to eqns. (5.8) and (5.9) but in this case M_{nm}, $Q^{\pm}_{nsm}$ and N_{nms} are given by eqns. (4.31), (4.38) and (4.34), respectively. Here again the $n = 1$ mode is sufficient to solve for the slot field, therefore one needs only to determine the coefficients A_{1m}' and B_{1m}'. These coefficients are found by solving the two equations in a way similar to the procedure followed in Chapter 4. Once the coefficients A_{1m}' are known, the slot field according to Section(4.5) can be shown to be

$$E^r_{\phi}(b,\phi,z) = \frac{T'}{\phi_0 J_0(\phi_0) N \cos\alpha} \frac{\sum_{m=1}^{\infty} A_{1n}' D_1'(K_{\rho_{1m}} b) \exp(\gamma_{1m} z')}{\sqrt{1 - (\frac{\phi - \alpha}{\phi_0})^2}}$$

(5.13)

where $z' = z - L$ and $T' = T A_{11} \exp(\gamma_{11} L)$.

The total slot field $E_s(b,\phi,z)$ is obtained by adding eqn.(4.57) and (5.13), and is given by

$$E_s(b,\phi,z) = \frac{T}{\phi_0 J_0(\phi_0) N \cos\alpha} \frac{1}{\sqrt{1 - (\frac{\phi - \alpha}{\phi_0})^2}} \{ \sum_{m=1} A_{1m} D'_1(K_{\rho_{1m}} b) \exp(-\gamma_{1m} z) + A_{11} \exp(-\gamma_{11} L) \sum_{m=1}^{\infty} A'_{1m} D'_1(K_{\rho_{1m}} b) \exp(-\gamma_{1m}(L - z)) \} \quad (5.14)$$

where $N = 1$ for a single slot,

$= 2$ for two diagonally symmetrical slots.

Equations (5.12) and (5.14) give the field on the surface of a finite slot of length L due to an incident TE_{11} mode. The results, as presented in the next Section show a standing wave pattern on the slot with a phase velocity that varies primarily with the operating frequency. This result, as well as the different factors affecting the field pattern, is discussed in the following Section.

5.1.2 Numerical Results of the Finite Slot Fields

The slot electric field, given by eqn.(5.12), (5.14) is evaluated for different slot length, width and ratio a/λ_0. Some of the results are given in Figs. 5.2 - 5.11. The graphs clearly reveal that the wavelength λ_s of the slot field, which is double the distance between any two successive maxima or minima, is always greater than the wavelength

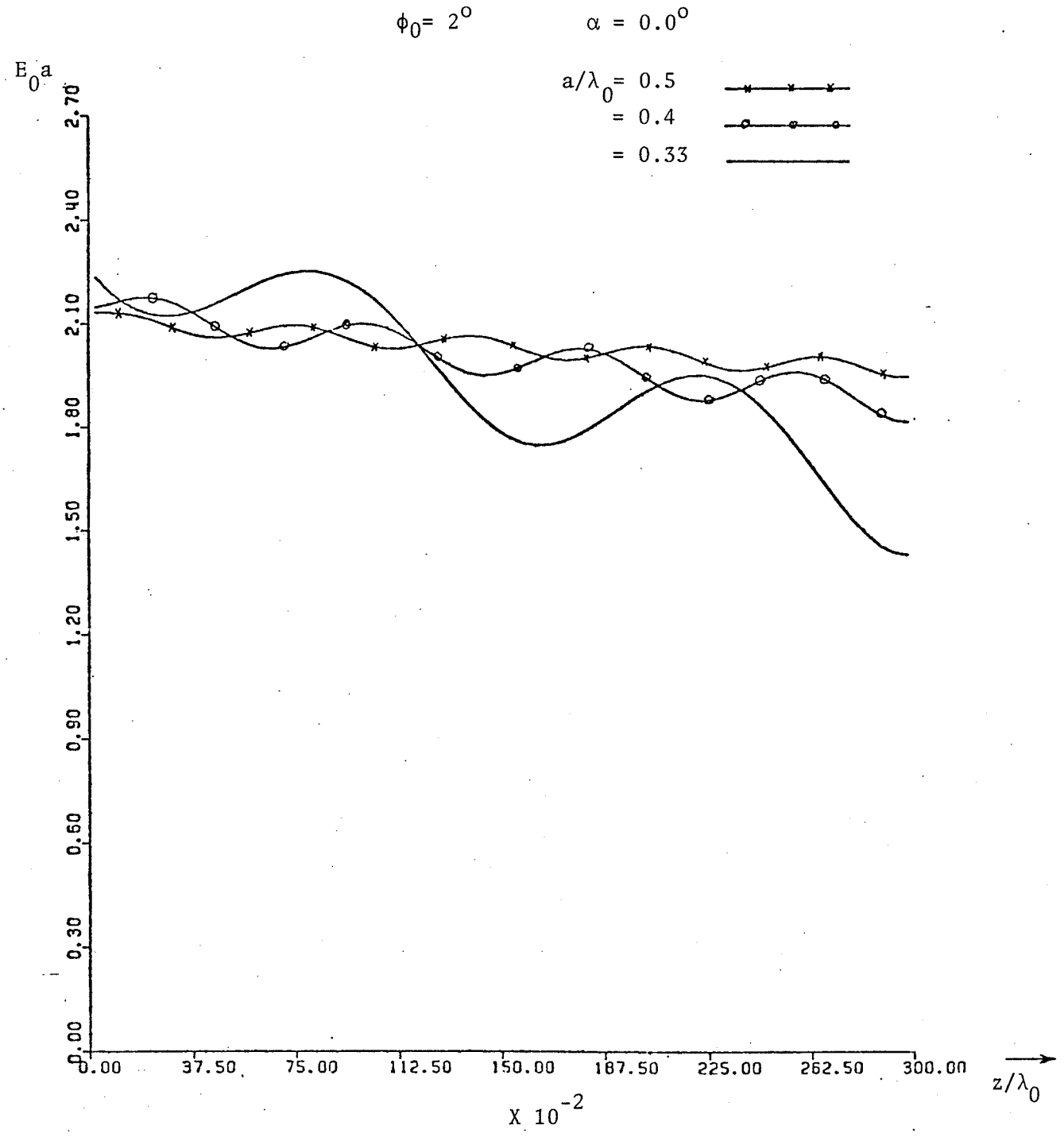

Fig. 5.2 . Tangential field E_0 on a finite slot of length 3 λ_0 , $\phi_0 = 2^o$. Single slotted waveguide.

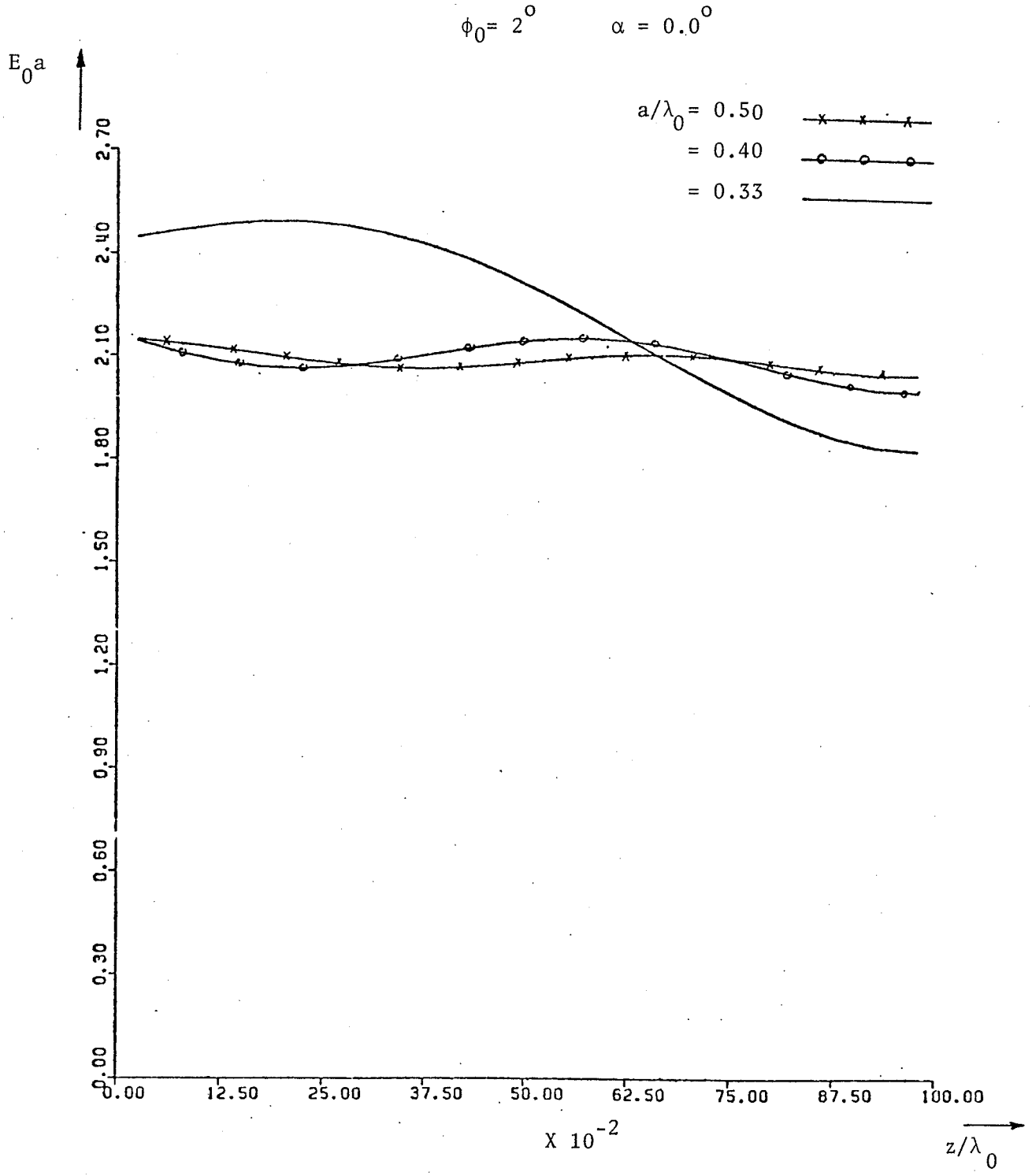

Fig. 5.3 . Tangential field E_0 on a finite slot of length λ_0 , ϕ_0 = 2°. Single slotted waveguide.

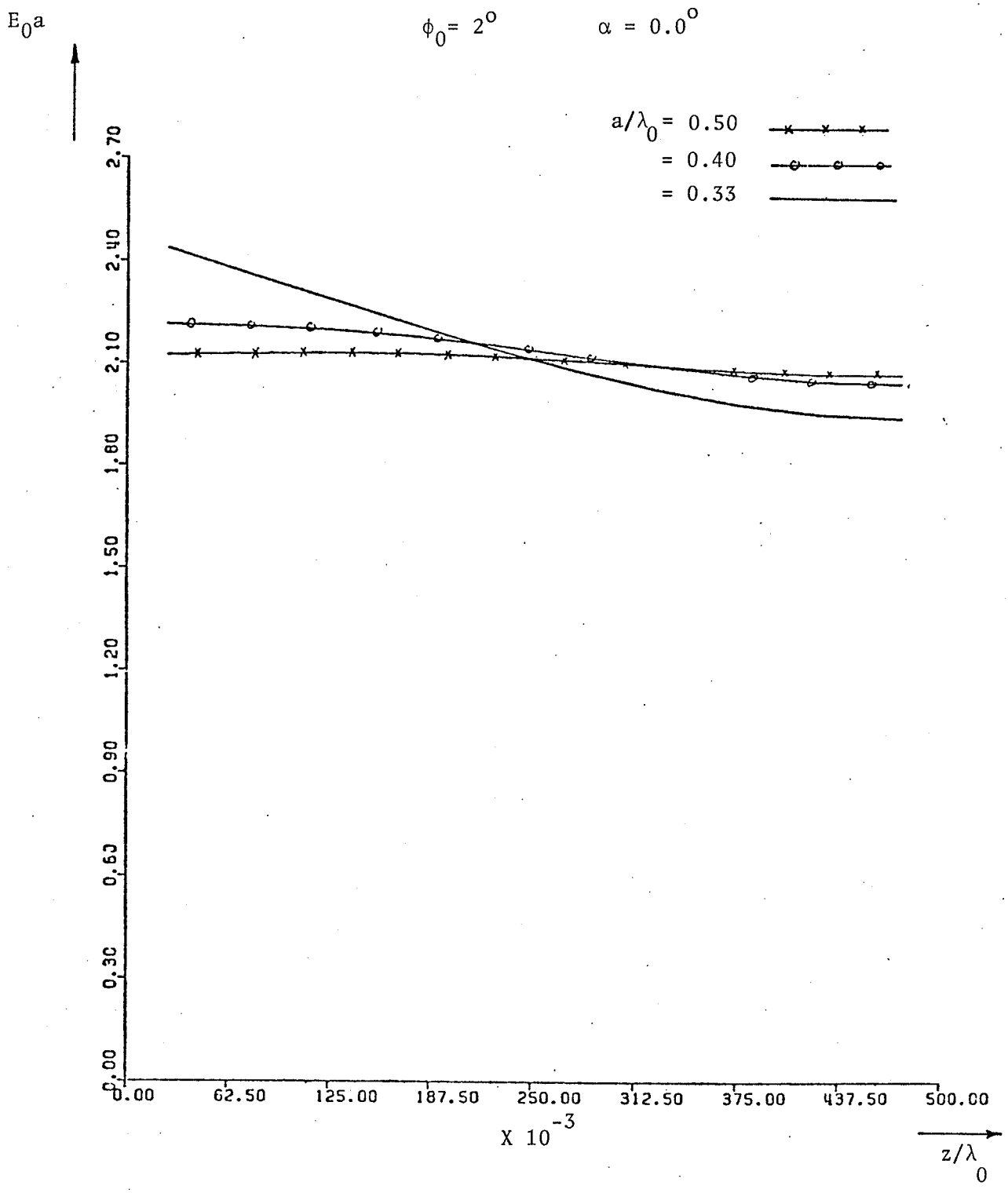

Fig. 5.4 . Tangential field E_0 on a finite slot of length $0.5\lambda_0$, $\phi_0 = 2^o$ Single slotted waveguide.

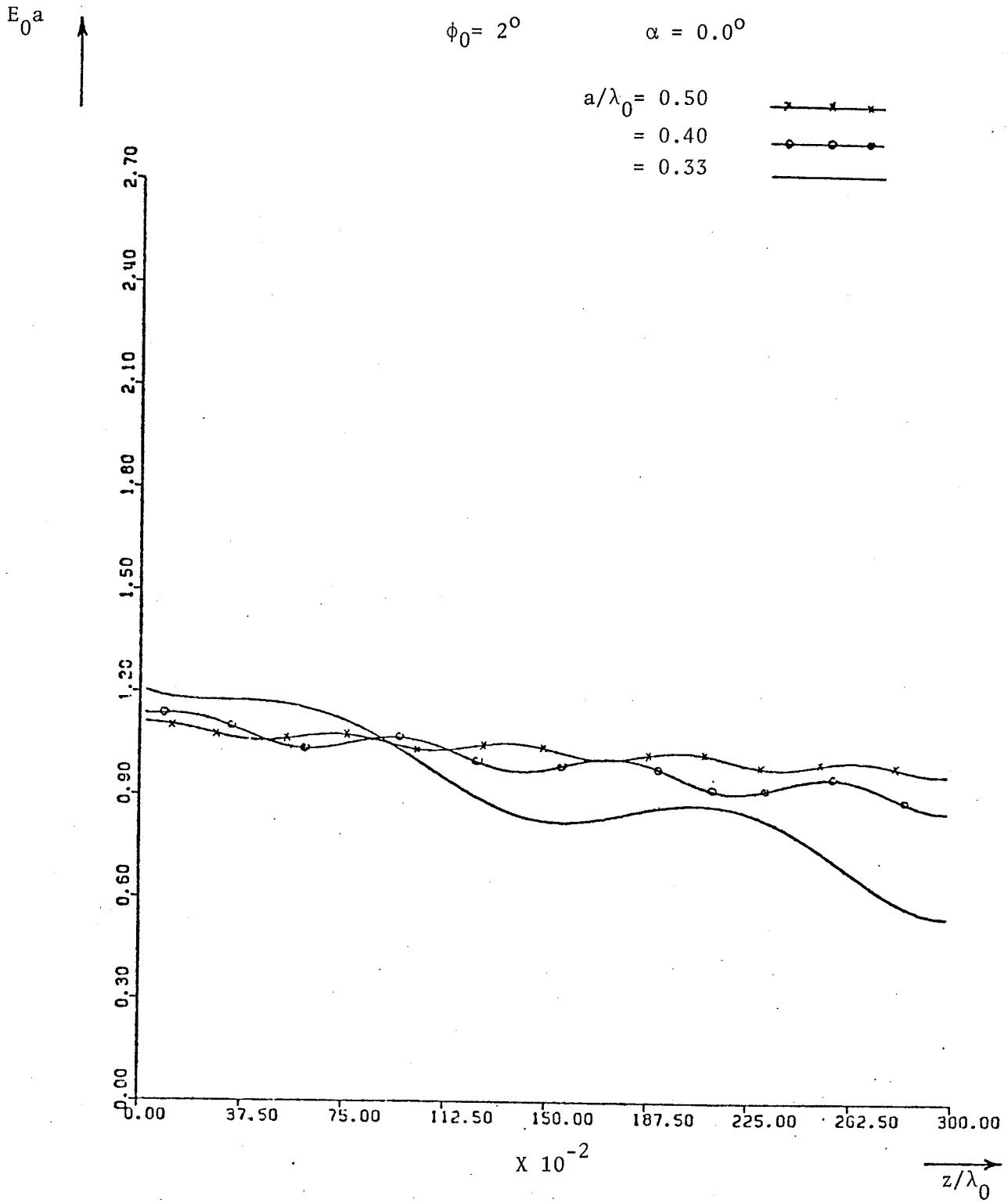

Fig. 5.5 . Tangential field E_0 on a finite slot of length $3\lambda_0$, $\phi_0 = 5^o$. Single slotted waveguide.

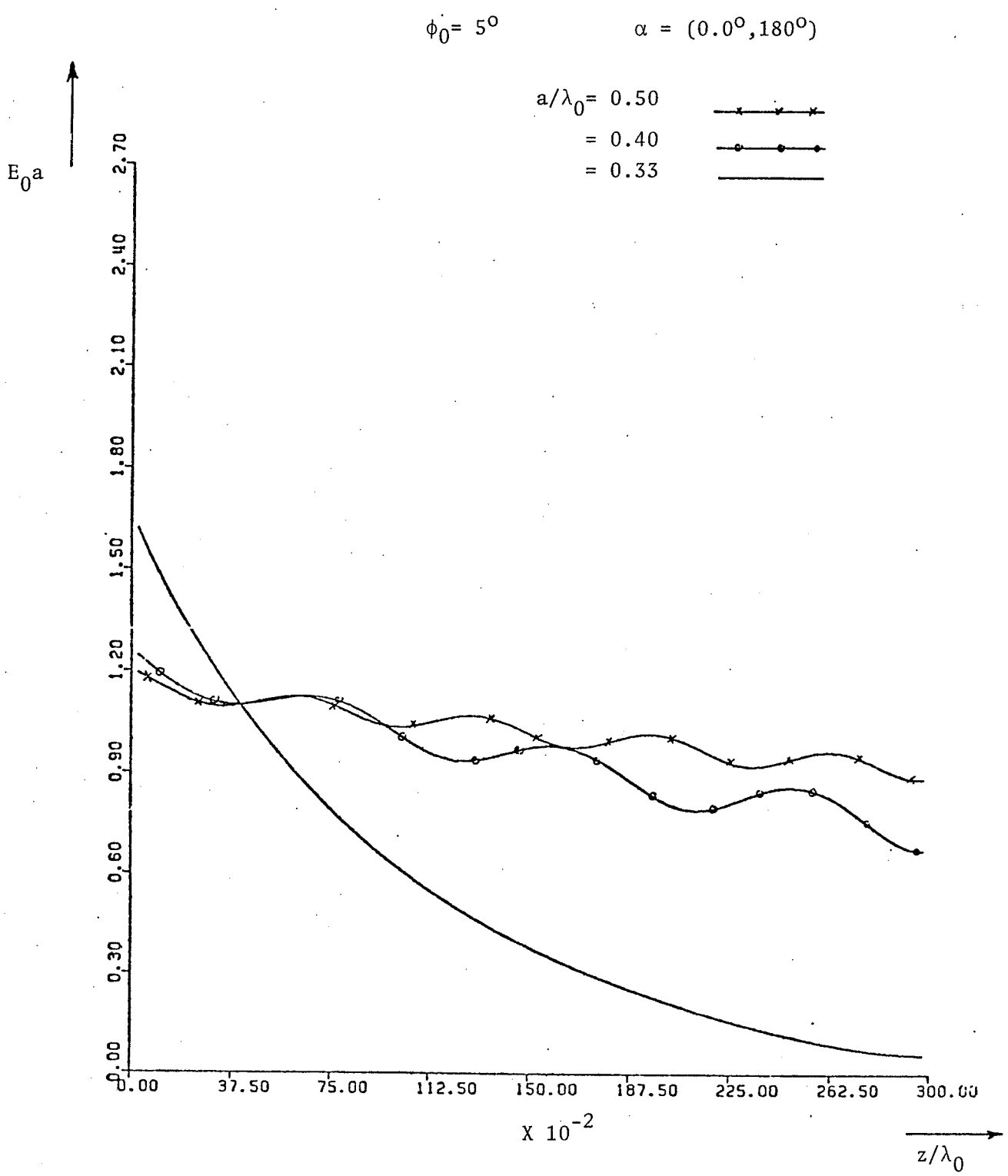

Fig. 5.6 . Tangential field E_0 on a finite slot of length $3\lambda_0$, $\phi_0 = 5^\circ$. Symmetrically double slotted waveguide.

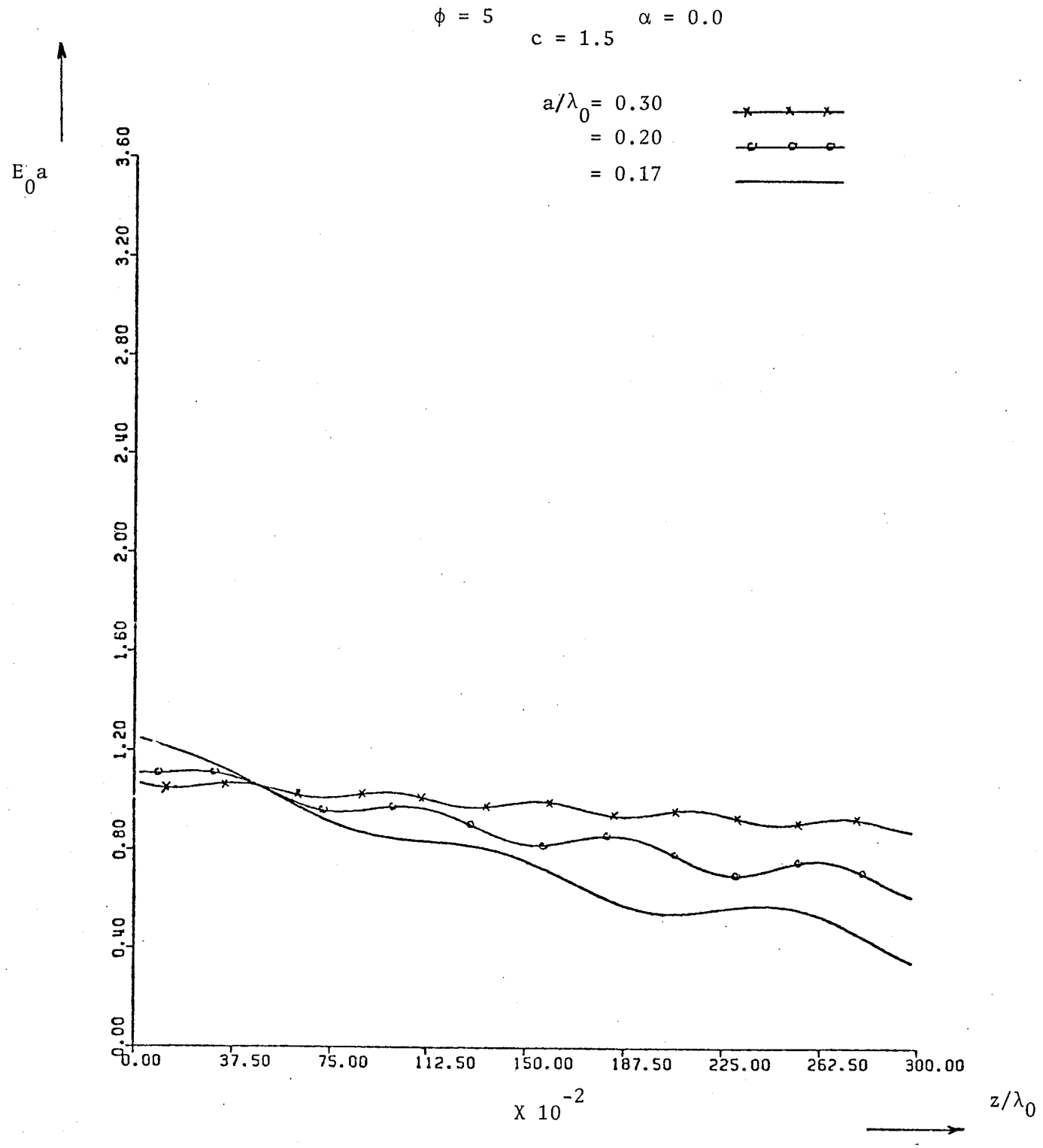

Fig. 5.7 Tangential field E_0 on a finite slot of length $3\lambda_0$, $\phi_0 = 5^o$. Single slotted coaxial line.

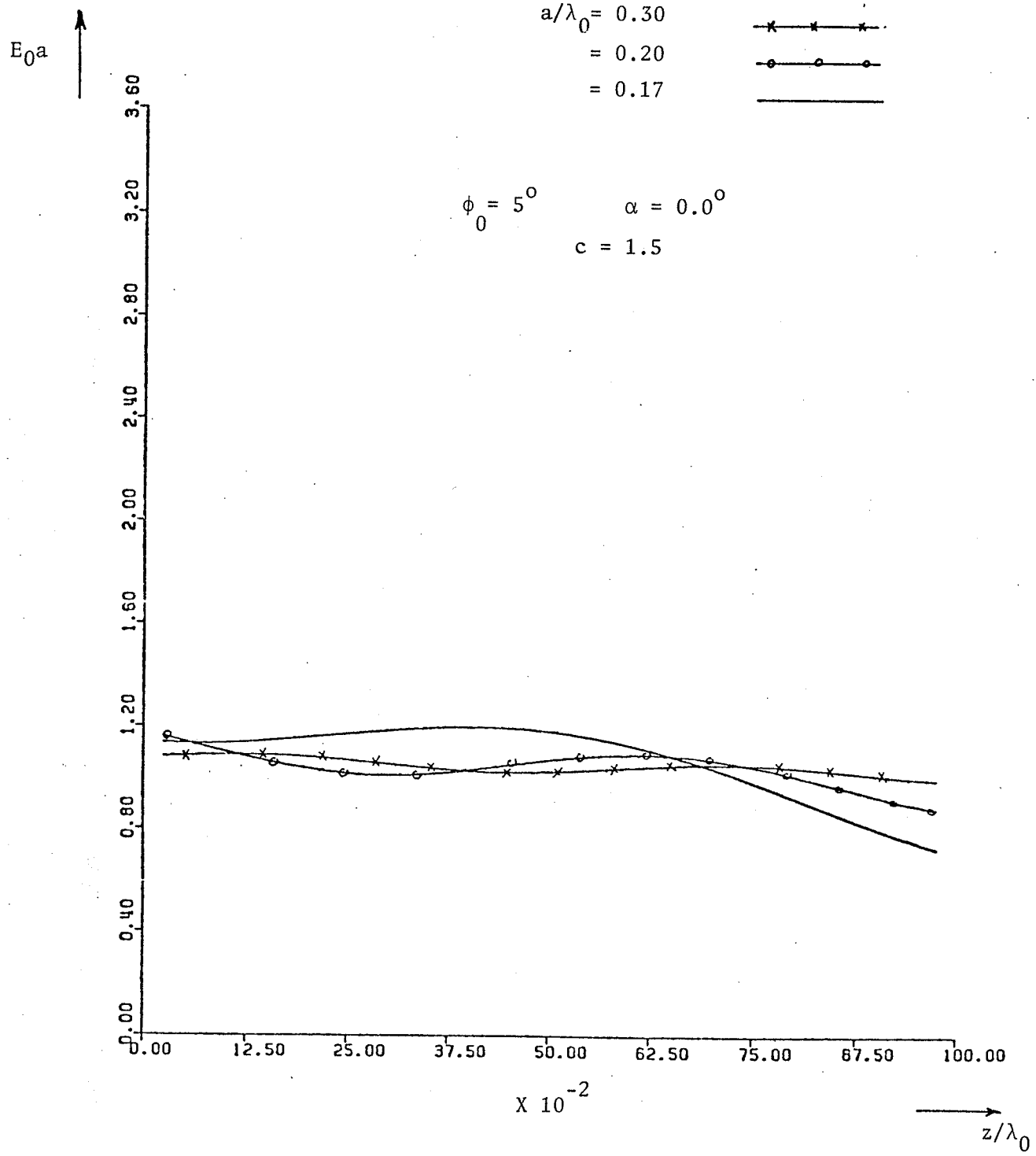

Fig. 5.8 . Tangential field E_0 on a finite slot of length λ_0 , $\phi_0 = 5^o$. Single slotted coaxial line.

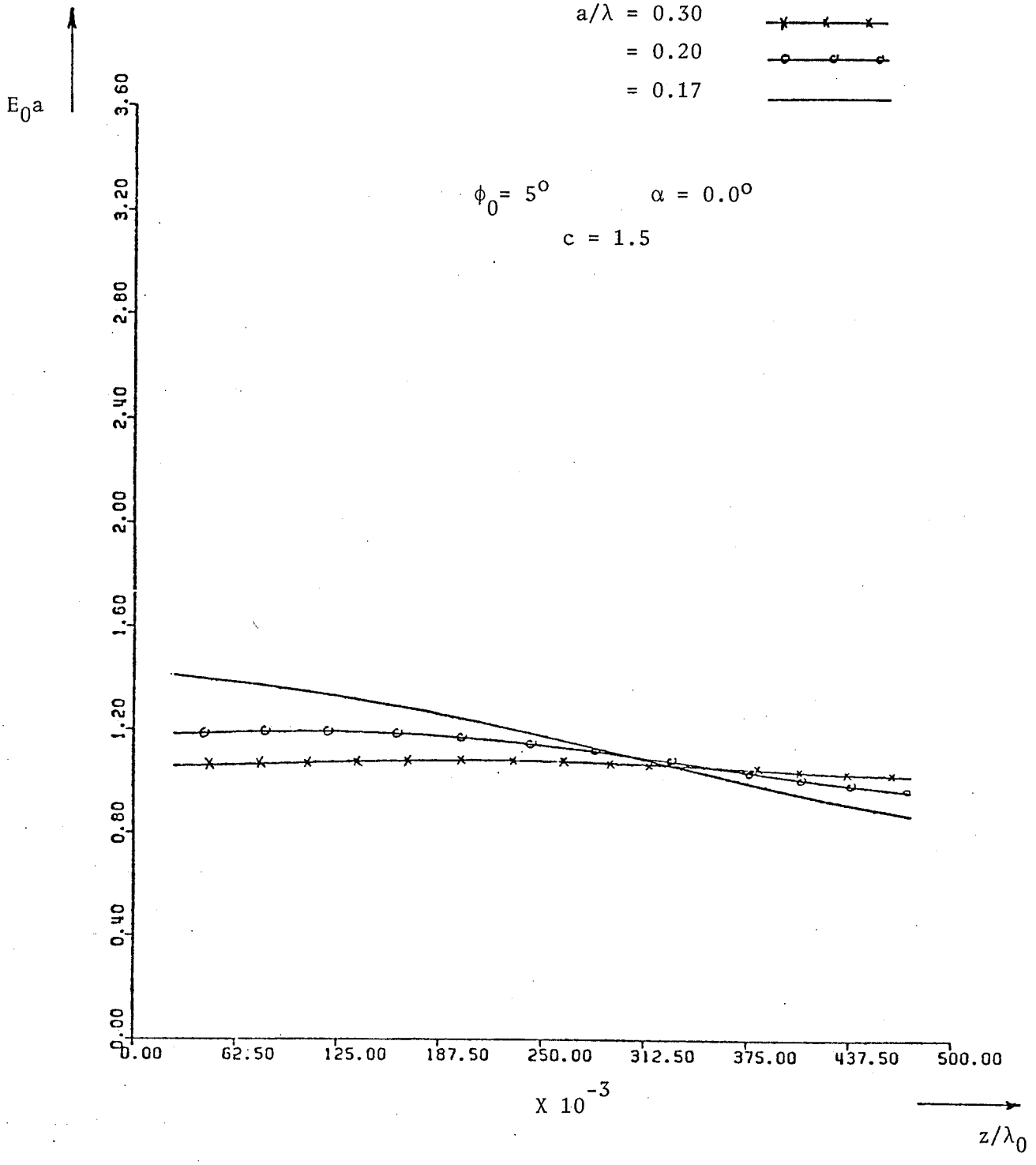

Fig. 5.9 . Tangential field E_0 on a finite slot by length 0.5 λ_0, $\phi_0 = 5^o$ Single slotted coaxial line.

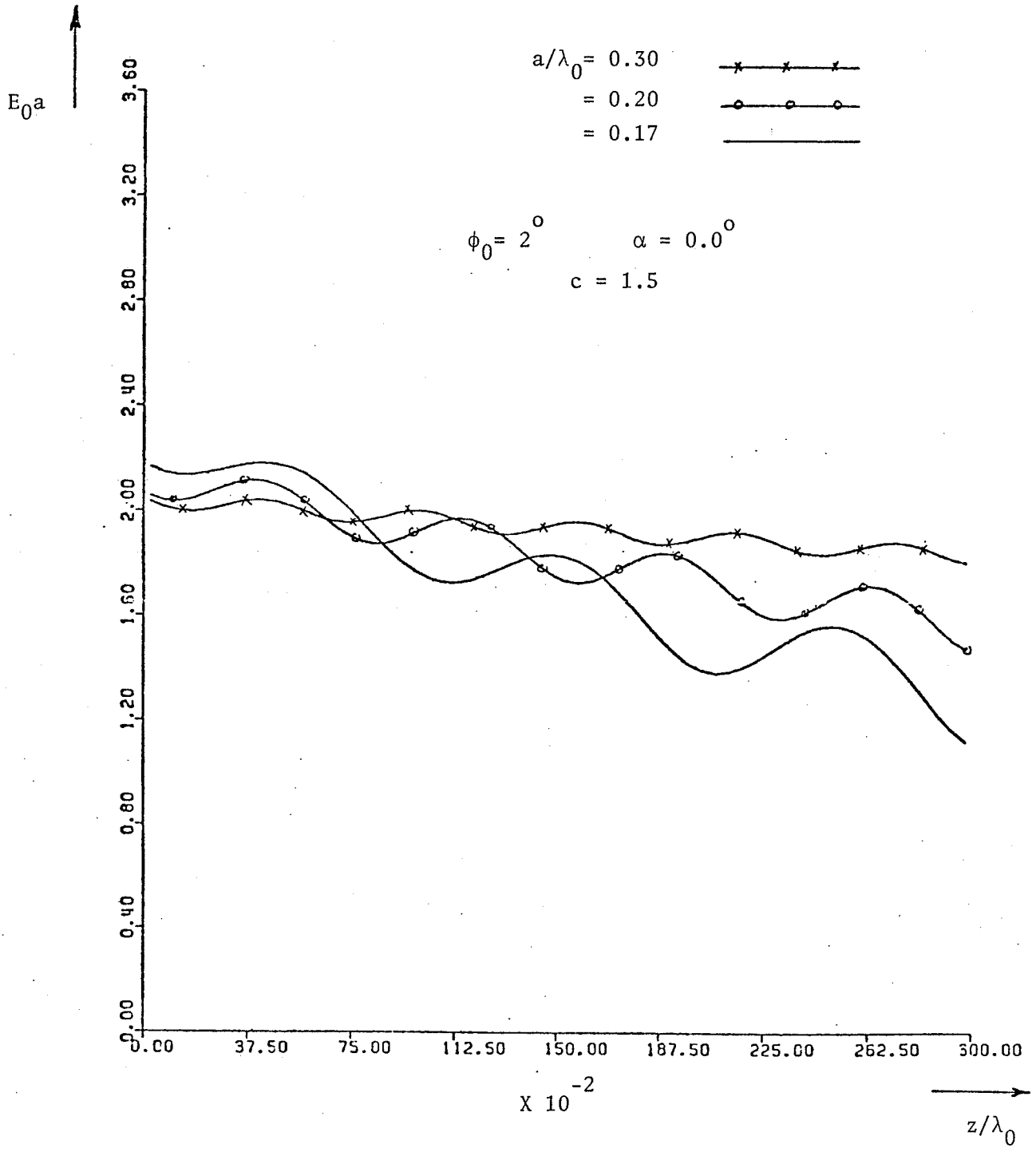

Fig. 5.10. Tangential field E_0 on a finite slot of length $3\lambda_0$, ϕ_0= 2° Single slotted coaxial line.

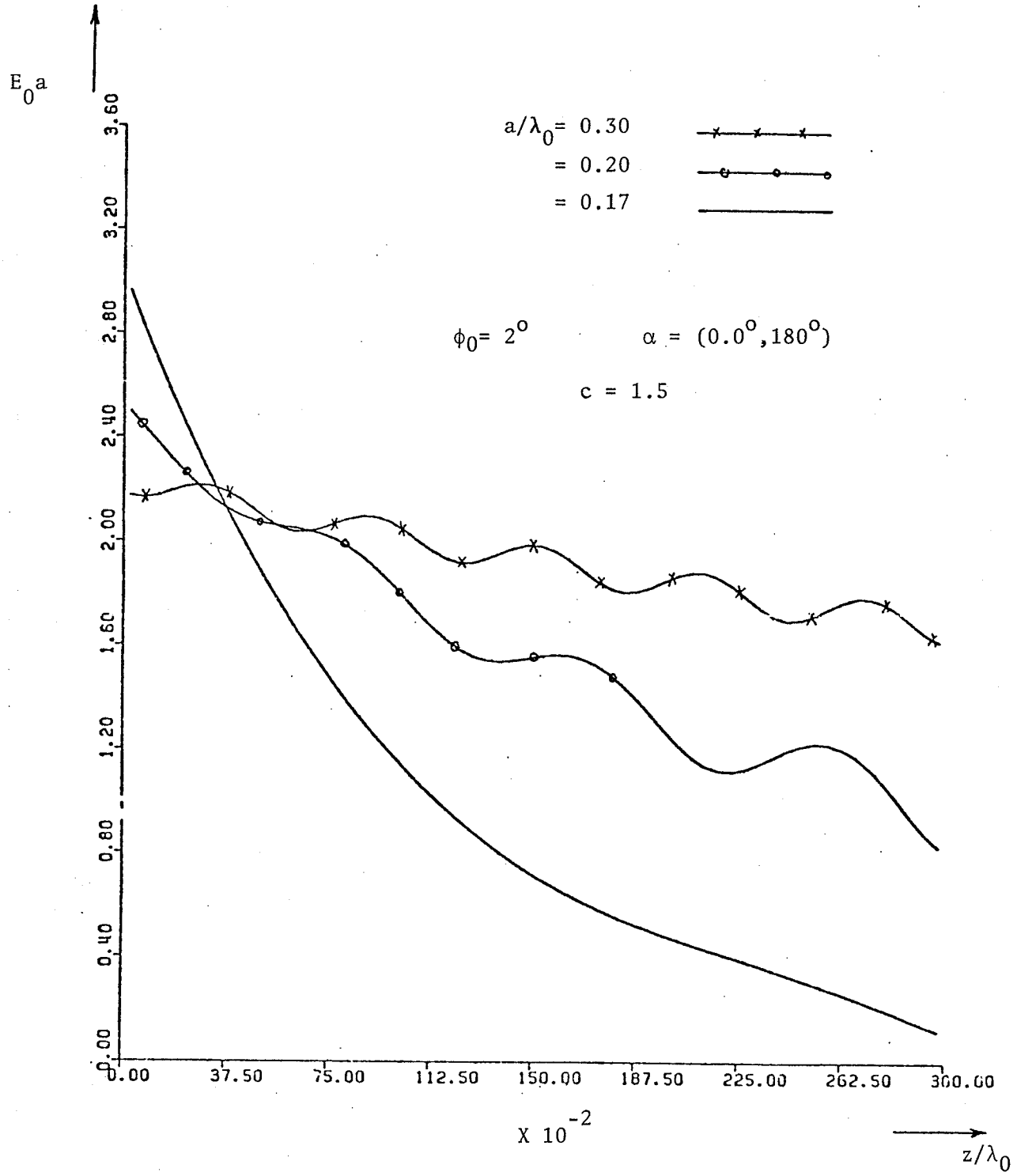

Fig. 5.11 . Tangential field E_0 on a finite slot of length $3\lambda_0$, $\phi_0 = 2^o$. Double symmetrically slotted coaxial guide.

of the operating frequency λ_0. This shows that the wave is a fast wave propagating with a phase velocity faster than the velocity of light. This comes as a direct result of the leaky wave nature of the field, where there is always a power flow away from the structure [14], [15], [28]. The figures show that as a/λ_0 approaches that of the cut-off frequency, the waves become faster as indicated by the longer wavelength λ_s. This implies that more power is radiated into the free space. This phenomenon was noticed before in Section (3.3.2) and Section (4.3.2) where it was shown that the field interior to the slotted waveguide is attenuated faster as a/λ_0 decreases. This fast attenuation of the field indicates more power radiation outside the structure. Further, comparing Figs. 5.5 and 5.6 for the slotted hollow waveguide or Figs. 5.19 and 5.11 for the slotted coaxial line, we see that for the double slotted guide the wave is faster than for the single slot case. Again one expects this result, since from Sections (3.3) and (4.3), the attenuation constant in the double slotted guide is higher than that of the single slotted one. The slot width does not seem to have much effect on the velocity of the waves, as is seen by comparing Figs. 5.2 and 5.5 or Figs. 5.7 and 5.10. More power radiation in the wider slot case may be attributed to its larger surface area, as discussed previously in Sections (3.2) and (4.2). One also should point out that the slot length has its influence on the slot field. Figs. 5.2 and 5.3 or Figs. 5.7 and 5.8 show that while the wave velocity is not affected by the slot length, the shape of the field changes. It is, however, interesting to note that for the particular slot length $0.5\ \lambda_0$ (Figs. 5.4 and 5.9) the field varies slowly along the slot and has no ripples. The form of the field in

this case resembles an exponentially decaying wave. This form was noticed in Sections (3.6) and (4.6) when studying the semi-infinite slotted guide. In This case one expects that the radiation characteristics of such a slot excitation are closely related to that of a semi-infinite slot. Here again the analyses and the results of this Chapter are restricted to narrow long slots. In defining a narrow long slot the criterion of Silver [35] introduced before on page 17 may be used. For a practical waveguide of dimension $a/\lambda_0 = 0.35$ and slot width 2^o, the criterion leads to a slot length L determined by $\log_{10}(82\ L)^2 \gg 1$. This determines the limits of validity of the present analyses. The numerical examples presented in this Chapter are merely for the purpose of illustrations.

5.2 Radiation Characteristics of Axial Slots

In this Section the radiation characteristics of the slotted waveguide in free space are studied. These radiation patterns present valuable and important information, especially when the structure is used as a radiating element to meet certain specific requirements. Since the slot field is already known, the radiation problem becomes simple. Application of the technique presented by Tyras [53] will serve to fully determine the far radiation field every where in space. In the following Section the radiation pattern of a single and two symmetrically located slots, as well as that for several successive slotted sections, is analyzed. The variation of the radiation field in both ϕ and θ are plotted and discussed.

5.2.1 Radiation Pattern of a Single and Double Axial Slots

Consider an axially slotted waveguide or coaxial line of infinite length, as shown in Figs. 3.5 and 4.4 , with a TE_{11} mode incident from the closed section (region I in both figures). Let the incident

field be given by eqn. (3.21) for the hollow waveguide and by eqn. (4.18) for the coaxial line. The resulting tangential field on the slot for both cases is given by eqns. (5.12) and (5.14), respectively. These can be written in the form

$$E_s(d,\phi,z) = \frac{1}{\phi_0 J_0(\phi_0) N} \frac{1}{\cos \alpha} \frac{\sum_{q=1} P_q \exp(-\gamma_{1q} z) + \sum_{q=1} P'_q \exp(\gamma_{1q} z)}{\sqrt{1 - (\frac{\phi - \alpha}{\phi_0})^2}} \tag{5.15}$$

where for the hollow waveguide

$$P_q = A_{1q} K_{\rho_{1q}} J'_1(K_{\rho_{1q}} a)$$

and (5.16)

$$P'_q = A_{11} \exp(-\gamma_{11} L) A'_{1q} K_{\rho_{1q}} J'_1(K_{\rho_{1q}} a) \exp(-\gamma_{1q} L)$$

with $d = a$, while for the coaxial guide

$$P_q = A_{1q} D'_1 (K_{\rho_{1q}} b)$$

and (5.17)

$$P'_q = A_{11} \exp(-\gamma_{11} L) A'_{1q} D'_1 (K_{\rho_{1q}} b)$$

with $d = b$.

Define a function $F_\phi(m,\theta)$ such that

$$F_\phi(m,\theta) = \int\int_{\text{aperture}} E_\phi(d,\phi',z')\exp[-j(m\phi' + K_o \cos\theta\, z')]d\phi'dz' \quad (5.18)$$

where m is an integer, ϕ' and z' are the local coordinates of the aperture, and θ and ϕ are the general spherical coordinates with the origin on the cylinder axis. With the definition of F_ϕ as given by (5.18), the electric and magnetic Hertzian potentials Π_z^e and Π_z^m (chosen in the z-direction) due to the aperture ϕ-polarized field are given by [53]

$$\Pi_z^e = 0.0$$

$$\Pi_z^m = \frac{\exp(jK_0 r)}{r} \frac{j}{2\pi^2 K_0 \omega\mu_0 \sin\theta} \sum_{m=-\infty}^{\infty} \frac{(-j)^{m+1} F_\phi(m,\theta)}{H_m^{(1)'}(K_0 d \sin\theta)} \exp(jm\phi) \quad (5.19)$$

where d stands for the radius of the hollow waveguide or the outer radius of the coaxial line. The radiated far electric and magnetic fields are given by [53]

$$E_\phi = \omega K_0 \mu_0 \sin\theta\, \Pi_z^m \quad , \quad E_\theta = 0$$

$$H_\theta = \frac{1}{\eta_0} E_\phi \quad , \quad H_\phi = 0 \quad (5.20)$$

where η_0 is the free space intrinsic impedance.

Now, using the slot field expression as given by (5.15) in eqn. (5.18) to determine the function $F_\phi(m,\theta)$, one gets

$$F_\phi(m,\theta) = \frac{1}{\phi_0 J_0(\phi_0) N} f(\alpha,\phi_0) \int_0^L \left(\sum_{q=1} P_q \exp(-\gamma_{1q} z') + \sum_{q=1} P_q' \exp(\gamma_{1q} z') \right) \cdot$$

$$\exp(-jK_0 \cos\theta\, z')dz' \qquad (5.21)$$

where

$$f(\alpha,\phi_0) = \frac{1}{\cos\alpha} \int_{\alpha-\phi_0}^{\alpha+\phi_0} \frac{\exp(-jm\phi')}{\sqrt{1-\left(\frac{\phi-\alpha}{\phi_0}\right)^2}} d\phi' \qquad \text{for a single slot}$$

$$= \frac{1}{\cos\alpha} \left\{ \int_{\alpha-\phi_0}^{\alpha+\phi_0} \frac{\exp(-jm\phi')}{\sqrt{1-\left(\frac{\phi-\alpha}{\phi_0}\right)^2}} - \int_{\pi+\alpha-\phi_0}^{\pi+\alpha+\phi_0} \frac{\exp(-jm\phi')}{\sqrt{1-\left(\frac{\phi-(\pi+\alpha)}{\phi_0}\right)}} \right\} d\phi'$$

for a two diagonally symmetrical slots

Using the result of Appendix[C], the function $f(\alpha,\phi_0)$ is shown to be equal to

$$f(\alpha,\phi_0) = \phi_0 J_0(m\,\phi_0)\pi \exp(-jm\alpha)/\cos\alpha \qquad \text{for a single slot}$$

$$= \frac{\phi_0 J_0(m\,\phi_0)\pi}{\cos\alpha} (\exp(-jm\alpha) - \exp[-jm(\alpha+\pi)]) \qquad (5.22)$$

for a double slot

Substituting (5.22) in (5.21), and carrying out the simple integration in eqn. (5.21), gives an explicit expression for $F_\phi(m,\theta)$. Using this

expression in eqn. (5.19) and with the aid of (5.20) the radiation field can be written as

$$E_{\phi}(r, \phi, \theta) = \frac{\exp(-jK_0 r)}{r} \frac{j}{2\pi} \frac{1}{\cos \alpha} R(\phi, \alpha, m)\, S(\theta, \gamma, a) \qquad (5.23)$$

where

$$S(\theta,\gamma,a) = \{ \sum_{q=1} P_q \left(\frac{\exp[-L(jK_0 \cos\theta + \gamma_{1q})] - 1}{-(jK_0 \cos\theta + \gamma_{1q})} \right)$$

$$+ \sum_{q=1} P'_q \left(\frac{\exp(-jK_0 \cos\theta\ L) - \exp(-\gamma_{1q}\ L)}{-(jK_0 \cos\theta - \gamma_{1q})} \right) \qquad (5.24)$$

and

$$R(\phi, \alpha, m) = \sum_{m} \varepsilon_m (-j)^{m+1} J_0(m\phi_0) \cdot \cos m(\phi - \alpha)/J_0(\phi_0) \cdot H_m^{(1)'}(K_0 d \sin\theta) \qquad (5.25)$$

As shown in Appendix[I], the summation over m is from 0 to ∞ for a single slot. For the double symmetrically located slot, the summation is over odd integers (i.e. 1, 3, . . . ∞).

This expression gives the radiation field of a single or double slot on a waveguide or a coaxial line. The expression contains the multiplication of two infinite summations, one over q and the other over m. It was shown in Sections (3.6) and (4.6) that the first few terms of P_q or P'_q is sufficient to achieve convergence. The summation over m depends largely on $K_0 d \sin\theta$ (or d/λ_0) and $J_0(m\phi_0)$. Since in practice $K_0 a$ or $K_0 b$ will always remain within the limit $0.15 < d/\lambda_0 < 0.5$, i.e. $0 < K_0 d \sin\theta < \pi$, the limiting values of the Hankel functions for large orders and the Bessel functions for large amplitudes [51] are

$$\sqrt{\frac{2}{\pi m}}\left(\frac{2m}{e\pi}\right)^m \frac{m}{\pi} < H_m^{(1)'}(K_0 d \sin\theta) \leq \infty$$

for large m

$$J_0(m\phi_0) \simeq \sqrt{\frac{2}{\pi m\phi_0}} \cos(m\phi_0 - \pi/4) \leq \sqrt{\frac{2}{\pi m\phi_0}}$$

This yields

$$\frac{J_0(m\phi_0)}{H_m^{(1)'}(K_0 d \sin\theta)} \simeq \frac{\pi}{\sqrt{\phi_0}}\left(\frac{e\pi}{2m}\right)^m \frac{1}{m}$$

which shows that the magnitude of the terms in the infinite summation decreases rapidly for $2m > e\pi$. This means that the first five or six terms are actually sufficient to obtain satisfactory results.

It is apparent that the radiation field depends on several factors such as the slot parameters ϕ_0 and L, the slot location α and $K_0 d$. It is worthwhile to throughly examine the influence of these parameters on the radiation pattern. The next Section is mainly devoted to this task.

5.2.2 Numerical Examples of the Radiation Pattern of a Single Slotted Waveguide Section

The radiation due to a finite slot, given by eqn. (5.23), is evaluated for several cases in both ϕ and θ directions. Figs. 5.12-5.14 give the ϕ variation of the field for double and single slots, respectively. The pattern of a single slot has a major forward lobe as shown in Fig. 5.12 . This agrees perfectly with the results reported by Wait[33].

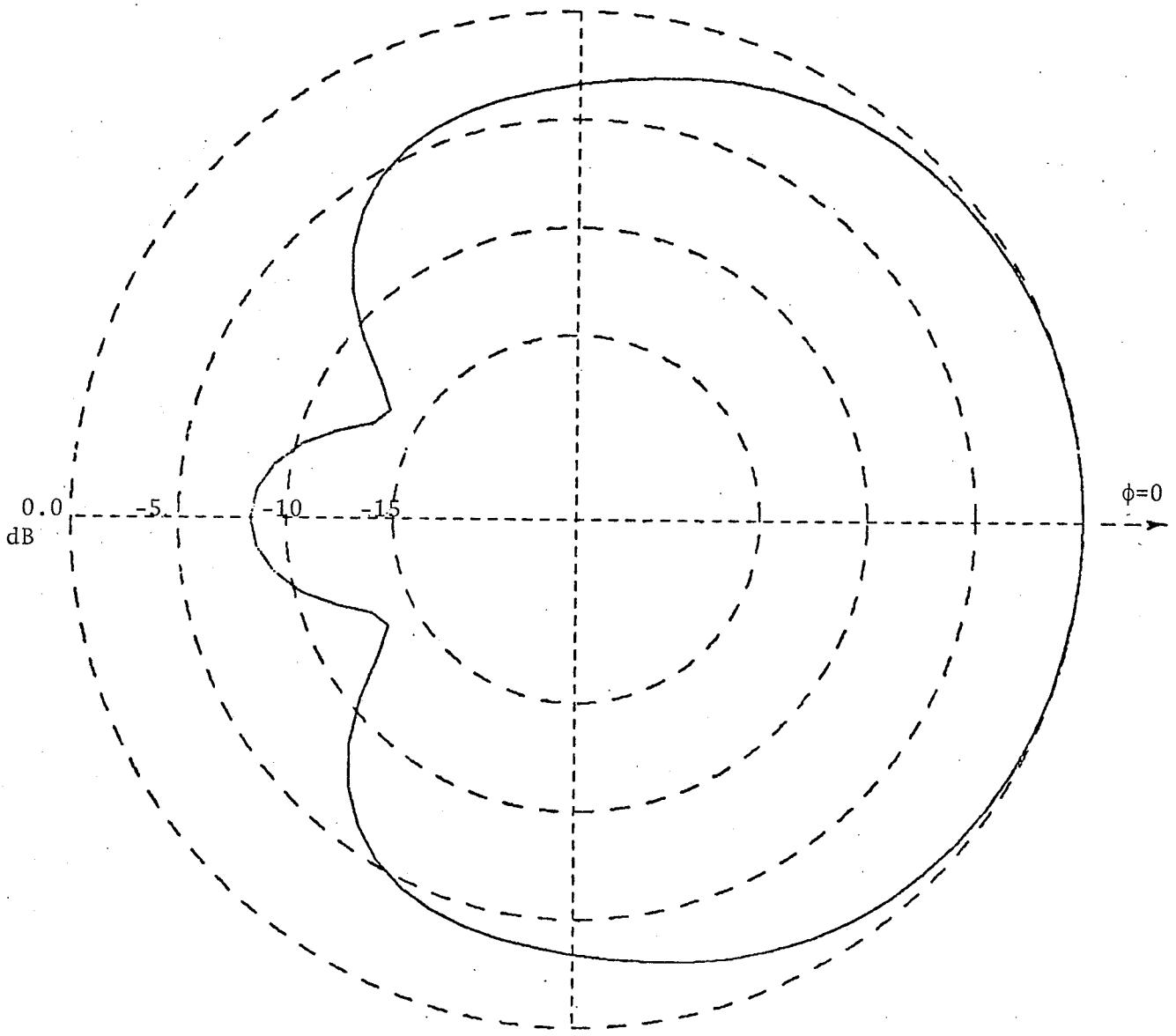

Fig. 5.12 . Radiation pattern of a finite slot in the ϕ-direction. Single slotted waveguide: $a/\lambda_0 = 0.4$, $\phi_0 = 5^{\circ}$, $\alpha = 0.0^{\circ}$.

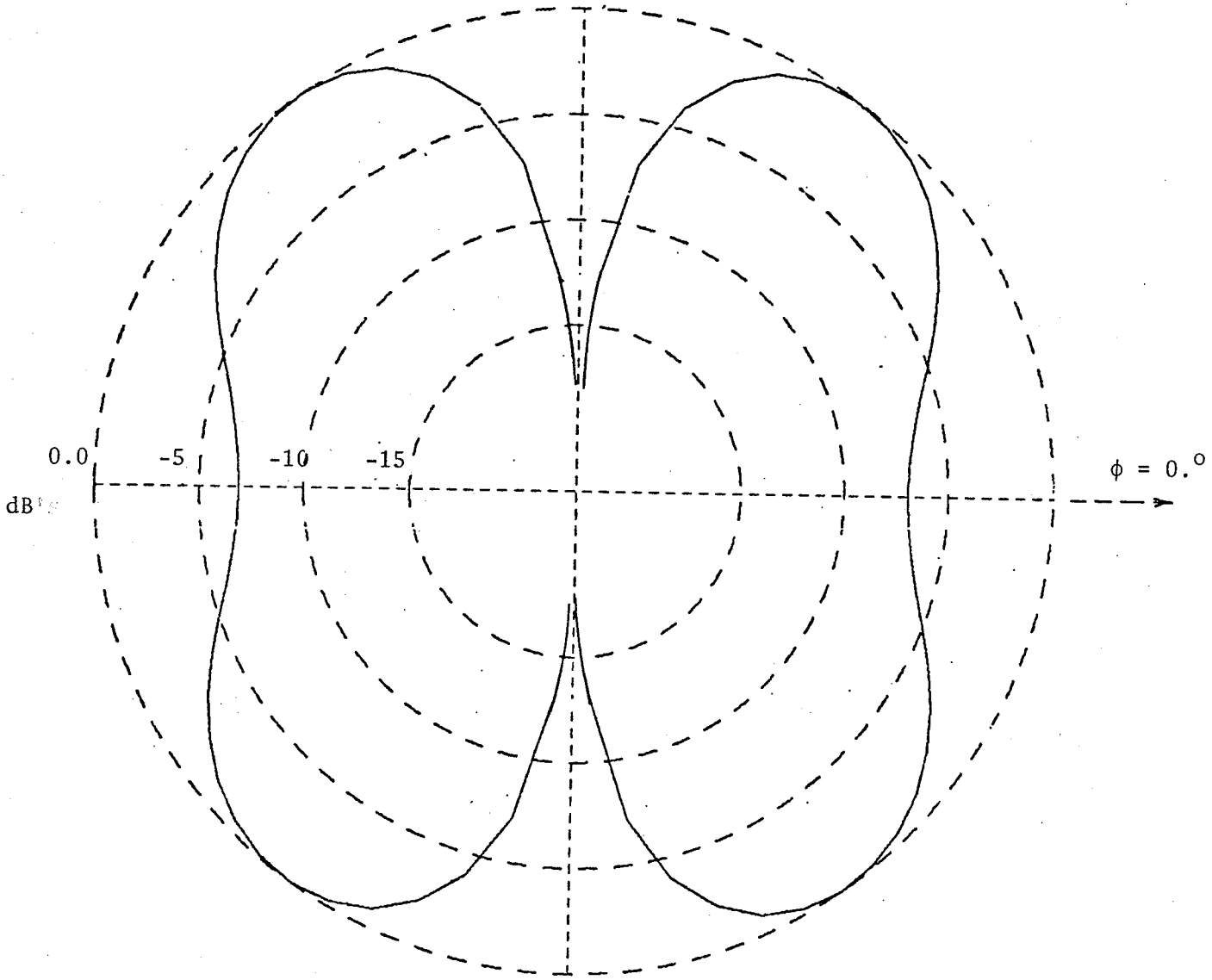

Fig. 5.13 . Radiation pattern of a finite slot in the ϕ-direction. Double symmetrical slots : $a/\lambda_0 = 0.4, \phi_0 = 5^{\circ}, \alpha = (0.0, 180^{\circ}), c = 1.5$

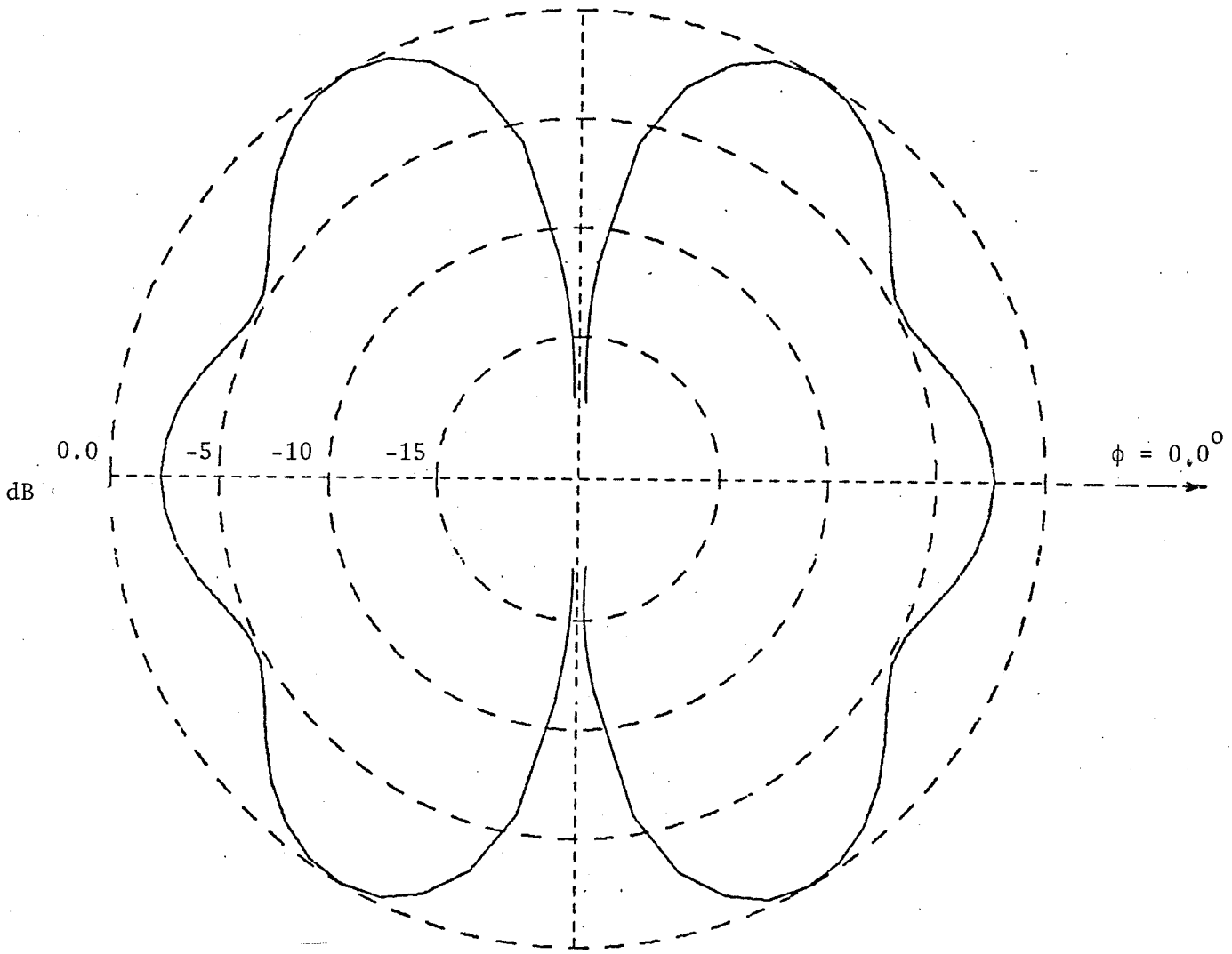

Fig. 5.14 . Radiation pattern of a finite slot in the ϕ-direction. Double slotted waveguide: $a/\lambda_0 = .5, \phi_0 = 5^o, \alpha = (0.0, 180^o), c = 1.5$

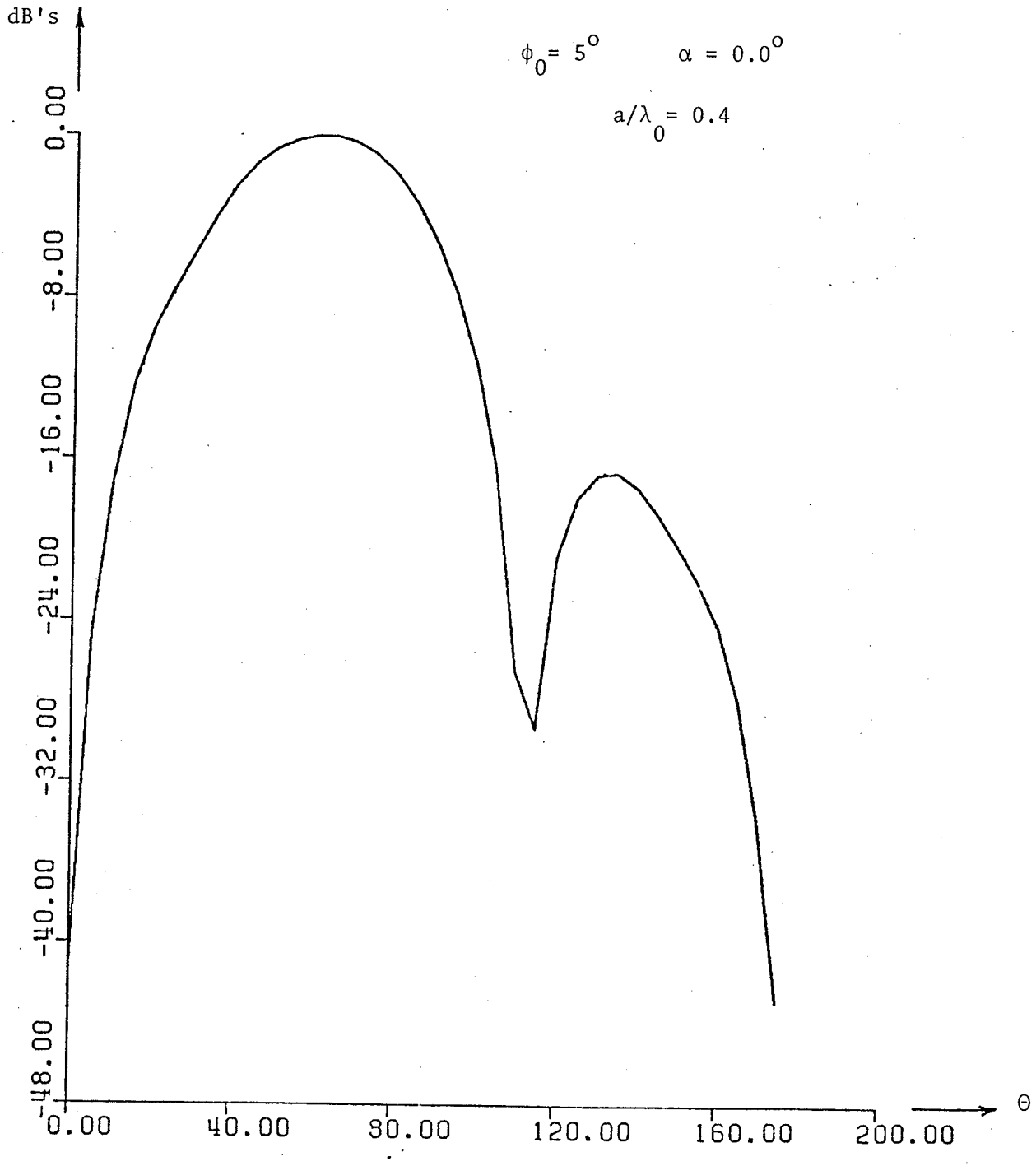

Fig. 5.15 . Radiation pattern of a finite slot in the θ-direction. Single slotted waveguide. $L = \lambda_0$

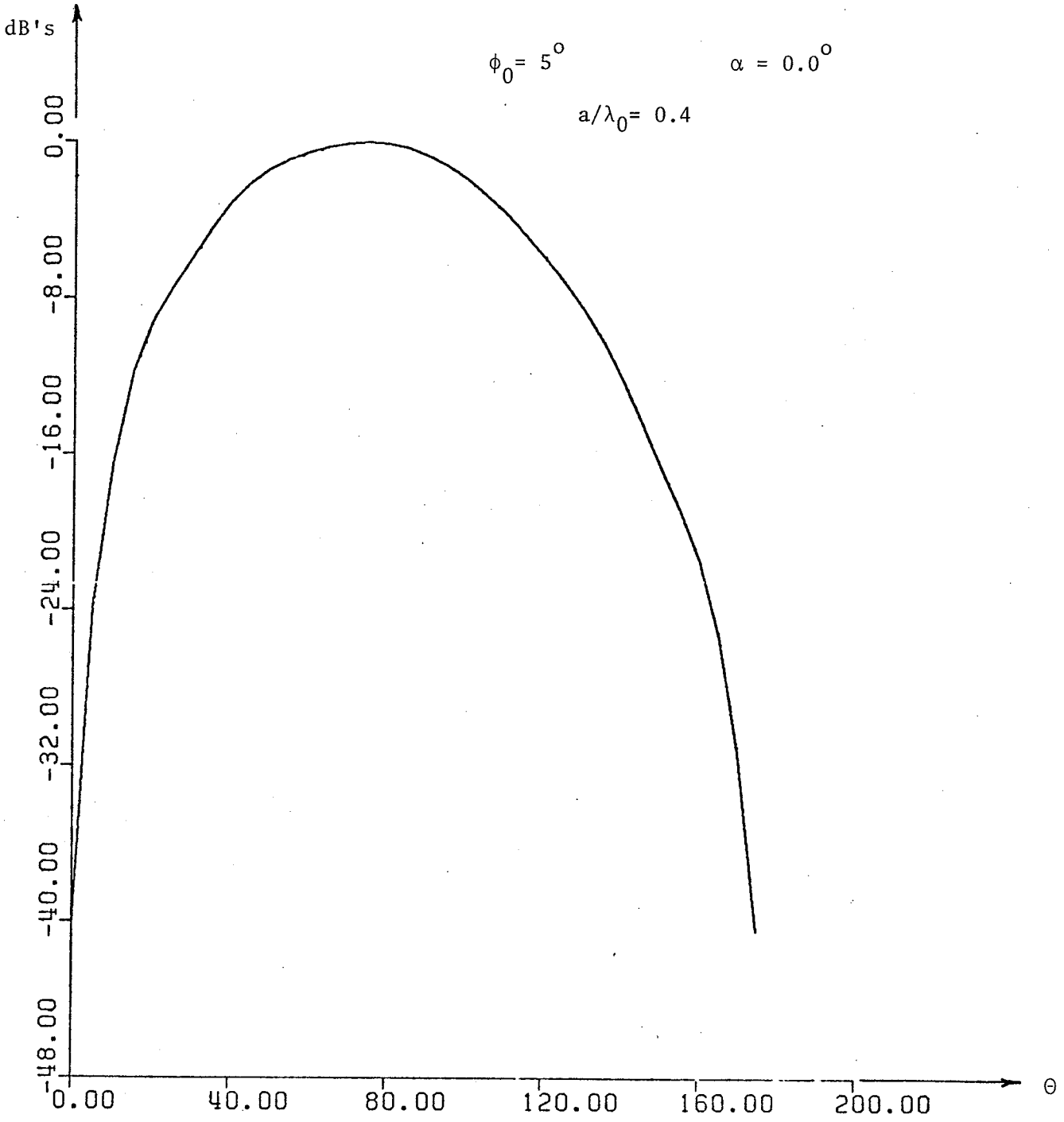

Fig. 5.16 . Radiation pattern of a finite slot in the θ-direction. Single slotted waveguide. $L = 0.5\lambda_0$

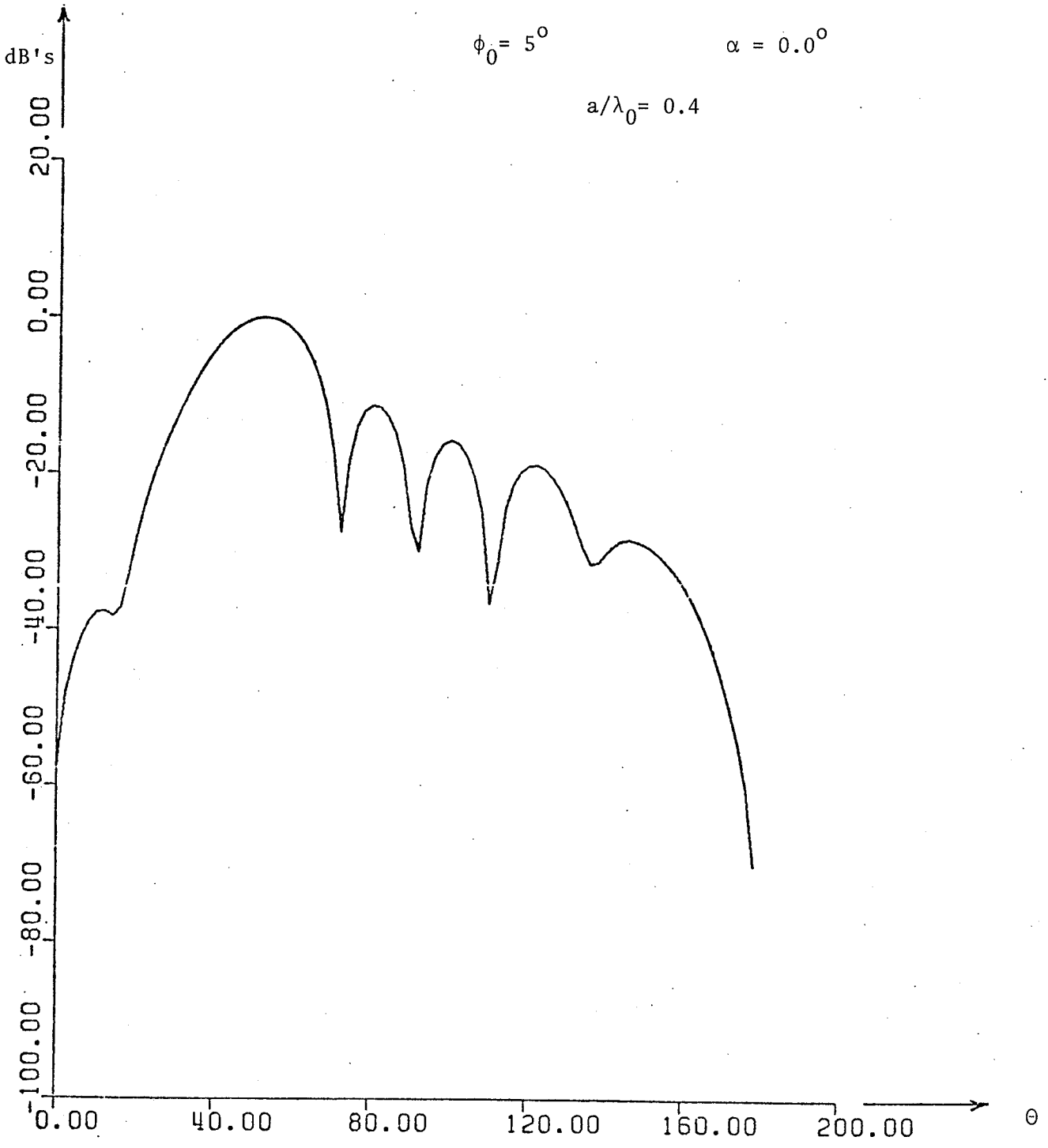

Fig. 5.17 . Radiation pattern of a finite slot in the θ-direction. Single slotted waveguide. $L = 3\lambda_0$

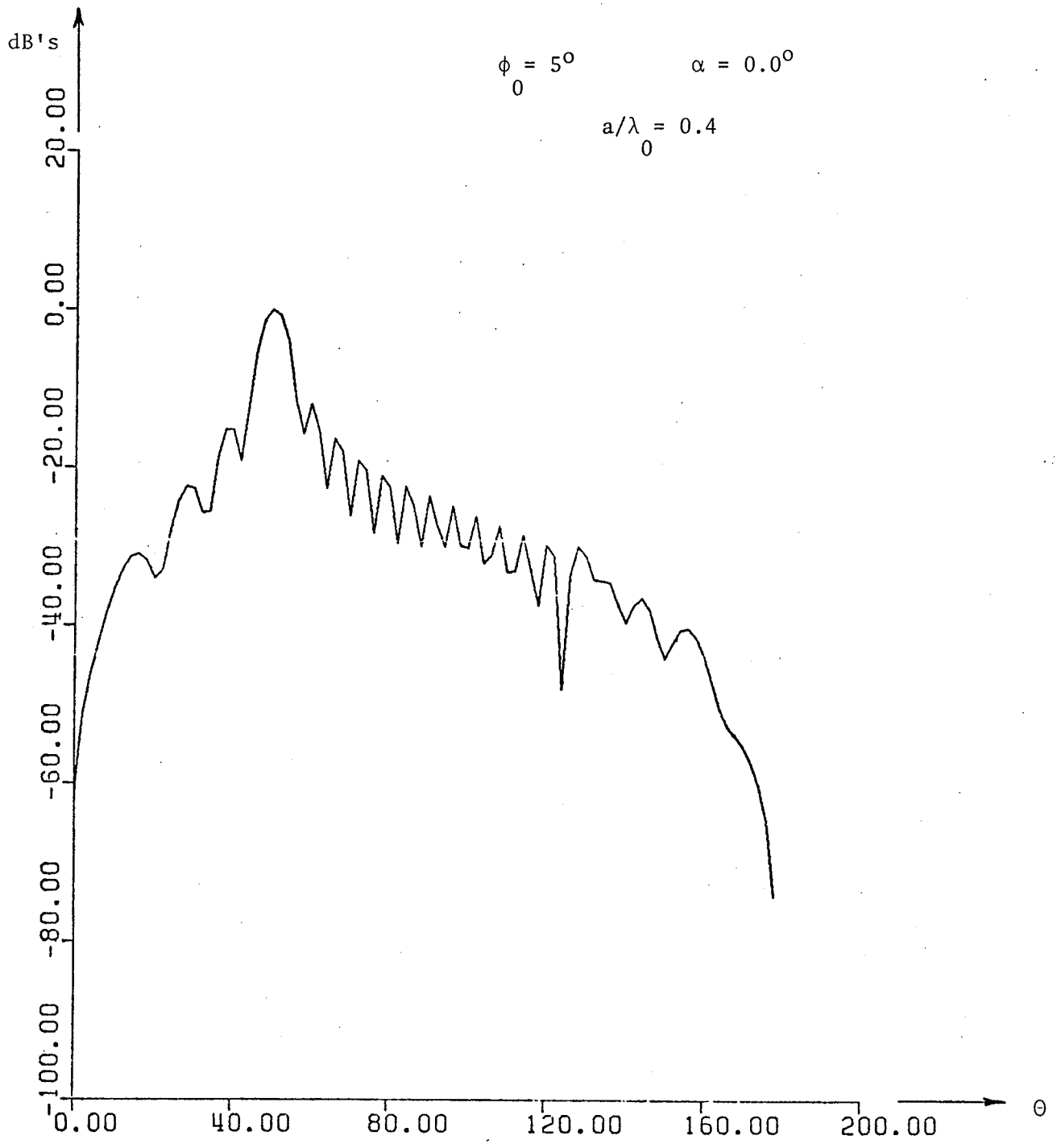

Fig. 5.18 Radiation pattern of a finite slot in the θ-direction. Single slotted waveguide. $L = 10\lambda_0$

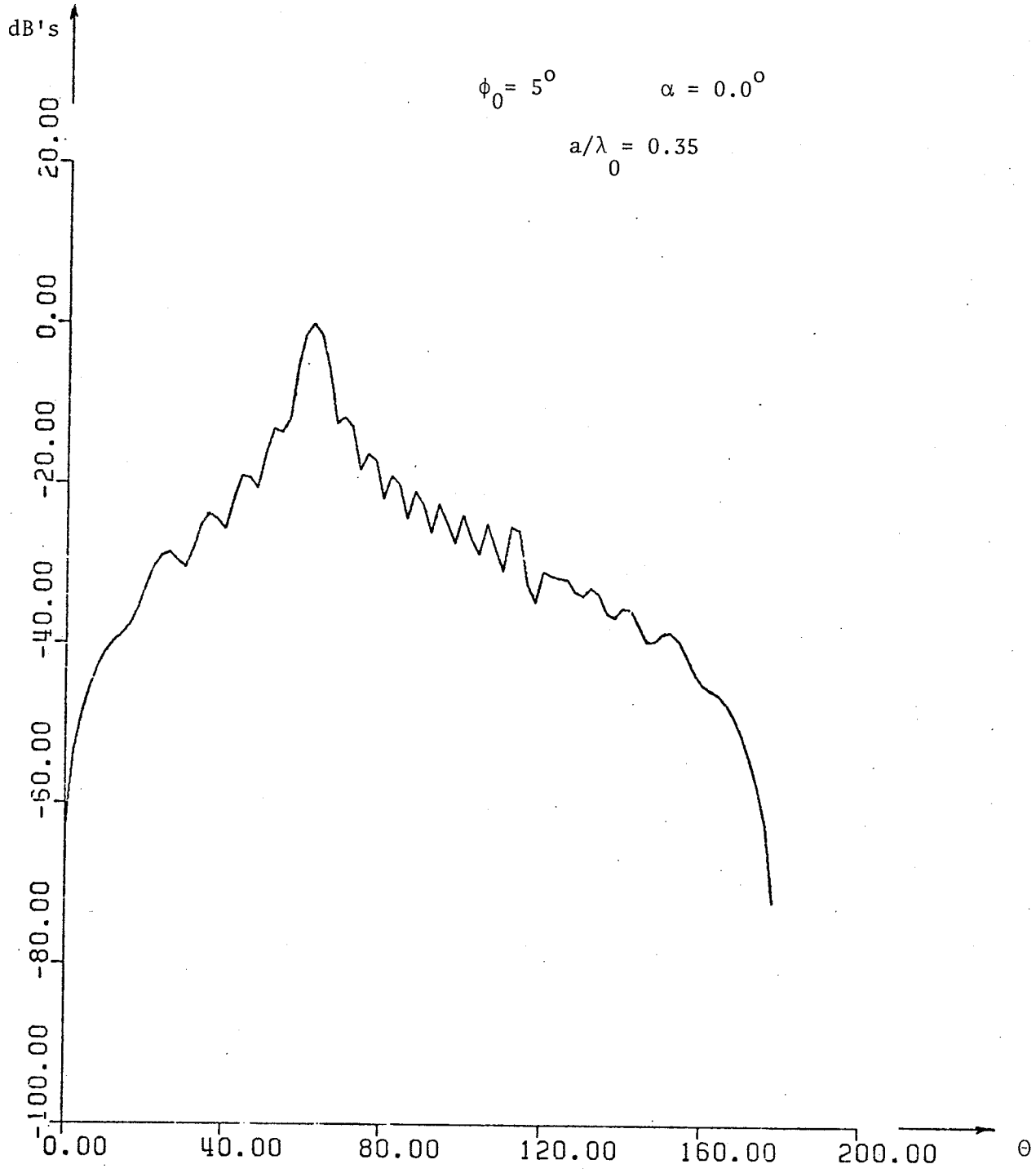

Fig. 5.19 . Radiation pattern of a finite slot in the θ-direction. Single slotted waveguide. $L = 10\ \lambda_0$

The radiation pattern of two symmetrical slots as shown in Figs. 5.13 and 5.14 is worth further study. Inspection of the positions of maxima and minima of these patterns and their displacement with the variation of frequency reveal quite an interesting result. Two slots act similar to two dipoles, 180° out of phase and separated by almost $2a/\lambda_0$, the distance separating the two slots. It is known that the pattern of two dipoles, 180° out of phase and at a distance ℓ from each other, is given by $\cos(K_0\ell/2 \cos\phi - \pi/2)$ [55]. This pattern goes to zero at $\phi = 90°$ and 270°, and its maxima occur at $\phi_{max} = \arccos(\lambda_0/2\ell)$. For $\ell/\lambda_0 = 0.8$ one finds $\phi_{max} = 51.3°, 138.7°, 231.3°$ and 308.7°. The corresponding case of two slots is shown in Fig. 5.13 for $2a/\lambda_0 = 0.8$. The maxima occur at about 54°, 126°, 234° and 306°. This resemblence of slot and dipole patterns preserves itself as a/λ_0 decreases. However, as a/λ_0 increases, the slot pattern shows two extra lobes at $\phi = 0.0, 180°$ as shown in Fig. 5.14. This may be due to the greater separation distance of two interacting slots, where their mutual interaction decreases. As a result, the back lobe of each slot tends to appear. Nevertheless, the location of the maxima still coincides with the corresponding case of two dipoles.

The patterns in a plane passing through the axis z, i.e. the variation with respect to θ are presented in Figs. 5.15 - 5.19 for different slot lengths and a/λ_0. One can see that each pattern has a number of major lobes in the forward direction. Further inspection of these figures shows that for every half wavelength along the slot each of the incident and reflected waves generate one major lobe. Thus, for a slot length $3\lambda_0$, the pattern has 6 major lobes. This is shown in

Fig. 5.17. Similar cases are shown in Figs. 5.15 - 5.19. However, as the slot length increases, the patterns tend to generate a distinct main lobe with progressively reducing side lobes, most of which are 20 dBs below the main lobe. It is interesting to note that, for a slot length of one half wavelength, the pattern has a major lobe with a 3dB beam width of about 50^{o} . The presence of a single lobe is obtained when the slot is infinetly long [14]. This shows similarity of radiation characteristics between the $\lambda_0/2$ and the infinetly long slot. The similarity was predicted in Section (5.1) when the slot fields were evaluated and plotted. The slot field in the $\lambda_0/2$ case was shown to vary along the slot in a manner similar to that of an infinetly long slot. It is also illuminating to point out that changing frequency steers the major lobe in space, but preserves its general features as shown in Fig. 5.18 - 5.19. In the following Section , further investigation of the radiation pattern is pursued. The radiation due to cascaded slotted sections are presented and discussed.

5.3 Cascaded Radiating Slotted Sections

The radiation pattern of a single slotted section was analysed in Section (5.2). It is apparent that with a single radiating section , both the radiated power and control of the radiation pattern is limited. It is therefore advantageous to study the radiation characteristics of several cascaded radiating slotted sections. The problem will be treated such that each section is a radiating element placed along the z axis,whose radiation pattern is already known. This is equivalent to taking the

integration of eqn.(5.18) over all the slots on the waveguide wall.

5.3.1 Analysis of the Radiation Pattern of Cascaded Slotted Sections

Consider the waveguide shown in Fig. 5.20. Let a dominant TE_{11} mode be incident toward section (1) with a wave function given by eqn. (5.1) as

$$\phi^{i}_{(1)} = T \quad J_1(x_{11}\rho/a) \cos\phi \exp(j\theta_{11}z) \tag{5.26}$$

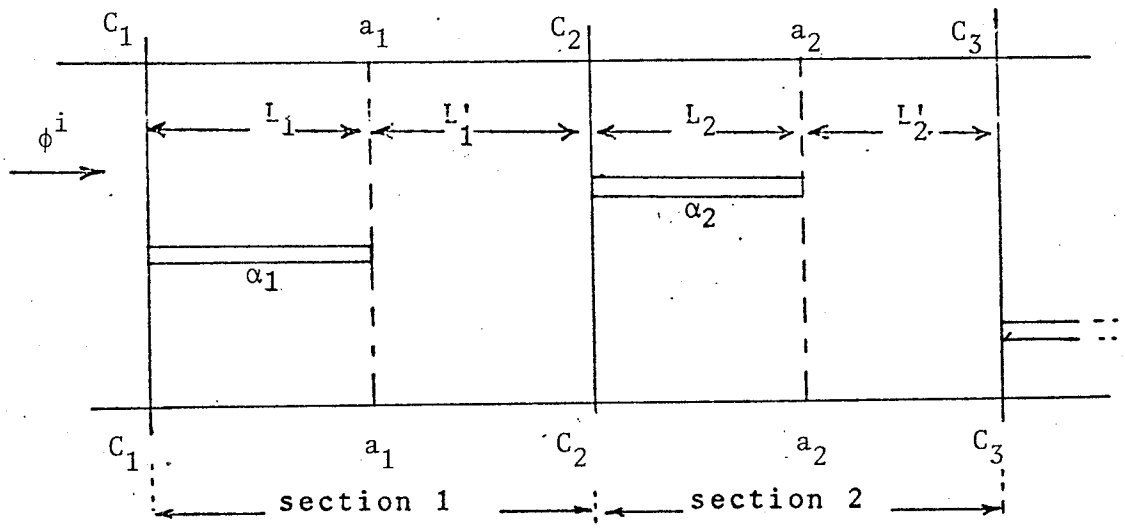

Fig. 5.20

Let the reflected field at C_1 - C_1 be represented by the wave function

$$\phi^{r} = T \sum_{n=0}^{\infty} \sum_{m=1}^{\infty} B_{nm} J_n(x\rho/a) \cos n\phi \exp(-j\theta_{nm}z) \tag{5.27}$$

and the transmitted field toward the slotted section be

$$\psi^t = T \sum_{n=0} \sum_{m=1} A_{nm} J_n(K_\rho \rho) \cos n\phi \exp(-\gamma_{nm} z) \qquad (5.28)$$

At the plane $a_1 - a_1$, the main remaining field is the first mode of the summation of eqn. (5.28) with its wave function given by

$$\psi^t_{11} = T A_{11} J_1(K_\rho \rho) \cos \phi \exp(-\gamma_n z)$$

Now, at the plane $a_1 - a_1$ the field suffers another reflection as previously analyzed in Section (5.1). According to that analysis, the reflected and the transmitted wavefunction ϕ'^r and ψ'^t, at the plane $a_1 - a_1$, respectively, are given by

$$\phi'^r = T A_{11} \exp(-\gamma_{11} L) \sum_{n=0} \sum_{m=1} A'_{nm} J'_n(K_\rho a) \cos n\phi \exp(-\gamma_{nm}(L - z)) \qquad (5.29)$$

$$\psi'^t = T A_{11} \exp(-\gamma_{11} L) \sum_{n=0} \sum_{m=1} B'_{nm} J'_n(x_{nm}\rho/a) \cos n\phi \exp(j\theta_{nm} z') \qquad (5.30)$$

where $z' = z - L$

The field given by (5.30) will continue to propagate toward the next section [section (2) in Fig. 5.20]. B'_{11} is the only transmitted coefficient that has an appreciable value and the rest of the coefficients B' are very small (with values similar to values of Table 3.9). Thus one can assume that the field incident on section (2) of Fig. 5.20 is given by

$$\phi^{i}_{(2)} = T\, A_{11}B'_{11} \exp(-\gamma_{11} L) \exp(j\theta_{11}L') J_1(x_{11}\rho/a) \cos\phi \exp(j\theta_{11}z'') \tag{5.31}$$

where $z'' = z - L - L'$

Now, comparing (5.31) and (5.26), one can see that as the field crosses successive sections, each section modifies the field by a factor V_ℓ given by

$$V_\ell = [A_{11}B'_{11} \exp(-\gamma_{11} L) \exp(j\theta_{11}L')]_\ell \tag{5.32}$$

where all the coefficients and parameters of (5.32) are those of the ℓ^{th} section, and L' is the spacing between the ℓ^{th} and the $\ell + 1^{th}$ slot. The factors V_ℓ will then modify the radiation field given previously by eqn. (5.23) such that for the ℓ^{th} section it takes the form

$$E^{(\ell)}_{\phi}(r,\phi,\theta) = \frac{\exp(-jK_0 r_\ell)}{\gamma_\ell} \frac{1}{2\pi \cos\alpha_\ell} (V_1 V_2 \cdots V_\ell)$$

$$R_\ell(\phi,\alpha,m) S'_\ell(\theta,\gamma,a) \tag{5.33}$$

where $R_\ell(\phi,\alpha,m)$ is given by (5.25) and r_ℓ and θ_ℓ are given by

$$r_\ell = \sqrt{r_0^2 + h^2 - 2r_0 \cos\theta}$$

$$\theta_\ell = \sin^{-1}\left(\frac{r_0}{r_\ell} \sin\theta_0\right)$$

Where h is the spacing between the first and the $\ell+1^{th}$ slot, and r_0, θ_0 are the observation point.

The function $S'_\ell(\theta,\gamma,a)$, however, is slightly different from the function given by (5.24). The analysis of Section (5.2), which led to

eqn. (5.24), assumes a single slotted section such that once the field passes this section it never reflects back. Thus the slot field in this case consists of two components only. These are the transmitted one at the plane $C_1 - C_1$ and the reflected one at $a_1 - a_1$ as shown in eqn. (5.15). The presence of another slotted section beyond the plane $a_1 - a_1$ causes a reflection at $C_2 - C_2$ back toward $a_1 - a_1$. At $a_1 - a_1$ this reflected field will be decomposed into two components. One component is transmitted to the slotted part of the first waveguide section and the other is reflected back toward the second section. The reflected component is negligibly small since it is the result of two successive reflections between $a_1 - a_2$ and $C_2 - C_2$. It's value does not exceed 2% of the existing field (eqn. 5.31) for a hollow waveguide of $a/\lambda_0 = .5$, and 1% for a coaxial guide of $a/\lambda_0 = 0.3$ Therefore it can be neglected. The second component which is transmitted into the slotted part of section (1) cannot, however, be neglected. For the ℓ^{th} section the mode function of this component $\psi^t_{\ell-(\ell+1)}$ could be shown to be equal to

$$\psi^t_{\ell-(\ell+1)} = [T\, A_{11}\exp(-\gamma_{11} L)\, B'_{11}\, \exp(j\theta_{11}L')]_{\ell} (B_{11}\exp(j\theta_{11}L))_{\ell+1} \cdot$$

$$\sum_{p=0} \sum_{q=1}^{\infty} A'_{pq} J_p(K_\rho a) \cos p\phi \exp(-\gamma_{pq}(Lz)) \qquad (5.34)$$

This field has to be added to the field of eqn. (5.29). This will change the slot field such that the factor P'_q of eqn. (5.24), which was given by (5.16) or (5.17), now assumes the form

$$P'_q = [A_{11}\exp(-\gamma_{11} L)]_{\ell}[1 + (B'_{11}\exp(j\theta_1 L')) \; {}_{\ell}(B_{11}\exp(j\theta_{11} L'))_{\ell+1}]$$

$$[A'_{1q}K_{\rho'_{1q}}J'_1(K_{\rho_{1q}}a)\exp(-\gamma_{1q}sL)]_{\ell} \qquad \text{for the hollow waveguide} \qquad (5.35)$$

and

$D'_1(K_{\rho_{1q}}b)$ replaces $K_{\rho_{1q}}J'_1(K_{\rho_{1q}}a)$ for the coaxial guide

The radiation field of all sections can finally be written as

$$E_\phi(r,\phi,\theta) = \sum_{\ell=1}^{L} \frac{\exp(-jK_0 r_\ell)}{r_\ell} \frac{1}{2\pi \cos\alpha_\ell} (V_1 V_2 \ldots V_\ell)$$

$$R_\ell(\phi,\alpha,m)\; S_\ell(\theta,\gamma,a) \qquad (5.36)$$

where L is the total number of slotted sections, V_ℓ, $R_\ell(\phi, \alpha, m)$ and S'_ℓ are given by (5.32), (5.25) and (5.24), respectively, where P'_q in (5.24) is replaced by its value given by (5.35)

The magnetic field is readily obtained from eqn. (5.20) as

$$H_\theta(r,\phi,\theta) = E_\phi(r,\phi,\theta)/120\,\pi \qquad (5.37)$$

This concludes the analysis of the radiation field of L cascaded slotted sections. Equation (5.36) is plotted for several parameters and the resulting pattern examined in each case.

5.3.2 The Radiation Pattern of Cascaded Slotted Sections

Equation (5.36) gives the radiation field of cascaded slotted waveguide sections in the far field zone. The waveguide diameter and the dimensions of various slotted sections as well as the mutual location of slots introduce a large number of parameters into the far field equation. All these parameters affect the radiation characteristics. Detailed investigation of their effects is too lengthy and beyond the scope of this Chapter. An attempt is made therefore to present the general features of the patterns for a particular arrangement of the slotted sections which simulates an array of in-phase slots, located at a fixed azimuthal location $\alpha = 0$. The slot length L and the axial distance L' between successive slots is chosen such that the incident field on all slotted sections is in phase. Because of the reflected fields the slot fields are not completely in-phase. However, if the reflected components are small (which depends on a/λ_0), the slot fields will almost have the same phase distribution.

Fig. 5.21 shows the radiation patterns for two different arrays of four and eight slotted sections. Since the slot fields are in phase, the general features of these patterns are similar to those of equi-phase point sources [55]. Thus, the beam width of the main and side lobes decreases as the number of radiating elements increases. This is also clear from Fig. 5.22 which shows the radiation pattern of 10 successive slotted sections. It is interesting to note that the slot length has considerable effect on the radiation pattern. Comparing Figs. 5.22 and 5.23, one can see that at the particular slot length $L = 0.5\,\lambda_0$, the back lobe is reduced and the radiation is mainly in the foward

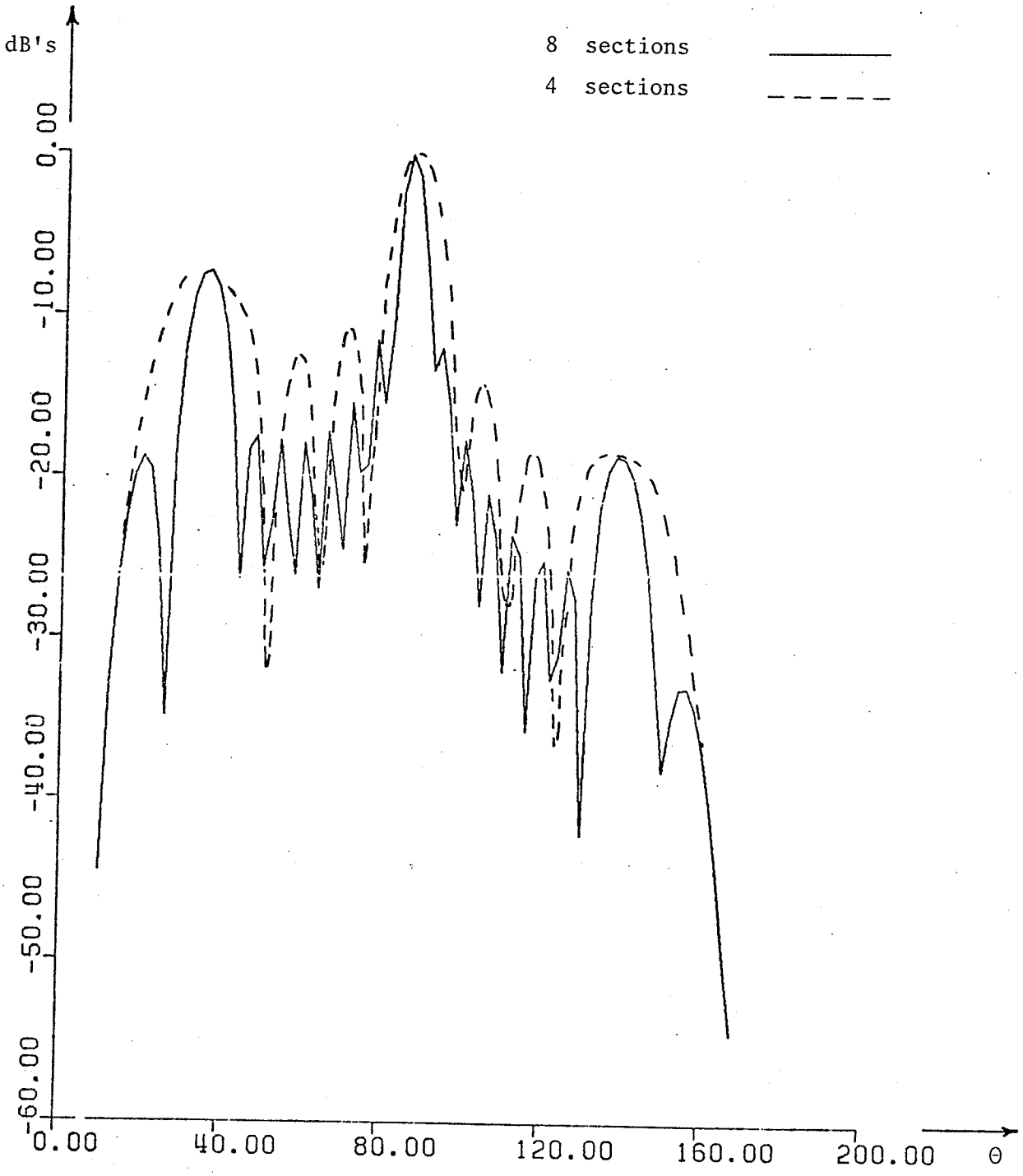

Fig. 5.21 . Radiation pattern in the θ direction of four and eight successive double slotted sections; $\alpha = (0.0, 180^{o})$, $L = 0.5\lambda_0$ $L' = 0.77\lambda_0, \phi_0 = 5^{o}$

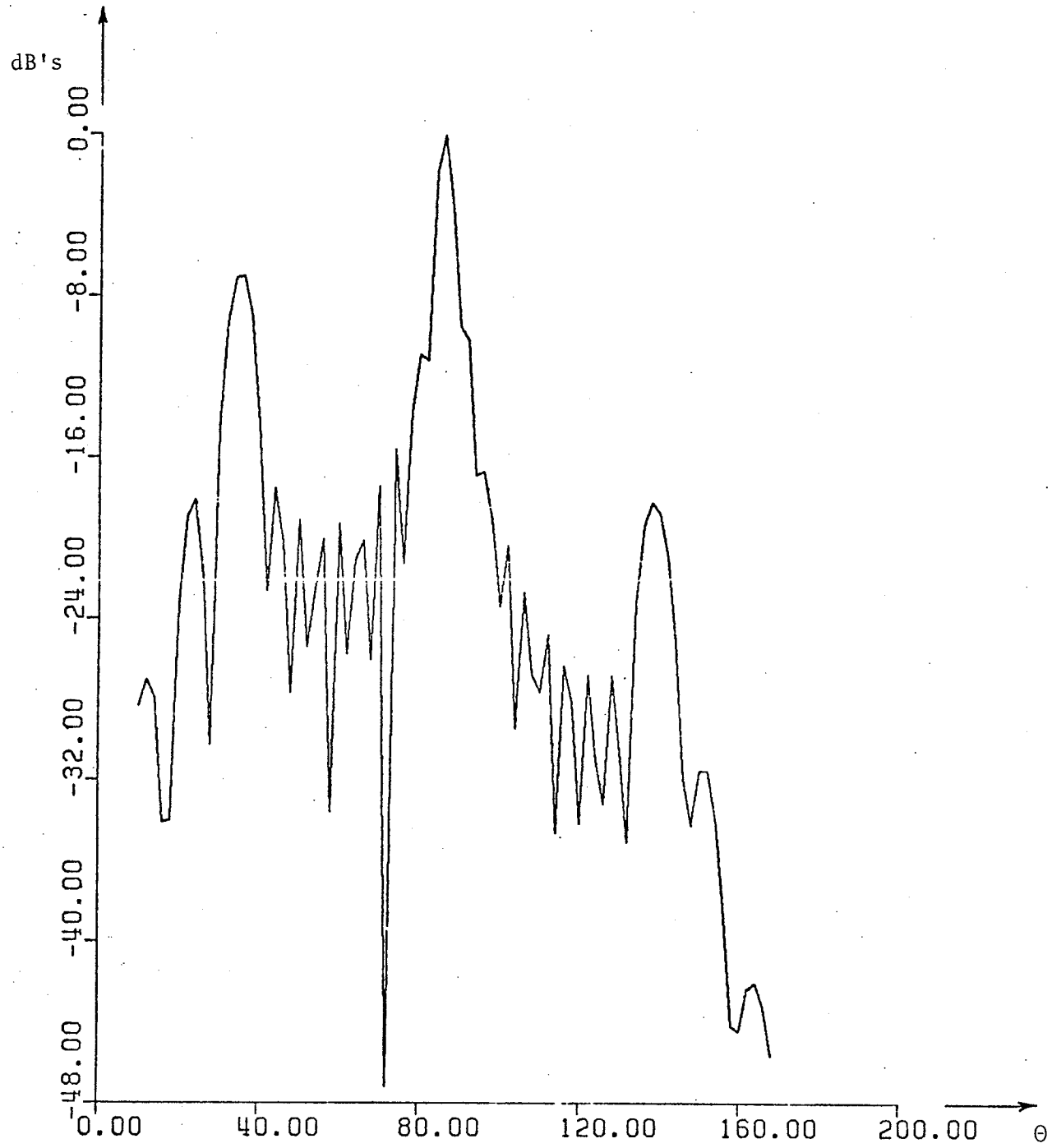

Fig. 5.22 . Radiation pattern in the Θ-direction of 10 successive double slotted sections : $\alpha = (0.0, 180^{o})$, $L = 0.5\lambda_0$, $L' = 0.77\lambda_0$, $\phi_0 = 5^{o}$

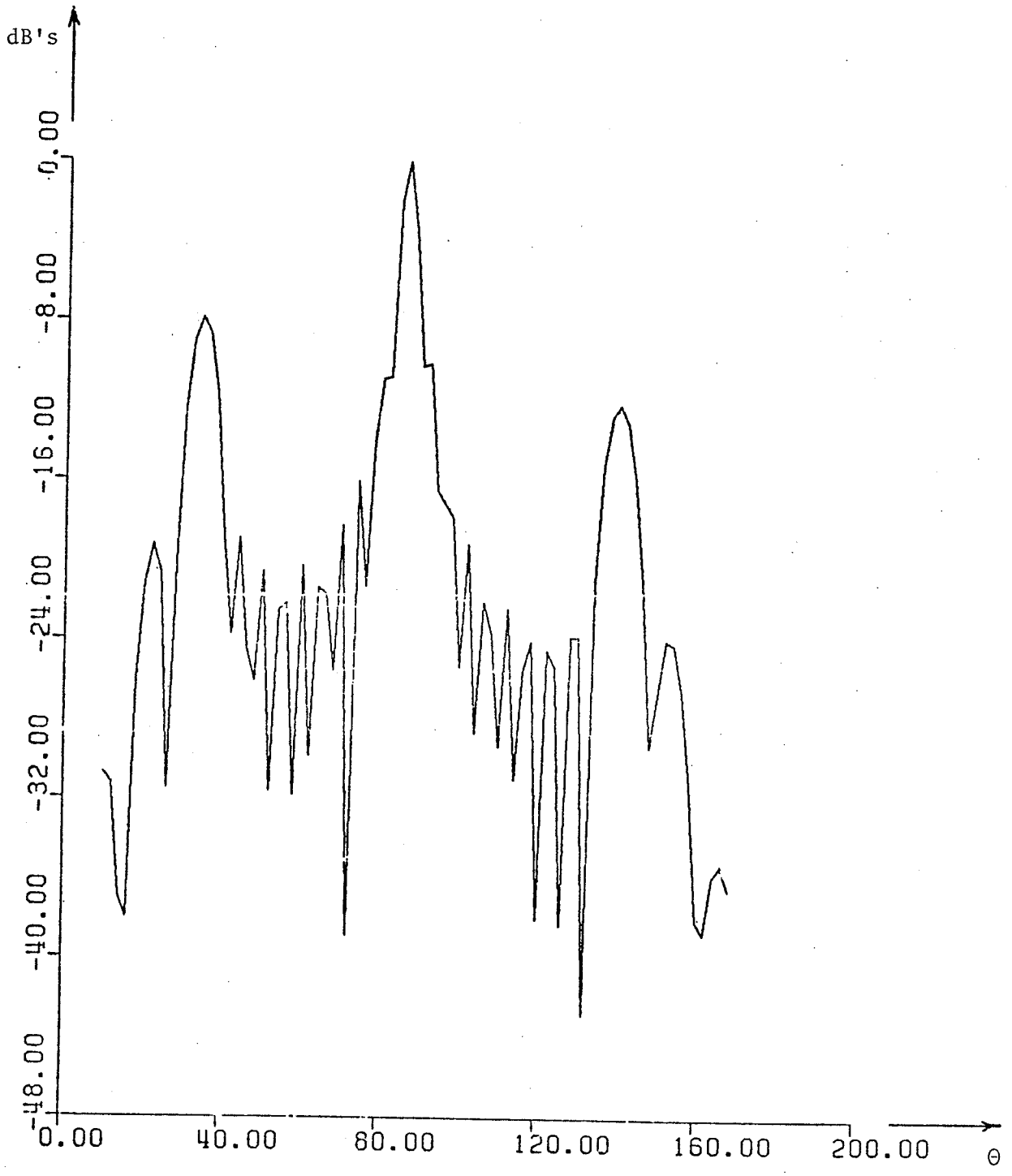

Fig. 5.23 . Radiation pattern in the Θ-direction of 10 successive double slotted sections: $\alpha = (0.0, 180^{o})$, $L=0.3\lambda_0$, $L' = 0.956\lambda_0$, $\phi_0 = 5^{o}$.

direction. This is possibly due to the fact that if the incident fields at the terminals of all slots are in phase, and if the values of L' and L are close, then for any slot the two reflected components of the slot field (discussed in Section 5.1) will be out of phase and almost cancel out. This leaves only the incident component responsible for forward radiation. It is also worth mentioning that the results for $L = 0.3\ \lambda_0$ (with parameters of Fig. 5.23) show that the radiated power of each section is about 5% of the power incident on that section. For the same parameters with $L = 0.5\ \lambda_0$ the radiated power rises to about 8.2% of the incident power. It is clear that each successive section radiates less power than the previous one. In the general case the amount of the radiated power per section can be controlled by changing the slot parameters. This opens a great number of possibilities for design of slotted waveguide antennas with a variety of interesting applications. The problem is certainly worth study and is left for future investigations.

This concludes the analysis of the present Chapter for the radiation characteristics of axially slotted hollow waveguides. The examples presented here were for the hollow waveguide case. The results of the coaxial line are similar and are not repeated.

It is advantageous to have a general look at problems discussed throughout this thesis and the possible extension of this work to related problems. The concluding Chapter is devoted to this purpose.

CHAPTER VI

CONCLUSION AND DISCUSSION

The leaky wave radiation through an axially slotted waveguide was studied throughout this thesis. The work was carried out for both hollow and coaxial waveguides, each with TE_{11} mode excitation. Several different electromagnetic techniques were employed in order to solve for the slot tangential field. The integral equation formulation for the slot impedance in the ρ direction was constructed. This formulation was modified to allow for the determination of the slot impedance in any arbitrary location around the waveguide. It was further extended to cover the combined impedance of two symmetrical and diagonally located slots along the guide wall. Following this, the transverse resonance technique was applied to the waveguide cross-section in the transverse plane (i.e. ρ and ϕ plane). To apply for this technique, the guide cross-section was represented by a radial transmission line in the ρ-direction terminated by the slot(s) impedance. When the transverse resonance equation was solved, the propagating modes in the slotted section of the waveguide (and coaxial line) were obtained. With the knowledge of these propagation constants, it was possible to set up a modal expansion of the field with unknown coefficients in the slotted section of the waveguide. A similar field expansion in the complete waveguide section was assumed and the tangential fields were matched across the plane separating the two guide sections. The resulting equations were solved numerically to yield the unknown coefficients of the field. In order to introduce the slot edge field condition an electrostatic field solution was utilized. This static solution together with the

coefficients of the electromagnetic field expansion as determined before, gave an approximate solution for the slot field.

The obtained solution shows clearly the leaky wave nature of the radiated field. For example, in Tables (3.1-3.6) and (4.1-4.6), one can see that the propagation in the transverse direction (ρ directions) is improper and the field magnitude is an ever increasing function of ρ. This was also apparent in Chapter 5 when the finite slot field was plotted and was shown to have a phase velocity faster than the velocity of light. The analyses show that the propagation in the ρ-direction is dependent on the geometry of the structure and not on the frequency of operation. The slot width $2\phi_0$, the slot orientation with respect to the incident field and the number of slots per section control the value of δ, and hence K_ρ. Stronger leaky waves were observed with wider slots and with slots located at $\phi = 0.0$. When the structure was modified to have two slots along the guide wall, it was shown that larger values of δ were obtained and accordingly faster waves were generated along the slot. One should also point out that the TE_{11} waves are characterized by the strongest leaky wave radiation, and that higher modes have less radiation as is evident from the values of δ given in Tables 3.4 and 4.4 .

The operating frequency seems to have two effects: it controls the magnitude and phase of the slot field, and it changes the direction of the main radiation beam in space. It is shown in Sections (3.6) and (4.6) that as one approaches the cut-off frequency, the ratio of the slot field to the field value at the waveguide centre (ρ= 0) increases. Because of this magnifying effect, it seems that the slotted waveguide acts as a step-up transformer with a transformation ratio

which depends on the ratio a/λ_0. This transformation ratio depends also on the slot width $2\phi_0$ and on the slot location α. As an example, for an incident TE_{11} wave function with unit amplitude in a hollow waveguide, the highest value of the field is at the origin and is equal to $E_\phi a = 0.9205$ V. This guide with a slot width $2\phi_0 = 4^o$, located at $\alpha = 0.0^o$ will generate an average slot field of approximately $E_0 a = 2.2$ V. at $a/\lambda_0 = 0.35$. At $a/\lambda_0 = 0.5$ the average slot field drops to $E_0 a = 2.1$ v. as shown in Fig. 3.13 and 3.14. There is, however, one point to consider when varying the ratio a/λ_0. The PRC at the interface between the slotted and the complete section rises rapidly as a/λ_0 approaches the cut-off frequency, as indicated in Figs. 3.6-3.7 and 4.5-4.6. Thus one must choose a suitable operating point according to these curves and avoid working too close to the cut-off point.

It is also interesting to notice that the transmitted field in the slotted section is basically TE_{11} as is evident from the results of Sections (3.4.4) and (4.4.4) . The slotted structure with the given dimensions is not able to support higher modes efficiently. This makes the ϕ - radiation pattern a rather uniform one as was demonstrated in Chapter 5.

A far more interesting result was obtained when the field of a single slotted section was compared to that of a doubly slotted section. In the hollow waveguide case the field changes by about 2% on aveage, which shows weak interaction between the slot fields. For the coaxial case the interaction is stronger, though still small, and the change may rise to about 7% . The interaction between slot fields of the same section is therefore weak and in most cases can be neglected as was discussed in Chapters

3 and 4. This suggests that the interaction between successive sections may as well be weak and can be neglected. This result is an important one in as much as it allows the analysis of this thesis to be extended to periodic leaky wave structures. An example of periodic structure consisting of a successive series of slotted sections was analyzed in Chapter 5.

The finite slot was also studied considering only the reflection at the slot far end. The slot field,when plotted,clearly reveals its fast-wave nature. It was shown that for the particular case of a half-wavelength slot the field variation is very much like that of a semi-infinite slot as studied in Chapter 3 and 4. This was tested further by inspecting the radiation pattern of this particular slot length , given in Fig. 5.15 and comparing it with the infinite slot as presented in reference [14].

The analyses was extended to a series of slotted sections forming an array of finite slots. The parameters of such an array can be utilized to control,over a very wide range,the radiation field of the array. It was shown that when the phase of the slot fields are adjusted such that they are all equal, the radiation pattern tends to have the same characteristics as those of a system of equi-phase point sources [55]. One more advantage of this structure was demonstrated in Section (5.3.2) . It was shown that about 60% power radiation was achieved for the case and parameters of Fig. 5.22. Extending the structure with several extra sections or changing the geometry of the slots will lead to very little power being carried to the far end of the structure. This reduces any possible mismatch problems, and provides an advantage over other radiating structures.

A comment on the accuracy and range of validity of the results is due . The stability of the numerical part of the analysis was tested by increasing the number of terms and then examining the magnitude of the coefficients. There were basically no changes in their values and the solution was found to be quite stable as presented in Section (3.4.4), Tables 3.11-3.12 and in Section (4.4.4), Tables 4.11-4.12 . The computational time to obtain these coefficients was very small and never exceeded 1 second on the IBM 370/157 computer model. The computation accuracy was tested by substituting back these coefficients into their respective equations and calculating the balancing error for each equation. The error was in all cases less than 10^{-5} in a single precision calculation, which shows an acceptable degree of accuracy.

The analytical part of the work is restricted to narrow and long slots since both the slot impedance and the static field used to introduce the edge condition are valid only in the narrow aperture limit. Further, for wide or very short slots mode coupling may arise and the analysis presented here may have to be modified to include the TM_{nm} excitation.

Suggestions For Future Investigations

Several interesting and challenging topics have arisen during the course of this work. The first and most related problem is to investigate the case of the multi-slotted waveguide. This can be done by studying the equivalent slots' impedance terminating the transmission line representation of the slotted guide,then proceeding as in Sec.(3.3) and Sec.(4.3) . This may provide extra control over the radiation pattern especially in the ϕ- direction. A second interesting problem would be to analyze the axially slotted guide for TM excitation. In this case the slot

tangential field is comprised of two components, E_ϕ and E_z, and if their relative magnitudes satisfy the McCormick relation[57] one may design a simple and efficient feed line suitable for spherical reflectors. A third problem would be to investigate the circumferentially slotted waveguide having TE_{11} excitation. The slot field in this case will also have both E_ϕ and E_z field components. Thus, to achieve a prescribed pattern in space one may use circumferential slots or a combination of circumferential and axial slots placed in succession.

A further problem is the tapered slotted waveguide, where the guide diameter is not constant but varies in the axial direction. This is necessary if it is required to maintain a variable main angle of radiation [6].

In most of these cases, as long as mode coupling does not exist, an integral equation formulation for the slot field can be constructed. This formulation involves a scalar Green's function similar to the analyses of Section (2.5). The solution, however, has to be investigated and it depends on the individual problem.

A problem that may be challenging is to investigate the wide axially slotted waveguide under TE excitation. In this case the mode coupling is certain to arise. The application of the scalar Green's function may not be valid in this case. One has to resort to the vector Green's function formulation, which makes the analysis highly complicated.

Finally, one may study in more depth the radiation problem of cascaded slotted sections as presented in this thesis. The parameters involved in the radiation equation (5.36) and their possible combinations are numerous. An optimization problem is likely to provide a variety

of patterns that may be important in feed lines and antenna designs.

APPENDIX A

TRANSVERSE RESONANCE EQUATION

Consider the system shown in Fig. A.1

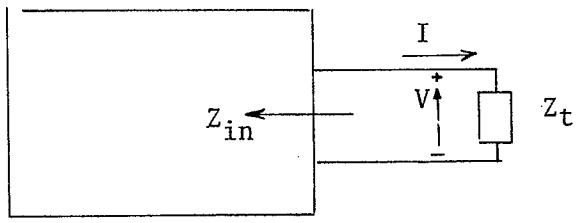

Fig. A.1 Transvrese resonance circuit

Z_t is a terminating impedance and Z_{in} is the input impedance of the system looking in the direction shown. Applying Ohm's law one gets

$$V = Z_t \quad I \tag{A.1}$$

If the network is source-free, then V is also equal to

$$V = - Z_{in} \quad I \tag{A.2}$$

Thus

$$Z_t \cdot I = - Z_{in} \quad I$$

which yields

$$Z_t + Z_{in} = 0 \tag{A.3}$$

which is the resonance equation of the system.

APPENDIX B

ELECTRIC FIELD AND MAGNETIC POLARIZABILITY OF AN AXIAL SLOT IN CYLINDRICAL WAVEGUIDE

In a cylindrical structure with an axial slot, it could be shown that the modal currents at the metallic surface and the electric field on the slot for the TE_{11} case are related through the relation [25]

$$I_1(a)h_{z1}(a,\phi) = \int_{-\phi_0}^{\phi_0} \sum_{\substack{n=0 \\ n\neq 1}}^{\infty} \overleftrightarrow{Y}_n(a)h_{zn}(a,\phi)h_{zn}(a,\phi')E_\phi(a,\phi')ad\phi' \tag{B.1}$$

where

$$h_{zn}(a,\phi) = \sqrt{\frac{\varepsilon_n}{2\pi}} \cos n\phi$$

$$\overleftrightarrow{Y}_n(a) = \vec{Y}_n + \overleftarrow{Y}_n \qquad \text{(looking in the direction of increasing } \rho\text{)}$$

$$I_1(a) = I_1'(a) - I_2'(a)$$

$I_1'(a)$ and $I_2'(a)$ are the modal current of the first mode at $\rho = a^-$ and $\rho = a^+$, respectively, and

$$\vec{Y}_n = \frac{K}{j\omega\mu a} \frac{H_n^{(1)}(K_\rho a)}{H_n^{(1)'}(K_\rho a)} \tag{B.2}$$

$$\overleftarrow{Y}_n = -\frac{K}{j\omega\mu a} \frac{J_n(K_\rho a)}{J_n'(K_\rho a)} \tag{B.3}$$

In order to diagonalize the above kernel $\overleftrightarrow{Y}(a)$, a set of static admittances is introduced as follows

$$\overleftrightarrow{Y}_{ns}(a) = - \frac{2K_\rho^2}{j\omega\mu n} \tag{B.4}$$

so that

$$\overleftrightarrow{Y}_n(a) = - \overleftrightarrow{Y}_{ns}(a) \rightarrow 0 \quad \text{for} \quad n >> K_\rho a \tag{B.5}$$

Using (B.4) in (B.1) and following the work in reference [25] one can show that for small ϕ_0 ,

$$E_\phi(a) \simeq \frac{1}{j\omega\varepsilon}\left(\frac{K_0}{K_\rho}\right)^2 \frac{I_1}{2a\sqrt{\pi}} \frac{1}{\ln(2/\phi_0)} \frac{1}{\sqrt{\phi_0^2 - \phi^2}} \tag{B.6}$$

The magnetic polarizability of the slot M_z could be defined as [25]

$$\int_{-\phi_0}^{\phi_0} \rho X E_t(\phi) a d\phi = \frac{1}{j\omega\varepsilon} M_z I_1 h_{z1}(a,0) \tag{B.7}$$

which by using (B.6) in (B.7), can be shown to have the form

$$M_z = \frac{\pi}{2}\left(\frac{K_0}{K_\rho}\right)^2 \frac{1}{\ln(2/\phi_0)} \tag{B.8}$$

APPENDIX C

EVALUATION OF THE INTEGRAL (3.6)

The integral $I(n)$ is given by

$$I(n) = \cos n\alpha \int_{-1}^{1} \frac{\cos(xn\phi_0)}{\sqrt{1 - x^2}}\, dx - \sin n\alpha \int_{-1}^{1} \frac{\sin(xn\phi_0)}{\sqrt{1 - x^2}}\, dx \tag{C.1}$$

Now, let

$$I_1(n) = \int_{-1}^{1} \frac{\cos(xn\phi_0)}{\sqrt{1 - x^2}}\, dx = -\int_{0}^{-1} \frac{\cos(xn\phi_0)}{\sqrt{1 - x^2}}\, dx + \int_{0}^{1} \frac{\cos(xn\phi_0)}{\sqrt{1 - x^2}}\, dx \tag{C.2}$$

and

$$I_2(n) = \int_{-1}^{1} \frac{\sin(xn\phi_0)}{\sqrt{1 - x^2}}\, dx = -\int_{0}^{-1} \frac{\sin(xn\phi_0)}{\sqrt{1 - x^2}}\, dx + \int_{0}^{1} \frac{\sin(xn\phi_0)}{\sqrt{1 - x^2}}\, dx \tag{C.3}$$

such that

$$I(n) = \cos n\alpha\, I_1(n) - \sin n\alpha\, I_2(n) \tag{C.4}$$

In the first term on the right-hand-side of both (C.2) and (C.3) let

$$x = -x$$

thus

$$I_1(n) = \int_0^1 \frac{\cos(xn\phi_0)}{\sqrt{1 - x^2}}\, dx + \int_0^1 \frac{\cos(xn\phi_0)}{\sqrt{1 - x^2}}\, dx = 2 \int_0^1 \frac{\cos(xn\phi_0)}{\sqrt{1 - x^2}}\, dx \qquad (C.5)$$

$$I_2(n) = -\int_0^1 \frac{\sin(xn\phi_0)}{\sqrt{1 - x^2}}\, dx + \int_0^1 \frac{\sin(xn\phi_0)}{\sqrt{1 - x^2}}\, dx = 0.0 \qquad (C.6)$$

The integral (C.5) is known [48] and is equal to

$$\int_0^1 \frac{\cos ax}{\sqrt{1 - x^2}}\, dx = \frac{\pi}{2} J_0(a)$$

Thus one finds

$$I(n) = \pi J_0(n\phi_0) \cos n\alpha \qquad (C.7)$$

APPENDIX D

CALCULATION of SLOTS CONDUCTANCE and SUSCEPTANCE

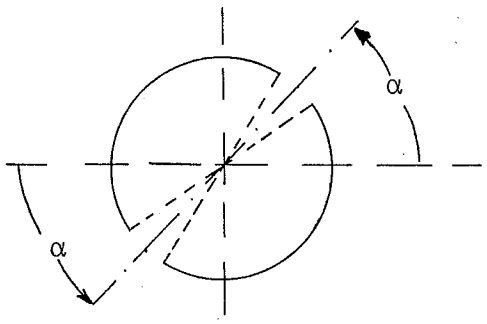

Fig. D.1 Symmetrically double slotted waveguide

Consider the slotted waveguide shown in Fig. (D.1). The structure could be regarded as a radial transmission line with the slots acting as terminating admittance at $\rho = a$ as shown in Fig. (D.2.)

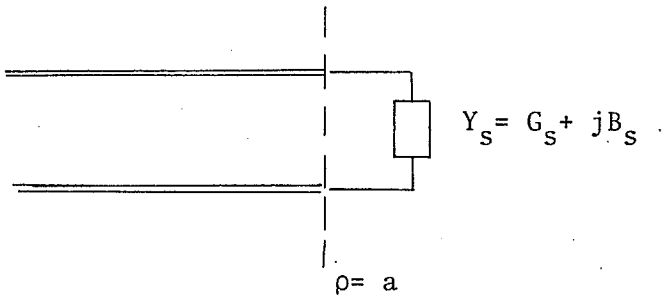

Fig. D.2 Transmission line representation of the double slotted waveguide

The transverse (to ρ)fields for the TE case (TE to z) are given by (equation 2.11)

$$E_t(\rho,\phi) = \sum_{n=0} V_n(\rho)\, e_n(\rho,\phi) \qquad (D.1)$$

$$H_t(\rho,\phi) = \sum_{n=0} I_n(\rho) h_n(\rho,\phi) \tag{D.2}$$

where $V_n(\rho)$ and $I_n(\rho)$ are the voltage and current modal amplitude respectively, and are related by [25]

$$\frac{I_n}{V_n} = \vec{Y}_n = \frac{K_\rho}{j\omega\mu a} \frac{H_n^{(2)}(Ka)}{H_n^{(2)'}(Ka)} \tag{D.3}$$

with $\vec{Y}_n$ the admittance of the n^{th} mode looking in the direction of increasing ρ at the slot ($\rho = a$), and the mode functions $e_n(\rho,\phi)$, $h_n(\rho,\phi)$ are given by [25]

$$\begin{aligned} h_{zn} &= \sqrt{\frac{\varepsilon_n}{\pi}} \cos n\phi \quad , \quad h_{\phi n} = \frac{\gamma}{K_\rho^2} \frac{n}{\rho} \frac{\sin n\phi}{\sqrt{\pi}} \\ e_{zn} &= 0 \quad , \quad e_{\phi n} = \sqrt{\frac{\varepsilon_n}{\pi}} \frac{\cos n\phi}{\rho} \end{aligned} \tag{D.4}$$

for which the following orthogonality relation holds

$$\int_0^{2\pi} (h_m \times \vec{a}_\rho \cdot e_n) \rho d\phi = \delta_{mn} \tag{D.5}$$

SLOT CONDUCTANCE

The conductance portion of the equivalent circuit which terminates the radial transmission line can be calculated from the relation [25]

$$G_s = P/|V|^2 \tag{D.6}$$

where P is the radial power flow per unit length and V_1 is the mode voltage of the $n = 1$ radial mode at the slot. The power P is given by

$$P = \mathrm{Re}\{\int_{\alpha-\phi_0}^{\alpha+\phi_0} E \times H^{*}\vec{a}_\rho a d\phi + \int_{\pi+\alpha-\phi_0}^{\pi+\alpha+\phi_0} E \times H^{*}\vec{a}_\rho a d\phi\}$$

$$= \mathrm{Re}\{(\int_{\alpha-\phi_0}^{\alpha+\phi_0} E_\phi H_z^{*} + \int_{\pi+\alpha-\phi_0}^{\pi+\alpha+\phi_0} E_\phi H_z^{*})\vec{a}_\rho a d\phi\} \qquad (D.7)$$

From (D.2) and (D.3) we have

$$H_z(\rho,\phi) = \sum_{n=0}^{\infty} I_{nz} h_{zn}(\rho,\phi)$$

$$= \sum_{n=0}^{\infty} \vec{Y}_n V_n h_{zn}(\rho,\phi) \qquad (D.8)$$

Using (D.1) and (D.5) V_n is readily obtained as

$$\int_0^{2\pi} h_n^{*}(\rho,\phi) x \vec{a}_\rho \cdot E_t(\rho,\phi) a d\phi = \sum_{n=0} V_n \int_0^{2\pi} h_n^{*}(\rho,\phi) x \vec{a}_\rho \cdot e_n(\rho,\phi) a d\phi$$

$$= V_n \qquad (D.9)$$

The integration on the left hand side of (D.9) exists only on the surfaces of the slots. Upon simplification, V_n becomes

$$V_n(a,\phi) = \int_{\alpha-\phi_0}^{\alpha+\phi_0} h_{zn}(a,\phi) E_\phi(a,\phi) a d\phi + \int_{\pi+\alpha+\phi_0}^{\pi+\alpha+\phi_0} h_{zn}(a,\phi) E_\phi(a,\phi) a d\phi \qquad (D.10)$$

Substituting V_n back in (D.8) gives

$$H_z(\rho,\phi) = \sum_{n=0}^{\infty} \vec{Y}_n h_{zn}(a,\phi) \Big[\int_{\alpha-\phi_0}^{\alpha+\phi_0} E_\phi h_{zn}(a,\phi')ad\phi' + \int_{\pi+\alpha-\phi_0}^{\pi+\alpha+\phi_0} E_\phi h_{zn}(a,\phi')ad\phi' \Big] \tag{D.11}$$

the power P using (D.7) and (D.11) becomes

$$P = \mathrm{Re}\{ \sum_{n=0}^{\infty} \vec{Y}_n \Big[\int_{\alpha-\phi_0}^{\alpha+\phi_0} E_\phi(a,\phi) h_{zn}(a,\phi) + \int_{\pi+\alpha-\phi_0}^{\pi+\alpha+\phi_0} E_\phi(a,\phi) h_{zn}(a,\phi) \Big] ad\phi$$

$$\Big[\int_{\alpha-\phi_0}^{\alpha+\phi_0} E_\phi(a,\phi') h_{zn}(a,\phi') + \int_{\pi+\alpha-\phi_0}^{\pi+\alpha+\phi_0} E_\phi(a,\phi') h_{zn}(a,\phi') \Big] ad\phi' \} \tag{D.12}$$

The conductance G_s by virtue of (D.6), (D.10) and (D.12) is given by

$$G_s = P \Big/ \left| \int_{\alpha-\phi_0}^{\alpha+\phi_0} h_{z1}(a,\phi) E_\phi(a,\phi) ad\phi + \int_{\pi+\alpha-\phi_0}^{\pi+\alpha+\phi_0} h_{z1}(a,\phi) E_\phi(a,\phi) ad\phi \right|^2 \tag{D.13}$$

with P given by (D.12).

SLOT SUSCEPTANCE

To calculate the slot susceptance, it is shown in Appendix[B] that the slot tangential field is related to the current discontinuity at the slot, I, and the slot dimension, ϕ_0, by the relation

$$E_\phi(\phi) \simeq \frac{-1}{j\omega\varepsilon}\left(\frac{K_0}{K_\rho}\right)^2 \frac{1}{2a\sqrt{\pi}} \frac{I}{\ln(2/\phi_0)} \frac{1}{\sqrt{\phi_0^2 - \phi^2}} ,$$

for the case $\alpha = 0$. For any arbitrary location one may assume the field to vary with a factor of $\cos\alpha$. This is in agreement with the type of excitation, TE_{11}. It is to be noted that the factor $\cos\alpha$ will adjust both the amplitude and the relative sign (i.e. direction) of the field. Accordingly,

$$E(a,\phi) = \frac{1}{-j\omega\varepsilon}\left(\frac{K_0}{K_\rho}\right)^2 \frac{1}{2a\sqrt{\pi}} \frac{|I_\alpha|}{\ln(2/\phi_0)} \frac{\cos\alpha}{\sqrt{\phi_0^2 - (\phi-\alpha)^2}} \qquad (D.14)$$

Where the expression has been modified to the slot location $\alpha - \phi_0 < \phi < \alpha + \phi_0$. The modal voltage of the $n = 1$ mode at the slot was given before [eqn. (D.9)], and is equal to

$$V_1 = \int_0^{2\pi} h_1^* \times \vec{a}_\rho \cdot E_t(a,\phi)\, a\, d\phi$$

$$= \int_{\alpha-\phi_0}^{\alpha+\phi_0} h_{z1}^*(a,\phi)\, \vec{a}_\rho \times E_t(a,\phi)\, a\, d\phi + \int_{\pi+\alpha-\phi_0}^{\pi+\alpha+\phi_0} h_{z1}^*(a,\phi) \cdot$$

$$\vec{a}_\rho \times E_t(a,\phi)\, a\, d\phi$$

$$\simeq h_{z1}^*(a,\phi) \int_{\alpha-\phi_0}^{\alpha+\phi_0} \vec{a}_\rho \times E_t(a,\phi)\, a\, d\phi + h_z^*(a, \pi+\alpha)$$

$$\int_{\pi+\alpha-\phi_0}^{\pi+\alpha+\phi_0} \vec{a}_\rho \times E_t(a,\phi)\, a\, d\phi \qquad (D.15)$$

Now, the integration

$$I_n = \int_{\alpha-\phi_0}^{\alpha+\phi_0} \vec{a}_\rho \times E_t(a,\phi)\,a\,d\phi$$

$$= \frac{-1}{j\omega\varepsilon}\left(\frac{K_0}{K_\rho}\right)^2 \frac{1}{2a\sqrt{\pi}} \frac{|I_\alpha|}{\ln(2/\phi_0)} \cos\alpha \int_{\alpha-\phi_0}^{\alpha+\phi_0} \frac{a}{\sqrt{1 - \left(\frac{\phi-\alpha}{\phi_0}\right)^2}}\, d(\phi/\phi_0)$$

Upon substituting $u = \phi - \alpha$ then $y = u/\phi_0$ the integration on the right hand side becomes

$$\int_{y=-1}^{1} \frac{dy}{\sqrt{1 - y^2}} = 2 \int_{0}^{1} \frac{dy}{\sqrt{1 - y^2}} = 2[\sin^{-1}]_0^1 = \pi$$

Thus

$$\int_{\alpha-\phi_0}^{\alpha+\phi_0} \vec{a}_\rho \times E_t(a,\phi)\,a\,d\phi = \frac{-1}{j\omega\varepsilon} |I_\alpha| \frac{\cos\alpha}{\sqrt{\pi}} \left(\frac{K_0}{K_\rho}\right)^2 \frac{\pi}{2} \frac{1}{\ln(2/\phi_0)} \tag{D.16}$$

But $\frac{\cos\alpha}{\sqrt{\pi}} = h_{z1}(a,\phi)$, therefore (D.16) could be written as

$$\int_{\alpha-\phi_0}^{\alpha+\phi_0} \vec{a}_\rho \times E_t(a,\phi)\,a\,d\phi = \frac{-M_z}{j\omega\varepsilon} |I_\alpha| \, h_{z1}(a,\alpha) h_{z1}^*(a,\alpha) \tag{D.17}$$

with

$$M_z = \left(\frac{K_0}{K_\rho}\right)^2 \frac{\pi}{2} \frac{1}{\ln(2/\phi_0)} \tag{D.18}$$

Substituting (D.17) in (D.15) taking into consideration that due to symmetry $|I_\alpha| = |I_{\pi+\alpha}|$ one may write

$$V_1 = -I_\alpha \frac{M_z}{j\omega\varepsilon}\{h_{z1}(a,\alpha)h^*_{z1}(a,\alpha) + h_{z1}(a,\pi+\alpha)h^*_{z1}(a,\pi+\alpha)\} \qquad (D.19)$$

so that

$$\frac{I_\alpha}{V_1} = jB_s = \frac{-j\omega\varepsilon}{M_z} \Big/ \left(\frac{\cos^2\alpha}{\pi} + \frac{\cos^2(\pi+\alpha)}{\pi}\right) \qquad (D.20)$$

APPENDIX E

INTEGRATION OF (3.25) AND (3.28)

Consider the integral

$$I_{\alpha\beta} = m^2 \int_0^1 \frac{J_m(\alpha y)J_m(\beta y)}{y}\, dy + \alpha\beta \int_0^1 J_m'(\alpha y)J_m'(\beta y)\, y\, dy \quad (E.1)$$

where α and β are constants. Using integration by parts applied to the second term of the right hand side one finds

$$I_{\alpha\beta} = m^2 \int_0^1 \frac{J_m(\alpha y)J_m(\beta y)}{y}\, dy + \alpha\{y\, J_m(\beta y)J_m'(\alpha y)\}\Big|_0^1$$

$$- \alpha \int_0^1 J_m(\beta y)\, y\, J_m''(\alpha y)\alpha\, dy - \alpha \int_0^1 J_m(\beta y)J_m'(\alpha y)\, dy$$

$$= \alpha\, J_m(\beta)J_m'(\alpha) + m^2 \int_0^1 \frac{J_m(\alpha y)J_m(\beta y)}{y}\, dy - \alpha \int_0^1 J_m(\beta y)J_m'(\alpha y)\, dy$$

$$- \alpha^2 \int_0^2 y\, J_m(\beta y)\{-\frac{1}{\alpha y} J_m'(\alpha y) - (1 - \frac{m^2}{\alpha^2 y^2})J_m(\alpha y)\}dy$$

(E.2)

where the Bessel equation

$$z^2 J_m'' + z\, J_m' + (z^2 - m^2)J_m = 0$$

has been used.

Collecting terms in (E.2) gives $I_{\alpha\beta}$ in the form

$$I_{\alpha\beta} = \alpha\, J_m(\beta)J'_m(\alpha) + \alpha^2 \int_0^1 y\, J_m(\beta y)J_m(\alpha y)\,dy \qquad (E.3)$$

which by interchanging α and β modifies to

$$I_{\alpha\beta} = \beta\, J_m(\alpha)J'_m(\beta) + \beta^2 \int_0^1 y\, J_m(\alpha y)J_m(\beta y)\,dy \qquad (E.4)$$

Equating these two equations, i.e. (E.3) and (E.4), gives

$$\int_0^1 y\, J_m(\alpha y)J_m(\beta y)\,dy = [\beta\, J_m(\alpha)J'_m(\beta) - \alpha\, J_m(\beta)J'_m(\alpha)]/(\alpha^2 - \beta^2) \qquad (E.5)$$

Now consider the integral in (E.5) for

i. α is a root of $J'_m(\alpha) = 0$

Thus, from (E.5) we have

$$\int_0^1 y\, J_m(\alpha y)J_m(\beta y)\,dy = \frac{\beta\, J_m(\alpha)J'_m(\beta)}{(\alpha^2 - \beta^2)}$$

Substituting this value back in (E.3) gives

$$I_{\alpha\beta} = \alpha^2\, \beta\, \frac{J_m(\alpha)J'_m(\beta)}{(\alpha^2 - \beta^2)} \qquad (E.6)$$

ii. If both α and β are roots of $J_m'(z) = 0$, $\alpha \neq \beta$, then the integral in (E.5) is zero, which upon substitution in (E.3) gives

$$I_{\alpha\beta} = 0 \tag{E.7}$$

iii. If both α and β are roots of $J'(z) = 0$ and $\alpha = \beta$ then by a simple limiting process of (E.5), or considering directly the results presented in [51], one has

$$\int_0^1 y J_m^2(\alpha y)\, dy = \frac{1}{2}\left(1 - \frac{m^2}{\alpha^2}\right) J_m^2(\alpha)$$

which upon substituting back in (E.4) or (E.3) gives

$$I_{\alpha\alpha} = \frac{\alpha^2}{2}\left(1 - \frac{m^2}{\alpha^2}\right) J_m^2(\alpha) \tag{E.8}$$

iv. For α and β being any two constants, other than the previous ones, one finds

$$I_{\alpha\beta} = \frac{\alpha^2\, \beta\, J_1(\alpha) J_1'(\beta) - \beta^2\, \alpha\, J_1(\beta) J_1'(\alpha)}{(\alpha^2 - \beta^2)} \tag{E.9}$$

APPENDIX F

MAGNETIC POLARIZABILITY OF AN AXIAL SLOT IN A COAXIAL GUIDE

In order to show that the magnetic polarizability of the slot in the coaxial line is approximately the same as in the hollow waveguide, one has to consider first the analysis of Appendix [B]. The same steps and equations as given there are applied in the case of the coaxial line, except for equation (B.3) which here takes the form

$$\overleftarrow{Y}''_n(b) = -\frac{K_\rho}{j\omega\mu}\left[K_\rho \frac{D_n(K_\rho b)}{D'_n(K_\rho b)}\right] \tag{F.1}$$

where $\overrightarrow{Y}''_n(b)$ for both the coxaial line and the hollow waveguide is identical and given by (B.2), and $D_n(K_\rho b)$ and $D'_n(K_\rho b)$ are given by (4.17).

The kernel $\overleftrightarrow{Y}''_n(b)$ of equation (B.1), namely

$$\overleftrightarrow{Y}''_n(b) = \overrightarrow{Y}''_n(b) + \overleftarrow{Y}''_n(b)$$

may be written here as

$$\overleftrightarrow{Y}''_n(b) = -\frac{K_\rho}{j\omega\mu b}\left[K_\rho \frac{D_n(K_\rho b)}{D'_n(K_\rho b)} - \frac{H_n^{(1)}(K_\rho b)}{H_n^{(1)'}(K_\rho b)}\right] \tag{F.2}$$

Using the asymptotic values of the Bessel and the Hankel functions for large orders gives [51]

$$J_n(Kb)Y'(Ka) \simeq \left(\frac{b}{a}\right)^n \frac{1}{\pi Ka}$$

$$J_n'(Ka)\ Y(Kb) \simeq -\left(\frac{a}{b}\right)^n \frac{1}{\pi Ka}$$

$$J_n'(Kb)Y'(Ka) \simeq \frac{n}{\pi}\left(\frac{b}{a}\right)^n \frac{1}{KaKb}$$

$$J_n'(Kb)Y'(Kb) \simeq \frac{n}{\pi}\left(\frac{a}{b}\right)^n \frac{1}{KaKb}$$

and

$$H_n^{(1)}(K_\rho b) \simeq -j\sqrt{\frac{2}{\pi n}}\left(\frac{2n}{e}\right)^n (Kb)^{-n}$$

$$H_n^{(1)'}(Kb) \simeq +j\sqrt{\frac{2}{\pi n}}\left(\frac{2n}{e}\right)^n (Kb)^{-n-1} \quad \text{for} \quad n >> Kb$$

Substituting the above expansions in eqn. (F.2) gives

$$\vec{Y}_n''(b) \simeq -\frac{K_\rho}{j\omega\mu b}\left[\frac{K_\rho b}{n}\ \frac{(c^{2n}+1)}{(c^{2n}-1)} + \frac{K_\rho b}{n}\right] \tag{F.3}$$

where $c = b/a$.

But since

$$\frac{c^{2n}+1}{c^{2n}-1} \simeq 1 \qquad n >> 1 \quad ,$$

therefore (D.3) becomes

$$\overleftrightarrow{Y}''(b) = -\frac{2K_\rho^2}{j\omega\mu n} \tag{F.4}$$

Equation (F.4) is identical to equation (B.4). Therefore, the steps and the results that follow there are applied here, and the expressions for E_ϕ and M_z, given by (B.6) and (B.8), are valid expressions for the coaxial line case.

APPENDIX G

EVALUATION OF $Z'(K_\rho b)$

From equation (4.7) we have

$$\overleftarrow{Z}_1(K_\rho b) = - \frac{j\omega\mu b}{K_\rho} \frac{D_n'(K_\rho b)}{K_\rho D_n(K_\rho b)}$$

with $D_n(Kb)$ and $D_n'(Kb)$ given by (4.17). Now

$$\frac{\partial \overleftrightarrow{Z}(K_\rho b)}{\partial K_\rho} \simeq \frac{\partial \overleftarrow{Z}_1(K_\rho b)}{\partial K_\rho} \Bigg|_{K_\rho b = z_{1m} c} =$$

$$- \frac{j\omega\mu b}{K_\rho} \left\{ \frac{J_1'(cz)aY_1''(z) + bJ_1''(cz)Y_1'(z) - aJ_1''(z)Y_1'(cz) - bJ_1'(z)Y''(cz)}{J_1(cz)Y_1'(z) - J_1'(z)Y_1(cz)} \right\} \tag{G.1}$$

where the relationship

$$J_1'(cz)Y_1'(z) - J_1'(z)Y_1'(cz) = 0$$

has been used, and the subscript 1m has been dropped for typing convinience. Also, the derivative of the slot impedance has been neglected [25].

Simplifying the expression (G.1) gives the required derivative of the $\overleftrightarrow{Z}(K_\rho b)$ as

$$\frac{\partial \overleftarrow{Z}(K_\rho b)}{\partial K_\rho} \Bigg|_{K_\rho b = cz} = -j \frac{\omega\mu b}{K_\rho} a\left\{\left(1 - \frac{1}{z^2}\right)\left(\frac{G_1(cz)}{C_1(cz)}\right) - c\left(1 - \frac{1}{c^2 z^2}\right)\right\} \tag{G.2}$$

where $G_1(cz)$ is given by (4.32) and $C_1(cz)$ is given by (4.17).

APPENDIX H

EVALUATION OF THE INTEGRAL (4.30) and (4.33)

Consider the integral

$$I = n^2 \int_1^c C_n(z_{nm}y)C_n(ty)\frac{dy}{y} + a^2 \int_1^c C_n'(z_{nm}y)C_n'(ty)ydy \qquad (H.1)$$

where $C_n(zy)$ and $C_n'(zy)$ are given by (4.17), and z_{nm} and C satisfies the condiction (4.20). In the following analysis all subscripts will be dropped for typing convenience. The integration of equation (H.1) can be written as

$$I = Y'(z)Y'(t)\{n^2 \int_1^c J(zy)J(ty)\,\frac{1}{y}\,dy + zt \int_1^c J'(zy)J'(ty)ydy\}$$

$$+ J'(z)J'(t)\{n^2 \int_1^c Y(zy)Y(ty)\,\frac{1}{y}\,dy + zt \int_1^c Y'(zy)Y'(ty)ydy\}$$

$$- Y'(z)J'(t)\{n^2 \int_1^c J(zy)Y(ty)\,\frac{1}{y}\,dy + zt \int_1^c J'(zy)Y'(ty)ydy\}$$

$$- J'(z)Y'(t)\{n^2 \int_1^c Y(zy)J(ty)\,\frac{1}{y}\,dy + zt \int_1^c Y'(zy)J'(ty)ydy\}$$

An integral similar to any of these four integrals has been carried out in Appendix[E],but with different limits. The result of these integrals upon simplification becomes

$$I = z^2 \int_1^c y\, C_n(zy) C_n(ty)\, dy \tag{H.2}$$

where the function $C_n(ty)$ is given by (4.17). Apparently both $C_n(zy)$ and $C_n(ty)$ satisfy the Bessel differential equation, namely

$$z^2 \frac{d^2w}{dz^2} + z \frac{dW}{dz} + (z^2 - n^2)W = 0 \tag{H.3}$$

Thus letting

$$U = C_n(zy) \quad \text{and} \quad V = C_n(ty) \tag{H.4}$$

one finds

$$y^2 \frac{d^2U}{dy^2} + y \frac{dU}{dy} + (z^2y^2 - n^2)U = 0$$

and

$$y^2 \frac{d^2V}{dy^2} + y \frac{dV}{dy} + (y^2t^2 - n^2)V = 0$$

Multiplying these equations, respectively, by V/y and U/y, their subtraction gives

$$(z^2 - t^2) \int_1^c y\, C_n(zy) C_n(ty)\, dy = [yt\, C_n(zy) C_n'(ty) - yz\, C_n'(zy) C_n(ty)]_1^c$$

The second term on the right hand side is zero at both limits, which gives

$$\int_1^c y\, C_n(zy)C_n(ty)dy = \frac{t}{z^2 - t^2}\{c\, C_n(cz)C_n'(ct) - C_n(z)C_n'(t)\} \tag{H.5}$$

Accordingly, using (H.5) and (H.2) one finds

$$I = \frac{z^2 t}{z^2 - t^2}\{c\, C_n(cz)C_n'(ct) - C_n(z)C_n'(t)\} \tag{H.6}$$

Consider now the two cases:

i. t is a root of eqn. (4.20), different from z. In this case both $C_n'(ct)$ and $C_n'(t)$ are zero, and the integration is zero.

ii. t is a root of eqn. (4.20) and equal to z .

Letting $t = xz$, and considering the limit as $x \to 1$, one finds

$$I = \lim_{x\to 1} z \{c\, C_n(cz) \frac{x}{1 - x^2}(J'(xcz)Y'(xz) - Y'(xcz)J'(xz))$$

$$+ C_n(z) \frac{1}{1 - x^2}(J'(xz)Y'(xz) - Y'(xz)J'(xz))\}$$

where the second term is always zero and I reduces to

$$I = -\frac{1}{2} cz\, C_n(cz)\{cz\, J''(cz)Y'(z) + z\, J'(cz)Y''(z) - cz\, Y''(cz)$$

$$J'(z) - z\, Y'(cz)J''(z)\} \tag{H.7}$$

Utilizing the Bessel equation (H.3) in (H.7) and simplifying the results one finds

$$I = \frac{z^2}{2}\{c^2(1 - \frac{1}{c^2z^2})[J(cz)Y'(z) - Y(cz)J'(z)]^2 - c(1 - \frac{1}{z^2})$$

$$[J(cz)Y'(z) - Y(cz)J'(z)][J(z)Y'(cz) - Y(z)J'(cz)]\} \qquad (H.8)$$

APPENDIX I

DERIVATION OF THE SUMMATION (5.25)

Consider the summation

$$S = \sum_{m=-\infty}^{\infty} \frac{J_0(m\phi_0)}{J_0(\phi_0)} \frac{(-j)^{m+1}}{H_m^{(1)'}(K_0 d \sin\theta)} \exp[jm(\phi - \alpha)] \qquad (I.1)$$

Choosing the p^{th} and the $-p^{th}$ terms one finds

$$S_p = \frac{J_0(p\phi_0)}{J_0(\phi_0)} \frac{(-j)^{p+1}}{H_p^{(1)'}(K_0 d \sin\theta)} \exp[jp(\phi - \alpha)] + \frac{J_0(-p\phi_0)}{J_0(\phi_0)} \cdot$$

$$\frac{(-j)^{-p+1}}{H_{-p}^{(1)'}(K_0 d \sin\theta)} \exp[-jp(\phi - \alpha)] \qquad (I.2)$$

This equation can be simplified by the following characteristic relations of the Bessel and the Hankel functions [51]

$$J_0(-p\phi_0) = J_0(p\phi_0) \qquad (I.3)$$

and

$$H_{-p}^{(1)'}(z) = \exp(jp\pi) H_p^{(1)'}(z)$$

$$= \frac{H_p^{(1)'}(z)}{[\exp(-j\pi)]^p}$$

$$= \frac{H_p^{(1)'}(z)}{(-j)^{2p}} \qquad (I.4)$$

That is, by substituting (I.3) and (I.4) in (I.2), it reduces to

$$S_p = \frac{J_0(p\phi_0)}{J_0(\phi_0)} \frac{(-j)^{p+1}}{H_p^{(1)'}(K_0 d \sin\theta)} 2\cos[p(\phi - \alpha)] \qquad (I.5)$$

Thus, the summation S of eqn. (I.1) can be modified to

$$S = \sum_{m=0}^{\infty} \varepsilon_m \frac{J_m(m\phi_0)}{J_m(\phi_0)} \frac{(-j)^{m+1}}{H_m^{(1)'}(K_0 d \sin\theta)} \cos m(\phi - \alpha) \qquad (I.6)$$

BIBLIOGRAPHY

[1] A.C. Ludwig, K. Woo, J. J. Gustincic and J. C. Harely, "Recent development of conical reflector antennas," G-AP Inter. Symp. 1973, pp. 314-317.

[2] R.C. Spencer, C.J. Sletten and J.E. Walsh, "Correction of spherical aberration by a phased line source," 1949 Proc. Nat'l Elect. Conf., p. 320.

[3] G.C. McCormick, "A line feed for spherical reflector," IEEE Trans. Antennas Propagat., Vol. AP-15, pp. 639-645, Sept. 1967.

[4] V.H. Rumsey, "On design and performance of feeds for correcting spherical aberration," IEEE Trans. Antennas Propagat., Vol. AP-18, pp. 343-351, May 1970.

[5] A.W. Love and J.J. Gustincic, "Line source feed for a spherical reflector," IEEE Trans. Antennas Propagat., Vol. AP-16, pp. 132-134, June 1968.

[6] L.C. Shen, "The field pattern of a long antenna with multiple excitation," IEEE Trans. Antennas Propagat., Vol. AP-16, pp. 643-646, Nov. 1968.

[7] J.W. Duncan and V.P. Minerva, "100:1 Bandwidth balun transformer," Proc. IRE, Vol. 48, pp. 156-164, Feb. 1960.

[8] N. Morcuvitz, "On field representations in terms of leaky modes or eigen-modes," IRE Trans. Antennas Propagat., Vol. AP-4, pp. 192-194, July 1956.

[9] T. Tamir and A.A. Oliner, "Guided complex waves, Part I, fields at an interface," Proc. Inst. Elect. Engrs. (London), Vol. 110, pp. 310-324, Feb. 1963.

[10] R.E. Collin, "Analytical solution for a leaky wave antenna," IRE Trans. Antennas Propagat., Vol. AP-10, pp. 561-565, Sept. 1962.

[11] A. Hessel, "On the influence of complex poles on the radiation pattern of leaky wave antennas," IRE Trans. Antennas Propagat., Vol. AP-10, pp. 646-647, Sept. 1962.

[12] T. Tamir and A.A. Oliner, "Guided complex waves, Part II, relation to radiation patterns," Proc. Inst. Elec. Engrs. (London). Vol. 110, pp. 325-334, Feb. 1963.

[13] L.O. Goldstone and A.A. Oliner, "Leaky wave antennas I: rectangular waveguides," IRE Trans. Antennas Propagat., Vol. AP-7, pp. 307-319, Oct. 1959.

[14] R. Collin and F.J. Zucker: Antenna Thoery, Part 2, Chap. 19 and 20, McGraw-Hill Book Company, N.Y., 1969.

[15] R.F. Hyneman, "Closely spaced transverse slots in waveguide," IRE Trans. Antennas Propagat., Vol. AP-5, pp. 335-342, October 1959.

[16] B. Clarricoats and B. Taylor, "Backward waves in waveguides containing dielectric," Proc. Inst. Elec. Engrs. (London), Vol. 108, pt. c, pp. 495-501, Sept. 1961.

[17] B. Clarricoats and B. Taylor, "Evanescent and propagation modes of dielectric-loaded circular waveguide," Proc. Inst. Elec. Engrs. (London), Vol. 111, pp. 1951-1956, Dec. 1964.

[18] A. Trivelpiece, A. Ignatius and P. Holscher, "Backward waves in longitudinally magnetized ferrite rods," J. Appl. Phys., Vo.. 32, pp. 259-267.

[19] A. Trivelpiece and R. Gould, "Space charge waves in cylindrical plasma columns," J. Appl. phys., Vol. 30, pp. 1784-1793, Nov. 1959.

[20] T. Tamir and A. Oliner, "The spectrum of electromagnetic waves guided by a plasma layer," Proc. IEEE, Vol. 51, pp. 317-332, Feb. 1963.

[21] R.E. Collin, "The characteristic impedance of a slotted coaxial line," IRE Trans. Microwave Theory and Techniques, Vol. MTT-4, pp. 4-8, January 1956.

[22] T. Hatsuda, "Computation of impedance of partially filled and slotted coaxial line," IEEE Trans. Microwave Theory and Techniques (correspondence), Vol. MTT-15, pp. 643-644, Nov. 1967.

[23] V. Rumsey, "Travelling wave slot antennas," J. Appl. Phys., Vol. 24, pp. 1358-1365, Nov. 1953.

[24] R.F. Harrington, "Propagation along a slotted cylinder," J. Appl. phys. Vol. 24, pp. 1366-1371, Nov. 1953.

[25] L. Goldstone and A. Oliner, "Leaky wave antennas II: circular wave guides," IRE Trans. Antennas Propagat., Vol. AP-9, pp. 280-290, May 1961.

[26] B. Clarricoats and K. Slinn, "Computer method of determining the propagation coefficient of slotted waveguide," Electronic Letters, Vol. 3., No. 5 pp. 191-192, May 1967.

[27] M.H. Chen, "Radial mode analysis of electromagnetic wave propagation on slotted cylindrical structure," IEEE Trans. Antennas Propagat., Vol. AP-21, pp. 314-320, May 1973.

[28] C.H. Walter: Travelling Wave Antennas, Chapt. 4 and 5. McGraw-Hill Book Company, N.Y., 1965.

[29] N. Marcuvitz, Waveguide Handbook, M.I.T. Rad. Lab. Ser., McGraw-Hill Book Company, N.Y., Vol. 10, 1951.

[30] R.F. Harrington, Time-Harmonic Electromagnetic Fields, McGraw-Hill Book Company, N.Y., 1961.

[31] J. Schwinger and D. Saxon, Discontinuities in Waveguides. Notes on lectures by J. Schwinger, Gordon and Breach Science Publishers. London, 1968.

[32] J. Wait and D. Hill, "Electromagnetic field on a dielectric coated coaxial cable with an interrupted shield,". AP.S. International symposium, Univ. of Illinois, pp. 423-424, June 1975.

[33] J.R. Wait, Electromagnetic Radiation From Cylindrical Structure, Pergamon Press, 1959, Chapter 16.

[34] W.F. Croswell, C.M. Knop, and D.N. Hatcher, "A dielectric coated circumferential slot array for omnidirectional coverage-age microwave frequencies," IEEE Trans. Antennas Propogat. , Vol. AP-15, No. 6, pp. 722-727 Nov. 1967.

[35] S. Silver (Editor), Microwave Antenna Theory and Design, Dover Publication, New York 1949.

[36] W.B. Wholey and W.N. Eldred, "A new type of slotted line section," Proc. IRE, Vol. 38, No. 3, pp. 244-248, March 1950.

[37] R.A. Hurd, "The field in a narrow circumferential slot in a coaxial waveguide," Can. J. Physics, No. 51, pp. 940-955, 1973.

[38] D.C. Chang, "Equivalent circuit representation and characteristics of a radiating cylinder driven through a circumferential slot," IEEE Trans. Antennas Propagat., Vol. AP-21, No. 6, Nov. 1973.

[39] J.R. Wait, "Scattering from a break in the shield of a braided coaxial cable - Theory," AEÜ 29, No. 11, pp. 467-473, Nov. 1975.

[40] D. Hill and J. Wait, "Scattering from a break in the shield of a braided coaxial cable. Numerical results," AEÜ 30, pp. 117-121, No. 3, March 1976.

[41] C.W. Harrison and R.W.P. King, "Excitation of a coaxial line through a transverse slot," IEEE Trans. Electromay. Compat., Vol. EMC-14, No. 4, pp. 107-112, Nov. 1972.

[42] P. Green and J. Richardson, "Aperture field of a leaky wave antenna," Elect. Letters, Vol. 2, No. 2, pp. 68-69, Feb. 1966.

[43] P. Clarricoats and P. Green, "Slot mode propagation in rectangular waveguide," Elect. Letters, Vol. 2, No. 8, pp. 307-308 Aug. 1966.

[44] J.R.Wait and D. Hill, "On the electromagnetic field of a dielectric coated coaxial cable with an interrupted shield," IEEE Trans. Antennas Prop., Vol. AP-23, No. 4, p. 470, July 1975.

[45] J.R. Wait and D. Hill, "Electromagnetic fields of a dielectric coated coaxial cable with an interrupted shield-quasi static approach," IEEE Trans. Antennas Prop., Vol. AP-23, No. 5, p. 679, Sept. 1975.

[46] D.C. Chang and T.T.Wu, "A note on the theory of end correction for thick monopole," Radio Sci., Vol. 3, No. 6, p. 639, 1968.

[47] T.T. Wu, "Input admittance of infinitely long dipole antennas driven from coaxial lines," J. Math. Phys., Vol. 3, No. 6 pp. 1298-1301, 1962.

[48] I. Gradshteyn and I. Ryzhik, Table of Integrals, Series and Products, Academic Press, New York. 1965.

[49] A. Wexler, "Solution of waveguide discontinuities by modal analysis," IEEE Trans. Microwave Theory and Techniques, Vol. MTT-15, No. 9, pp. 508-517, Sept. 1967.

[50] P. Morse and H. Feshbach, Methods of Theoretical Physics, Vol II, McGraw-Hill, New York, 1953. Chapt. 11.2.

[51] M. Abramowitz and I.Stegun, Handbook of Mathematical Functions, Dover Publications, New York, 1968.

[52] R. Collin, Field Theory of Guided Waves, McGraw-Hill, New York, 1960.

[53] G. Tyras, Radiation and Propagation of Electromagnetic Waves, Academic Press, N.Y., 1969.

[54] C. Montgomery, R. Dicke and E. Purcell, Principles of Microwave Circuits, McGraw-Hill, N.Y., 1948.

[55] J. Kraus, Antennas, McGraw-Hill, N.Y., 1950.

[56] J. Stratton, Electromagnetic Theory, McGraw-Hill, N.Y., 1941.